Cover Page

The handle http://hdl.handle.net/1887/36568 holds various files of this Leiden University dissertation

Author: Scholten, Florine E.M.
Title: Host factors involved in chikungunya virus replication
Issue Date: 2015-12-10

Host factors involved in chikungunya virus replication

Florine Elisabeth Maria Scholte

Host factors involved in chikungunya virus replication

Proefschrift ter verkrijging van
de graad van Doctor aan de Universiteit Leiden,
op gezag van Rector Magnificus prof. mr. C.J.J.M. Stolker,
volgens besluit van het College voor Promoties
te verdedigen op donderdag 10 december 2015
klokke 16.15 uur

door

Florine Elisabeth Maria Scholte
Geboren 17 december 1985
te Hoogeveen

PROMOTIECOMMISSIE

Promotor:

Prof. dr. E.J. Snijder

Co–promotor:

Dr. M.J. van Hemert

Overige leden:

Prof. dr. A. Merits (University of Tartu, Estonia)
Prof. dr. R.C. Hoeben
Dr. G.P. Pijlman (Wageningen University)
Prof. dr. J.M. Smit (University of Groningen)

"Wisdom comes from experience.
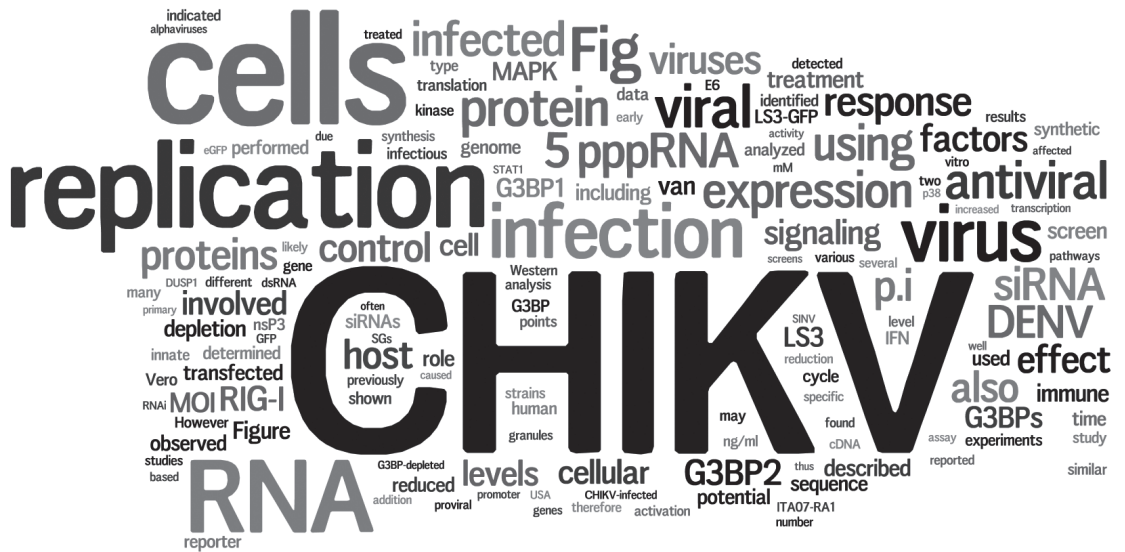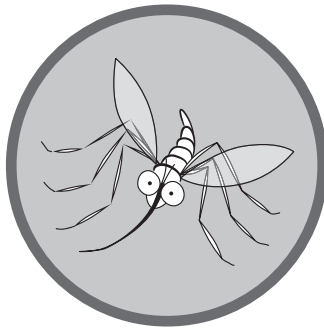Experience is often a result of lack of wisdom."

Terry Pratchett

TABLE OF CONTENTS

1.

General Introduction

Chikungunya virus: from neglected pathogen to global public health concern

In 2005 a mysterious virus suddenly surfaced on several islands in the Indian Ocean. It caused high fever and severe joint pains, and infected a large proportion of the islands' populations. The unidentified virus spread rapidly and attracted the attention of the scientific community as well as the media. Soon it was discovered that the chikungunya virus (CHIKV) was responsible for this outbreak, causing the non-lethal but debilitating and untreatable chikungunya fever (CHIKF). CHIKV is a mosquito-borne virus belonging to the alphavirus genus of the *Togaviridae* family. CHIKF is characterized by the abrupt onset of high fever, headache, nausea, skin rash, myalgia and a characteristic arthralgia that can persist for weeks or even months (1, 2). Its name is a descriptive Kimakonde term and can loosely be translated as 'disease that bends up the joints', referring to the contorted posture of many of patients. The disease is usually self-limiting and rarely fatal, but the arthralgia can be extremely painful and debilitating. Severe complications are rare, but can include myocarditis, retinitis, hepatitis, acute renal disease, and neurological complications, such as meningoencephalitis, Guillain-Barré syndrome, paresis or palsies (brain damage resulting in muscle weakness or paralysis) (reviewed in (3)). Especially newborns and patients with underlying conditions are at risk for these severe complications, which can occasionally result in death. Maternal-fetal (vertical) transmission has been reported and often leads to neurological birth defects (4, 5). CHIKV likely originates from Africa, where it was first isolated at the Makonde plateau in Tanzania in 1952 (6). The virus subsequently spread to Asia (7) and in the next three decades caused several localized and limited outbreaks, as well as larger outbreaks in urban areas in India and other parts of Asia (reviewed in (8)). However, CHIKV remained a rather neglected pathogen and did not receive much attention from the media, medical, or scientific community. This changed when in 2004 a major outbreak started in Kenya (9), which spread to numerous islands in the Indian Ocean, India and other countries in southern Asia (1). By January 2005, CHIKV had reached the Comoros, and subsequently the French territory island of La Reunion, where it infected roughly a third of the island's population (at least 270.000 cases) and gained global attention (10, 11). Aided by trade-related traffic and infected (air) travelers, CHIKV continued to spread globally, and infected millions of people, mostly in India, Africa and South-East Asia (12, 13).

By the end of 2013, CHIKV had also crossed the Atlantic Ocean and reached the Caribbean, yet another area with an immunologically naïve population. CHIKV rapidly spread over many islands and territories in the region and caused over a million suspected and confirmed cases in the Americas in about a year's time, resulting in severe human suffering and economic damage (13, 14). Many islands in the Caribbean and the Indian Ocean region, such as the Seychelles and Maldives, are popular holiday destinations. Therefore, returning travelers brought home CHIKV to countries all over the world, including Japan, Canada, Australia, the USA and many European countries (15, 16). Also the Netherlands is receiving CHIKV-infected travelers, especially due to the ties with the Dutch Antilles and Suriname. Because CHIKV is not a notifiable disease in many countries, including the Netherlands, exact numbers remain

1

unclear. However, the amount of returning travelers is thought to be substantial, since already 181 CHIKV cases were laboratory-confirmed in the Netherlands from September to November 2014 (19). CHIKV infections are probably still underdiagnosed due to limited awareness clinicians (20). If an infected traveler arrives in a country where a competent mosquito vector is present, local (autochthonous) transmission can occur, potentially starting a new outbreak. Indeed, in 2007 a local outbreak was reported in the Emilia-Romagna region of Italy, involving over 200 cases (21, 22). This outbreak was caused by a returning traveler
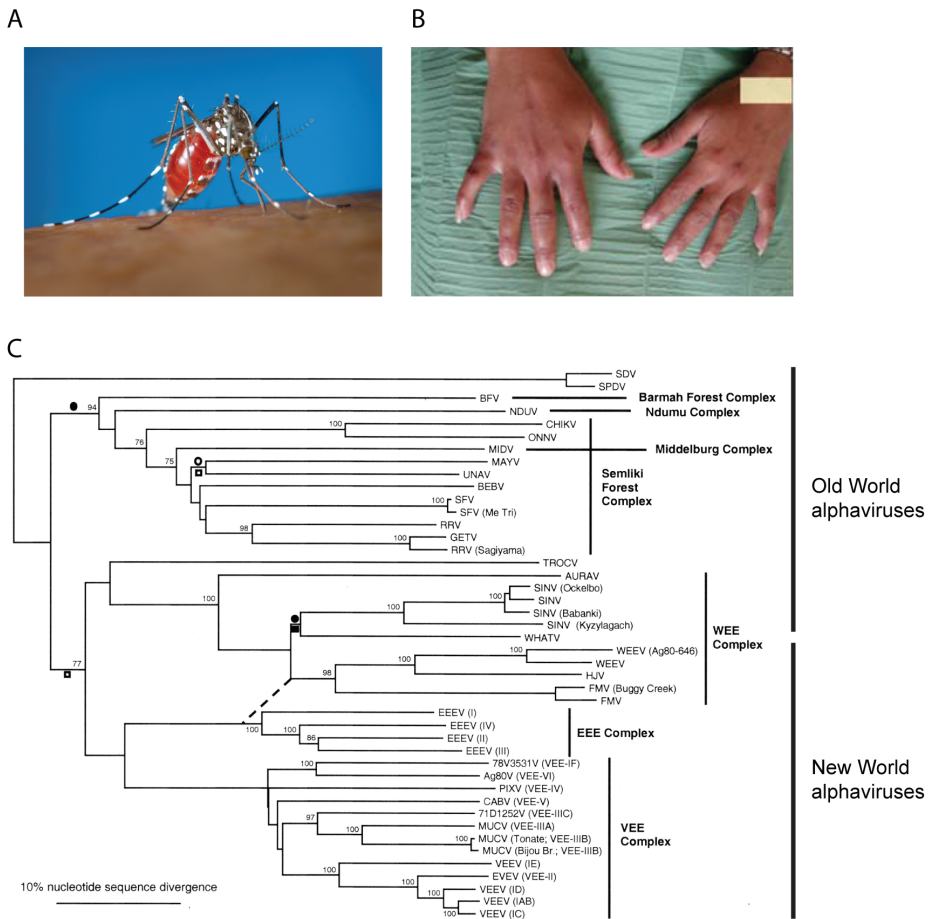
Figure 1. Chikungunya virus is an arthropod–borne virus belonging to the New World alphaviruses. (A) CHIKV is transmitted mostly by infected *Aedes* mosquitoes, especially *Aedes aegypti* and *Aedes albopictus* (depicted here). During the 2004 Indian Ocean outbreak CHIKV acquired a mutation in its glycoprotein (E1-A226V) that facilitated spread via *Aedes albopictus* (CDC/James Gathany). **(B)** Infection with CHIKV results in chikungunya fever, which is characterized by fever, headache, skin rash, joint swelling and arthralgia. Reprinted with permission from (17). **(C)** Phylogenetic tree of New and Old World alphaviruses. In addition, alphaviruses can be divided in different serological complexes based on antigenicity. CHIKV belongs to the Old World alphaviruses that are associated with arthralgia, whereas the New World alphaviruses are associated with encephalitis. Adapted from (18).

from India and supported by a local population of *Aedes (Ae.) albopictus* mosquitoes (22, 23). Local transmission in Europe was reported again in the summer of 2010 in France, when two young girls were found to be infected with CHIKV while they had not been out of the country recently (24, 25). Some years later, locally-acquired CHIKV infections were again reported from France (Montpellier, 2014) when 12 people living in the vicinity of a CHIKV patient that had returned from Cameroon (26, 27) became infected. The outbreak in the Caribbean (late 2013-present) greatly increased the number of CHIKV-infected travelers returning to the USA. Especially the southern USA hosts competent mosquito vectors, and it was therefore not surprising that local CHIKV transmission in the continental USA was reported from Florida in July 2014 (28). Since the start of the CHIKV epidemic in the Caribbean a relatively low number of local transmissions have been reported (11 cases), and it is not expected that this number will increase enormously. It is expected that CHIKV transmission in the USA will be similar to that of dengue virus (DENV), which causes sporadic local transmission but no large outbreaks (29) (although increasing numbers of CHIKV-infected travelers increase the likelihood). However, the risk of CHIKV becoming endemic in Latin America is very real (8). These countries host several competent mosquito vectors, together with a human population that is largely immunologically naïve and spends a lot of time outdoors or in rooms without window screens or air-conditioning, thus increasing their exposure to mosquitoes. In addition, the surveillance and diagnostic capacity in these countries is limited, paving the way for unhindered, initially unnoticed, outbreaks.

Based on phylogenetic analysis, three major CHIKV genotypes can be distinguished: West African, East/Central/South African (ECSA), and Asian (7). These names reflect their original geographic distribution, but the distribution of these CHIKV genotypes is no longer restricted to the areas they were originally named after. The genome sequences of these three genotypes differ about 3-5% from each other. The recent Indian Ocean and Indian strains form a monophyletic group within the ECSA lineage, dubbed IOL (Indian Ocean Lineage), of which some members acquired the E1-A226V mutation, and others did not (10, 30, 31).

CHIKV is the causative agent of the largest outbreaks caused by any alphavirus, resulting in an estimated 4-7 million cases in over 40 countries worldwide since 2004 (Figure 2). Other alphavirus family members include Sindbis virus (SINV), Semliki Forest virus (SFV), Ross River virus (RRV), Barmah Forest virus, o'nyong-nyong and Mayaro virus. These viruses are considered the 'Old World' alphaviruses, and are generally associated with arthralgia and myalgia (reviewed in (32)). In contrast, the 'New World' alphaviruses: Eastern, Western and Venezuelan equine encephalitis (EEEV, WEEV and VEEV) are mostly associated with encephalitis (33). SINV and SFV are well-studied model viruses within the alphavirus genus, but especially SINV is quite distantly related to CHIKV (Figure 1C). O'nyong-nyong is the alphavirus most closely related to CHIKV, and for a period was even thought to be a strain of CHIKV, but it was later shown to be genetically distinct and to have diverged probably thousands of years ago (7).

In total the alphavirus genus comprises ~30 virus species, which are able to infect a range of vertebrates (mammals, fish, birds etc.) as well as invertebrates. Most alphaviruses are arthropod-born, although the particular vector may differ from virus to virus. CHIKV is typically transferred by infected *Aedes* species, such as *Ae. aegypti and Ae. albopictus (35, 36)*. However, during the 2005 outbreak CHIKV acquired a mutation in its envelope protein (E1-A226V) that enabled a more efficient transmission by *Ae. albopictus* (37, 38). This mutation was acquired independently by different CHIKV lineages through convergent evolution (10, 39-42). *Ae. albopictus* is better known as the Asian tiger mosquito, and is an aggressive daytime biter that prefers urban areas (Figure 1B). In recent years, it has quickly spread throughout large parts of the world, including parts of Europe and the Americas (43). This - in combination with the acquisition of the A226V mutation by CHIKV – dramatically increased the epidemic potential of CHIKV in the early 2000s. Therefore it is worrisome that licensed vaccines or specific antiviral drugs to prevent or treat CHIKV infection are currently not available. CHIKF can only be treated symptomatically using analgesics, and protection from mosquito bites is the only way to prevent CHIKV infection. Research on this quickly spreading pathogen is hampered because CHIKV is a biosafety level 3 pathogen in most countries, including the Netherlands. In addition, it is considered a potential 'dual-use agent' by the Dutch government and is listed as a category C priority pathogen by the US National Institute of Allergy and Infectious Diseases (NIAID). This means that CHIKV is considered a pathogen
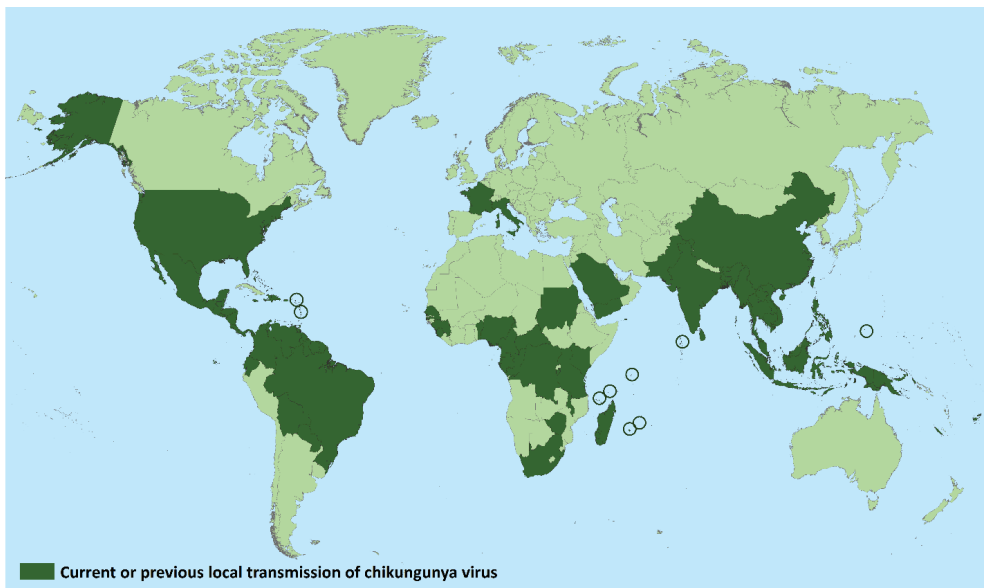
Figure 2. Geographic distribution of CHIKV. Prior to 2004, CHIKV was geographically restricted to Africa, India and South-East Asia. Adaptation to the tiger mosquito (*Ae. Albopictus*) and wide-spread distribution of that vector facilitated the dispersion of CHIKV across the globe. At present, cases have been reported in 101 countries and territories, divided over all inhabited continents. Local CHIKV transmission was reported in 44 countries or territories (indicated in dark green). Reprinted with permission from (34).

that could potentially be engineered for mass dissemination, and has the potential for high morbidity and mortality rates, resulting in a major health impact.

The CHIKV replicative cycle

Alphaviruses share a common genome organization and replication strategy (44, 45). SINV and SFV are well-studied members of the alphavirus genus, in part because they do not cause serious disease in humans. Studies on these viruses have yielded many important insights into the molecular details of alphavirus replication. The insights into the alphaviral replication cycle obtained using the SINV and SFV models often form the fundament on which hypotheses and further studies on CHIKV replication are based.

Alphavirus particles are spherical, enveloped and ~70 nm in diameter. The envelope is comprised of a host-derived lipid bilayer and trimeric spikes consisting of E2-E1 glycoprotein heterodimers. The envelope surrounds a ~40 nm capsid core containing the viral RNA genome (Figure 3). The replicative cycle starts when the virion attaches to a host cell using E2 and one or more cellular receptors (Figure 5) (44, 45). For many alphaviruses, including CHIKV, these receptors have not been (convincingly) identified. Laminin was proposed to be a receptor during SINV entry, as well as heparin sulphate (46, 47). The cellular receptor needed for SFV remains unidentified thus far. After internalization of the viral particle, glycoprotein E1 mediates low-pH induced fusion, resulting in the release of the nucleocapsid into the cytoplasm (48, 49). Replication takes places in invaginations of the plasma membrane or modified endosomal/lysosomal membranes, termed cytopathic vacuoles CPV) (50-52). Alphaviruses possess a ~12 kb positive-strand RNA genome, that is capped and polyadenylated, and contains two open reading frames (ORFs) encoding two polyproteins (Figure 4). The first polyprotein can be directly translated from the incoming genome and contains the four non-structural proteins (nsP1-nsP2-nsP3-nsP4) (44, 45). Most CHIKV strains
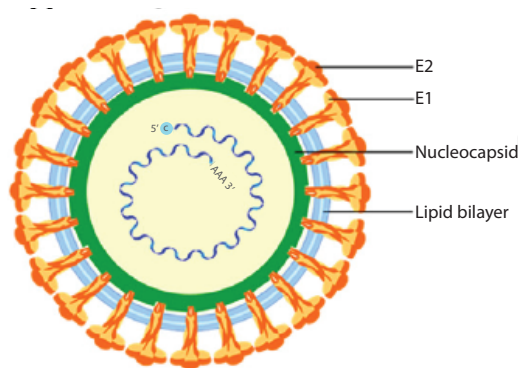
Figure 3. Schematic overview of a CHIKV particle. The ~12 kb single stranded, positive-sense RNA genome is encapsidated and enveloped by a host-derived lipid bilayer. This lipid bilayer contains 80 glycoprotein spikes composed of E1 and E2 heterotrimers. The spikes facilitate attachment and entry via low pH-dependent endocytosis. The viral genome is capped and polyadenylated and can be directly translated into the viral non-structural proteins upon its release in the cytoplasm. Adapted from (57).

have an opal stop codon at the end of the nsP3-coding region and occasional translational read-through results in production of nsP4 (53, 54). A portion of the four nsPs assemble into the replication complex (RTC), presumably together with host factors, whereas another subset of the nsPs is associated with other compartments of the cell, performing additional functions (44). Alphavirus nsP1 anchors the RTC to the plasma membrane and contains the methyl- and guanylyltransferase activities that are needed to cap the (sub)genomic RNA (55, 56).

Alphavirus nsP2 has protease and helicase activity, and nsP2 of the Old World alphaviruses induces transcriptional and translational host shut off (58). The exact function of nsP3 has not been elucidated yet, but it contains a macro domain that can bind ADP-ribose, DNA and RNA (59), a zinc-binding domain (60), and an unstructured region that binds to cellular factors, such as G3BP (61-63). NsP4 is the RNA-dependent RNA-polymerase (RdRp). Proteolytic cleavage by nsP2 releases the individual nsPs from the polyprotein. The extent to which the non-structural polyprotein is proteolytically processed determines the polarity of the newly synthesized RNA. RTCs that contain uncleaved nsP123 produce only negative strand RNA. Proteolytic cleavage of the nsP1-2 site results in complexes that produce both + and – RNA, whereas RTCs containing completely processed nsPs exclusively produce +RNA (64).

The structural polyprotein (C-E3-E2-6K-E1) is produced from a subgenomic RNA that is transcribed under control of the 26S subgenomic promoter in the minus strand (45, 65). The subgenomic RNA of most alphaviruses includes a translational enhancer sequence, which allows the continued translation of structural proteins when cellular translation is blocked (induced by nsP2 and/or stress granule formation) (66-68). This translational enhancer sequence has not been identified for CHIKV. The virus may contain one, as it is able to produce structural proteins after host shut-off has been induced (69). However, the characteristic stemloop structure has not been found in the 5' region of the subgenomic RNA. Assembly of alphavirus particles begins when capsid proteins bind genomic RNA, thus forming the nucleocapsid in the cytoplasm (44). The viral RNA is encapsidated by 240 copies of the capsid protein, which contains a putative coiled-coil α-helix, needed for core assembly (70). The completely assembled nucleocapsid binds to the cytoplasmic tails of the viral glycoprotein spikes embedded in the plasma membrane and buds through that membrane to acquire a lipid envelope containing E1-E2 trimers (71, 72). Glycoprotein E3 is not associated with mature virions, but likely prevents premature fusion activity and E1 trimerization by binding to the E2-E1 dimer (73-75).
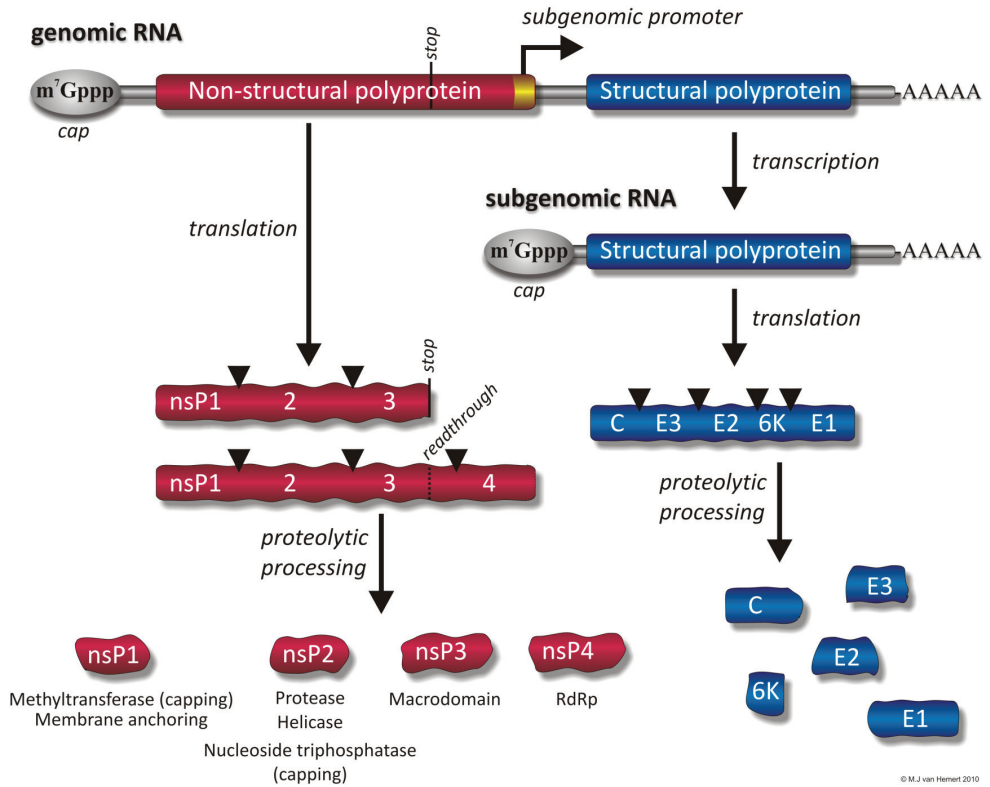
Figure 4. Genome organization of chikungunya virus. The CHIKV genome is ~12 kb in length, capped and polyadenylated. It contains two open reading frames, which encode the non-structural and the structural proteins, respectively. The first open reading frame can directly be translated from the incoming genome and proteolytic processing produces the individual non-structural proteins that subsequently assemble into the viral replication complex. Transcription of the genomic RNA results in a double-stranded replication intermediate. This replication intermediate contains a subgenomic promoter that directs the synthesis of the subgenomic mRNA from which the second open reading frame, encoding the structural proteins, is translated. The structural polyprotein is processed by a combination of viral and host proteases, generating the mature structural proteins.
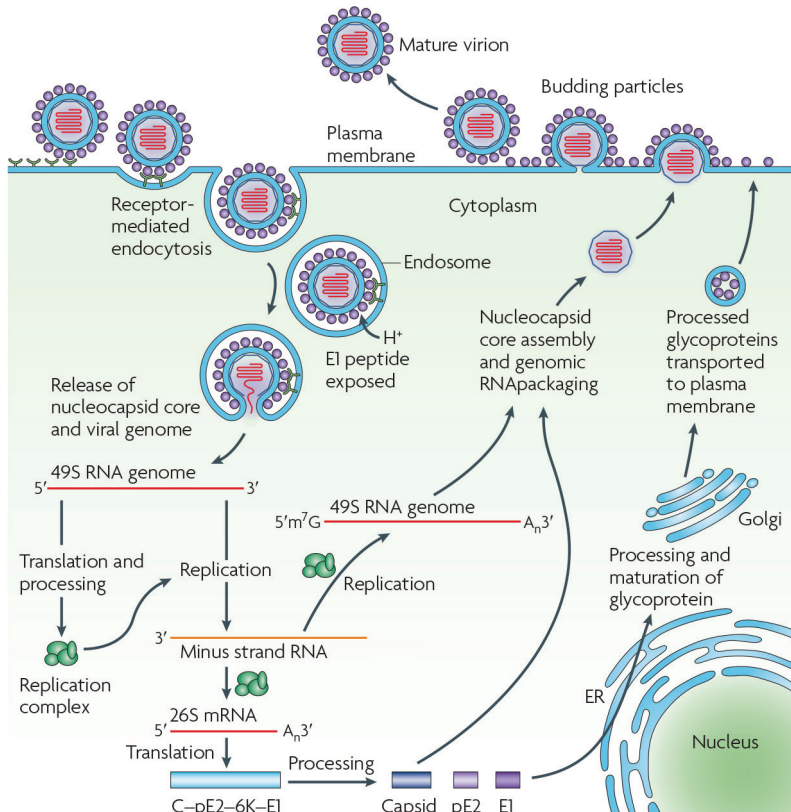
Figure 5. Replicative cycle of chikungunya virus. The CHIKV replicative cycle starts when the virus particle attaches to the host cell using its E2 glycoprotein and a thus far unidentified cellular receptor. The virion is internalized using receptor-mediated endocytosis, the local low pH triggers a conformational change, which results in fusion with the cellular membrane, and the viral genome is released in the cytosol. The 5'-proximal ORF of the incoming genome can directly be translated into the non-structural polyprotein, and proteolytic processing yields the four individual nsPs, which assemble into the viral replication complex. This replication complex initially produces negative-sense RNA which can be used as a template to produce more genomic RNA. It also contains a subgenomic promoter to generate a subgenomic mRNA for expression of the structural proteins. The structural polyprotein is proteolytically processed by both viral and host proteases. The glycoprotein precursors are further processed in the endoplasmatic reticulum (ER) and Golgi system. The mature glycoproteins form E2-E1 heterodimers which gather at the cell surface as trimeric spikes. The viral RNA is encapsidated by capsid proteins to form nucleocapsids, which interact with the cytoplasmic tails of the glycoprotein spikes to trigger budding. Adapted from (76).

The host (immune) response to CHIKV – pathogenesis and chronic disease

CHIKV is able to infect a wide range of cell lines, including hamster, human, monkey, and insect cells. Permissive cells include epithelial cells, endothelial cells, fibroblasts, and monocyte-derived macrophages (*in vitro*) (77). During a natural infection, CHIKV is transmitted via the bite of an infected mosquito. It replicates initially in the skin, and subsequently spreads to the joints, muscles and organs via the blood stream (Figure 6) (78-80). CHIKV infection results in a brief viraemia, usually lasting 5-7 days, which is controlled primarily by interferon (IFN) α and antibodies (Figure 7) (81-84). The innate immune response to CHIKV typically includes elevated levels of IFN-α, INF-β, IFN-γ, monocyte chemoattractant protein 1 (MCP-1), interleukin (IL)-1β, and IL-6 (85, 86). Like other alphaviruses, CHIKV induces a strong, protective IFN response, and mice lacking the IFNα receptor are highly susceptible to CHIKV infection (79). CHIKV has been described to counteract the type I IFN response through various mechanisms, including transcriptional and translational host shut off, which renders the host cell unable to respond to IFN (69, 87-89). In addition, nsP2 interferes with the JAK-STAT signaling pathway and blocks STAT phosphorylation (90). Besides induction (and suppression) of innate immune responses, CHIKV infection also induces an adaptive immune response, although the role of T cells in controlling CHIKV infection is less well characterized. In the sera of acutely infected patients elevated levels of activated CD4+ and CD8+ T cells were detected, as well as NK and dendritic cells (91-93). Acute lymphopenia (abnormally low levels of lymphocytes in the blood) is often observed in CHIKV-infected patients (94). Since CHIKV does not infect T and B cells, this most likely is an indirect effect caused by the IFN response, which results in both cell death and migration of lymphocytes from the blood stream into tissue (95).

Generally, chikungunya fever is regarded as a self-limiting disease, typically lasting from a few days to a couple of weeks. However, many patients report persisting joint pain (polyarthralgia and/or polyarthritis) that can last up to months or even years. The chronic joint pain often presents as relapses, which can be extremely painful and debilitating. Especially elderly people are at risk for developing such long-term symptoms (86, 91, 96-99). These persisting pathologies illustrate that - despite low mortality rates – CHIKV is a serious pathogen that causes severe morbidity. The persistent arthralgia can seriously affect the quality of life of a large group of patients.

Besides CHIKV there are several other alphaviruses that can cause chronic joint pain, although often less severe than CHIKV. For example, also SINV, RRV, Barmah Forest virus, o'nyong-nyong and Mayaro virus were described to cause rheumatic symptoms (reviewed in (32, 100)). Chronic alphaviral rheumatic disease is thought to arise from inflammatory responses to virus in joint tissues, which persists despite robust antiviral immune responses. The exact mechanism behind this prolonged arthralgia has not been elucidated, yet several possible mechanisms have been proposed, including (I) an autoimmune response, (II) tissue damage caused by inflammation, and (III) low levels of persistent replication. It has been suggested repeatedly that auto-immune responses are responsible for the CHIKV-induced arthralgia, but thus far convincing evidence supporting this hypothesis has not been obtained. A

1
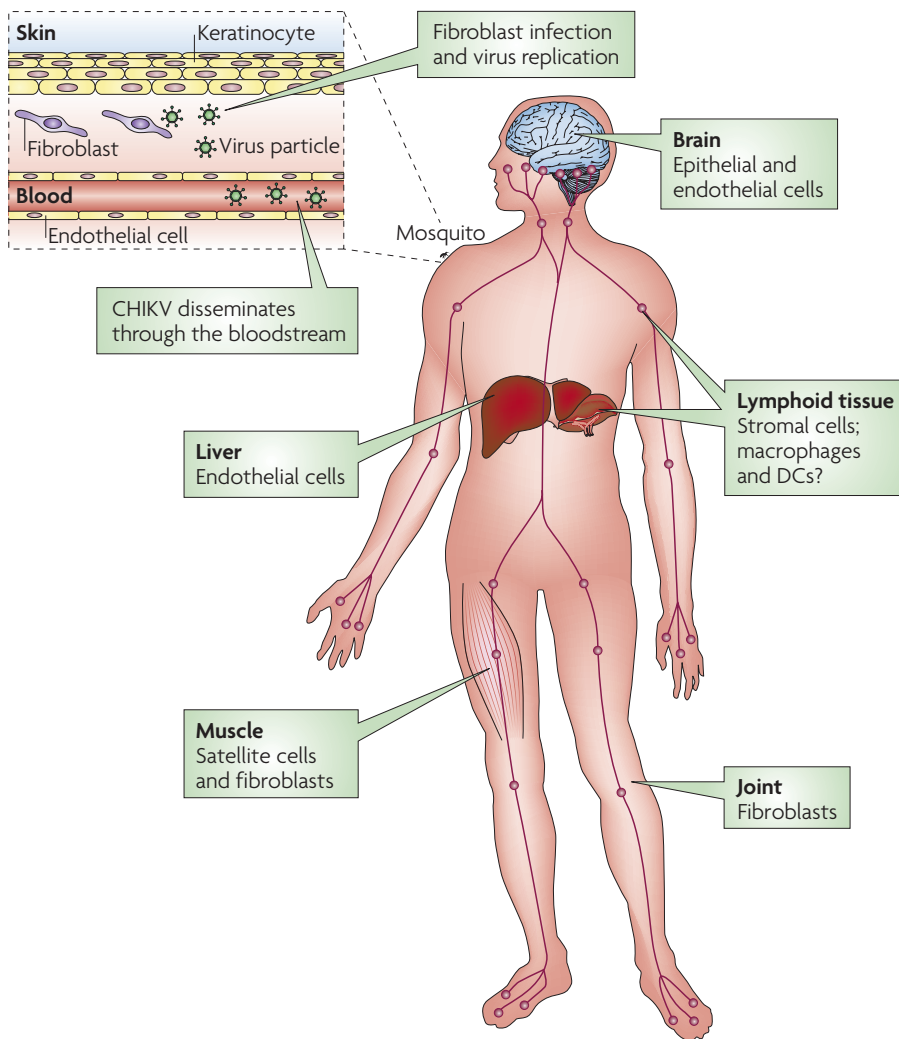
Figure 6. Dissemination of chikungunya virus. The viral replicative cycle starts when a CHIKV-infected mosquito bites a susceptible host. Virus particles are released with the mosquito's saliva and infect fibroblasts in the skin. The virus replicates locally and newly formed particles are released into the bloodstream, enabling their spread to various organs, muscle and joint tissue. In rare cases the virus can cross the blood-brain barrier and cause encephalitis, which happens mostly in new-borns. Reproduced with permission from (76).

number of research groups have attempted but failed to detect autoimmune or rheumatoid markers in chronic patients (99, 101, 102), with the exception of one study on La Reunion (103). However, multiple arthritogenic viruses have been shown to cause inflammation by replicating within joint tissues, which is mediated primarily by infiltrating macrophages and the complement system (100, 104, 105). Several studies have suggested that CHIKV is able to establish a chronic infection in joint cells. For example, viral antigen was found in satellite cells in a muscle biopsy three months after initial infection, and it was confirmed that CHIKV could replicate in cultured primary human satellite cells (80). In another patient, viral RNA and proteins were found in perivascular synovial macrophages 18 months after onset of the disease (91). This suggests that CHIKV may invade and persistently infect joint tissues.

Macrophages likely are the main cellular reservoir during persistent infection, and macrophage infiltrates were found in affected joints, suggesting they are involved in pathogenesis (104, 106). Clodronate is a macrophage-specific inhibitor that can specifically deplete macrophages from organs and tissues. Treatment of CHIKV-infected mice with clodronate reduced foot swelling (83). However, clodronate treatment prolonged CHIKV viraemia, indicating that macrophages also play a role in clearance of the virus (83). In conclusion, these studies indicate that macrophages are a target of infection, promote viral clearance and are involved in the development of rheumatic disease.

Strikingly, joint inflammation does not occur simultaneously with the peak of viraemia, but the maximum joint swelling occurs after the virus has already been cleared from circulation, around 4 d.p.i. in animal experiments (83, 107). Knockout mice lacking T and B lymphocytes needed for adaptive immunity (RAG2-/-) developed persistent viraemia, but no signs of inflammation, suggesting a key role for humoral responses during CHIKV infection. CD4-/- and CD8-/- mice experienced normal viraemia, but the peak of joint swelling, infiltrates and tissue damage was reduced in the CD4-/- but not CD8-/- mice, indicating that CD4+ T cells are involved in CHIKV-induced joint pathology (93).

Taken together, the experimental field of CHIKV-induced rheumatic disease is still immature and various controversial findings and conflicting results have been reported. Our current knowledge is by far not sufficient to understand, let alone prevent or treat this CHIKV-induced pathology. However, increasing numbers of studies are performed to identify the mechanism(s) behind rheumatic disease caused by alphaviruses, and slowly more light is shed on this interesting and important clinical disease sign.

CHIKV diagnosis and misdiagnosis

CHIKV can be diagnosed using several laboratory tests, including virus isolation, real time (RT-)PCR and serological testing. These tests detect either virus, viral RNA, virus-specific IgM and IgG or neutralizing antibodies. Virus isolation from patient material is the most definitive diagnostic method. However, infectious virus can usually be isolated only within the first three days after the onset of symptoms, requires a BSL-3 laboratory and may take up to one or two weeks. RT-PCR is a quick diagnostic tool that is highly sensitive and specific, but is only

suitable during the first 7 days after onset of symptoms and requires reagents and equipment that may not be available in diagnostic laboratories throughout the world. After 7 days, CHIKV infection can be detected using IgM and IgG serology, however, these tests are often unable to differentiate between a recent past infection and an acute infection. In addition, cross-reactivity with other alphaviruses can occur.

A laboratory-confirmed CHIKV diagnosis is important, as there are many other diseases causing symptoms like fever, headache, skin rash and myalgia, with or without arthralgia. For example, CHIKV infections often occur in areas where DENV is also endemic, and both viruses initially cause very similar symptoms. Unfortunately, both viruses occur in regions where the capacity to perform differential diagnoses is often limited. In retrospect, many cases that were attributed to DENV infections, may very well have been CHIKV infections, making it likely that the incidence of CHIKV disease is much higher than reported (108). In addition to cases of mistaken identity, CHIKV-DENV co-infections have been reported (109-113), although it remains unclear how this impacts the replication and pathogenesis of both viruses. Malaria is another infectious agent that often occurs in areas where people are at risk of contracting CHIK fever, and generally can give rise to similar symptoms.
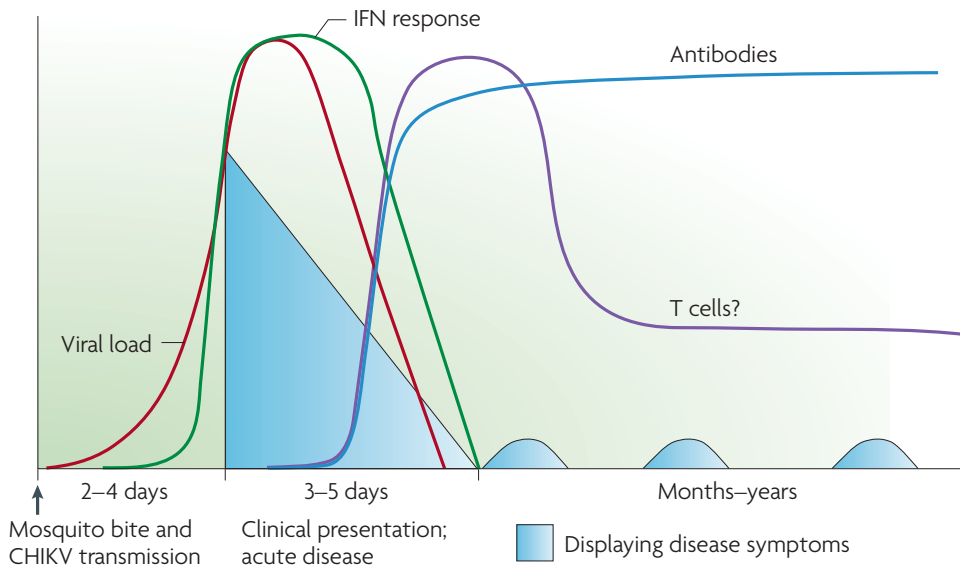
Figure 7. Host immune response to chikungunya virus infection. CHIKV infection typically induces a strong, protective IFN response, which controls the viral load together with the humoral (antibody) response. The role of T lymphocytes during CHIKV replication is less well characterized. CHIKV-infected patients display an increased T cell activation, but lymphopenia (depletion of lymphocytes) is also commonly observed. CHIKV infection results in CHIKV-specific IgG and IgM, which can typically be detected from 7 after onset of symptoms. The acute phase of CHIKV infection usually resolves after ~7-10 days, but relapses (arthralgia) are often reported. Reproduced with permission from (76).

Research tools

CHIKV research tools are indispensable in order to increase our understanding of this important human pathogen. The virus was regarded as rather obscure for quite a while, so many research tools have only been developed in the last decade, when the impact of CHIKV on health and society became clear. Obviously, the development of CHIKV-specific tools greatly benefited from the knowledge and tools created for the well-studied SINV and SFV alphaviruses. Research tools include antibodies, in vitro assays, animal models, virus-like particles, replicons and infectious cDNA clones.

Full-length cDNA clones from which infectious viral RNA can be transcribed are invaluable tools to study many aspects of the viral life cycle, including virus-host interactions, attenuation/virulence markers and immunogenicity. Such clones enable manipulation of the viral genome through reverse genetics, allowing for example the construction of a mutant virus expressing a reporter gene to facilitate the quantification of virus replication. Replicons are self-replicating RNA molecules that encode the CHIKV replication machinery (nsPs) but lack the structural protein gene, and therefore infectious particles cannot be produced. CHIKV RNA replicons can be handled at the more convenient biosafety level 2 to study certain aspects of CHIKV replication, such as translation, polyprotein processing and RNA synthesis. Replicon-based assays are also useful to exclude the involvement of antiviral compounds or host factors in entry or assembly/release. Several replicons and full-length clones have been created for CHIKV, including some based on the sequence of the La Reunion outbreak strain (LR2006 OPY1) (62, 69, 114-117). These CHIKV cDNA clones often contain a reporter gene under control of a subgenomic promoter. However, most of these infectious clones are based on the sequence of a single genome of a clinical isolate, which may have adapted to the specific patient or to cell culture passaging during isolation procedures. Therefore it is possible that different infectious cDNA clones yield viruses with different properties. It would be prudent to repeat key experiments with several different virus isolates.

Host factors in CHIKV replication

RNA viruses are highly dependent on the exploitation and subversion of host proteins, structures and pathways to facilitate their replication. For example, viruses depend on cellular receptors and (clathrin-mediated) endocytosis for entry, the translational machinery of the host cell to produce viral proteins, and the cellular plasma membrane to acquire the viral envelope during budding. Furthermore the anabolic capacity of the host cell is used as a source of NTPs, amino acids and lipids, and cellular factors are part of the RNA replication machinery. To facilitate their replication, viruses manipulate many cellular pathways, including stress and antiviral responses, to create a cellular environment that is optimally suited to their specific needs. Therefore it is of great importance to understand the interplay between viral proteins and host factors, as this will help us to understand how the virus can influence the host cell and vice versa. In recent years, many efforts have been made to identify cellular factors involved in +RNA virus replication and a multitude of (potentially)

involved genes have been discovered. However, only a handful of the host factors involved in CHIKV replication have been identified (118-122). Their specific role, and the specific step(s) of the viral replication cycle in which they are involved, also remains largely unclear. Identification and characterization of the cellular factors needed for CHIKV replication is a crucial step to improve our understanding of this important human pathogen. In addition, knowledge of host factors co-opted by the virus can potentially be used to counter emerging antiviral resistance. Most +RNA viruses lack proofreading capability and can therefore rapidly acquire mutations that provide resistance against specific antiviral treatment. Traditional approaches to develop antiviral drugs have mostly focused on viral proteins, but antiviral strategies that target cellular factors required for virus replication could reduce the risk of the development of viral drug resistance, as host factors are far less likely to change/mutate. An additional advantage of targeting cellular factors instead of a viral protein is that the antiviral agent is more likely to be effective against a wide(r) range of pathogens/viruses. Cellular factors involved in CHIKV replication can thus provide interesting starting points for novel antiviral strategies, besides the fact that their identification sheds more light on the replication cycle of this virus.

There is a range of techniques available to identify host factors involved in viral replication. The first host factors were identified by studying physical interactions between viral and host proteins using co-immunoprecipitation and antisera specific to viral and host proteins. At present, roughly the same technique is still being used, often aided by viral proteins equipped with affinity tags and the analysis of pull-down samples by mass spectrometry, which greatly increases the number of interaction partners that can be identified. Other techniques to study molecular interactions between viral and host proteins include yeast two-hybrid (Y2H) screening, virus overlay protein binding assay (VOPBA), tandem affinity purification, and glutathione S-transferase (GST) protein purification. However, interactions identified in *in vitro* assays do not necessarily reflect functional *in vivo* interactions. In addition, weak or transient interactions may be missed. Most of the above-mentioned assays are limited to direct protein-protein interactions, meaning that host proteins that are part of a virus/host-protein complex but lacking a direct physical interaction with viral proteins will be missed, as well as proteins that exert their function during viral replication in an indirect manner. The discovery of RNA interference (RNAi) by Fire and Mello in 1998 and the adaptation of its application to high-throughput screening formats started a revolution in the genomics field, as it allowed genes to be specifically silenced at a large scale (123). The advantage of RNAi is that it can be used to identify functional interactions between proteins that directly physically interact with viral proteins, as well as host proteins that affect replication indirectly, e.g. because they are part of viral replication complexes, bind to viral RNA, or are involved in signaling pathways that affect viral replication. RNAi screens enable large-scale loss-of-function studies in cell culture, and have been performed in recent years to identify cellular factors involved in the replication of a variety of +RNA viruses, including hepatitis C virus (HCV) (124-127), West Nile virus (WNV) (128), yellow fever virus (YFV) (129) and DENV (130,

131). These studies have provided valuable insights into the replicative cycle of these viruses, and the cellular proteins and pathways involved.

Previous efforts to identify host factors involved in alphavirus replication included two genome-wide RNAi screens aimed at identifying factors involved in SINV entry (132, 133), a SINV *in vivo* RNAi screen (134), a study of cellular components of the SFV replication complex (119), as well as a genome-wide RNAi screen aimed at the identification of host factors involved in SFV replication (135). Other studies have sought to identify interaction partners of SINV nsP2, -3 and -4 by applying tagged nsPs, expressed by plasmids or recombinant viruses (136-138). For CHIKV mainly differential proteome analyses (121, 139-144) have been performed, in addition to a Y2H screen (122). However, differential proteome analysis is not a very suitable technique to identify host factors, since it mostly aims to detect cellular changes upon infection by monitoring changes in cellular protein abundance. Such changes are often linked to antiviral responses or host shut-off. Targets identified in CHIKV proteomic studies generally cluster in distinct functional pathways/groups, including energy metabolism, transcription, translation, stress response and apoptosis (summarized in (142, 145)). However, the sets of potential host factors identified in the above-mentioned studies share only a very limited overlap. This might be due to the use of different viruses, expression systems, cell lines, experimental conditions, and/or differences in data interpretation. Some hits were found in more than one screen, for example, nsP2 of both SINV and CHIKV was found to bind hnRNP K and vimentin (122, 136, 146). A serious drawback of many of the studies summarized above is that the importance of most of the (potential) host factors identified has not been validated using an alternative technical approach. Consequently the presence of false-positive hits cannot be excluded, which may for example be caused by off-target effects, aspecific binding of host proteins to the tagged viral protein, or general effects on the cell's ability to support viral replication.

In summary, although in recent years many efforts have been made to identify host factors that play a role during CHIKV replication, the involvement of only a relatively small number of proteins was confirmed and systematic large-scale RNAi screens have not been reported for CHIKV. The number of host factors whose precise function is known is even smaller. Further elucidating the replicative cycle of this increasingly important human pathogen will aid us in developing antiviral strategies, thus providing means to combat the extensive socio-economic burden CHIKV is currently causing in large parts of the world.

1

Outline of this thesis

In this thesis the interplay of CHIKV with cellular (host) factors involved in its replication is addressed. An in-depth understanding of the interactions between the viral proteins and those of their host within the infected cell is required for the elucidation of molecular mechanisms underlying viral replication. A variety of proteins and pathways involved in CHIKV replication were identified in this thesis, and the role of a selection of those is described. First, the construction and characterization of a novel synthetic CHIKV full-length cDNA clone is described in **chapter 2.** The CHIKV genome sequence of this construct was based on the consensus sequence of CHIKV strains containing the A226V mutation, rather than on the genome of a single isolate. The virus derived from this clone is a valuable tool to study many aspects of the viral replicative cycle, including virus-host interactions. In **chapter 3** the synthetic reporter gene-expressing virus described in chapter 2 was used to screen a siRNA library targeting the human kinome, aiming to identify cellular kinases involved in CHIKV replication. We identified dozens of cellular factors and pathways that are potentially involved in CHIKV replication and validated a selection of these hits using a secondary siRNA screen. **Chapter 4** describes the response of the p38 MAPK and MEK/ERK signaling pathways in CHIKV-infected human cells. In contrast to the distantly related alphavirus VEEV, CHIKV does not induce MEK/ERK signaling, nor is its replication affected by either inhibition or stimulation of this signaling cascade. **Chapter 5** describes the unexpected proviral role of stress granule components G3BP1 and G3BP2 early during CHIKV infection. Stress granules are cellular protein-mRNA aggregates formed in response to stress, such as viral infection. Generally, their formation is considered to be part of an antiviral response, inhibiting viral replication. This chapter describes G3BP1- and G3BP2-containing granules that are formed in response to CHIKV infection, but differ from *bona fide* stress granules in composition, morphology and behavior. We demonstrate that the G3BPs are likely needed for the switch from translation to amplification of the CHIKV genome. In **chapter 6** the inhibitory effect of a RIG-I agonist (5'pppRNA) on CHIKV and DENV replication is described. A low, non-cytotoxic dose of 5'pppRNA stimulates RIG-I and leads to a robust antiviral response, which is dependent on an intact RIG-I/MAVS/TBK1/IRF3 signaling axis but not on the type 1 IFN response. This might open up therapeutic options against these two important human pathogens. Finally, **Chapter 7** discusses the findings described in this thesis, and places them in a broader context regarding the existing knowledge about alphaviruses and chikungunya virus.

2.

Characterization of synthetic Chikungunya viruses based on the consensus sequence of recent E1–226V isolates
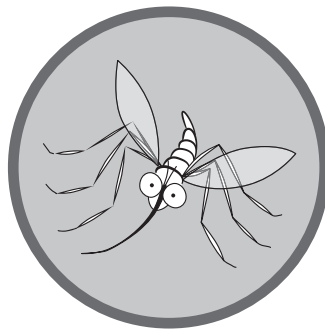
Florine E.M. Scholte[1], Ali Tas[1], Byron E.E. Martina[2], Paolo Cordioli[3], Krishna Narayanan[4], Shinji Makino[4], Eric J. Snijder[1], and Martijn J. van Hemert[1*]

[1]Molecular Virology Laboratory, Department of Medical Microbiology, Leiden University Medical Center, Leiden, The Netherlands; [2]Department of Viroscience, Erasmus Medical Center, Rotterdam, The Netherlands; [3]Istituto Zooprofilattico Sperimentale della Lombardia e dell'Emilia Romagna, Brescia, Italy; [4]Department of Microbiology and Immunology, University of Texas Medical Branch, Galveston, Texas, USA.

ABSTRACT

Chikungunya virus (CHIKV) is a mosquito-borne alphavirus that re-emerged in 2004 and has caused massive outbreaks in recent years. The lack of a licensed vaccine or treatment options emphasize the need to obtain more insight into the viral life cycle and CHIKV-host interactions. Infectious cDNA clones are important tools for such studies, and for mechanism of action studies on antiviral compounds. Existing CHIKV cDNA clones are based on a single genome from an individual clinical isolate, which is expected to have evolved specific characteristics in response to the host environment, and possibly also during subsequent cell culture passaging. To obtain a virus expected to have the general characteristics of the recent E1-226V CHIKV isolates, we have constructed a new CHIKV full-length cDNA clone, CHIKV LS3, based on the consensus sequence of their aligned genomes. Here we report the characterization of this synthetic virus and a green fluorescent protein-expressing variant (CHIKV LS3-GFP). Their characteristics were compared to those of natural strain ITA07-RA1, which was isolated during the 2007 outbreak in Italy. In cell culture the synthetic viruses displayed phenotypes comparable to the natural isolate, and in a mouse model they caused lethal infections that were indistinguishable from infections with a natural strain. Compared to ITA07-RA1 and clinical isolate NL10/152, the synthetic viruses displayed similar sensitivities to several antiviral compounds. 3-deaza-adenosine was identified as a new inhibitor of CHIKV replication. Cyclosporin A had no effect on CHIKV replication, suggesting that cyclophilins -opposite to what was found for other +RNA viruses- do not play an essential role in CHIKV replication. The characterization of the consensus sequence-based synthetic viruses and their comparison to natural isolates demonstrated that CHIKV LS3 and LS3-GFP are suitable and representative tools to study CHIKV-host interactions, screen for antiviral compounds and unravel their mode of action.

2

INTRODUCTION

Chikungunya virus (CHIKV) re-emerged in 2004 and has caused unprecedented outbreaks in Asia and Africa since 2005. The estimated number of cases exceeds 2 million and over a thousand infected travelers have returned to Europe and the USA since 2006 (15, 147). CHIKV generally causes a fever that resolves within several days, a maculopapular rash, and a characteristic arthralgia that can be extremely painful and may persist for months. During the recent outbreaks also more severe clinical manifestations have been reported occasionally, such as neurological complications and even deaths, usually in the elderly, patients with underlying conditions, and newborns (148, 149). A licensed vaccine or specific antiviral therapy are currently not available.

CHIKV is an alphavirus with an 11.7 kb positive-stranded RNA genome that contains two open reading frames (ORFs). The 5' ORF encodes the nonstructural polyproteins P123 and P1234. The latter results from translational read-through of an opal termination codon that is present at the end of the nonstructural protein (nsP) 3 coding sequence of most CHIKV isolates. Assuming that CHIKV follows the typical alphavirus life cycle, proteolytic processing of the nonstructural polyproteins by the protease domain in nsP2 will ultimately lead to the release of nsP1, nsP2, nsP3, and nsP4. These nsPs and their precursors possess a variety of functions and the enzymatic activities, including protease, helicase, methyltransferase, and RNA-dependent RNA polymerase (RdRp) activity that drive CHIKV replication (44). In addition to replication of its genomic RNA, CHIKV also transcribes a subgenomic (sg) RNA encoding a precursor polyprotein that is processed by viral and cellular proteases into the structural proteins C, E3, E2, 6K and E1. CHIKV nsPs will - presumably together with host factors - assemble into replication and transcription complexes (RTCs) that associate with membrane structures derived from the plasma membrane and/or endosomes, as observed for other alphaviruses (44, 51, 52).

The CHIKV strains that emerged during the 2005-2006 outbreaks had acquired a mutation (A226V) in the E1 envelope glycoprotein, which facilitated transmission of the virus via a new vector, the Asian tiger mosquito *Aedes albopictus*, and consequently dramatically increased the epidemic potential of CHIKV (10, 37). Later studies suggested that recent Indian and Indian Ocean epidemics have emerged separately as the result of at least three independent events, and that convergent evolution of East-Central-South African lineage strains in different geographical regions ultimately led to the emergence of strains with the A226V substitution in E1 (39, 40, 42, 150). More recently, other amino acid positions and epistatic interactions were also shown to play an important role in the emergence of these new CHIKV variants, which are now even replacing endemic strains that have been circulating in Asia for decades (151). *Aedes albopictus* also thrives in more temperate climates and its geographical distribution has rapidly expanded. Over the past decades, parts of southern Europe and large areas of the USA have been invaded by this mosquito, providing imported cases of CHIKV with a competent mosquito vector, thus paving the road for outbreaks in non-endemic-areas such as the USA and Europe. Indeed, autochthonous infections have been reported from Italy in

2007 and France in 2010 (22, 25). The recent and ongoing CHIKV outbreaks are characterized by their rapid geographical spread, high numbers of infected people and high morbidity, emphasizing the need to gain more insight into the replicative cycle of this important human pathogen.

Infectious cDNA clones of viruses have become invaluable tools that allow reverse genetics studies to elucidate the contribution of specific amino acids or RNA structures to viraemia, virulence, antigenicity, replication kinetics, interactions with host factors, adaptation to new vectors, and many other aspects of the viral life cycle. The use of cDNA clones is also instrumental in mechanism of action studies to pinpoint the viral target of antiviral compounds by selecting for and genotyping compound-resistant viruses, followed by reverse engineering of the identified mutations to assess their individual phenotypic contribution to resistance. Finally, the generation of cDNA clones of reporter viruses, like those expressing green fluorescent protein (GFP), greatly facilitates high throughput screening, e.g. for antiviral compounds or host factors that affect replication.

Several CHIKV cDNA clones have been constructed in the past, which - except for the West African lineage strain 37997 strain that was isolated from a mosquito - were all based on clinical isolates from infected humans (93, 114-116, 152-154). Each natural isolate is expected to have evolved its own specific characteristics in terms of sequence, virulence and virus-host interactions as a result of specific selective pressures within the infected host (tissue) and possibly also during subsequent passaging in cell culture. Intrahost evolution and quasispecies diversity is expected to be substantial, especially compared to the relatively low level of interhost variation when the consensus sequences of CHIKV genomes isolated from different hosts are aligned. The low level of interhost variation is a typical trait of arboviruses, due to evolutionary constraints imposed by the alternating replication in vertebrate and arthropod hosts. A recent study on the distantly related Ross River virus indeed reported a high level of intrahost diversity (155). The existing CHIKV molecular clones can be considered to represent a single individual genome (or fragments of several individual genomes) out of the whole spectrum of viruses present in the CHIKV quasispecies population that has been shaped by intrahost evolution and probably a complex set of environmental factors. In contrast, most deposited CHIKV genome sequences represent the consensus (or master sequence) of a viral quasispecies population.

To obtain a virus that - in terms of virulence, sensitivity to antiviral compounds, and CHIKV-host interactions - is expected to have the general characteristics of the E1-226V CHIKV strains that were circulating during the 2005-2009 outbreaks, we have constructed a completely synthetic CHIKV cDNA clone based on the consensus sequence of the aligned genomes of these recent isolates. This new infectious clone, CHIKV LS3 (Leiden Synthetic 3), and a variant that expresses the eGFP reporter gene under control of a duplicated subgenomic promoter (CHIKV LS3-GFP), were created by custom DNA synthesis.

The properties and replicative cycle of the new synthetic viruses were characterized in detail, and comparison with a field isolate (ITA07-RA1) from the 2007 CHIKV outbreak in Italy

demonstrated that they have similar characteristics. The sensitivity of LS3 to a number of antiviral compounds was compared to those of ITA07-RA1 and clinical isolate NL10/152. All compounds tested had a similar antiviral activity against LS3 and the natural isolates. These experiments also identified 3-deaza-adenosine as a novel inhibitor of CHIKV replication. This study describes a detailed characterization of the CHIKV replication cycle at the molecular level and demonstrates that a new synthetic infectious clone-derived virus is a useful and representative tool to gain more insight into the replicative cycle of CHIKV, its interactions with the host, and the mode of action of antiviral compounds, which should aid in the development of antiviral strategies against this important human pathogen.

MATERIALS AND METHODS

Cells and viruses. Vero E6, *Ae. albopictus* C6/36 (156) and 293/ACE2 cells (157) were maintained in Dulbecco's modified Eagle's medium (DMEM; Lonza), supplemented with 8% fetal calf serum (FCS; PAA), 2 mM L-glutamine, 100 IU/ml of penicillin and 100 µg/ml of streptomycin. 293/ACE2 cells were grown in the presence of 12 µg/ml blasticidin (PAA) and C6/36 medium was supplemented with non-essential amino acids (Lonza). BHK-21 cells were cultured in Glasgow's Modified Eagles Medium (Gibco) supplemented with 7.5% FCS, 10 mM HEPES pH 7.4, 8% tryptose phosphate broth (Gibco), and antibiotics. The mammalian cell lines were grown at 37°C and C6/36 cells at 30°C in 5% CO_2. CHIKV strain ITA07-RA1 (GenBank accession number EU244823) was isolated from *Ae. albopictus* during the 2007 outbreak in Ravenna, Italy, and was passaged twice on BHK-21 cells. CHIKV NL10/152 (GenBank KC862329) was isolated at the Erasmus Medical Center in Rotterdam from the serum of an infected traveler that returned from Indonesia and was passaged twice on Vero cells. Working stocks of CHIKV were routinely produced in Vero E6 cells at 37°C, typically yielding titers of ~10^7 PFU/ml. Infections were performed in Eagle's minimal essential medium (EMEM; Lonza) with 25 mM HEPES (Lonza) supplemented with 2% FCS, L-glutamine, and antibiotics. After 1 h, the inoculum was replaced with fresh culture medium. All procedures with live CHIKV were performed in a biosafety level 3 facility at the Leiden University Medical Center.

Construction of synthetic CHIKV full-length cDNA clones. A cDNA clone of the synthetic CHIKV strain LS3-GFP, which contains a duplicated subgenomic promoter and expresses the eGFP reporter gene, was designed *in silico* as described in the results section. Three DNA fragments together forming a cDNA copy of CHIKV LS3-GFP were chemically synthesized (GeneArt, Germany). Using standard cloning techniques, these fragments were assembled and cloned into the *Asc*I-*Not*I sites of vector pUC19AN, a pUC19-derived plasmid in which the original polylinker was replaced by one with *Asc*I-*Nco*I-*Eco*RV-*Xho*I-*Not*I sites. The resulting plasmid (pCHIKV-LS3-GFP) contains the genomic cDNA of CHIKV LS3-GFP directly downstream of a phi2.5 promoter and followed by a unique *Spe*I linearization site for DNA linearization prior to *in vitro* transcription. The 'wild type' synthetic pCHIKV-LS3 construct was made by deleting the 920 bp eGFP-containing *Sac*I fragment from pCHIKV-LS3-GFP (Fig. 1).

A third variant with a duplicated subgenomic promoter and a multiple cloning site behind subgenomic promoter 1 (pCHIKV-LS3-MCS), which allows the introduction of e.g. a reporter gene, was generated by removing the 737 bp *Asi*SI-*Pac*I fragment from pCHIKV-LS3-GFP. The constructs were verified by sequencing.

***In vitro* transcription and RNA transfection.** RNA was transcribed from plasmids with the phi2.5 promoter (158) using the AmpliScribe T7 high yield transcription kit (Epicenter), the m[7]GpppA RNA cap structure analog (NEB) and 0.7 μg of template DNA that had been linearized with *Spe*I. After a 3-h reaction at 37°C, template DNA was digested with DnaseI and RNA was purified by precipitation with 7.5 M LiCl (Ambion). The concentration of *in vitro* transcribed RNA was determined with a NanoDrop spectrophotometer (Thermo Scientific) and its integrity was checked by agarose gel electrophoresis. BHK-21 cells (2 x 10^{6}) were electroporated with 1 μg of RNA using program T-20 of the Amaxa Nucleofector and Kit T (Lonza) according to the manufacturer's instructions. Electroporated cells were plated in 6-well clusters and incubated at 37°C in the same medium used for CHIKV infection experiments.

Sequencing of CHIKV genomes. CHIKV RNA was isolated from virions using the QIAamp Viral RNA mini kit. Four overlapping amplicons were generated by a two-step reverse transcriptase (RT) PCR. In the first step cDNA was synthesized using RevertAid H Minus Reverse transcriptase (Fermentas) and primers AT-39 (GACTGCAGATGCCCGCCATT), AT-41 (CGCTCGGTCCAGGCAACTCT), AT-43 (CGTGGTGTTTGCCAACAGGC), or AT-52 (CGCCGTTTTTTTTTTTTTTTTTTTTTTTTTTT). In the second step 4 PCR products were generated using combinations of primers AT-38 (ATGGCTGCGTGAGACACACG) and AT-39, AT-40 (TGCACCCAAGTGTACCACAA) and AT-41, AT-42 (CAGGAGAGTGCATCCATGGC) and AT-43, or AT-44 (GAATGCGCGCAGATACCCGT) and AT-52. The resulting RT-PCR products were purified and directly sequenced (50 ng template) using the BigDye Terminator Cycle Sequencing Kit v1.1 (Applied Biosystems) and a 3130 Genetic Analyzer automatic sequencer (Applied Biosystems). PCR conditions and primer sequences are available upon request.

Virus titration and infectious center assay. Viral titers were determined by plaque assay on Vero E6 cells. Six-well clusters containing confluent monolayers of Vero E6 cells were incubated with 0.5-ml volumes of 10-fold serial dilutions of CHIKV-containing samples. After a 1-h incubation at 37°C, the inoculum was replaced with 2 ml of DMEM containing 1.2% Avicel RC-581 (FMC BioPolymer), 2% FCS, 25 mM HEPES, and antibiotics. After a 66-h incubation at 36°C, monolayers were fixed with 3.7% formaldehyde in PBS and plaques were visualized by crystal violet staining. For infectious center assays 10-fold serial dilutions of electroporated cells were added to 6-well clusters already containing a monolayer of 1 x 10^{6} BHK-21 cells per well. After a 1-h incubation at 37°C, a DMEM/Avicel overlay was applied and cells were incubated at 37°C for 48 h. Plaques were visualized as described above.

RNA isolation, denaturing agarose electrophoresis and in-gel hybridization. Total RNA was isolated from 7×10^5 cells by lysis in 0.5 ml of 20 mM Tris-HCl (pH 7.4), 100 mM LiCl, 2 mM EDTA, 5 mM DTT, 5% (w/v) lithium dodecyl sulfate, and 100 µg/ml proteinase K. After acid phenol (Ambion) extraction, RNA was precipitated with isopropanol, washed with 75% ethanol, and dissolved in 1 mM sodium citrate (pH 6.4). Samples containing RNA from 4.7×10^4 cells were mixed with 3 volumes of 67% formamide, 23% formaldehyde, 6.7% glycerol, 13 mM MOPS (pH 7.2), 6.7 mM NaAc, 2.7 mM EDTA, 0.07% SDS, and 0.03% bromophenol blue. After denaturation for 15 min at 75°C, RNA was separated in 1.5% denaturing formaldehyde-agarose gels using the MOPS buffer system as described (159). RNA molecules were detected by direct hybridization of the dried gel with ^{32}P-labeled oligonucleotides essentially as described previously (160). Positive-stranded genomic and subgenomic CHIKV RNAs were visualized with probe CHIKV-hyb4 (5'-TGTGGGTTCGGAGAATCGTGGAAGAGTT-3') that is complementary to the 3' end of the genome. Negative-stranded RNA was detected with probe CHIKV-hyb2 (5'-AACCCATCATGGATCCTGTGTACGTGGA-3') that is complementary to the 3' end of the minus strand. 18S ribosomal RNA (loading control) was detected with the oligonucleotide probe 5'-ATGCCCCCGGCCGTCCCTCT-3'. Probes (10 pmol) were labeled with 10 µCi [γ-^{32}P]ATP (PerkinElmer) in a 1h reaction using 10 U of T4 polynucleotide kinase (Invitrogen) in 10 µl of the supplied forward reaction buffer (Invitrogen). Prehybridization (1 h) and hybridization (overnight) were done at 55°C in 5x SSPE (0.9 M NaCl, 50 mM NaH$_2$PO$_4$, 5 mM EDTA, pH 7.4), 5x Denhardt's solution, 0.05% SDS, and 0.1 mg/ml homomix I. Hybridized gels were washed twice in 5x SSPE with 0.05% SDS before they were exposed to Storage Phosphor screens. After scanning with a Typhoon-9410 scanner (GE Healthcare), quantification of RNA levels was done with Quantity One v4.5.1 (Biorad) and corrections for loading variations were made based on the quantity of 18S ribosomal RNA in the same lane. The results of two or three independent experiments were quantified (one representative experiment is shown in figures).

Western blot analysis. Total protein samples were prepared by lysing 7×10^5 cells in 0.5 ml of 4x Laemmli sample buffer (100 mM Tris-HCl, pH 6.8, 40% glycerol, 8% SDS, 40 mM DTT, 0,04 mg/ml bromophenol blue). Proteins were separated by SDS-PAGE in 12% polyacrylamide gels and were transferred to Hybond-LFP membranes (GE Healthcare) by semi-dry blotting. After blocking with 1% casein (Sigma) in PBS with 0.1% Tween-20 (PBST), membranes were incubated overnight with rabbit antisera against CHIKV nsP1 (raised using the peptide EVEPRQVTPNDHAN), nsP4 (raised using the peptide ASSRSNFEKLRGPV) or E2 (161) in PBST with 0.5% casein. Mouse monoclonal antibodies against β-actin (Sigma), or the transferrin receptor (Zymed) were used for detection of loading controls. Biotin-conjugated swine-α-rabbit (DAKO) or goat-α-mouse (DAKO), and Cy3-conjugated mouse-α-biotin (Jackson) were used for fluorescent detection of the primary antibodies with a Typhoon-9410 scanner (GE Healthcare).

Metabolic labeling with ³H-uridine. At various time points post infection approximately 2 x 10^5 CHIKV-infected or mock-infected 293/ACE2 cells in 12-well clusters were incubated with 40 µCi of ³H-uridine in medium and incorporation was allowed to proceed for 60 minutes at 37°C. Total RNA was isolated and analyzed in a denaturing agarose gel as described above. For fluorographic detection of ³H-labeled RNA, the gel was soaked in methanol for 1 hour (one change) and then incubated with 3% 2,5-diphenyloxazole in methanol for at least 3 hours. After incubation in milliQ for 30 minutes, the gel was dried and a Fuji RX film was placed on top. Films were developed after a 1-4 day exposure at -80°C and scanned with a Biorad GS-800 densitometer. To check equal sample loading, the gel was hybridized with a ³²P-labeled 18S ribosomal RNA-specific probe as described above. In addition, incorporation of ³H-uridine into RNA was quantified by analyzing 2-µl samples of isolated total RNA with a liquid scintillation counter (Beckman LS 6500 IC). In control samples, cellular transcription was inhibited by adding Actinomycin D (Sigma) to a final concentration of 5 µg/ml.

Metabolic labeling of proteins with ³⁵S-methionine and ³⁵S-cysteine. At various time points post infection approximately 2 x 10^5 CHIKV-infected or mock-infected 293/ACE2 cells in 12-well clusters were starved in DMEM lacking L-methionine and L-cysteine (Invitrogen) for 30 min., and subsequently incubated with 44 µCi EasyTag EXPRESS ³⁵S protein labeling mix (PerkinElmer) for 30 min. Total protein samples were analyzed by SDS-PAGE as described above. Gels were stained with Coomassie to check equal sample loading and ³⁵S-labeled proteins were detected by drying the gels and exposing them to a Storage Phosphor screen, which was scanned 1-2 days later with a Typhoon-9410 scanner (GE Healthcare).

Indirect immunofluorescence microscopy. CHIKV- or mock-infected Vero E6 cells grown on coverslips were fixed with 3% paraformaldehyde in PBS. After quenching with 10 mM glycine in PBS, cells were permeabilized with 0.1% Triton in PBS for 10 min. and coverslips were incubated with primary antibodies diluted in PBS with 5% FCS for 1 h. Double-stranded RNA was detected with a 1:200 dilution of mouse monoclonal antibody J2 (English & Scientific Consulting). CHIKV E2 was visualized with a 1:8000 dilution of a polyclonal rabbit antiserum (161). Detection of primary antibodies was done with donkey-α-mouse-Cy3, goat-α-rabbit-Cy3 or goat-α-rabbit-Alexa488 (1:500; Jackson). Nuclei were stained with Hoechst 33342. The coverslips were mounted with Prolong (Invitrogen) and analyzed using an Axioskop2 Mot Plus fluorescence microscope with Axiocam HRc camera and AxioVision software (Zeiss).

Virus neutralization assay. Mouse monoclonal antibodies raised against CHIKV particles of strain ITA07-RA1 (IZSLER, Brescia, Italy) were heat-inactivated for 30 min. at 56°C. Two-fold serial dilutions of the neutralizing monoclonal antibody 1H7 and non-neutralizing control antibody 3H9 (162) were incubated with an equal volume of medium containing 100 PFU of CHIKV. These mixtures were incubated for 60 min. at 37°C and transferred to 96-well clusters

containing 2×10^4 Vero E6 cells per well. After incubation at 37°C for 2 days, the wells were fixed with 3.7% formaldehyde and CPE was detected by staining with crystal violet.

Antiviral compound assays. Chloroquine, 6-aza-uridine and ribavirin were dissolved in PBS. Cyclosporin A and 3-deaza-adenosine were dissolved in DMSO. Mycophenolic acid was dissolved in ethanol. All compounds were obtained from Sigma. For CPE reduction assays, 96-well clusters with ~1×10^4 Vero E6 cells/well were incubated with 50 PFU of virus per well, corresponding to a multiplicity of infection (MOI) of 0.005, and 2-fold serial dilutions of the compound in medium. Wells without cells, uninfected cells, infected untreated cells and infected cells treated with solvent alone were included as controls. Four days post-infection cell viability was assessed using the CellTiter 96® AQueous Non-Radioactive Cell Proliferation Assay (Promega). CPE reduction experiments with ribavirin were done with BHK-21 cells in a similar way, except that viability was assessed 2 days post infection. For eGFP reporter gene assays, ~1×10^4 Vero E6 cells/well in black 96-well plates were infected with CHIKV LS3-GFP at an MOI of 0.05. After a 42-h incubation in medium containing the compound, the cells were fixed with 3% paraformaldehyde in PBS. eGFP expression was quantified using a Berthold Mithras LB 940 plate reader, with excitation and emission wavelengths of 485 and 535 nm, respectively. The fluorescence in wells containing mock-infected cells was used to correct for background signal. IC_{50} and CC_{50} values were calculated with GraphPad Prism 5 using the nonlinear regression model.

Mouse experiments. All animal experiments described in this paper were carried out in the BSL3 facilities of the Erasmus Medical Center in accordance with the Dutch guidelines for animal experimentation and were approved by the institute's independent animal ethics committee. Twelve-day old C57BL/6 mice were injected intraperitoneally with 100 $TCID_{50}$ of CHIKV S27, CHIKV LS3 or CHIKV LS3-GFP. After the challenge the mice were monitored daily for signs of illness or death. The infection was considered lethal when the animals reached humane end-points and needed to be euthanized. Viral RNA was extracted from brain samples using the automated MagnaPure method (Total nucleic acid isolation kit, Roche Diagnostics, the Netherlands) according to the manufacturer's instructions, and quantified using a one-step RT-PCR TaqMan protocol (EZ-kit, Applied Biosystems) and an ABI PRISM 7500 detection instrument. The primers and probe used for CHIKV RNA quantification were essentially as described (163) except that probe Fam-CCAATGTCTTCAGCCTGGACACCTTT-Tamra was used. Dilutions of virus suspensions of known titer were included to make a calibration curve, which was used to express results as $TCID_{50}$ equivalents per gram of brain tissue.

Ethics statement. All animal experiments described in this paper were carried out in the BSL3 facilities of the Erasmus Medical Center in accordance with the Dutch guidelines for animal experimentation. A Dutch Government-approved and independent animal experimentation

ethical review committee (Stichting DEC Consult) approved the animal studies (permit nr. EMC2838/122-12-29).

Nucleotide sequence accession numbers. The GenBank accession numbers for the full-length cDNA clones pCHIKV-LS3, pCHIKV-LS3-GFP and pCHIKV-LS3-MCS are JX911334, JX911335, and JX911336 respectively. The Genbank accession numbers for the genomic RNA sequences of CHIKV LS3, LS3-GFP, LCS3-MCS and NL10/152 are KC149888, KC149887, KC149889, and KC862329, respectively.

RESULTS

***In silico* design and construction of synthetic CHIKV full-length cDNA clones.** The complete genomes of the 13 CHIKV strains carrying the E1-A226V mutation (Table 1) that were available in GenBank at the time of *in silico* design (November 2009) were aligned using MAFFT (164) and the resulting consensus sequence formed the basis for the synthetic full-length cDNA clones. A 40 nucleotide polyA tail was added to the 3' end of the consensus sequence and a translationally silent point mutation (A7435G) was introduced to create a *Sac*I restriction site required for cloning. The virus encoded by the resulting sequence was termed CHIKV LS3 (GenBank accession KC149888). Variants containing a duplicated subgenomic promoter and a multiple cloning site (CHIKV LS3-MCS; GenBank KC149889) or an eGFP reporter gene (CHIKV LS3-GFP; GenBank KC149887) were also designed. The eGFP reporter gene was placed under control of the native subgenomic promoter and upstream of a second subgenomic promoter that drives expression of the viral structural polyprotein, as this configuration was previously reported to result in a more stable reporter gene expression (114). The CHIKV cDNAs were placed downstream of a phi2.5 T7 promoter, and a unique *Spe*I site for linearization prior to *in vitro* transcription directly followed the polyA tail. The phi2.5 promoter was used because the 5' ends of capped transcripts generated from this
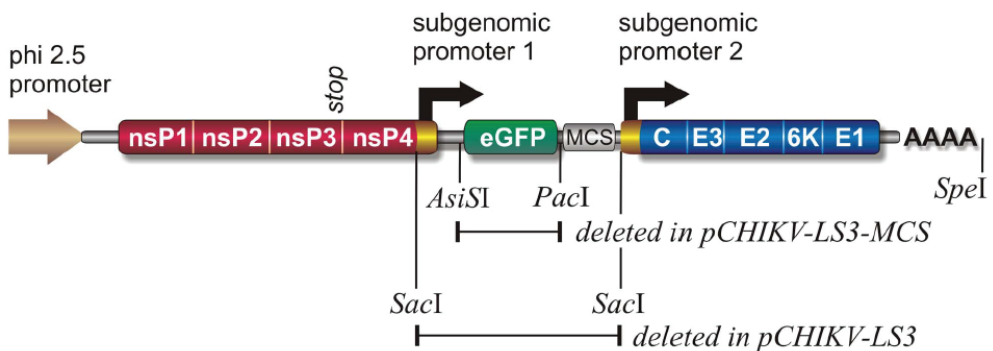

Figure 1. Schematic overview of the synthetic infectious clone pCHIKV–LS3–GFP. The 'wild type' full-length clone pCHIKV-LS3, which lacks the eGFP reporter gene, was generated by deleting the *Sac*I fragment; the variant pCHIKV-LS3-MCS, containing a multiple cloning site (MCS) preceded by subgenomic promoter 1, was generated by removing the *Asi*SI-*Pac*I fragment.

promoter with T7 polymerase and the m⁷Gppp**A** cap analog are identical to the 5' end of the genomes of naturally occurring CHIKV strains. In contrast, capped RNAs generated by *in vitro* transcription from the frequently used SP6 promoter will contain m⁷Gppp**G** at their 5' terminus, i.e. will contain an additional 5'-terminal G residue. However, existing CHIKV cDNA clones that contain the SP6 promoter also efficiently yield infectious virus and it is assumed that the additional 5'-terminal G residue is removed during subsequent rounds of replication. In line with this, *in vitro* transcribed RNA from pCHIKV-LS2, a variant of plasmid pCHIKV-LS3 in which the phi2.5 promoter was replaced with the SP6 promoter also yielded infectious virus. Plasmid pCHIKV-LS3-GFP, the infectious clone encoding the eGFP-expressing reporter virus, was created by assembling the chemically synthesized DNA fragments as described in the Materials and Methods section. Plasmid pCHIKV-LS3, the infectious clone encoding the synthetic 'wild type' strain CHIKV LS3, and plasmid pCHIKV-LS3-MCS were generated from pCHIKV-LS3-GFP by deleting specific restriction fragments, as described in Materials and Methods (Fig. 1). In the original alignment, strains DRDE-07 (GenBank U372006) and D570/06 (GenBank EF012359) shared the highest sequence similarity with LS3, with 3 amino acid differences (Table 2). However, a BLAST search performed in March 2013, three years after the design of CHIKV LS3, and alignment of the retrieved complete CHIKV genomes revealed that strains IND-06-AP3 (GenBank EF027134), IND-GJ53 (GenBank FJ000065), and CHIK31 (GenBank EU564335) share the highest degree of nucleotide sequence identity with CHIKV LS3 (>99.9%), with only 5-7 nucleotide differences respectively (supplemental table S1). Interestingly, these Indian strains were not included in the original alignment on which the

2
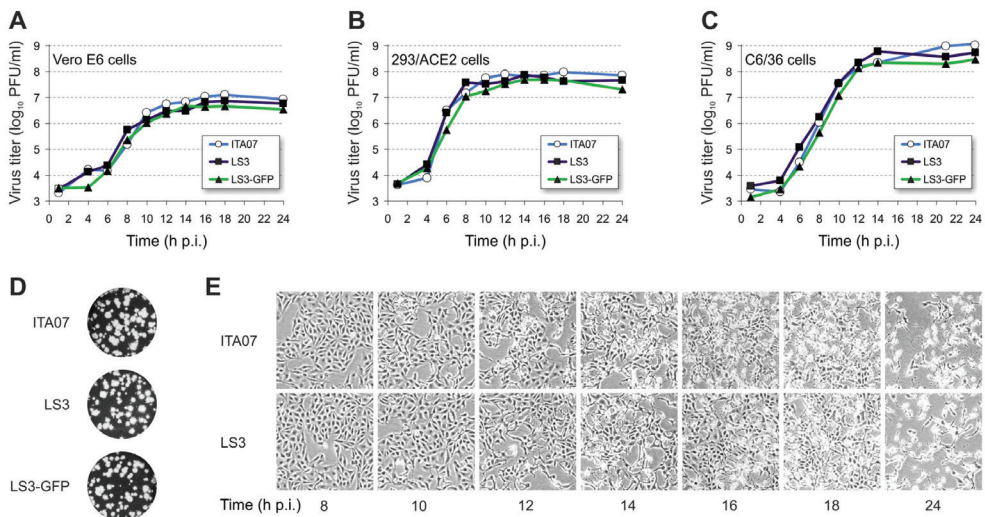
Figure 2. Growth kinetics of CHIKV LS3, LS3–GFP and ITA07–RA1 on various cell lines. Growth kinetics of CHIKV on Vero E6 **(A)**, 293/ACE2 **(B)** and mosquito C6/36 cells **(C)**. Cells were infected at an MOI of 5 and the viral progeny titers in the supernatant were determined at various time points post infection. **(D)** Plaque morphology of ITA07, LS3 and LS3-GFP on Vero E6 cells. **(E)** Induction of CPE by ITA07 (upper panel) and LS3 (lower panel) on Vero E6 cells at different time points post infection.

LS3 sequence was based, as they do not contain the E1-A226V mutation (Table 1). However, nsP1234 of LS3 is identical to that of IND-06-AP3. At the amino acid level, CHIKV LS3 differs at 4 positions from LR2006_OPY1 and at 3 positions from ITA07-RA1 (Table 2).

Growth kinetics of synthetic CHIKV strains and comparison to a natural isolate. To determine whether infectious virus could be generated from the synthetic CHIKV clones, *in vitro* transcribed RNA was electroporated into BHK-21 cells. Strong eGFP fluorescence was readily detected 16 h after transfection of CHIKV LS3-GFP RNA. For CHIKV LS3 and LS3-GFP RNA specific infectivities of approximately 10^5 PFU/μg of RNA were found in infectious center assays, which is similar to what has been found for other CHIKV cDNA clones (114, 116). Virus titers in cell culture supernatants 16 h after electroporation, were generally in the range of 10^5 - 10^6 PFU/ml. This is lower than the peak viral titers that are obtained during infection experiments, but can be explained by the early time point of harvesting and the fact that not all cells were transfected. As expected, electroporation of BHK-21 cells with uncapped CHIKV RNA did not result in the release of infectious virus.

To assess the stability of eGFP reporter expression, CHIKV LS3-GFP was serially passaged (MOI 0.5) in both 293/ACE2 and Vero E6 cells. Virus harvested during each passage was used to infect Vero E6 cells at an MOI of 0.2 and immunofluorescence microscopy revealed that at passage 10, over 95% of the E2-positive foci still displayed robust eGFP expression. Sequencing of cDNA obtained by RT-PCR amplification of RNA extracted from extracellular virions revealed that, after 3 passages on Vero E6 cells, the consensus genome sequence of CHIKV LS3-GFP was identical to the original *in silico* designed sequence. These results demonstrated that the synthetic viruses are viable, genetically stable, and able to retain stable expression of the reporter gene.

Since we aim to use CHIKV in siRNA screens and proteomics studies to identify host factors involved in replication, various human cell lines were evaluated for their ability to support CHIKV replication. CHIKV LS3-GFP was able to productively infect HeLa, MRC-5, Huh7, 293, and 293/ACE2 cells (data not shown). Infection of HeLa and Huh7 cells was not very efficient and these cells were therefore not used for any further experiments. 293/ACE2 cells were selected for this study, as they supported high levels of CHIKV LS3-GFP replication, could be efficiently transfected with siRNAs, and - unlike regular 293 cells - adhered well to tissue culture plastics. 293/ACE2 cells stably express angiotensin-converting enzyme 2 (ACE2), the receptor for SARS-coronavirus. ACE2 expression is not required for CHIKV infection, but these cells were chosen because of the aforementioned advantages and the fact that they have been previously used in our lab in siRNA screens for host factors that affect corona- and arterivirus replication ((165, 166); Wannee et al., in preparation). Using these cells in similar siRNA screens with CHIKV and other alphaviruses would allow direct comparison of data sets with those obtained for corona- and arteriviruses, which could lead to the identification of common (broad spectrum) pro- and antiviral host factors.

To determine whether the synthetic viruses behave like natural isolates, their growth kinetics in Vero E6, 293/ACE2, and C6/36 cells were compared to those of ITA07-RA1, which was isolated during the 2007 CHIKV outbreak in Italy (Fig. 2A-C). The growth curves of CHIKV LS3 on all three cell lines were found not to differ significantly from those of ITA07-RA1, with virus titers reaching a maximum 14-18 h post infection (p.i.). Peak virus titers on mosquito cells were approximately 1-log higher than those on mammalian cells. CHIKV LS3-GFP replicated slightly slower than the other viruses in all three tested cell lines, which is not unusual for recombinant reporter viruses.

eGFP expression could be detected as early as 6 h p.i. and peaked around 22 h p.i. The plaque morphology of the synthetic viruses was similar to that of ITA07-RA1 (Fig. 2D). CHIKV LS3 induced a cytopathic effect (CPE) indistinguishable from the natural isolate. On Vero E6 cells early signs of CPE started to appear around 12 h p.i. and CPE was complete by 24 h p.i. (Fig. 2E).

To study CHIKV-induced transcriptional host shut-off, the incorporation of ^{3}H-uridine into cellular and viral RNA was analyzed by metabolic labeling of infected 293/ACE2 cells at various time points post infection (MOI of 5). A strong reduction in the incorporation of ^{3}H-uridine into RNA was observed at 10-12 h p.i. in cells infected with CHIKV LS3 or ITA07, as determined by liquid scintillation counting of total RNA samples (Fig. 3A). Inhibition of cellular transcription with actinomycin D for 30 min. prior to metabolic labeling at 12 h p.i. revealed the contribution of viral RNA synthesis to the total signal. Fluorographic detection of ^{3}H-labeled RNA analyzed in denaturing gels also showed a decrease in cellular transcription during the course of the infection, while the synthesis of CHIKV RNA became clearly detectable by 6 h p.i (Fig. 3B). Transcriptional shut-off occurred around 10-12 h p.i. and was induced
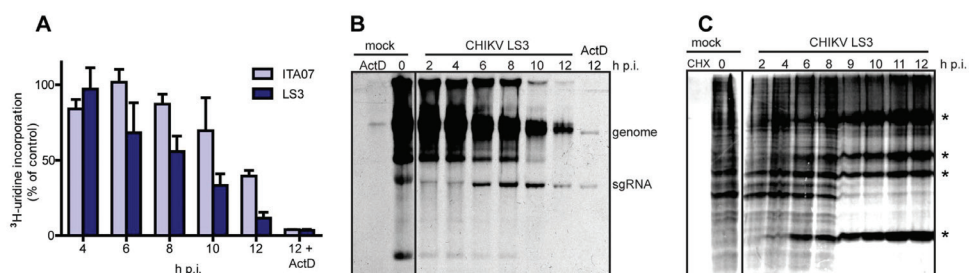
Figure 3. Transcriptional and translational shut–off induced by CHIKV. 293/ACE2 cells were infected with CHIKV LS3 or ITA07-RA1 at an MOI of 5, and at the indicated time points post infection metabolic labeling with ^{3}H-uridine **(A, B)** or ^{35}S-Cys and ^{35}S-Met **(C)** was performed to analyze total RNA and protein synthesis, respectively. **(A)** Incorporation of ^{3}H-uridine into viral and cellular RNA as measured by liquid scintillation counting of total RNA samples taken at various time points post infection. **(B)** ^{3}H-uridine incorporation into viral and cellular RNA during CHIKV LS3 infection as detected by denaturing gel electrophoresis and fluorography. In control samples (ActD) 5 ug/ml Actinomycin D was added 30 min. prior to metabolic labeling to inhibit cellular transcription. **(C)** Synthesis of ^{35}S-labeled viral and cellular proteins during CHIKV LS3 infection. The control lane labeled CHX contains proteins from cells treated with the translation inhibitor cycloheximide prior to metabolic labeling. CHIKV-specific proteins are indicated with a *.

by CHIKV LS3 and ITA07 with similar kinetics, although LS3 seemed to act slightly faster. To examine CHIKV-induced translational shut-off, the synthesis of ^{35}S-labeled viral and cellular proteins during the course of CHIKV LS3 infection was analyzed by metabolic labeling of infected 293/ACE2 cells with ^{35}S-Met and ^{35}S-Cys (Fig. 3C). A clear shut-off of host translation was observed 8-9 h p.i. Beyond 9 h p.i. the bulk of newly produced protein appears to be of viral origin, likely C, E1, E2 and their precursors (indicated with * in Fig. 3C). CHIKV ITA07 and LS3 induced translational host shut-off in a similar manner (only results obtained with LS3 are shown in Fig. 3C).

Both CHIKV ITA07-RA1 and the synthetic viruses established non-cytopathic persistent infections in C6/36 mosquito cells. All characterization experiments have been performed in both 293/ACE2 and Vero E6 cells, with similar results. For simplicity only the results for 293/ACE2 cells are shown, except for immunofluorescence experiments, which were done with Vero E6 cells as they had a more suitable morphology.

Kinetics of RNA synthesis of CHIKV ITA07-RA1 and the synthetic viruses. The replication cycle of the synthetic viruses and ITA07-RA1 was characterized in more detail to assess whether the synthetic viruses behaved like their natural counterpart. The kinetics of RNA synthesis was analyzed by isolating total RNA from 293/ACE2 cells infected with CHIKV LS3, LS3-GFP, or ITA07-RA1 at various time points post infection. Negative- and positive-stranded RNAs were detected by hybridization with ^{32}P-labeled oligonucleotide probes (Fig. 4A). Both negative- and positive-strand RNAs were readily detected in cells infected with the various strains starting at 6 h p.i. The negative-strand RNA was less abundant than the positive strand, it was easily detected relatively early in infection (Fig. 4A top panel, Fig. 4B), and appeared to decrease at later time points as has also been observed for other alphaviruses. This apparent decrease is probably not only due to degradation of minus strands, but at least partly due to a hampered detection caused by the large excess of positive-strand RNA present at late time points. This excess of positive-strand RNA competes with the radioactively labeled minus-strand specific probe. In support of this, we observed that mixing RNA isolated from CHIKV-infected cells at 6 h p.i. with *in vitro* transcribed positive-strand RNA reduced the amount of negative strand that could be detected (data not shown). Furthermore, when samples taken at 6 and 14 h p.i. were treated with single-strand-specific RNase A/T1 before hybridization, the negative-strand levels at the late time point were approximately 70% of that at 6 h p.i, instead of the approximately 50% in untreated samples (data not shown). Using a positive-strand-specific probe, both the 49S genomic and 26S sgRNA could be detected, and both RNAs accumulated until 12 h p.i (Fig. 4A middle panel, Fig. 4C). The ratio of genomic to sgRNA varied between 1:3.5 and 1:5.5 during the course of infection, similar to the ratios reported for Semliki forest virus and SINV (167). The kinetics of RNA synthesis and RNA accumulation levels were similar in CHIKV LS3- and ITA07-RA1-infected cells. In cells infected with CHIKV LS3-GFP, the additional subgenomic RNA encoding the eGFP reporter gave rise to an extra band above the 26S RNA band, and its expression level was calculated to be approximately

half of that of the 26S RNA. The individual levels of the two sgRNAs expressed by CHIKV LS3-GFP were lower than those of ITA07 or LS3, but their combined abundance was comparable to that of the viruses expressing a single sgRNA (Fig. 4C).

CHIKV protein synthesis and dsRNA accumulation in cells infected with ITA07-RA1 or the synthetic viruses. To monitor viral protein expression, 293/ACE2 cells were infected with CHIKV LS3, LS3-GFP, or ITA07-RA1 and total protein was isolated at various time points post infection. These samples were analyzed by Western blotting with antisera against the nonstructural proteins nsP1 and nsP4, and the structural protein E2. Expression of nsP1, E2,
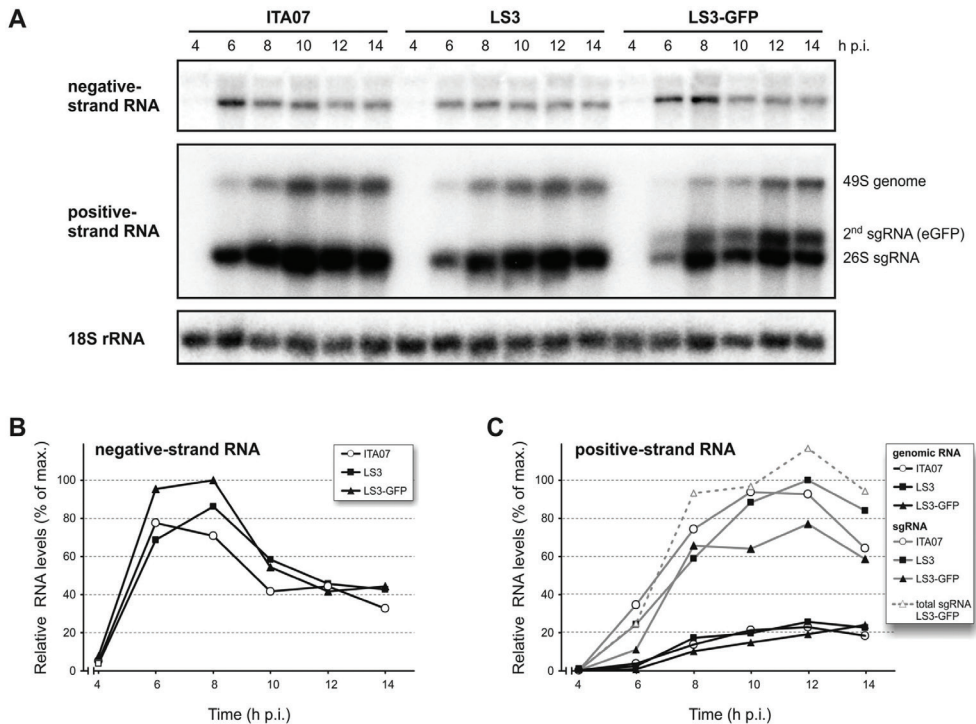
Figure 4. Accumulation of negative– and positive–strand CHIKV RNA in infected cells. (A) 293/ACE2 cells were infected with CHIKV LS3, LS3-GFP or ITA07-RA1 at an MOI of 5, total RNA was isolated at different time points post infection and strand-specific detection was performed with radioactively labeled oligonucleotides complementary to the 3' end of either negative- (top panel) or positive-strand (middle panel) CHIKV RNA. Cellular 18S ribosomal RNA was probed as a loading control (lower panel). The positions of genomic RNA, the 26S sgRNA and the second eGFP-encoding sgRNA are indicated to the right of the middle panel. **(B)** Plot representing the kinetics of CHIKV negative-strand RNA accumulation, based on quantification of data from panel A. After correction for variations in sample loading based on the 18S rRNA signal, the relative abundance of the RNAs was determined by normalizing to the highest value observed (CHIKV LS3-GFP, 8 h p.i.). **(C)** Kinetics of CHIKV positive-strand RNA accumulation. The relative abundance of RNA was calculated as before, except that data were normalized to the value measured for LS3 sgRNA at 12 h p.i (100%). Genomic RNA levels are indicated with black lines, sgRNA levels with gray lines. The total level of both sgRNAs expressed by LS3-GFP is indicated with the gray dotted line.

and the E3E2 precursor could be detected as early as 6 h p.i. and the proteins accumulated over time, reaching a plateau around 12 h p.i. (Fig. 5). The RdRp nsP4 could not be detected in infected cells using a CHIKV nsP4-specific antiserum capable of detecting the purified bacterially expressed protein. This was probably due to the low affinity of the antibody, the low expression level and relative instability of nsP4 in infected cells, as was also observed for other alphaviruses (168). In addition, a quantitative proteomics study on CHIKV-infected cells also suggested that at 10 h p.i. the amount of nsP4 was at least 200-fold lower than that of nsP1 (121).

Indirect immunofluorescence analysis of Vero E6 cells infected with CHIKV LS3, LS3-GFP, or ITA07-RA1 at various time points showed that the localization and expression kinetics of E2 and dsRNA were similar for the natural isolate and the synthetic viruses (Fig. 6). Double-stranded RNA, which is assumed to be generated during replication of CHIKV in infected cells (169), could be detected as early as 4 h p.i. and remained clearly visible throughout the infection. The dsRNA localized to foci throughout the cytoplasm. The E2 protein could be detected from 6 h p.i. onwards with maximum expression reached by 12 h p.i. The E2 protein mainly localized to the plasma membrane of infected cells. eGFP produced by the reporter virus was visible from 6 h p.i. onwards, reaching a maximum level around 12 h p.i. (Fig. 6C).

Neutralization of CHIKV LS3 by a monoclonal antibody raised against ITA07-RA1. CHIKV LS3 and ITA07-RA1 were compared in a neutralization assay using the neutralizing monoclonal antibody 1H7 that was raised in mice against CHIKV ITA07-RA1 virions, and appears to recognize a linear epitope in E2 (162). The non-neutralizing mAb 3H9 was used as a control. Both the natural isolate and CHIKV LS3 were neutralized with similar characteristics by 1H7, while their infectivity was not affected by 3H9 (Fig. 7).

The synthetic viruses cause lethal infections in a mouse model. Newborn mice are highly susceptible to CHIKV infection and they develop symptoms as lethargy, dragging of
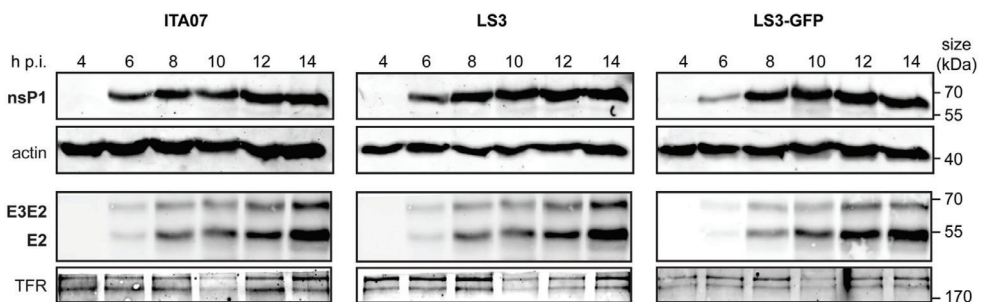
Figure 5. Western blot analysis of CHIKV nsP1 and E2 expression at different time points post infection. 293/ACE2 cells were infected with CHIKV ITA07, LS3 or LS3-GFP at an MOI of 5. At the indicated time points cells were lysed, proteins were separated by SDS-PAGE and viral proteins were detected by Western blotting. The anti-E2 antiserum also recognized the E3E2 (p62) precursor of E2. Actin and the transferrin receptor were used as loading controls.

hind limbs, flaccid paralysis, and reduced weight gain (170). 12-day old mice were injected intraperitoneally with 100 TCID$_{50}$ of CHIKV LS3, LS3-GFP or prototype strain S27 as a control. The animals were euthanized when their humane end points were reached 3 or 4 days post infection and viral RNA levels in brain tissue were analyzed (Fig. 8). Both synthetic viruses behaved like the natural isolate *in vivo,* causing lethal infections with similar kinetics (Fig. 8A). In addition, the viral titers in the brains of CHIKV S27-infected mice were similar to those of mice infected with the synthetic viruses (Fig. 8B).

Sensitivity to antiviral compounds. To evaluate their suitability for analyzing the potency and mechanism of action of antiviral compounds, the sensitivity of CHIKV LS3 and LS3-GFP to a number of such compounds was determined and compared to ITA07-RA1. Cyclosporin A, which through its effect on cellular cyclophilins inhibits the replication of a variety of viruses, had no specific effect on CHIKV replication, not even at a (cytotoxic) dose of 32 μM (data not shown). The compounds 3-deaza-adenosine, 6-aza-uridine, chloroquine, and mycophenolic acid were tested in CPE reduction assays with Vero E6 cells infected at an

Figure 6. Immunofluorescence analysis of dsRNA and E2 expression in time. Vero E6 cells grown on coverslips were infected with CHIKV ITA07, LS3 or LS3-GFP at an MOI of 5. At the indicated time points the coverslips were fixed and stained with antibodies specific for dsRNA **(A)** or E2 **(B)**. **(C)** eGFP fluorescence in CHIKV LS3-GFP infected cells (green). Nuclei (blue) were visualized by Hoechst staining.

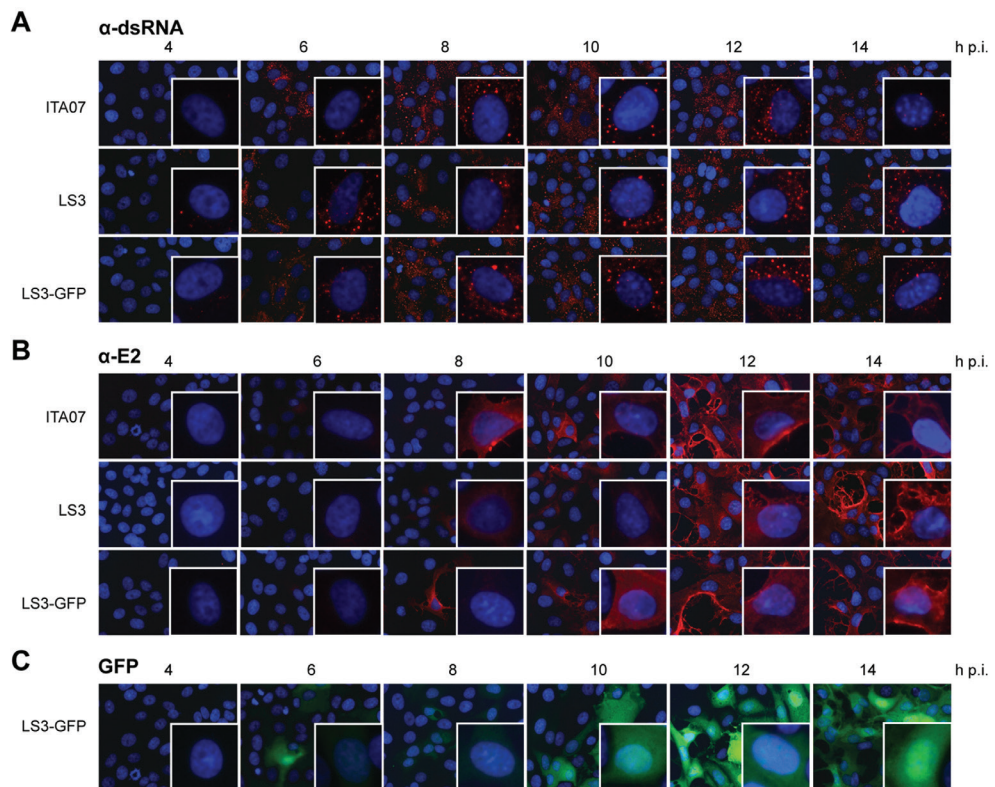MOI of 0.005 and analyzed 4 days p.i. They were all found to inhibit CHIKV replication with IC_{50}s in the low micromolar range and with minimal cytotoxicity (Fig. 9A-D). No substantial differences were observed between the IC_{50} values calculated for ITA07-RA1, LS3 and LS3-GFP. The four compounds also clearly reduced eGFP reporter gene expression in Vero E6 cells infected with CHIKV LS3-GFP (Fig. 9F). Slightly lower IC_{50} values were obtained for 6-aza-uridine and chloroquine, and a significantly higher IC_{50} was observed for 3-deaza-adenosine in this assay, compared to the CPE-based assay. This might be due to the mode of action of 3-deaza-adenosine and/or due to differences in experimental set-up compared to the CPE-based assay (MOI 0.05 vs. 0.005; measurement 42 h p.i. vs. 4 d p.i.). Ribavirin is a known inhibitor of CHIKV replication, but in our CPE reduction assay with Vero E6 cells it was not very effective in inhibiting replication of the various strains, as IC_{50} values of over 400 μM were obtained (Fig. 9E, gray lines). This is likely due to the inefficient conversion of ribavirin to its active phosphorylated form in Vero E6 cells (171). Therefore, we have also analyzed the effect of ribavirin in a 2-day CPE reduction assays with BHK-21 cells, which are able to metabolize ribavirin (172, 173) and found IC_{50}s of 15-21 μM for the various strains. Clinical isolate NL10/152 was also included in the assays and appeared to be somewhat more sensitive to the antiviral compounds than LS3 and ITA07-RA1. However, the slower replication kinetics of this strain made it impossible to directly compare NL10/152 and LS3 in the same CPE reduction assays, despite the fact that virus yields and cytopathic effect of NL10/152 and LS3 were comparable (data not shown).

DISCUSSION

The massive CHIKV outbreaks that have been occurring in Asia and the Indian Ocean region since 2005 are associated with the emergence of strains with the A226V substitution in the E1 glycoprotein, which allowed their transmission by a novel mosquito vector, *Aedes albopictus* (10, 37, 39, 40, 42, 150). These East-Central-South African lineage-derived strains even appear to be replacing the Asian lineage CHIKV strains that have been endemic in the region for
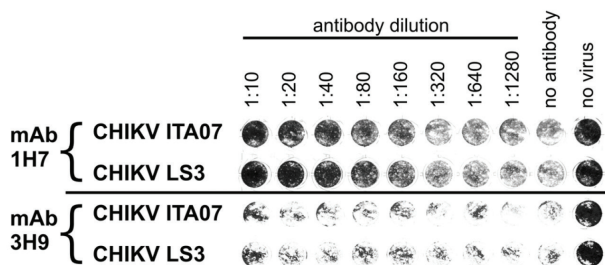
Figure 7. Neutralization of CHIKV ITA07 and LS3 by mouse monoclonal antibodies raised against ITA07–RA1. 100 PFU of the CHIKV strains were incubated with serially diluted antibodies in 96-well clusters containing confluent monolayers of VeroE6 cells. After 2 days the wells were fixed with formaldehyde and stained with crystal violet. Either the neutralizing antibody 1H7 or non-neutralizing control antibody 3H9 were used.

decades. Since the 1980s, the geographic distribution of *Aedes albopictus* has dramatically expanded and now also includes large parts of the USA and several European countries. This creates concern for locally transmitted outbreaks in Europe and the USA, which could be initiated by viraemic travelers arriving from countries where CHIKV is endemic, like India and Indonesia. Locally transmitted CHIKV infections have indeed already been reported from Italy in 2007 and France in 2010 (22, 25) and recent studies suggest that also the USA is at risk for locally transmitted CHIKV outbreaks (174, 175). Besides its large medical and societal impact in endemic countries, the increased risk of CHIKV outbreaks in Europe and the USA underlines the importance of studying the replication of this important human pathogen and its interactions with the host to develop safe and effective vaccines and antiviral therapy. Infectious cDNA clones have proven to be important tools to study many aspects of the viral life cycle, and molecular clones of a variety of natural isolates have been instrumental in several recent CHIKV studies (93, 114-116, 152-154). The existing CHIKV molecular clones can be considered to be derived from a single genome (or fragments of single genomes) out of the whole spectrum of viruses present in a CHIKV quasispecies population. In contrast, most of the complete CHIKV genome sequences that have been deposited in GenBank represent the consensus (or master sequence) of a viral quasispecies population.
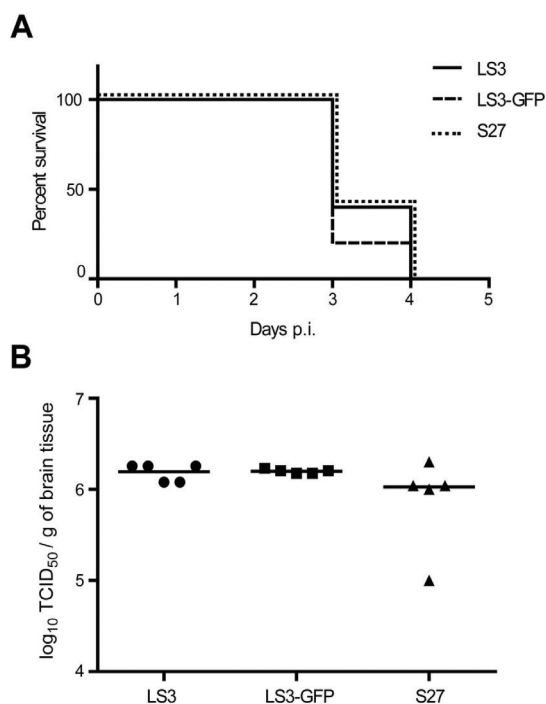
Figure 8. Replication of synthetic CHIKV strains *in vivo*. (A) Survival of mice after intraperitoneal injection with 100 $TCID_{50}$ of CHIKV LS3, LS3-GFP or S27 (5 mice per group). **(B)** CHIKV titers (in $TCID_{50}$ equivalents per mg of tissue) in the brains of the mice infected with the 3 CHIKV strains.
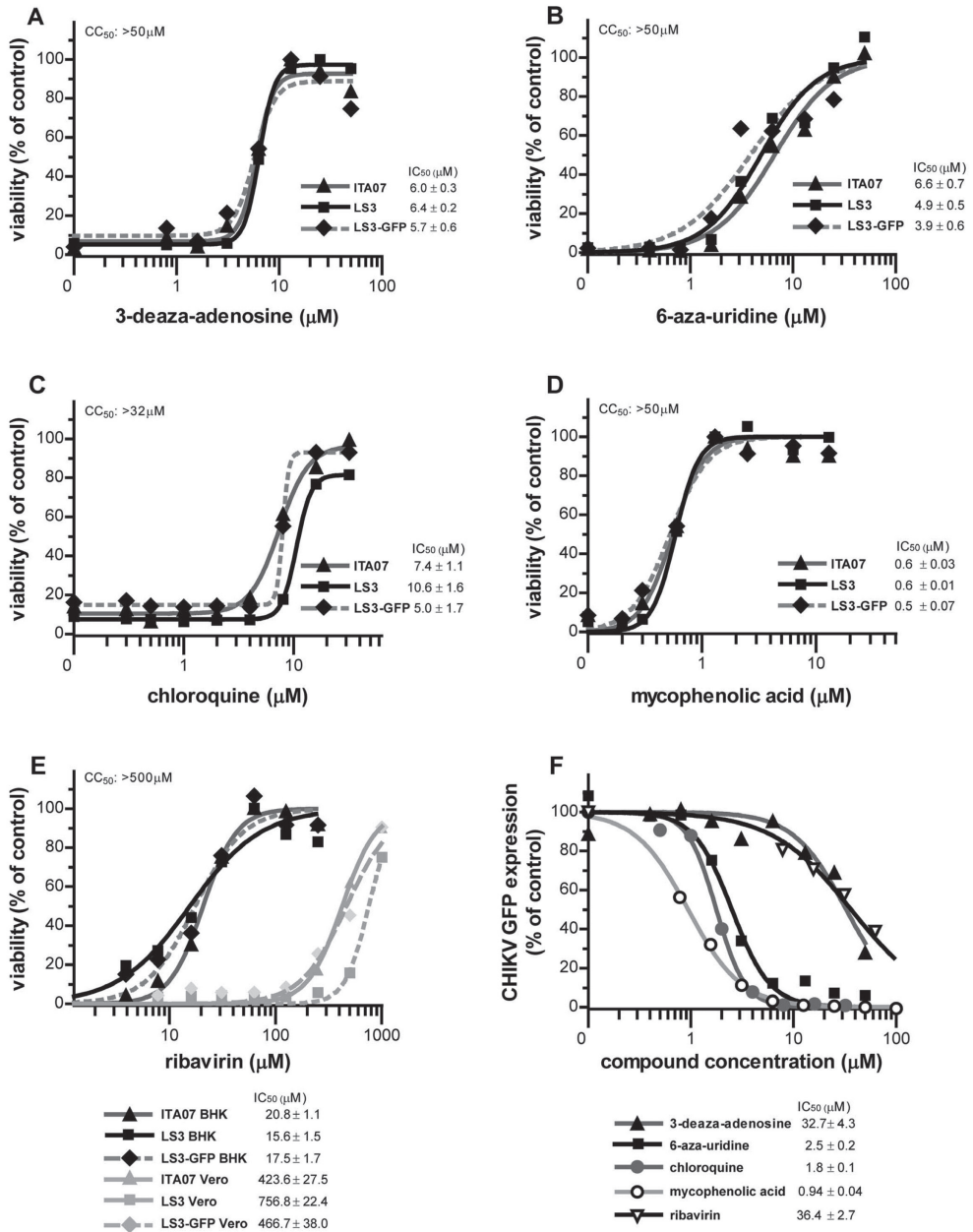
Figure 9. Effect of antiviral compounds on the replication of various CHIKV strains. Dose dependent reduction of CHIKV-induced CPE by **(A)** 3-deaza-adenosine, **(B)** 6-aza-uridine , **(C)** chloroquine and **(D)** mycophenolic acid in Vero E6 cells infected with CHIKV strains ITA07-RA1, LS3 and LS3-GFP (MOI 0.005). **(E)** Antiviral effect of ribavirin on CHIKV replication in BHK-21 (black lines) and Vero E6 cells (gray lines). Cell viability was normalized to untreated uninfected cells (100%). The 50% cytotoxic concentration (CC_{50}) of the compounds is indicated in the top left of each panel. **(F)** Dose-response curves showing the effect of five antiviral compounds on the eGFP expression in Vero E6 cells infected with CHIKV LS3-GFP (MOI 0.05) at 42 h p.i. Values were normalized to eGFP fluorescence in untreated infected cells (100%).

The diversity (and evolution) of a CHIKV quasispecies population has probably been shaped by the characteristics of the individual host and the specific tissue source (serum) from which it was isolated. For Ross River virus it was observed that the level of intrahost genetic variation in patient serum samples, was considerably larger than that observed at the epidemiological scale, which can be explained by the purifying selection for replication in both arthropod and vertebrate hosts (155). Advances in sequencing techniques now allow a more detailed view on quasispecies diversity and intrahost evolution, and also for CHIKV a recent study has provided more insight into quasispecies dynamics and the effect of purifying selection by host alternation (176). A link was observed between increased fitness as a result of alternating passaging and reduced quasispecies complexity, which restricted adaptability to novel selective pressures like antiviral treatment or antibody-mediated neutralization (176).

Individual CHIKV isolates or molecular clone derived viruses could have their specific properties in terms of replication kinetics, vector specificity, dissemination within the host, virulence, virus-host interactions or sensitivity to antiviral compounds. We were interested in studying the general characteristics of the life cycle and virus-host interactions of the E1-226V CHIKV strains that were circulating during the 2005-2009 outbreaks. Therefore, we have constructed a fully synthetic cDNA clone, CHIKV LS3, based on the consensus sequence of the aligned genomes of these recent E1-226V isolates, rather than on a single genome from a clinical isolate. In addition, a variant with a (duplicated) subgenomic promoter that expresses the eGFP reporter gene was created (CHIKV LS3-GFP). The current possibilities of gene synthesis allowed the design of these clones *in silico*, with sequences tailored to our requirements, e.g. already containing a reporter gene under control of a duplicated subgenomic promoter and including (translationally silent) mutations to create restriction sites that facilitate cloning and reverse genetics studies.

Alignment of all 148 complete CHIKV genomes that were in GenBank by June 2013 yielded a consensus sequence that differed only at 3 nucleotide positions from the sequence of LS3 that was designed 3 years earlier. These were position 7,435 at which we introduced a translationally silent restriction site (G7435A), a synonymous U→C substitution at position 3,397, and position 10,670, which is a C in 68% of all deposited genomes (strains with E1-226A), while the remaining (E1-226V) strains have a U at this position. An interesting observation was that 6% of the sequenced CHIKV strains, including the prototype strains S27 and Ross, contain an arginine codon instead of the opal stop codon that is present between the nsP3- and nsP4-coding regions of most CHIKV isolates. The presence or absence of this opal codon might be influenced by the passage history of the isolate as has been observed for other alphaviruses (177). This might also explain why the sequence of the original clinical isolate of LR2006-OPY1 (Genbank DQ443544.2) contains the opal termination codon near the end of the nsP3 coding region, while the infectious clone of this strain (Genbank EU224268.1) contains an arginine codon at this position.

To assess whether the synthetic viruses are representative models, their characteristics were compared to those of the natural strain ITA07-RA1. Like the natural isolate, the synthetic

viruses caused cytopathic infections in Vero E6 and 293/ACE2 cells (Fig. 2E), whereas non-cytopathic persistent infections were observed in the mosquito cell line C6/36. In vertebrate cells all strains caused a shut-off of cellular translation around 8-9 h p.i. and a strong inhibition of cellular transcription by 10-12 h p.i. The accumulation of negative- and positive-strand viral RNA, the kinetics of non-structural and structural viral protein expression, as well as the growth kinetics and plaque morphology of the synthetic viruses were indistinguishable from those of CHIKV ITA07-RA1 (Fig. 2-6). In addition, the synthetic viruses caused lethal infections in 12-day old mice, with virus spreading to the brain, as observed for natural isolates (Fig. 8). Although this demonstrates that the synthetic viruses replicate *in vivo*, this mouse model does not allow comparison of strains for more subtle differences in virulence and pathogenesis. The genomic stability of CHIKV LS3-GFP was assessed and after 3 passages its (consensus) sequence was found to be identical to the original *in silico* designed sequence. The expression of the eGFP reporter gene was stable for at least 10 passages, making the synthetic viruses suitable tools for high-throughput screens for antiviral compounds, (reverse genetics) studies into their mechanism of action, and systematic functional genomics screens for host factors affecting CHIKV replication.

To evaluate whether CHIKV LS3 and LS3-GFP are suitable to analyze the potency and mechanism of action of antiviral compounds, their sensitivity to a number of such compounds was determined and compared to ITA07-RA1. The lysosomotropic agent chloroquine and nucleoside analog 6-aza-uridine inhibited the replication of the synthetic viruses and natural isolates with IC_{50}s that were in the same range and comparable to values previously reported by others (77, 117, 178-181). The inhibitory effect of chloroquine on the replication of many viruses including alphaviruses has been known for decades. For CHIKV it is a useful reference compound in cell-based studies, but a small scale clinical trial on the island of La Reunion suggested it is not effective in the treatment of CHIKV infections in patients (178). The nucleoside analog 6-aza-uridine has previously been reported to inhibit the replication of a variety of viruses, including CHIKV (117, 181). The compound could interfere with cellular UTP metabolism and may be incorporated into CHIKV RNA, leading to chain termination and/or increased error frequency, ultimately resulting in 'error catastrophe'. Mycophenolic acid is a non-competitive inhibitor of inosine monophosphate dehydrogenase (IMPDH), causing a depletion of the intracellular guanosine pool. It is a known inhibitor of various viruses, including CHIKV (117, 182). Ribavirin is a synthetic nucleoside analog with broad spectrum antiviral effect due to potential effects on the cellular IMPDH enzyme, viral RNA synthesis and capping (171). However, not all cell lines are able to perform the necessary conversion of this compound to its active phosphorylated form, explaining the contradictory reports on the antiviral activity of this compound (172, 173, 183). In our hands, ribavirin inhibited CHIKV replication in BHK-21 cells with an IC_{50} of around 18 µM, while it was hardly effective in Vero E6 cells, with IC_{50} values of over 400 M. The IC_{50} that we obtained with BHK-21 cells is in the same range as those previously reported for the antiviral effect of ribavirin on CHIKV replication (117, 181). Cyclosporin A, which through its effect on the cellular

cyclophilins, inhibits the replication of a variety of viruses (for recent review see (184)), had no effect on CHIKV replication. We identified 3-deaza-adenosine as a novel inhibitor of CHIKV replication with an IC_{50} of approximately 6 μM and a CC_{50}>50 μM. This compound has previously been identified as inhibitor of a broad spectrum of viruses, although many other +RNA viruses appeared to be rather insensitive or not affected at all (reviewed in (185)). The antiviral activity of 3-deaza-adenosine was attributed to its inhibitory effect on the cellular enzyme S-adenosylhomocysteine hydrolase, leading to an accumulation of S-adenosylhomocysteine, which inhibits S-adenosylmethionine-dependent methylation reactions (185). In this manner the enzyme plays a key role in S-adenosylmethionine-dependent methylation reactions and inhibition of viral methylation reactions (e.g. of viral RNA) apparently can be achieved at compound concentrations that do not notably interfere with cellular methylation reactions. Our observation warrants a more detailed analysis of the mode of action of 3-deaza-adenosine and analogs, also to evaluate their potential for use in antiviral therapy to treat CHIKV infections. Overall, no large differences were observed between the IC_{50} values calculated for ITA07-RA1, LS3 and LS3-GFP, indicating that the synthetic viruses are suitable for use in antiviral screens. For most compounds, a faster and simpler assay with CHIKV LS3-GFP reporter virus showed a good dose-dependent response that correlated well with results obtained in the CPE-based assay.

Clinical isolate NL10/152 exhibited slightly slower replication kinetics and appeared to be more sensitive to antiviral compounds than ITA07 and the synthetic viruses. Differences in the sensitivity to antiviral compounds among clinical isolates is not an uncommon phenomenon. NL10/152 differs at 7 amino acid positions from LS3 and it will be interesting to determine the contribution of these mutations, in particular the R88S substitution in nsP4, to the slower replication kinetics (and higher sensitivity to antivirals).

Taken together the detailed characterization of the CHIKV replication cycle at the molecular level demonstrated that our new synthetic consensus-based viruses behave like natural isolates and are suitable tools to study various aspects of the CHIKV life cycle, which should ultimately provide a basis for the development of antiviral therapy.

ACKNOWLEDGMENTS

TABLE 1. CHIKV E1–226V strains that were aligned to produce the CHIKV LS3 consensus sequence.

CHIKV strain	Origin	Year	GenBank accession
BNI-CHIKV_899	Mauritius	2006	FJ959103.1
D570/06	Mauritius	2006	EF012359.1
LR2006_OPY1	La Reunion	2006	DQ443544.2
TM25	Mauritius	2006	EU564334.1
Wuerzburg 1	Mauritius	2006	EU037962.1
DRDE-07	India	2007	EU372006.1
ITA07-RA1	Italy	2007	EU244823.2
RGCB80/KL07	India	2007	GQ428212.1
RGCB120/KL07	India	2007	GQ428213.1
0810aTw	Bangladesh	2008	FJ807898.1
0810bTw	Malaysia	2008	FJ807899.1
RGCB355/KL08	India	2008	GQ428214.1
RGCB356/KL08	India	2008	GQ428215.1

position in protein	nspP1								nsP2	nsP3			nsP4	C		E2		E1	
	128	157	184	230	314	326	376	391	539	155	376	472	88	23	27	191	252	4	226
LS3	K	H	M	G	M	V	M	F	L	A	T	S	R	S	V	T	K	V	V
IND-06-AP3	.	.	.	.	.	.	.	.	.	.	.	.	.	.	.	.	.	.	A
IND-MH51	.	.	.	.	.	.	.	L	.	.	.	.	.	.	.	.	.	.	A
CHIK31	.	.	.	.	.	.	.	.	.	.	.	N	.	.	I	.	.	.	A
DRDE-07	.	.	T	.	L	.	.	.	.	.	.	.	.	.	.	.	.	A	.
D570/06	T	.	.	.	.	.	T	.	.	.	.	.	.	P	.	.	.	.	.
ITA07-RA1	.	.	.	R	.	.	.	.	.	.	I	.	.	.	I	.	.	.	.
LR2006_OPY1	T	.	.	.	.	M	T	.	.	.	.	.	.	P	.	.	.	.	.
NL10/152	.	Y	.	.	.	.	.	.	S	T	.	.	S	.	I	S	Q	.	.

TABLE 2. Comparison of the amino acid sequences of CHIKV LS3 and various natural isolates. The CHIKV LS3 amino acid sequences were aligned with those of several highly similar natural isolates, and clinical isolate NL10/152. Only amino acid differences are indicated and identity is represented by dots. The numbering is based on the sequence of LS3, which is also equal to that of LR2006_OPY1. It is important to note that - like all other CHIKV strains in this table - clinical isolate LR2006-OPY1 (Genbank DQ443544) also contains an opal stop codon in the 3'-end of the nsP3 coding region, while its infectious clone with Genbank accession number EU224268 lacks this stop codon.

SUPPLEMENTARY FIGURE

Table S1. Comparison of CHIKV LS3 with the genome sequences of various closely related natural isolates. Only differences between LS3 and each of the other strains are summarized. Dots indicate that the nucleotide at that position is identical to that at the corresponding position in the sequence of LS3. Genomes were aligned with MAFFT and analyzed in Jalview. Numbering is based on the sequence of LR2006_OPY1 (and is equal to LS3 numbering). The nucleotide at position 10670 (indicated in gray) determines whether the strain has the A226V mutation in the E1 protein. Strains with a T at this position have the A226V mutation. Differences not included in the comparison are the 35 nt, 5 nt and 23 nucleotides that are missing from the 3'UTR of the sequences of DRDE-07, D570/06 and ITA07-RA1, respectively. The missing first 19 nt, missing last 13 nt and the insertion of an A after position 11564 in the sequence of IND-06-AP3 were also not included in this comparison.

strain	nt position	LS3	IND-06-AP3	CHIK31	IND-MH51	LR2006_OPY1	DRDE-07	D570/06	ITA07-RA1
5'-UTR	1	A	-	.	T	.	.	.	T
nsP1	358	T	.	.	.	C	.	C	.
	459	A	.	.	.	C	.	C	.
	499	T	.	.	C	.	.	.	.
	568	C	.	.	.	.	T	.	.
	627	T	.	.	.	.	C	.	.
	757	T	.	.	.	.	.	.	C
	764	G	.	.	.	.	.	.	A
	862	G	C	.	.	.	.	.	.
	985	T	.	.	.	.	.	.	C
	1016	A	.	.	.	.	T	.	.
	1052	G	.	.	.	R	.	.	.
	1203	T	.	.	.	C	.	C	.
	1247	T	.	.	C	.	.	.	.
	1381	T	.	.	.	.	.	.	G
	1603	C	.	.	.	.	T	.	.
nsP2	2014	A	.	.	.	.	.	.	G
	2944	G	.	.	.	.	A	.	.
	3325	C	.	.	.	.	.	.	T
	3397	T	.	.	.	.	.	.	C
	3481	C	.	.	.	.	.	.	T
	3724	T	.	.	.	A	.	A	.
nsP3	4167	A	.	.	.	R	.	.	.
	4300	T	.	.	C	.	.	.	.
	5049	G	.	.	.	K	.	.	.
	5122	T	.	.	.	.	.	C	.
	5202	C	.	.	.	.	.	.	T
	5248	C	.	.	T	.	T	.	.
	5377	G	.	.	.	.	.	.	A
	5490	G	.	A	.	.	.	.	.
	5491	C	.	T	.	.	.	.	.
nsP4	5744	C	.	.	.	.	.	.	T
	6397	C	.	.	T	.	.	.	.
	6547	G	.	.	.	A	.	A	.
	6706	C	.	T	.	.	.	.	.
	7435	G	A	A	A	A	A	A	A
	7450	C	.	.	.	.	.	.	T
C	7633	T	.	.	.	C	.	C	.
	7645	G	.	A	.	.	.	.	A
	7983	C	.	.	.	.	.	.	T
	8127	C	.	.	.	.	.	.	T
E3	8385	C	.	.	.	.	T	.	.
E2	8910	T	.	.	.	C	.	C	.
	8985	T	.	.	.	A	.	.	.
	9114	A	.	.	.	G	.	.	.
	9207	T	.	.	A	.	.	.	.
	9633	T	.	.	.	C	.	C	.
	9681	G	.	.	.	.	.	.	A
E1	10004	T	.	.	.	.	C	.	.
	10314	T	.	.	C	C	.	C	.
	10377	T	.	.	.	.	.	.	C
	10670	T	C	C	C	.	.	.	.
	10743	A	.	.	.	G	.	G	.
	11127	T	.	.	.	C	.	C	.
	11256	T	.	.	.	.	.	C	.
3'-UTR	11360	T	.	.	.	.	C	.	.
	11499	G	T	.	.	.	.	.	.
	11600	C	.	.	.	.	.	.	T
	11640	A	.	.	.	.	.	.	G
	11723	T	-	.	.	.	.	.	.
	11762	T	.	.	.	.	.	-	.
	11763	C	.	.	.	.	.	.	.
	11765	C	.	.	.	.	T	.	.
	11770	C	.	.	.	.	A	.	.
	11776	G	.	.	.	.	C	.	.
	11784	G	-	.	.	.	.	-	.
total nt difference			5	7	9	16	16	16	21

3.

Identification of host factors involved in chikungunya virus replication by RNAi screening of the human kinome
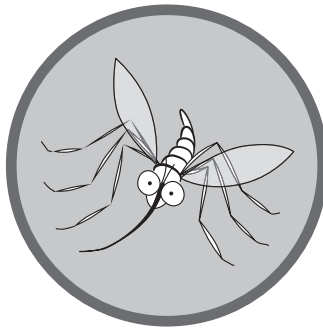
Florine E.M. Scholte[1], Ali Tas[1], Adriaan H. de Wilde[1], Kazimier F. Wannee[1], Jelle Goeman[2#], Peter ten Dijke[3], Eric J. Snijder[1], and Martijn J. van Hemert[1*]

[1]Molecular Virology Laboratory, Department of Medical Microbiology; [2]Department of Medical Statistics; [3]Department of Molecular Cell Biology, Leiden University Medical Center, Leiden, the Netherlands. [#] Current address: Biostatistics, Department for Health Evidence, Radboud University Medical Center, Nijmegen, the Netherlands

ABSTRACT

Chikungunya virus (CHIKV) is a mosquito-borne alphavirus that causes severe and often persistent arthritis. The virus re-emerged in 2004, causing large epidemics in the Indian Ocean region and Asia. It reached the Caribbean in December 2013, where it quickly spread. Presently, CHIKV is endemic in large parts of the world and encroaching on both Americas. CHIKV relies, as other RNA viruses, heavily on host factors for its replication. However, the identity of most of these proteins remains unknown. Identifying these proteins will greatly improve our understanding of the replication of this important human pathogen, and they can potentially include interesting targets for antiviral therapy. Kinases, for example, are a common drug target as they play a key role in numerous cellular processes, and are therefore likely also involved in virus replication. Here we describe a siRNA library-mediated screen targeting the human kinome to identify cellular factors involved in CHIKV replication. We identified numerous proviral factors that could be placed in distinct cellular pathways, including (control of) mitogen-activated protein kinase (MAPK) and ErbB (epidermal growth factor receptor family) signaling, indicating that these pathways may play an important role in CHIKV replication. We performed a secondary screen to validate a selection of our hits, including the 20 genes that scored highest on our annotated hit list. We were able to confirm the identification of 10 proviral and 2 potential antiviral factors, including FGFR2, SHC1, DUSP1 and LATS2. The pro- and antiviral host factors described here expand our understanding of CHIKV replication and form perfect starting points for further in-depth mechanistic studies.

Abbreviations host factors

BLNK	b-cell linker
BUB1B	budding uninhibited by benzimidazoles (yeast homologue) 1 beta
CDC2L5/CDK13	cell division cycle 2-like 5
COPB2	coatomer protein complex, subunit beta 2
DMPK	dystrophia myotonica protein kinase
DUSP	dual specificity phosphatase
FGFR2	fibroblast growth factor receptor 2
FN3K	fructosamine 3 kinase
FN3KRP	fructosamine 3 kinase related protein
LATS2	large tumor suppressor kinase 2
MAPKAPK3	mitogen-activated protein kinase-activated protein kinase 3
MAPK4	microtubule affinity-regulating kinase 4
MMP2	matrix metalloproteinase
PFKFB3	6-phosphofructo-2-kinase/fructose-2,6-biphosphatoase 3
RPS6KC1	ribosomal protein S6 kinase, 52kDa, polypeptide 1
RPS6KL1	ribosomal protein S6 kinase-like 1
SHC1	Src homology 2 domain containing transforming protein
SOCS	suppressor of cytokine signaling 1
TRIM/TRAT	T-cell receptor-interacting molecule / T cell receptor associated transmembrane adaptor 1

INTRODUCTION

Chikungunya virus (CHIKV) is a mosquito-borne alphavirus that re-emerged in 2004 during an explosive outbreak of unprecedented magnitude, which took place in the Indian Ocean area. During this outbreak the virus acquired a mutation in its envelope protein (E1-A226V) that facilitated its spread via a novel vector, the Asian tiger mosquito (*Aedes albopictus*) (10, 30, 37, 152). The E1-A226V mutation, in combination with the rapidly expanding geographical distribution of *Aedes albopictus* has dramatically increased the epidemic potential of CHIKV (30, 37, 186). By the end of 2013, the virus had reached the Caribbean and subsequently Latin America (8, 13, 14) and by the beginning of 2015 already over one million people in the Americas had been infected with CHIKV (12, 13). Consequently also thousands of infected travelers returned to the USA and Europe. Hence, CHIKV no longer only causes human suffering and financial loss in the regions where the virus is (now) endemic, but it also affects the quality of life of people in non-endemic countries. The recent outbreak in the Caribbean also puts the United States at risk for (limited) local outbreaks, and indeed local transmission has already occurred in Florida (28). CHIKV transmission has been reported from all inhabited continents, and especially Latin America is facing potentially large outbreaks. Its population is largely immunologically naïve while the local capacity for surveillance and diagnostic is limited, enabling initially unnoticed outbreaks that may expand quickly once established. CHIKV causes a fever that usually resolves within several days, a maculopapular rash and a characteristic, debilitating arthralgia that can be extremely painful and may persist for months (1, 2). A licensed vaccine or effective antiviral therapy are currently not available.

Alphaviruses possess a ~12 kb positive-strand RNA genome that contains two open reading frames (ORFs). The 5' ORF encodes the four nonstructural proteins (nsP1-4), whereas the structural proteins (capsid, E3, E2, 6K and E1) are produced from a subgenomic RNA (44, 76). A portion of the four nonstructural proteins assemble into the replication complex, likely together with cellular co-factors, whereas another fraction of the nsPs is thought to have other functions, e.g. modulating the immune response, inducing host shut off and interfering with SG formation (62, 87, 90, 118, 187). Due to their relative small genome size, RNA viruses like CHIKV rely heavily on cellular host factors for all stages of their replicative cycle. However, till date only a handful of host factors involved in CHIKV replication have been identified (e.g. (62, 118, 119, 121, 122, 188)), and in general their exact role during viral replication is poorly understood. Many studies on the interplay between CHIKV infection and cellular proteins have focused on changes in the cellular proteome following CHIKV infection (121, 139-144). These studies provided valuable information on the cellular response to CHIKV infection, but do not necessarily provide insight into the factors that restrict infection or those that are required for virus replication. Another strategy to identify host factors involved in CHIKV replication encompasses screening for interacting partners of viral (nonstructural) proteins using Y2H (yeast two-hybrid) or VOPBA (viral overlay protein binding assay) (122, 188, 189), although a physical interaction does not necessarily translate into functional relevance. In addition, cellular proteins that interact with viral proteins indirectly or transiently will

be missed, as will host proteins that interact with the viral RNA. RNAi screening enables large-scale loss of function studies to identify cellular factors that are directly or indirectly involved in viral replication. It focusses on protein function rather than physical interaction, therefore potentially providing more biological relevant data. Making an inventory of the proteins involved in CHIKV replication will improve our understanding of this important human pathogen, and they may comprise useful starting points for the development of novel antiviral strategies. Antiviral strategies that target cellular factors instead of viral proteins are expected to be less sensitive to the development of antiviral resistance. RNAi screens have already been performed for a number of +RNA viruses, including Sindbis virus (SINV) (133), hepatitis C virus (HCV) (124-127), West Nile virus (128), yellow fever virus (129), and dengue virus (DENV) (130, 131). These studies have provided valuable insights into the cellular proteins and pathways involved in the replication of these viruses.

Here we describe a kinome-targeted RNAi library screen to identify cellular factors involved in CHIKV replication. Kinases play a key role in a wide range of cellular processes like proliferation, signaling and immunity, and are therefore also likely involved in the replication of various viruses. Indeed, previously several kinases have been found to be indispensable for viral replication, for example for HCV, DENV, severe acute respiratory syndrome coronavirus (SARS-CoV) and influenza virus (124, 131, 166, 190, 191). Little is known about the involvement of cellular kinases in alphavirus replication. We therefore set out to investigate which kinases and pathways are involved in the replicative cycle of CHIKV. In this study 66 proteins were identified that potentially play a proviral role in CHIKV replication. These proteins can be placed in specific pathways likely involved in the CHIKV replicative cycle, including (control of) the MAPK cascade and ErbB (epidermal growth factor receptor family) signaling. We confirmed a selection of hits by performing a secondary screen using different siRNA, and could confirm 10 potential proviral proteins and 2 potential antiviral proteins, including MAPKAPK3, FGFR2, MARK4, SHC1, DUSP1 (proviral), and CDC2L5 and LATS2 (antiviral).

MATERIALS AND METHODS

Cells, viruses and titration. MRC5 and Vero E6 cells were cultured as described previously (69, 192). The production and titration of virus stocks and routine infections were performed as described (69). The primary and secondary screens were executed with a CHIK reporter virus expressing eGFP from a duplicated subgenomic promoter (CHIKV LS3-GFP; GenBank KC149887). All procedures with live CHIKV were performed in a biosafety level 3 facility at the Leiden University Medical Center.

RNA interference (primary screen). The ON-TARGETplus SMARTpool Protein Kinases siRNA library (# G-103505) and scrambled control siRNAs (Non-Targeting Pool; D-001810-10) were obtained from Dharmacon. The Protein Kinases siRNA library contained 779 SMARTpools, each comprised of 4 single siRNA duplexes, targeting the human kinome and some additional targets. MRC5 cells (1 x 10^4 per well of a 96-well plate) were transfected with

a final concentration of 100 nM siRNA using DharmaFECT1 (Dharmacon) according to the manufacturer's instructions. At 48 h post-transfection (p.t.), the transfection and knockdown efficiency was determined using siRNAs targeting GAPDH (D-001830-10) in combination with the KDalert™ GAPDH assay kit (Ambion) to determine remaining GAPDH activity. Two days post transfection, the siRNA-treated cells were infected with CHIKV LS3-GFP at an MOI of 0.05. At 24 h p.i., the cells were fixed with 3% paraformaldehyde in PBS and GFP expression was quantified using a Berthold Mithras LB 940 96-well plate reader. In duplicate plates, the viability of siRNA-transfected uninfected cells was assessed at 48 h p.t. using the CellTiter 96® AQueous Non-Radioactive Cell Proliferation Assay (Promega). Absorbance was quantified using a Berthold Mithras LB 940 96-well plate reader.

Data analysis (primary screen). Raw GFP measurements and cell viability data were analyzed using the Bioconductor/R package cellHTS2, with minor adaptations. Raw data were log2 transformed and normalized using the NPI (normalized percent inhibition) method to remove plate-to-plate variation. Log scores were calculated, resulting in log-fold changes that were calculated back to fold change. The variance of the normalized intensities was not adjusted (cellHTS2 default). Values were normalized to infected cells transfected with control siRNA, and mock-infected wells. The ranked list was further processed by removing hits of which the siRNA pools reduced cell viability to less than 80% (cut-off was based on our experience). Statistical significance was calculated by R using a two-tailed unpaired Student's t-test. Values were considered to be significant if $p < 0.05$. Each siRNA SMARTpool in a screen was tested in triplicate and the complete screen was performed 3 times.

Pathway analysis. Proteins from the hit list were grouped according to their function using DAVID (http://david.abcc.ncifcrf.gov/). Visualization of protein interaction networks was performed using STRING (http://string-db.com).

RNA interference (secondary screen). For the secondary screen, single siRNAs against selected targets were obtained from Sigma (MISSION pre-designed Nano Scale siRNA), with the exception of BLNK, COPB2, SHC1 and TRIM/TRAT, for which no Nano Scale siRNA were available and standard Sigma pre-designed siRNA were obtained. Transfection and infection procedures were identical as to those described for the primary screen.

Data analysis (secondary screen). Statistical significance was calculated by GraphPad5 using a two-tailed unpaired Student's t-test. Values were considered to be significant if $p < 0.05$. All values represent the average of triplicate wells, experiments were performed in duplicate or triplicate. The values presented in the graphs represent the mean values of triplicate wells with the error bars indicating the standard deviation of the mean. P-value: *$p < 0.05$, **$p < 0.01$, ***$p < 0.001$.

Compound screening. BCl was obtained from Axon Medchem BV (cat. no. 2178) and dissolved in DMSO. MRC5 cells were infected with CHIKV (MOI 5 for 8 h) or CHIKV-GFP (MOI 0.05 for 24h), and BCl was added to the culture media at 1 h p.i. To induce DUSP1 protein expression, cells were treated with various concentrations of arsenite (Sigma) in culture media for 30 min. Cells were washed with PBS and fresh culture medium was added. Five hours after arsenite treatment, the cells were harvested and protein expression was analyzed using western blotting.

Western blot analysis. Western blot analysis was performed essentially as described previously (69).

RESULTS

Kinome-targeted siRNA library screen identifies host factors involved in CHIKV replication. To identify host factors involved in CHIKV replication we screened a siRNA library targeting the human kinome. This library consists of siRNA targeting 779 genes, each gene is targeted with a SMARTpool containing 4 distinct siRNAs. The use of SMARTpools (i.e. a mix of siRNA duplexes) allows the use of a lower concentration of each single siRNA, which reduces their potential off-target effects. MRC5 cells were selected for this study as they are human cells (fibroblasts) that can be transfected efficiently before subsequent infection with CHIKV. Furthermore, MRC5 cells are not immortalized and exhibit a functional innate immune response (192). Transfected MRC5 cells were infected with a reporter virus (CHIKV-GFP) at a multiplicity of infection (MOI) of 0.05. The GFP expression was quantified as a measure for viral replication at 24 h post infection (p.i.) (Figure 1). In theory, this experimental set-up with multiple rounds of virus replication allows the identification of host factors involved in any step of the replicative cycle, including assembly and the release of infectious progeny virus. In duplicate plates the viability of siRNA-transfected uninfected cells was assessed using a colorimetric assay. The efficiency of siRNA delivery and knockdown was assessed using siRNAs targeting GAPDH and subsequent determination of the remaining GAPDH activity at 48 h post transfection (data not shown). The kinase siRNA library was screened three times, with each screen using triplicate wells for each siRNA pool, after which the data were analyzed using the R package cellHTS2. This package transformed raw measurements into an annotated hit list. The data were normalized using reference controls (scrambled siRNA and uninfected wells), and the 'normalized percent inhibition' (NPI) method, provided in cellHTS2. Normalization was applied on a per-plate basis to correct for plate effects. siRNA pools that induced cytotoxicity (<80% remaining cell viability as compared to the control siRNAs) were discarded. Targets were considered potential proviral factors when their knockdown reduced the CHIKV-driven GFP signal at least 3-fold. Analysis of the fold-change scores identified 66 genes of which knockdown met these criteria, suggesting they are relevant for CHIKV replication. This means that ~8% of the genes targeted by the siRNA library influences CHIKV replication (Figure 2). This may appear a rather large fraction, but

one has to keep in mind that the library does not target a random selection of genes, but kinases that often occupy key positions in important cellular pathways. The largest reduction (32-fold) in CHIKV replication was induced by depletion of BUB1B (budding uninhibited by benzimidazoles (yeast homologue) 1 beta), a mitotic checkpoint kinase. Knockdown of the majority of the targets in our annotated hit list reduced CHIKV GFP expression 3- to 4-fold. Strikingly, we could not identify any strong antiviral hits, as depletion of none of the targeted proteins increased the CHIKV-GFP signal to a sizable extent. The strongest increase in GFP signal (a mere 1.4-fold) was observed when DMPK (Dystrophia myotonica protein kinase))
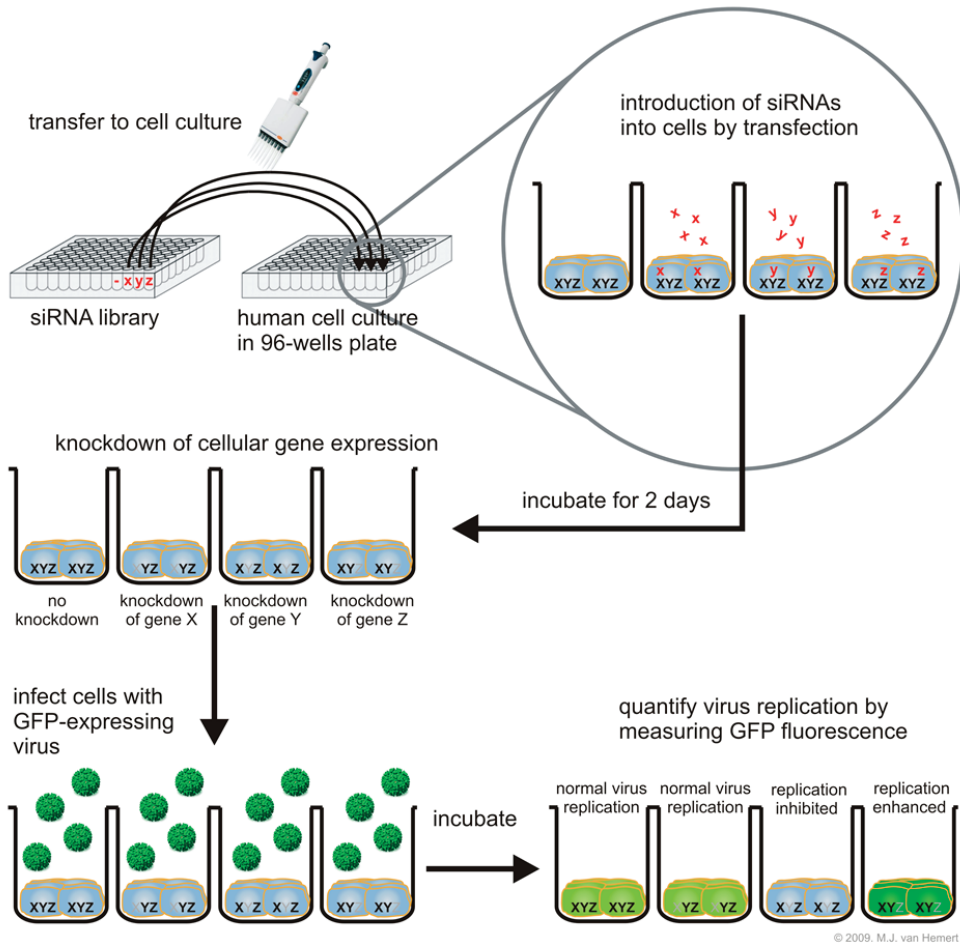

Figure 1. Schematic overview of the siRNA library screening set–up. MRC5 cells were transfected with siRNA pools targeting the human kinome. After two days the cells were transfected with CHIKV-GFP (MOI 0.05) and GFP was quantified 24 h p.i. as a measure of viral replication. GFP values were normalized to cells transfected with control siRNAs. Potential cytotoxicity was determined in parallel plates using a colorimetric assay.

Accession	GeneID	pvalues	fold reduction
NM_001211	BUB1B	0.06686	32.7
NM_020341	PAK7	0.05317	18.3
NM_002627	PFKP	NA	16.6
NM_006549	CAMKK2	0.09021	11.5
NM_004635	MAPKAPK3	0.09654	11.3
NM_005374	MPP2	0.00664	7.3
NM_013314	BLNK	0.03012	6.6
NM_004417	DUSP1	0.00911	6.1
NM_007199	IRAK3	0.01626	6.0
NM_024046	CAMKV	0.00039	5.8
NM_005607	PTK2	0.04976	5.7
NM_000141	FGFR2	0.00004	4.9
NM_016388	TRIM	0.00053	4.8
NM_002019	FLT1	0.00378	4.3
NM_003913	PRPF4B	0.07238	4.1
NM_002654	PKM2	0.03065	4.1
NM_031417	MARK4	0.01179	4.1
NM_004766	COPB2	0.00116	4.0
NM_005400	PRKCE	0.05786	4.0
NM_025052	YSK4	0.01752	3.9
NM_017859	URKL1	0.04994	3.9
NM_018423	STYK1	0.00244	3.9
NM_003029	SHC1	0.00079	3.8
NM_002822	PTK9	0.09095	3.8
NM_000616	CD4	0.00003	3.8
NM_002461	MVD	0.02391	3.8
NM_003674	CDK10	0.01997	3.8
NM_005592	MUSK	0.01334	3.7
NM_006206	PDGFRA	0.06630	3.7
NM_001320	CSNK2B	0.00481	3.7
XM_496631	TPRXL	0.00661	3.7
NM_000222	KIT	NA	3.7
NM_016308	UMP-CMPK	0.01234	3.7
NM_002715	PPP2CA	0.01109	3.6
NM_004566	PFKFB3	0.01209	3.5
NM_004420	DUSP8	0.02581	3.5
NM_003745	SOCS1	0.00296	3.4
NM_022740	HIPK2	0.00958	3.4
NM_000291	PGK1	0.00131	3.4
NM_002766	PRPSAP1	0.01596	3.4
NM_006648	PRKWNK2	0.03450	3.3
NM_002741	PRKCL1	0.05409	3.3
NM_002611	PDK2	0.08607	3.3
NM_024619	FN3KRP	0.00590	3.3
NM_003390	WEE1	0.00770	3.3
NM_022158	FN3K	0.00680	3.2
NM_018571	ALS2CR2	0.00243	3.2
NM_006182	DDR2	0.00733	3.2
NM_005235	ERBB4	0.00402	3.2
NM_016586	MBIP	0.02999	3.2
NM_003646	DGKZ	0.00276	3.2

Accession	GeneID	pvalues	fold increase
NM_004409	DMPK	0.03715	1.41
NM_014572	LATS2	0.00685	1.33
NM_005627	SGK	0.02699	1.31
NM_021158	TRIB3	0.05770	1.29
NM_004439	EPHA5	0.07760	1.29
NM_005406	ROCK1	0.20881	1.29
NM_033116	NEK9	0.13891	1.27
NM_133494	NEK7	0.27599	1.24
NM_003557	PIP5K1A	0.28191	1.24
NM_173354	SNF1LK	0.16225	1.24
NM_018425	PI4KII	0.02370	1.24
NM_006510	RFP	0.50783	1.22
NM_002419	MAP3K11	0.24946	1.21
NM_000024	ADRB2	0.24424	1.20
NM_153273	IHPK1	0.08559	1.19
NM_003718	CDC2L5	0.02539	1.19
XM_291107	NEK1	0.38310	1.19
NM_006260	DNAJC3	0.12814	1.19
NM_138293	ATM	0.27700	1.18

3

Figure 2. Hit list of primary kinome–directed siRNA screen. Raw GFP data were converted to fold-change using Bioconductor/R package cellHTS2. Potential proviral factors are indicated in green, potential antiviral factors in red. Statistical significance was calculated by R using a two-tailed unpaired Student's t-test. Statistical significance is indicated in yellow. Values were considered to be significant if p<0.05

was depleted (Fig. 2). This modest increase might still be relevant, and we therefore decided to include some potential antiviral hits in our follow-up experiments.

Analysis of primary screen data. Some of the proteins that were identified in this screen have clear, well-characterized functions and some have been implicated in the replication of other viruses or the immune response, which makes it easy to explain their effect on CHIKV replication. These hits help to confirm the validity of our data and lend more credibility to other identified potential host factors. One example is COPB2 (coatomer protein complex, subunit beta 2), a protein involved in retrograde vesicular transport. Blocking this transport has been shown to be detrimental for replication of several RNA viruses, including poliovirus, SARS-CoV, and HCV (124, 131, 133, 166, 193-198). Here, we could also confirm a role for COPB2 during CHIKV replication. PLK1 (polo-like kinase 1) is often used as a positive control for siRNA transfection efficiency, as PLK1 depletion results in growth reduction and apoptosis (199, 200). Indeed, also in our hands siRNA targeting PLK1 reduced cell viability extensively (data not shown). SOCS1 (suppressor of cytokine signaling 1) is another proviral hit with an anticipated effect on CHIKV replication, which further corroborates the validity of the data yielded by this screen. SOCS1 is a member of the STAT-induced STAT inhibitors, and is part of a negative feedback system that regulates cytokine signal transduction (201). Depletion of this protein should result in a stronger antiviral response upon CHIKV infection. Indeed, it was previously shown that SOCS1 negatively regulates IFN signaling during HCV (202) and influenza virus infection (203).

Furthermore, several proteins involved in ribosomal function were identified, such as RPS6KC1 and RPS6KL1. CHIKV relies on the host cellular translation machinery for the production of viral proteins, therefore disturbing this machinery should affect virus replication. However, these ribosomal proteins were not selected for additional validation, as they are indispensable for normal cellular function and are therefore not suitable as potential therapeutic targets.

Identification of cellular pathways involved in CHIKV replication. The potential proviral host factors of which depletion resulted in >2-fold reduction in CHIKV-GFP were functionally analyzed using Gene Ontology (GO) biological process terms. Not surprisingly, considering the fact that we tested a kinome-directed siRNA library, a strong enrichment for (protein) phosphorylation and protein modification processes was found (data not shown). Placing the hits in distinct pathways revealed a significant enrichment for several signaling pathways, including MAPK signaling, regulation of MAPK signaling, ErbB signaling, neurotrophin signaling, and the cell cycle (Figure 3). Mapping the network connectivity of the 66 potential proviral cellular proteins revealed that many of them are highly interconnected (Figure 4).

We identified several proteins that are involved in glucose metabolism (fructosamine 3 kinase (FN3K), fructosamine 3 kinase related protein (FN3KRP), phosphofructokinase, platelet (PFKP), and 6-phosphofructo-2-kinase/fructose-2,6-biphosphatoase 3 (PFKFB3)).

Several viruses have been described to depend on endogenous glucose or regulate glucose uptake and glycolytic flux, as enhancement of these processes leads to increased glycolytic ATP production (204-207). However, cellular glucose deprivation using either 2-deoxy-D-glucose or glucose-free cell culture media did not specifically affect CHIKV replication, nor did the addition of extra glucose (data not shown). Extreme glucose deprivation had a strong negative effect on cell viability, which complicated further experiments, and made it impossible to determine whether it had an effect on CHIKV replication other than through its nonspecific effect on metabolism.

Evaluation of hits from the primary screen. In order to validate a selection of the hits from the primary screen, we performed a secondary screen using siRNAs from a different supplier and with different sequences. We selected 31 targets for this secondary screen, including the 20 siRNA pools that caused the largest reduction in CHIKV GFP expression (potential proviral factors), the 5 siRNA pools that caused the largest (significant) increase in CHIKV GFP expression (potential antiviral factors), and a few genes that were of special interest to us because of their particular function (e.g. DUSP5 and DUSP8). For each gene, we separately tested two individual siRNA duplexes for their effect on CHIKV GFP expression (Figure 5), except for BLNK, COPB2, SHC1 and TRIM/TRAT, for which only a single siRNA was tested as described in the materials and methods section. Cell viability was determined in parallel plates and transfection of none of the siRNAs duplexes was found to induce cytotoxicity (data not shown). A target was considered a confirmed hit if at least one of the two siRNA duplexes reduced CHIKV GFP expression by 40% or more (in

the case of potential proviral targets). Using this method, 10 (out of 25) potential proviral hits from the primary screen could be validated (indicated in bold in Fig. 5A), including MAPKAPK3, MARK4, WEE1, BLNK, COPB2, SHC1 and DUSP1. Of these confirmed targets, COPB2, SHC1 and WEE1 were also found in a genome-wide siRNA screen for SINV, a (distantly) related alphavirus (133). This indicates that these targets are most likely involved in alphavirus replication in general. In total we tested 46 single siRNA duplexes (targeting 25 potential proviral genes), of which 27 induced a significantly reduction in GFP expressed by CHIKV compared to the non-targeting control siRNA. Together they covered 20 of the 25 genes (Fig. 5B).

Although only 10 genes met the cut-off criteria (40% reduction), this indicates that a larger fraction of the genes tested here may be true hits. The modest, but statistically significant effect on CHIKV-GFP may be due to sub-optimal siRNA design and/or modifications.

Transfection of two (out of 12) single siRNA targeting potential antiviral hits resulted in the expected increase in CHIKV-GFP: CDC2L5 (also known as CDK13) and LATS2 (Figure 5B). Similar as in the primary screen, the observed increase in GFP expressed by CHIKV was modest (~130% and ~140% respectively), but statistically significant.

Taken together, a substantial number of hits from the primary screen could be confirmed in the secondary RNAi screen. We were able to validate a larger fraction of the proviral factors (40%), compared to the potential antiviral hits initially found (17%). This is not surprising

Category	Term	Count	PValue	Genes	Fold Enrichment
KEGG	MAPK signaling pathway	20	3.1E-07	FGFR2, FGFR4, MAPKAPK5, MAPKAPK3, STK3, DUSP5, DUSP4, DUSP2, MAPK12, DUSP1, PAK2, MAPK3, RAC1, PDGFRA, MAPK9, MAPK8, MAPK8IP1, DUSP8, MAP2K7, DUSP6	4.0
BIOCARTA	Regulation of MAP Kinase Pathways Through Dual Specificity Phosphatases	7	3.2E-07	DUSP4, DUSP2, DUSP1, MAPK3, MAPK8, DUSP8, DUSP6	19.0
KEGG	ErbB signaling pathway	12	4.7E-07	PAK7, PTK2, CDKN1B, PAK2, ERBB4, PAK4, MAPK3, MAPK9, MAPK8, CAMK2B, SHC1, MAP2K7	7.3
KEGG	Neurotrophin signaling pathway	12	1.6E-05	IRAK3, YWHAH, MAPK12, MAPK3, RAC1, YWHAQ, MAPK9, MAPK8, CAMK2B, SHC1, MAP2K7, IRS1	5.1
BIOCARTA	MAPKinase Signaling Pathway	12	7.5E-05	PAK2, MAPK12, MAP3K9, MAPKAPK5, MAPK3, RAC1, MAP3K10, MAPKAPK3, MAPK9, MAPK8, SHC1, MAP2K7	4.1
KEGG	Type II diabetes mellitus	7	2.1E-04	PKM2, SOCS1, MAPK3, MAPK9, MAPK8, PRKCE, IRS1	7.9
KEGG	Wnt signaling pathway	11	4.6E-04	CSNK2A2, CSNK1A1, ROCK2, PPP2CA, RAC1, CSNK1A1L, CSNK2B, MAPK9, MAPK8, WIF1, CAMK2B	3.9
KEGG	T cell receptor signaling pathway	9	8.4E-04	PAK7, PAK2, MAPK12, PAK4, MAPK3, ZAP70, MAPK9, CD4, MAP2K7	4.4
KEGG	Focal adhesion	12	1.2E-03	PAK7, PTK2, FLT1, PAK2, ROCK2, PAK4, MAPK3, RAC1, PDGFRA, MAPK9, MAPK8, SHC1	3.2
BIOCARTA	BCR Signaling Pathway	6	1.9E-03	MAPK3, RAC1, CAMK1, MAPK8, SHC1, BLNK	6.3
KEGG	Cell cycle	9	2.2E-03	CDC7, CDKN1B, YWHAH, CDKN2D, YWHAQ, BUB1B, TTK, ATR, WEE1	3.8
BIOCARTA	Angiotensin II mediated activation of JNK Pathway via Pyk2 dependent signaling	6	2.3E-03	PTK2, MAPK3, RAC1, CAMK1, MAPK8, SHC1	6.0
KEGG	Toll-like receptor signaling pathway	8	2.6E-03	MAPK12, TBK1, MAPK3, RAC1, MAPK9, MAPK8, TLR6, MAP2K7	4.2
KEGG	Fc epsilon RI signaling pathway	7	3.2E-03	MAPK12, MAPK3, RAC1, MAPK9, MAPK8, PRKCE, MAP2K7	4.8
KEGG	Insulin signaling pathway	9	3.5E-03	PRKAR2B, PHKG2, SOCS1, MAPK3, MAPK9, MAPK8, SHC1, IRS1, PCK1	3.5
BIOCARTA	Fc Epsilon Receptor I Signaling in Mast Cells	6	3.7E-03	PAK2, MAPK3, CAMK1, MAPK8, SHC1, MAP2K7	5.4
BIOCARTA	T Cell Receptor Signaling Pathway	6	6.4E-03	MAPK3, RAC1, ZAP70, CAMK1, MAPK8, SHC1	4.8
BIOCARTA	PTEN dependent cell cycle arrest and apoptosis	5	6.9E-03	PDK2, PTK2, CDKN1B, MAPK3, SHC1	6.2
BIOCARTA	Cell Cycle: G2/M Checkpoint	5	8.1E-03	YWHAH, CDKN2D, YWHAQ, ATR, WEE1	5.9
BIOCARTA	Links between Pyk2 and Map Kinases	5	1.3E-02	MAPK3, RAC1, CAMK1, MAPK8, SHC1	5.2
BIOCARTA	Agrin in Postsynaptic Differentiation	5	1.4E-02	MUSK, PTK2, MAPK3, RAC1, MAPK8	5.0
KEGG	Regulation of actin cytoskeleton	10	1.8E-02	FGFR2, PAK7, FGFR4, PTK2, PAK2, ROCK2, PAK4, MAPK3, RAC1, PDGFRA	2.5
BIOCARTA	Multiple antiapoptotic pathways from IGF-1R signaling lead to BAD phosphorylation	4	2.5E-02	YWHAH, MAPK3, SHC1, IRS1	6.0
KEGG	Insulin Signaling Pathway	4	2.9E-02	MAPK3, MAPK8, SHC1, IRS1	5.7
BIOCARTA	IGF-1 Signaling Pathway	4	2.9E-02	MAPK3, MAPK8, SHC1, IRS1	5.7
BIOCARTA	Integrin Signaling Pathway	5	3.2E-02	PTK2, BCR, MAPK3, MAPK8, SHC1	4.0
KEGG	Axon guidance	7	3.3E-02	PAK7, PTK2, PAK2, ROCK2, PAK4, MAPK3, RAC1	2.9
KEGG	GnRH signaling pathway	6	3.6E-02	MAPK12, MAPK3, MAPK9, MAPK8, CAMK2B, MAP2K7	3.2
KEGG	Adipocytokine signaling pathway	5	3.6E-02	MAPK9, MAPK8, IRS1, PCK1, CAMKK2	4.0
BIOCARTA	Deregulation of CDK5 in Alzheimers Disease	3	3.9E-02	CSNK1A1, CDK5R1, PPP2CA	9.0
KEGG	Renal cell carcinoma	5	4.1E-02	PAK7, PAK2, PAK4, MAPK3, RAC1	3.8
BIOCARTA	Growth Hormone Signaling Pathway	4	4.2E-02	SOCS1, MAPK3, SHC1, IRS1	4.9
BIOCARTA	Phospholipids as signalling intermediaries	4	4.7E-02	PTK2, MAPK3, RAC1, PDGFRA	4.7

Figure 3. Pathway enrichment of targets identified in the primary screen. Targets of which depletion caused at least a 2-fold reduction in CHIKV-GFP were functionally analyzed using Gene Ontology (GO) biological process terms.
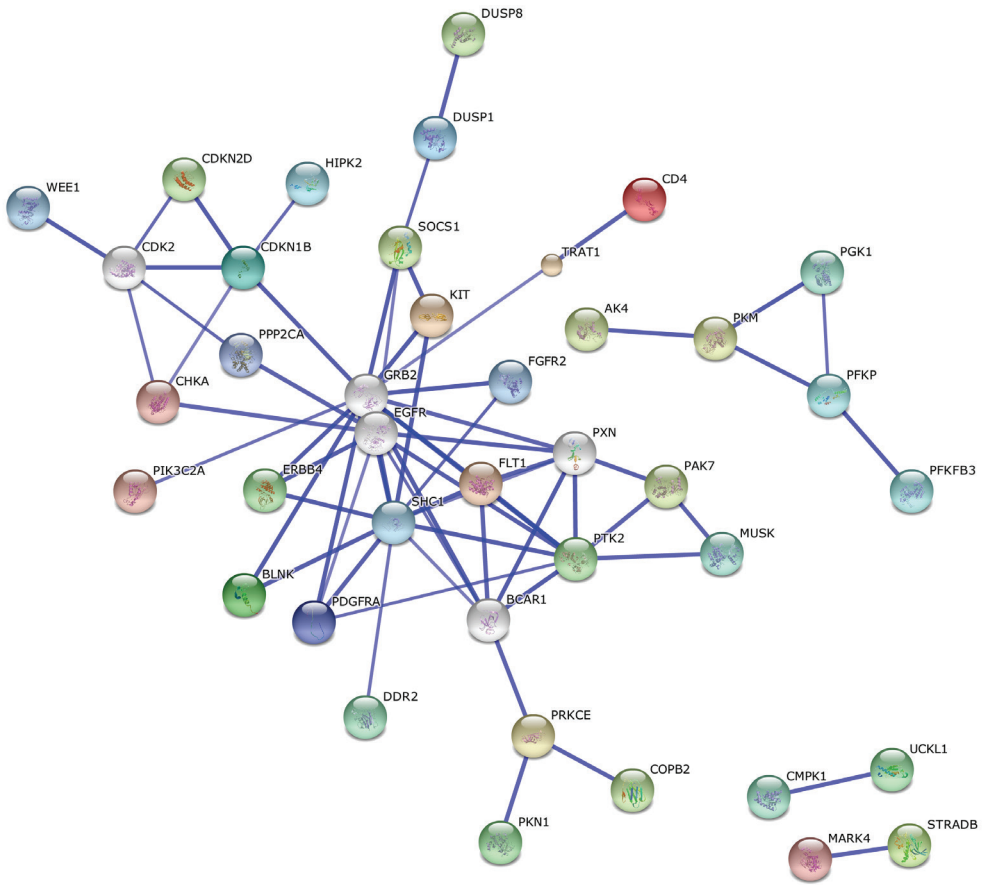
Figure 4. Network connectivity of potential proviral factors. STRING analysis (string-db.com) was used to determine the network connectivity of the 66 potential proviral factors identified in this screen. Confidence was set on high and 5 extra nodes (in white) were added. A thicker line represents a stronger association.

given the fact that also during the primary screen the observed increase in CHIKV-GFP was modest. The hits from the primary screen that we could not confirm might either constitute off-target hits, or the secondary siRNAs may have been less efficient.

Regulation of MAPK signaling by DUSPs. Mitogen-activated protein kinase (MAPK) signaling and regulation thereof was strongly represented in our data set (Figure 2, 3). MAPKs are serine/threonine kinases that regulate gene expression, protein translation, protein stability, protein localization and enzyme activity, thus influencing cell proliferation, differentiation, survival and death (208-210). Depletion of MAPKAPK3, MAPKAPK5, MAPK12, MAPK3, MAPK8, MAPK9, MAP2K7, MAPK8IP1, Rac1, or PAK2 resulted in at least a 2-fold reduction of CHIKV-GFP expression. Depletion of MAPKAPK3 even resulted in an 11-fold lower expression of GFP, although it did not reach statistical significance due to a relatively

large spread in GFP values. However, this high p-value does not reflect a lack of biological significance (as the effect on CHIKV-GFP was substantial); therefore we decided to include this hit in our secondary screen. MAPKAPK3 is phosphorylated by members of several MAPK signaling cascades (MEK/ERK, p38 MAPK and Jun N-terminal kinase), indicating that it is an integrative element of signaling of both mitogen- and stress-driven responses (211, 212). MAPKAPK3 is one of potential proviral targets that we could confirm in our secondary screen and is therefore likely involved in CHIKV replication (see Fig. 5A & discussion). The
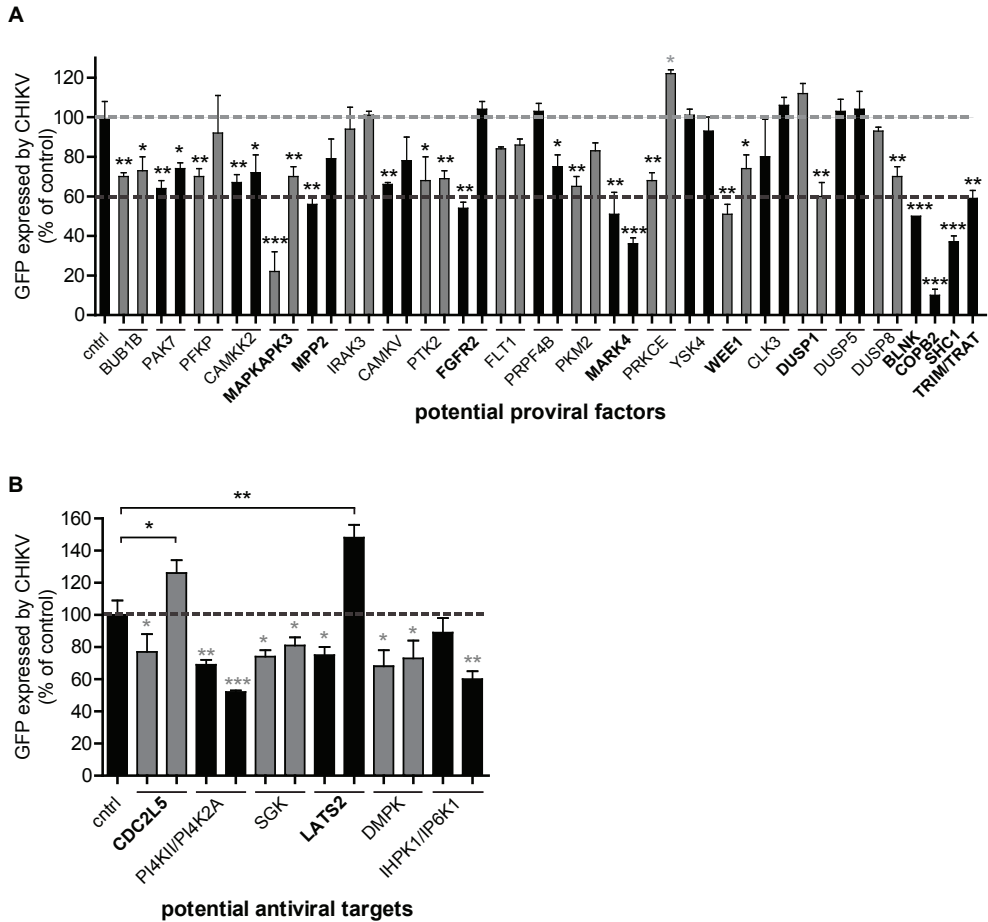
Figure 5. Secondary siRNA screen to validate potential proviral (A) or antiviral (B) factors. MRC5 cells were transfected with siRNA and 48h later infected with CHIKV-GFP, MOI 0.05. GFP expression was determined at 24 h.p.i. as a measure for viral replication and normalized to cells transfected with control siRNAs. Two single siRNA duplexes were used for each gene, with the exception of BLNK, COPB2, SHC1 and TRIM/TRAT, for which single siRNAs were tested. An initial hit was considered confirmed when at least one siRNA from the secondary screen reduced CHIKV-GFP with at least 40%. The values presented in the graphs represent the mean values of triplicate wells with the error bars indicating the standard deviation of the mean. P-value: * p<0.05, **p<0.01, ***p<0.001.

MAPK pathway is negatively regulated by dual specificity phosphatases (DUSPs). Our ranked hit list contains a substantial number of DUSPs/MKPs, including DUSP1/MKP-1, DUSP2/PAC1, DUSP4/MKP-2, DUSP5, DUSP6/MKP-3 and DUSP8 (Figure 6B). Strikingly, this includes all members of the mitogen- and stress-inducible nuclear MKP subfamily (DUSP1, DUSP2, DUSP4 and DUSP5). Several DUSPs have been implicated in viral replication (213-215), and it is therefore likely that they are also involved in CHIKV replication.

3

A
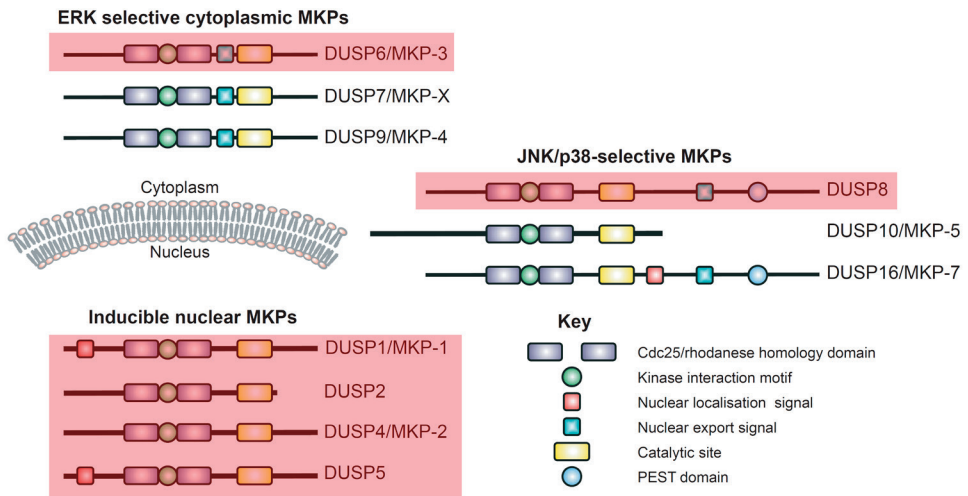
B

Accession	GeneID	pvalues	fold reduction
NM_004417	**DUSP1**	0.00911	6.1
NM_004420	**DUSP8**	0.02581	3.5
NM_004419	**DUSP5**	0.01451	3.1
NM_004418	**DUSP2**	0.01179	2.4
NM_001946	**DUSP6**	0.00908	2.3
NM_001394	**DUSP4**	0.00287	2.1
NM_020185	**DUSP22**	0.01234	2.0
NM_007207	**DUSP10**	0.21584	1.2

Figure 6. Structure, localization and classification of the DUSPs. (A) DUSPs (dual-specificity phosphates), also known as MKPs (MAPK phosphates), can be divided in three subclasses. The classification is based on their localization, substrate specificity and sequence similarity. The JNK/p38-selective MKPs are evenly distributed between nucleus and cytoplasm and are therefore depicted to the side. With red shading is indicated which DUSPs were identified in our kinome-directed siRNA screen targeting host factors involved in CHIKV replication. Adapted from (216). **(B)** DUSPs/MKPs identified in the primary siRNA screen. DUSPs of which depletion induced >3-fold decrease in CHIKV-GFP were considered a proviral hit (indicated in green). Hits with p-values of p<0.05 were considered significant (indicated in yellow).

DUSP1 expression during CHIKV replication. Several viruses induce the expression of DUSP1 mRNA (213-215). Therefore, we examined if CHIKV infection would also result in higher DUSP1 levels. Arsenite treatment causes oxidative stress and can function as a positive control for DUSP1 induction. Indeed, treating cells with increasing concentrations of arsenite resulted in increased DUSP1 protein levels (Figure 7A). Next, we examined DUSP1 protein levels at different time points post CHIKV infection (Fig. 7B).

DUSP1 remained undetectable in mock-treated, uninfected or CHIKV-infected cells. This suggests that CHIKV infection does not induce DUSP1 expression, at least not to levels that can be detected with our antibody. We cannot entirely exclude the possibility that the protein levels were too low to be detected by the antibody.

BCl is an allosteric inhibitor of DUSP1 and DUSP6 phosphatase activity. We examined the effect of BCl-treatment on CHIKV replication. MRC5 cells were infected with CHIKV (MOI 5) and 1 h p.i. various concentrations of BCl were added (Fig. 7C). As expected, BCl treatment resulted in increased levels of phosphorylated p38 MAPK, confirming that the compound blocks phosphatase activity. In addition, BCl treatment strongly reduced CHIKV nsP2 levels at 8 h p.i., suggesting that DUSP1 is needed for CHIKV replication, which is in line with the results obtained using our siRNA screen. However, when BCl was used during a multiple cycle experiment (using an MOI of 0.05, analyzed at 24 h p.i.) the effect of BCl on CHIKV-GFP seemed mostly caused by a general cytotoxic effect induced by the compound (Fig. 7D). Possibly, this is caused by an intolerance of the cells to prolonged DUSP1 inhibition. Alternatively, since DUSP signaling is highly regulated, it is possible that the cells have adapted to the presence of the compound during the extended experiment.

DISCUSSION

CHIKV is an arthrogenic alphavirus that re-emerged in 2004 and has caused unprecedented outbreaks in the years that followed. Licensed vaccines or approved antiviral drugs to prevent or treat CHIKV infection are currently not available. Alphaviruses rely, as other +RNA viruses, heavily on host factors for all steps of their replicative cycle. Unfortunately, the identity of the majority of these host factors involved in CHIKV replication remains elusive. Here we describe a kinome-directed RNAi study aimed at identifying host factors involved in CHIKV replication. We identified 66 potential proviral proteins that could be placed in cellular pathways likely involved in CHIKV replication, including DUSP-mediated control of MAPK signaling. Using a secondary screen we could confirm a substantial number of hits found in our primary screen, including DUSP1, MAPKAPK3, MARK4 and COPB2 (Figure 5). Not surprisingly, the dataset described here displays limited overlap with previously identified CHIKV host factors. Our approach focused mainly on kinases and related proteins, whereas the proteomics studies identified a varied subset of different proteins from the total cellular proteome. More importantly, the fundamentally different questions that are answered by siRNA and proteomics approaches (what happens to the virus if a host factor is depleted? vs. what happens to the host during infection?) obviously will lead to different results. We did identify

a handful of potential proviral proteins during CHIKV replication that were also found in a recent RNAi screen for SINV (COPB2, SHC1 and WEE1) (133). In addition, some proteins in our hit list were previously identified in various screens aimed at the identification of host factors involved in influenza virus replication. For example, knockdown of MAPK13 reduced CHIKV-GFP expression by 2-fold in our screen, and was identified in three independent influenza virus screens (217-219). Knockdown of CAMK2B or CDC42BPA reduced CHIKV-GFP expression 2-fold in our hands, and were both found in two influenza virus screens (193, 218, 219). FGFR2 knockdown reduced CHIKV-GFP 5-fold in both our primary and secondary screen, and was previously found in two influenza virus screens (193, 218).

Strikingly, we identified mostly proviral host factors in this kinome screen. This might be due to our experimental set-up, or to the fact that CHIKV is already replicating optimally in the chosen cell line. Alternatively, antiviral proteins might work in concert (redundancy in antiviral mechanisms), and reducing the levels of just one factor is not sufficient to have a significant effect on viral replication. In addition, the virus might already have evolved mechanisms to evade its antiviral effect, thus depletion has no additive effect. Some of the proteins that are
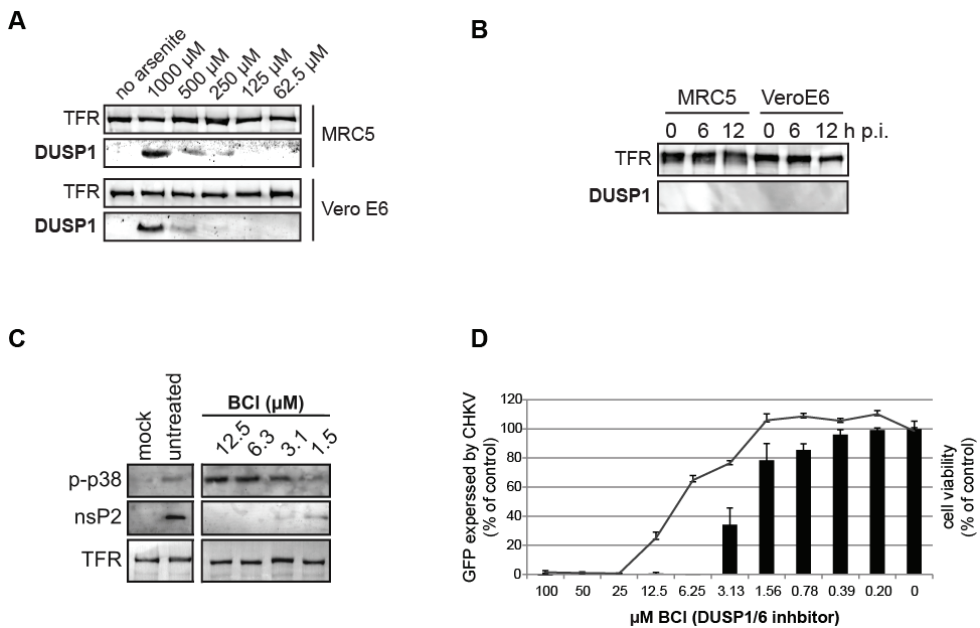
Figure 7. DUSP1 during CHIKV replication. (A) MRC5 or Vero E6 were treated with increasing concentrations of arsenite. DUSP1 protein levels were examined using western blot. **(B)** Cells were infected with CHIKV (MOI 5) and harvested at the indicated time points post infection. DUSP1 protein levels were examined using western blot. **(C)** MRC5 cells were infected with CHIKV (MOI 5), and 1 h p.i. various concentrations of the DUSP1/6 inhibitor BCl was added. Protein samples were harvested 8 h p.i. and the indicated protein levels were analyzed. **(D)** MRC5 cells were infected with CHIKV-GFP (MOI 0.05), and 1 h p.i. various concentrations of BCl was added. The cells were fixed 24 h p.i. and GFP expression was determined. Potential cytotoxicity was determined in parallel.

on the 'antiviral' side of the ranked hit list can easily be explained. For example, ROCK1 is described to be a pro-apoptotic protein. Depletion would increasecell viability and/or delay onset of (virus-induced) apoptosis.

Targets confirmed in the secondary screen

MAPKAPK3

Mitogen-activated protein kinase-activated protein kinase 3 (MAPKAPK3), is a serine/ threonine protein kinase that is activated by stress and growth inducers. Main functions of MAPKAPK3 (or MK3/3pK) are cell cycle control, posttranscriptional regulation of cytokines (e.g. TNF-α and IL-6) and regulation of chromatin and actin remodeling (reviewed in (212)). MAPKAPK3 was previously reported to play a role during HCV infection. HCV replication induced MAPKAPK3 RNA and protein levels, and MAPKAPK3 silencing reduced viral protein and infectious progeny levels (220). It was found that MAPKAPK3 binds to the HCV core protein, and may therefore be a functional part of the viral replication machinery (220). MAPKAPK3 was also implicated in influenza virus infection, where virally induced activation of MAPKAPK3 indirectly inhibited PKR activation and thus the block of cellular protein translation (221). Both HCV and influenza virus replication induce the upregulation of MAPKAPK3 in the infected cell. It would therefore be interesting to see if CHIKV also affects MAPKAPK3 protein levels, and whether overexpression of MAPKAPK3 would reduce CHIKV replication. MAPKAPK5 is a paralog and its depletion reduced CHIKV-GFP with 2.8-fold.

MARK4

Microtubule affinity-regulating kinase 4 (MARK4) is a proviral hit that was also confirmed in our secondary screen. Both single siRNAs reduced CHIKV-driven GFP expression with at least 50% (Figure 5A). MARK4 is a serine/threonine protein kinase that phosphorylates microtubule-associated proteins (reviewed in (222)). Phosphorylated microtubule-associated proteins detach from microtubules, which increases their dynamics and enables cell cycle control, cell division, and cell shape. Also MARK4 involvement with clathrin-coated vesicles during endocytosis was confirmed (223). CHIKV replication was demonstrated to be dependent on microtubules and clathrin-coated vesicle formation (224), possibly explaining its dependency on MARK4.

MMP2

Matrix metalloproteinase 2 (MMP2) belongs to a family that is involved in the breakdown of extracellular matrix in normal physiological processes. However, in recent years it was acknowledged that MMPs are also involved in other cellular processes, including host defence. At present, MMPs are considered important modulators of inflammation and innate immunity (reviewed in (225)), and may therefore very well be involved in CHIKV replication.

FGFR2 & SHC1

Fibroblast growth factor receptor 2 (FGFR2) is a membrane-spanning protein with a cytoplasmic kinase domain. The extracellular portion of the protein interacts with fibroblast growth factors, downstream inducing mitogenesis and differentiation. Ligand binding results in downstream activation of PLCγ, MAPK (MEK/ERK) and PI3-K/Akt signaling.

FGFR2 is an interesting confirmed hit, because it was also implicated in influenza virus replication in two independent RNAi screens (193, 218). Activated FGFR2 phosphorylates SHC1 (Src homology 2 domain containing transforming protein), another confirmed hit in our secondary screen. SHC1 is a signaling adapter protein that couples activated tyrosine kinases (such as FGFR2) to signaling pathways. For example, SHC1 can activate the Ras-Raf-MEK-ERK cascade by recruitment of the GRB2/SOS complex. There are three SHC1 isoforms of which one is a downstream target of p53 and is needed for the induction of apoptosis by stress-activated p53 (226). Depletion of SHC1 would therefore delay the onset of apoptosis, for example upon viral infection. Silencing of SHC1 reduced WNV but not DENV replication (128), and SHC1 was also implicated in HCV entry (227).

DUSPs – negative regulators of MAPK signaling. MAPKs play important roles in many signaling transduction pathways and are activated by a range of stimuli, including virus infection. MAPK activation is tightly controlled by phosphatases including dual-specificity phosphatases (DUSPs). DUSPs that are specifically dedicated to MAPK control are dubbed MAP kinase phosphatases (MKPs, reviewed in (216)). The DUSPs/MKPs differ in substrate specificity, tissue distribution, subcellular localization and sensitivity to extracellular stimuli, and can be subdivided accordingly (Figure 6A) (reviewed in (216, 228)). They form a negative regulatory network and determine the duration, magnitude and spatiotemporal profile of MAPK responses after stimulation. DUSPs may be very specific for a single MAPK or able to regulate multiple MAPK pathways. They can provide mechanisms of crosstalk between distinct MAPK pathways, as well as between MAPK signaling and other signaling modules (216).

Several DUSPs have been implicated in viral replication. For example, mRNA of DUSP4 and DUSP5 is upregulated during influenza virus (delNS1) infection, and the coronavirus infectious bronchitis virus induces the expression of DUSP1 to counteract the induction of IL-6 and IL-8 (213, 214). DUSP1 was also found to be upregulated in HIV-infected cells (215). Another study showed that DUSP10/MKP5 expression is induced by influenza virus (229). DUSP10 was shown to directly dephosphorylate IRF3, thus dampening the innate immune response. DUSP10-/- mice displayed increased levels of IRF3 activation and IFN expression and were resistant to influenza infection (229).

Here we show that siRNA-mediated depletion of DUSP1, DUSP2, DUSP4, DUSP5, DUSP6, DUSP8 and DUSP22 all resulted in at least a 2-fold reduction in CHIKV replication. We confirmed the involvement of DUSP1 and DUSP8 in our secondary screen. Transfection of siRNAs targeting DUSP5 had no effect in our secondary screen, but it needs to be noted that

knockdown efficiency was not determined. DUSP2, DUSP4, DUSP6 and DUSP22 did not meet our criteria for inclusion in the secondary screen. To our knowledge, this is the first time that DUSPs are linked to alphavirus replication. The kinase library also included DUSP22, but depletion of this target did not influence CHIKV replication. Of course, it is possible that sufficient knockdown was not achieved using this siRNA pool.

As mentioned earlier, several viruses can induce the upregulation of DUSP1 upon infection (213-215). Unfortunately, we were unable to demonstrate DUSP1 induction during CHIKV infection (Fig. 7B), although this does not necessarily mean it does not occur. High concentrations of arsenite were needed to visualize an induction of DUSP1 using western blot, indicating that the antibody might not be sensitive enough to show a more modest increase in DUSP1 protein levels upon CHIKV infection. RT-qPCR would be a more sensitive technique to monitor DUSP1 induction. Alternatively, it is possible that we examined DUSP1 protein levels at a time point too late in infection, as DUSP1 signaling is highly regulated and possesses negative feedback loops.

DUSPs/MKPs are connected to the innate immune response. For example, DUSP1 induction reduces the anti-inflammatory response and excessive cytokine induction. Overexpression of DUSP1 efficiently blocks MAPK-dependent transcription. In line with these observations, DUSP1/MKP-1 and DUSP10/MKP5 knockout mice display enhanced innate immune responses and cytokine production (229, 230). DUSP family members are considered promising drug targets to manipulate MAPK-dependent immune responses, both to boost or subdue immune responses in cancer, infectious diseases and inflammatory responses (231). It would be very interesting to further explore the (immunomodulatory) role of DUSPs during CHIKV replication.

Concluding remarks

With all large(r)-scale screens, concerns arise regarding the biological relevance of the data gathered. Off-target effects are an ever-present concern during siRNA experiments, especially during large-scale screens. Despite better-designed siRNA sequences and modifications, aimed to minimize off-target effects, it is unfortunately not possible yet to completely abolish these effects. The usage of siRNA pools does decrease the chance of off-target effects, as lower concentrations of each siRNA duplex can be used. However, caution still needs to be used when interpreting RNAi screening data, and independent validation is indispensable. False-positive or –negative hits remain a problem, which is illustrated by the fact that it is often difficult to confirm initial hits in secondary screens and additional follow-up experiments. In this study, we were able to confirm 12 of the 31 factors (~40%) tested in the secondary validation screen. It remains a possibility that we failed to confirm a number of initial hits because these genes are not expressed in the chosen cell line, and are thus to be considered false positives.

Host factors and viral factors together form a complex interaction network, and understanding the role of a single protein in this virus-host interplay proves challenging. In this study we

describe the identification of numerous host factors that are potentially involved in CHIKV replication, which can be extrapolated to several pathways that appear to play a role during CHIKV replication. We confirmed the involvement of several proteins/networks previously described, such as COPB2 and ribosomal proteins (RPSs), but also identified novel cellular factors involved in CHIKV replication, including the DUSP/MKP family. This dataset provides a valuable starting point for further research into the role of the numerous cellular proteins and pathways that affect CHIKV replication, which might eventually even lead to the development of (host-directed) antiviral strategies.

3

4.

MEK/ERK and p38 MAPK signaling is not induced by nor affecting chikungunya virus replication
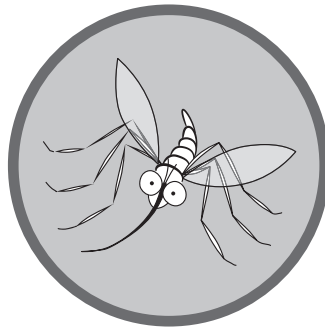
Florine E.M. Scholte, Ali Tas, Eric J. Snijder, and Martijn J. van Hemert[*]

Molecular Virology Laboratory, Department of Medical Microbiology, Leiden University Medical Center, Leiden, the Netherlands.

ABSTRACT

Mitogen-activated protein kinase (MAPK) signaling is an important part of the cellular response to viral infection. It plays an essential role in the expression of pro-inflammatory cytokines and is manipulated by many RNA viruses. With the exception of Venezuelan equine encephalitis virus (VEEV), little is known about the involvement of MAPK signaling in alphavirus replication. Activation of the extracellular signal-regulated kinase (ERK) cascade during VEEV infection was reported, and inhibition of ERK1/2 reduced virus replication. Surprisingly, ERK signaling responds differently to CHIKV infection. In contrast to VEEV infection, ERK1/2 signaling was not activated by CHIKV replication, and inhibition of ERK1/2 did not have any effect. CHIKV did induce phosphorylation of p38 MAPK very late in infection, but this was likely linked to apoptosis. Neither chemical inhibition nor stimulation of ERK or p38 MAPK signaling affected CHIKV replication, suggesting that they do not play an important role in CHIKV replication.

RESULTS

Mitogen-activated protein kinase (MAPK) cascades are important cellular signaling pathways that regulate many processes, including gene expression, proliferation, differentiation and immune responses (reviewed in (208)). MAPK signaling can be activated by a range of stimuli and mediates physiological and pathological changes in cell function by phosphorylating a plethora of proteins, including other kinases and transcription factors. Each MAPK pathway is formed by a three-tiered kinase cascade, consisting of a MAP kinase kinase kinase (MAPKKK, MAP3K, MEKK or MKKK), a MAP kinase kinase (MAPKK, MAP2K, MEK or MKK) and a MAPK, mediating an extremely sensitive response to various stimuli. The MAPK family consists of three major subgroups: extracellular signal-regulated kinase (ERK), p38 MAPK and c-Jun N-terminal kinase (JNK). In general, the ERK pathway is activated by mitogenic stimuli, whereas the other two pathways are mainly activated by stresses or inflammatory cytokines. Generally speaking, ERK activation promotes cell survival, whereas activation of p38 MAPK and JNK promotes apoptosis. Activation of MAPK signaling upon infection has been described for a number of RNA viruses, including influenza viruses (221, 232-235), hepatitis C virus (236), coxsackievirus B3 (237, 238) and infectious bronchitis virus (213). Except for Venezuelan equine encephalitis virus (VEEV) (239), little is known about the induction of MAPK signaling by alphaviruses and its involvement in replication. We therefore set out to determine the role of MAPK signaling during chikungunya virus (CHIKV) replication in cell culture. To investigate whether MAPK signaling is activated during CHIKV replication, we infected human fibroblast (MRC5) cells, which possess functional innate immune responses (192), and analyzed total and phosphorylated p38 MAPK and ERK1/2 levels (Fig. 1a). At 6 h p.i. no differences in p38 MAPK phosphorylation could be detected between infected and control cells, whereas a strong increase in phosphorylated p38 MAPK (p-p38 MAPK) levels was observed in infected cells by 12 h p.i. In contrast, ERK1/2 phosphorylation (p-ERK1/2) was not, or only marginally, induced by CHIKV infection at any of the time points analyzed.
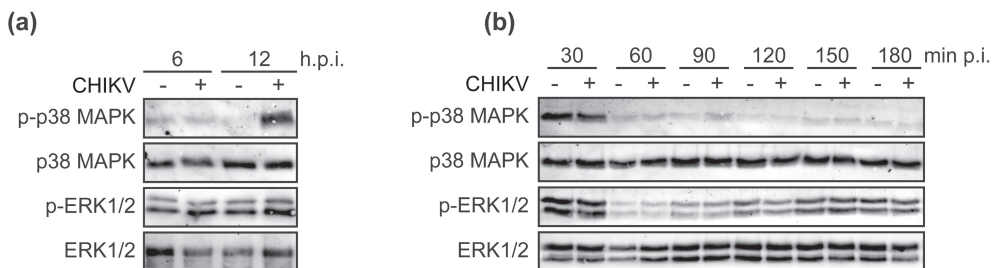
4

Figure 1. Phosphorylation of ERK1/2 and p38 MAPK in CHIKV–infected cells. (a)/(b) MRC5 cells were mock-infected or infected with CHIKV LS3 at an m.o.i. of 5 and lysed at the indicated time points post infection, essentially as described (69). Expression levels of the indicated proteins were determined by Western blotting using polyclonal antibodies specific for p38 MAPK, ERK1/2, and their respective phosphorylated forms (cat. nr. #9212, #9211, #9102, #9101, Cell Signaling Technology), or a rabbit CHIKV nsP1-specific antiserum.

CHIKV infection of Vero E6 cells yielded similar results (data not shown), indicating that this is not a cell type-specific observation. The distantly related alphavirus VEEV was reported to induce phosphorylation of ERK1/2 during the first two hours of infection (239), and we therefore also assessed MAPK activation in the first three hours of CHIKV infection at 30-min intervals. We did observe a strong increase in phosphorylation of both p38 MAPK and ERK1/2 at 30 min p.i., but this effect was detected in both CHIKV-infected and mock-infected cells (Fig. 1b). Therefore, it was most likely caused by the handling of the cells, which involved taking them out of the incubator and replacing the medium at 0 and 60 min p.i. The sharp increase in phosphorylated p38 MAPK observed at 30 min p.i. was short-lived, as barely any p-p38 MAPK could be detected by 60 min p.i., or at any of the other early time points tested (Fig. 1b). Also ERK1/2 phosphorylation was strongly reduced between 30 and 60 min p.i., although it slowly reappeared between 90 and 150 min p.i. Again, the same fluctuation in p-ERK1/2 levels was observed both in infected and control cells, indicating it did not result from CHIKV-infection, but rather from the experimental procedures (Fig. 1b). Taken together, these data suggest that also early in infection CHIKV did not induce p38 MAPK or ERK1/2 phosphorylation.

Next, we examined the effect of commonly employed chemical inhibitors of p38 MAPK (SB203580) or ERK1/2 MAPK (U0126) on CHIKV replication. MRC5 cells were infected with a GFP-expressing reporter CHIKV (CHIKV-GFP; m.o.i. 0.05) and various concentrations of the compounds were added at 1 h p.i. At 24 h p.i., CHIKV-driven GFP expression was determined as a measure of viral replication (Fig. 2a, b). In parallel, the viability of compound-treated, uninfected cells was determined using a colorimetric assay (CellTiter 96 Aqueous Non-Radioactive Cell Proliferation Assay; Promega), as described (69). Figures 2a and 2b show that CHIKV replication was not affected by these compounds, not even when cells were pretreated for 24 h (data not shown). To exclude the possibility that the absence of an effect on CHIKV replication was due to inactivity of the compound, we examined a downstream target of U0126.

This chemical inhibitor blocks MEK kinase activity and thus the phosphorylation of its downstream target ERK1/2 (240). Figure 2c shows that ERK1/2 phosphorylation was indeed blocked by U0126 at all concentrations tested, whereas it was not sensitive to SB203580 treatment, as expected. To determine if U0126 was still capable of blocking ERK1/2 phosphorylation during CHIKV infection, we treated infected (m.o.i. 5) and mock-infected MRC5 cells with various concentrations of U0126. Western blot analysis of samples harvested at 8 h p.i. showed that U0126 reduced the level of phosphorylated ERK1/2 to a similar extent in mock- and CHIKV-infected cells (Fig. 2c). Furthermore, treatment of cells with SB203580 or U0126 did not affect CHIKV capsid protein levels (Fig. 2c), which is in line with the results obtained with the eGFP-expressing reporter virus (Fig. 2a, b). The observation that U0126 does not affect CHIKV replication is in line with a previous publication on VEEV (239), although the same authors reported that another ERK1/2 inhibitor, Ag-126, did inhibit VEEV replication

(239). We therefore also tested this compound, but strikingly found that also Ag-126 does not affect CHIKV replication (Fig. 2d).

It is possible that pharmacological inhibition of MAPK signaling has no effect on CHIKV replication because the virus already blocks MAPK signaling, which would preclude observing an additional effect of chemical inhibitors. To investigate this possibility we incubated CHIKV-infected cells with compounds that are known to activate p38 MAPK (sorbitol) or ERK (ceramide C6) signaling (241, 242). MRC5 cells were infected with CHIKV-GFP (m.o.i. 0.05 for 24 h) and ceramide C6 or sorbitol was added at 1 h p.i. (Fig. 3a, b). Ceramide C6 reduced cell viability at concentrations above 5 μM. At non-cytotoxic concentrations (0.04-0.63 μM) it caused a slight stimulation of CHIKV replication, which did not reach statistical significance (Fig. 3a). Also in a single-cycle experiment (m.o.i. 5; analyzed at 8 h p.i.) ceramide C6 treatment did not stimulate replication, but even reduced CHIKV protein levels (nsP2) (Fig. 3c). The fact that ceramide C6 has no effect on the CHIKV-driven expression of GFP or the level of CHIKV nsP2, is in contrast with the data reported for VEEV, for which increased viral protein levels and progeny titers were reported upon ceramide C6 treatment (239). We therefore also

4
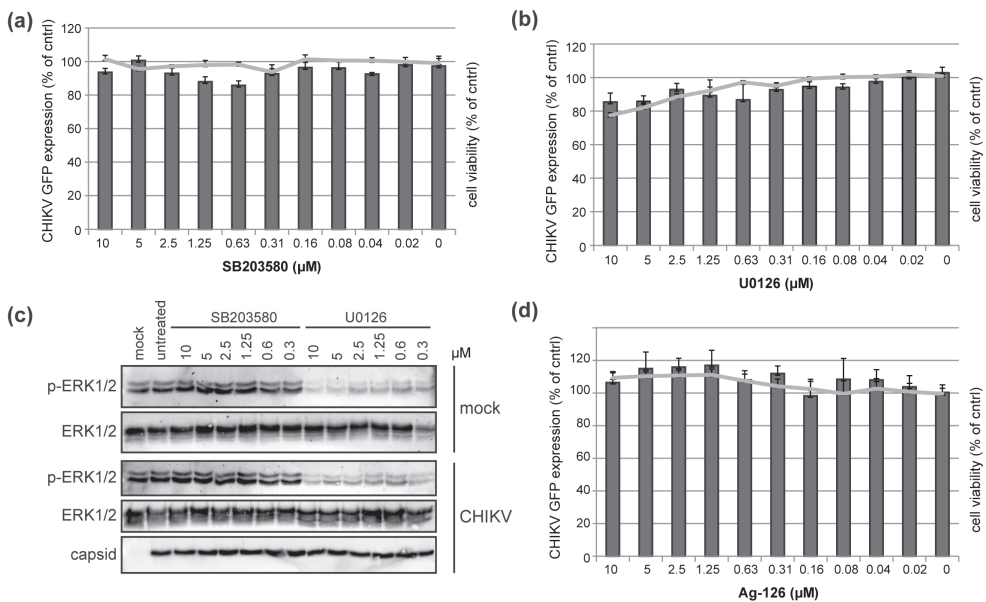
Figure 2. Chemical inhibition of ERK1/2 and p38 MAPK signaling during CHIKV replication. MRC5 cells were infected with CHIKV-GFP at an m.o.i. of 0.05 and at 1 h p.i. SB203580 **(a)**, U0126 **(b)** or Ag-126 **(d)** was added. Cells were fixed at 24 h p.i. and CHIKV-driven eGFP expression was determined using a Berthold plate reader as described (69). Cell viability was assessed using a colorimetric assay and is represented by the grey line. Both CHIKV-driven GFP expression and cell viability were normalized to an untreated control. **(c)** Western blot analysis of (p-)ERK1/2 and CHIKV capsid protein. MRC5 cells were infected with CHIKV LS3 (m.o.i. 5), the compounds were added 1 h p.i. and total cell lysates were harvested at 8 h p.i. In parallel, compound-treated mock-infected cells were analyzed as control. The values presented in graphs represent the mean values of triplicate experiments with the error bars indicating the standard deviation of the mean.

analyzed the production CHIKV infectious progeny by plaque assay and found that treatment with 2-4 μM of ceramide C6 slightly increased viral titers, but merely by 3-fold (Fig. 3e).

Similar to ceramide C6 treatment, non-toxic concentrations of sorbitol (2-125 mM) had no effect on CHIKV-GFP replication in MRC5 cells. The induction of p38 MAPK phosphorylation was clearly observed when using 250-1000 mM sorbitol (Fig. 3d), and no differences were observed between CHIKV- and mock-infected cells (data not shown). The sorbitol concentrations that induced p38 MAPK phosphorylation did not stimulate CHIKV replication, but rather blocked nsP2 expression completely. Analysis of infectious progeny titers released from sorbitol-treated cells (Fig. 3f) indicated that sorbitol concentrations above 125 mM reduced CHIKV titers, likely due to a general negative effect on cellular physiology. Lower sorbitol concentrations (15-62.5 mM) had no effect on CHIKV titers.

Taken together, our study establishes that, in contrast to what was reported for VEEV, the replication of CHIKV does not induce ERK1/2 signaling. CHIKV does induce p38 MAPK signaling, but only late in infection (12 h p.i.), when host shut-off has already been established and the first signs of cytopathology become apparent. Therefore, at this time point, p38 MAPK phosphorylation is most likely associated with the onset of cell death/ apoptosis, rather than with a belated antiviral response. In addition, CHIKV replication was not affected by the pharmacological modulation of p38 MAPK or ERK1/2 signaling, which further strengthens the notion that p38 MAPK and ERK signaling do not play a prominent role during CHIKV replication. This is rather surprising, as especially the ERK signaling cascade has been associated with the replication of several RNA viruses. For example, replication of Influenza virus, coxsackievirus B3 and Junin virus activates ERK1/2 signaling (233, 238, 243, 244). ERK1/2 are signal-transducing molecules that are activated in response to type I interferons (IFNα/β) (245, 246). Type I IFN is produced in many cells as an early innate immune response to virus infection, inducing an antiviral state and influencing the subsequent immune response. However, replication of many RNA viruses, including the aforementioned Influenza virus, coxsackievirus B3 and Junin virus, appears to benefit from the activation of ERK signaling, and inhibition of MEK/ERK reduces infectious viral progeny (233, 238, 243, 244). Virus-induced upregulation of RAS-RAF-MEK-ERK is thought to result in downregulation of the IFN response, thus enhancing viral replication (247, 248). These studies suggest that an activated Ras-Raf-MEK-ERK pathway renders cells less responsive to type I IFN, which can be restored with MEK inhibitor U0126. It is therefore striking that CHIKV does not induce ERK signaling, nor is it affected by pharmacological manipulation of this pathway.

This can be explained by the notion that CHIKV already blocks the IFN response at another level, for example by inducing transcriptional and translational host shut off (69, 249), or via the nsP2-mediated block in STAT phosphorylation (90). In addition, CHIKV does not induce a particular strong IFN response, especially when compared with other alphaviruses such as SFV. Nikonov et al. demonstrate that CHIKV generates less IFN-inducing RNAs that activate RIG-I signaling (250).
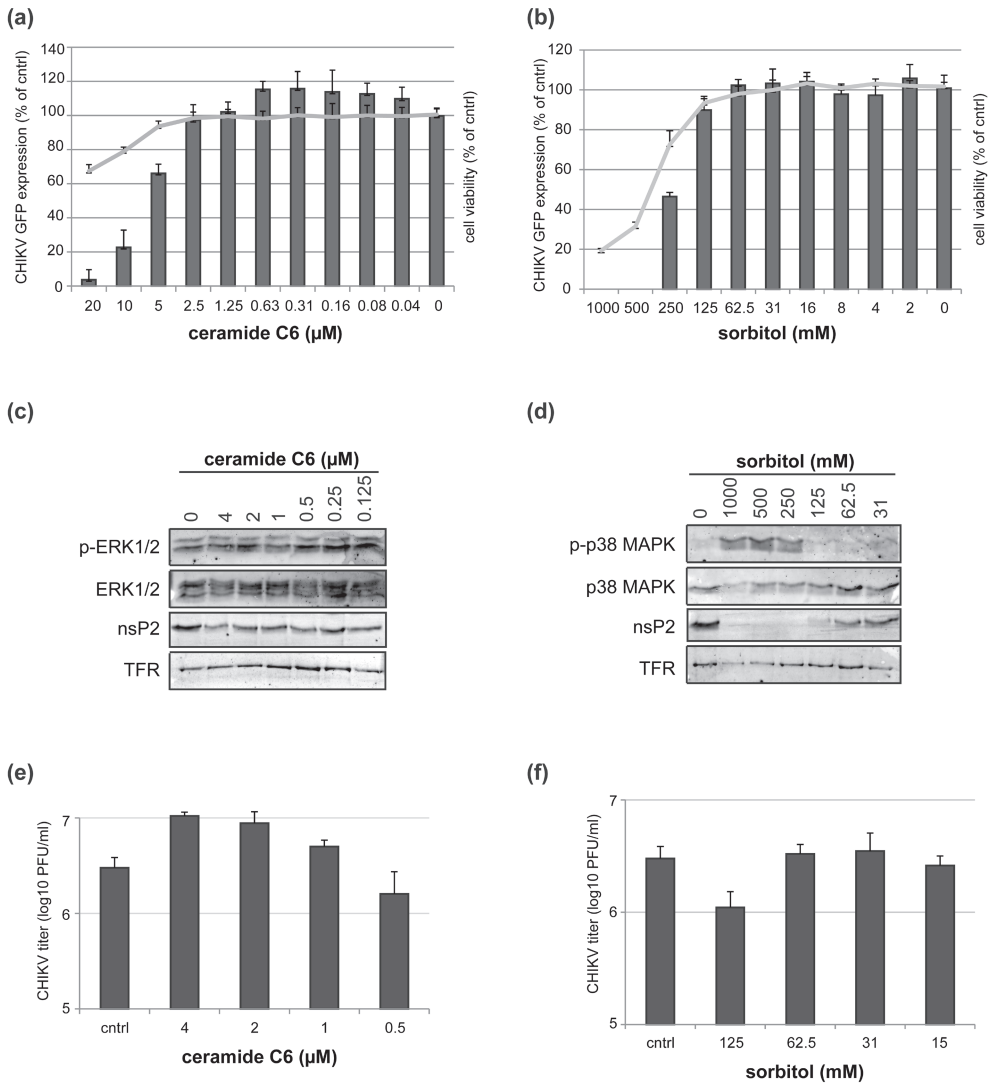
Figure 3. Chemical stimulation of ERK1/2 and p38 MAPK signaling during CHIKV replication. MRC5 cells were infected with CHIKV-GFP at an m.o.i. of 0.05 and ceramide C6 **(a)** or sorbitol **(b)** was added at 1 h p.i. Cells were fixed at 24 h p.i. and CHIKV-driven eGFP expression was determined using a Berthold plate reader. Both CHIKV-driven GFP expression and cell viability was normalized to an untreated control. **(c)** Western blot analysis of (p-)ERK1/2 and CHIKV nsP2 protein levels. MRC5 cells were infected with CHIKV LS3 (m.o.i. 5), ceramide C6 was added 1 h p.i. and total cell lysates were harvested at 8 h p.i. **(d)** Western blot analysis of (p-)p38 MAPK and CHIKV nsP2 protein levels. MRC5 cells were infected with CHIKV LS3 (m.o.i. 5), sorbitol was added at 1 h p.i. and total cell lysates were harvested at 8 h p.i. The transferrin receptor (TFR) was used as a loading control. Infectious progeny titers of ceramide C6 **(e)** or sorbitol **(f)** treated cells, determined by plaque assay. MRC5 cells were infected with CHIKV (m.o.i. 1), compound was added 1 h p.i. and viral titer was determined 24 h p.i. The values presented in graphs represent the mean values of triplicate experiments with the error bars indicating the standard deviation of the mean.
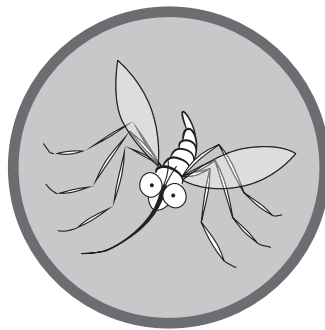
ACKNOWLEDGEMENTS

5.

Stress granule components G3BP1 and G3BP2 play a proviral role early in chikungunya virus replication

Florine E.M. Scholte[1], Ali Tas[1], Irina C. Albulescu[1], Eva Žusinaite[2], Andres Merits[2], Eric J. Snijder[1], and Martijn J. van Hemert[1#]

[1]Molecular Virology Laboratory, Department of Medical Microbiology, Leiden University Medical Center, Leiden, the Netherlands; [2]Institute of Technology, University of Tartu, Tartu, Estonia

ABSTRACT

Stress granules (SGs) are protein-mRNA aggregates that are formed in response to environmental stresses, resulting in translational inhibition. SGs are generally believed to play an antiviral role and are manipulated by many viruses, including various alphaviruses. GTPase-activating protein (SH3 domain)-binding protein 1 (G3BP1) is a key component and commonly used marker of SGs. Its homolog G3BP2 is a less extensively studied SG component. Here, we demonstrate that chikungunya virus (CHIKV) infection induces cytoplasmic G3BP1- and G3BP2-containing granules that differ from bona fide SGs in terms of morphology, composition, and behavior. For several Old World alphaviruses it has been shown that nonstructural protein 3 (nsP3) interacts with G3BPs, presumably to inhibit SG formation, and we have confirmed this interaction in CHIKV-infected cells. Surprisingly, CHIKV also relied on G3BPs for efficient replication, as simultaneous depletion of G3BP1 and G3BP2 reduced viral RNA levels, CHIKV protein expression, and viral progeny titers. The G3BPs colocalized with CHIKV nsP2 and nsP3 in cytoplasmic foci, but no colocalization with nsP1, nsP4, or dsRNA was observed. Furthermore, G3BPs could not be detected in a cellular fraction enriched for CHIKV replication/transcription complexes, suggesting that they are not directly involved in CHIKV RNA synthesis. Depletion of G3BPs did not affect viral entry, translation of incoming genomes, or nonstructural polyprotein processing but resulted in severely reduced levels of negative-stranded (and consequently also positive-stranded) RNA. This suggests a role for the G3BPs in the switch from translation to genome amplification, although the exact mechanism by which they act remains to be explored.

IMPORTANCE

Chikungunya virus (CHIKV) causes a severe polyarthritis that has affected millions of people since its reemergence in 2004. The lack of approved vaccines or therapeutic options and the ongoing explosive outbreak in the Caribbean underline the importance of better understanding CHIKV replication. Stress granules (SGs) are cytoplasmic protein-mRNA aggregates formed in response to various stresses, including viral infection. The RNA-binding proteins G3BP1 and G3BP2 are essential SG components. SG formation and the resulting translational inhibition are generally considered an antiviral response, and many viruses manipulate or block this process. Late in infection, we and others have observed CHIKV nonstructural protein 3 in cytoplasmic G3BP1- and G3BP2-containing granules. These virally induced foci differed from true SGs and did not appear to represent replication complexes. Surprisingly, we found that G3BP1 and G3BP2 were also needed for efficient CHIKV replication, likely by facilitating the switch from translation to genome amplification early in infection.

5

INTRODUCTION

Chikungunya virus (CHIKV) is a reemerging arbovirus that is currently causing a large outbreak in the Caribbean, affecting 41 countries and territories with ~1 million suspected and ~22,500 confirmed cases (http://www.cdc.gov/chikungunya/geo/americas.html). CHIKV will likely continue to spread throughout the Americas, as competent vectors are present in many countries in the region, including parts of the United States. The magnitude of this recent outbreak and the fact that CHIKV might soon be endemic in many parts of the world stress the need for a deeper understanding of this important human pathogen.

In the past decade, there has been an increasing interest in stress granules (SGs) and their interplay with the replication of a variety of viruses (reviewed in references (251, 252)). SGs are cytoplasmic ribonucleoprotein condensations formed in eukaryotic cells in response to environmental stress, and their appearance is linked to inhibition of translation (253). SGs contain stalled translation preinitiation complexes and are characterized by the presence of cellular mRNAs, translation initiation factors (e.g., eIF3 and eIF4B), the small ribosomal subunit, and RNA-binding proteins such as T-cell-restricted intracellular antigen 1 (TIA-1), TIA-1-related protein (TIAR), and GTPase-activating protein (SH3 domain)-binding protein 1 (G3BP1) (254-256). Environmental stress is sensed by double-stranded RNA (dsRNA)-dependent protein kinase (PKR) (257), PKR-like endoplasmic reticulum kinase (PERK) (258), general control nonderepressible 2 (GCN2) kinase (259), or heme-regulated inhibitor kinase (HRI) (260). Upon their activation, these kinases phosphorylate the α-subunit of eukaryotic translation initiation factor 2 (eIF2α), which, in turn, leads to dephosphorylation of G3BP1 and enables G3BP1 multimerization and subsequent SG formation (255). RNA-binding proteins TIA-1 and TIAR play a similar role in SG formation (261). The G3BP1 homolog G3BP2 is relatively poorly characterized, but it also localizes to SGs (262, 263). The G3BPs share a conserved acidic domain, a nuclear transport factor 2-like domain, a number of SH3 domain binding motifs, an arginine/glycine-rich box, and an RNA recognition motif. The last two elements are associated with RNA binding. The G3BPs may be partly functionally redundant, but there are also functional differences. For example, G3BP1 has phosphorylation-dependent endoribonuclease activity, which has not been reported for G3BP2 (264). Furthermore, only G3BP2 binds the N-terminal domain of IκBα (265) and differences in the number of SH3 domain binding motifs (PxxP) suggest that G3BP1 and G3BP2 differ in their interactions with other proteins. RNA viruses commonly induce SG formation via dsRNA replication intermediates that are sensed by PKR, although in some cases activation of PERK by ER stress is involved (reviewed in reference (251)). Alphaviruses also induce the formation of SGs or aggregates resembling those, as G3BP1-containing foci have been observed in cells infected with Semliki Forest virus (SFV) and Sindbis virus (SINV) or transfected with a CHIKV replicon (62, 63, 66, 138). Several laboratories have demonstrated colocalization and coimmunoprecipitation of alphavirus nsP2, nsP3, or nsP4 with G3BPs, and it was therefore speculated that these host proteins might be associated with the alphavirus replication machinery (62, 136-138, 266). The interaction of nsP3 with G3BP1 has been studied extensively (61, 137, 138, 266, 267), and

the induction of SGs by SFV has also been characterized in detail (61, 63, 66). SFV induces SGs early in infection; these are disassembled around 8 h postinfection (p.i.) following recruitment of G3BPs by nsP3 (63). Colocalization of G3BPs with SFV nsP1 and dsRNA suggests that they are recruited to replication and transcription complexes (RTCs) (63). Fros et al. showed that expression of CHIKV nsP3 was sufficient to induce G3BP-containing foci (62). The C-terminal repeat of SFV nsP3 that allows G3BP binding is conserved among Old World alphaviruses and was demonstrated to be responsible for the interaction between CHIKV nsP3 and both G3BPs as well (61), although earlier studies suggested the involvement of another nsP3 domain (62). In general, SG formation is considered an antiviral response that limits translation, and it has been hypothesized that alphaviruses prevent SG formation through the nsP3-mediated sequestering of G3BPs into cytoplasmic granules (62, 63). Despite the reported CHIKV nsP3-G3BP1 interaction and the SG-like aggregates that have been described to occur in cells transfected with a CHIKV replicon (62), it remains unclear whether such aggregates are formed in the context of a complete CHIKV infection and what the role of these SG-like G3BP aggregates might be. We therefore set out to elucidate the role of SGs, in particular that of the G3BPs, in the CHIKV replicative cycle. Rather than focusing only on G3BP1, we also analyzed the role of the often-overlooked G3BP2 and assessed the impact of their combined knockdown on CHIKV replication. We show that late in the CHIKV replication cycle, the bulk of G3BP1 and G3BP2 is not associated with the viral RTCs but sequestered in nsP3-G3BP aggregates, likely to prevent the formation of bona fide SGs. Surprisingly, we discovered that the G3BPs, in particular G3BP2, also have a proviral function early in CHIKV replication, as their knockdown delayed the accumulation of negative-stranded RNA. The G3BPs appear to play a regulatory role in the switch from genome translation to negative-strand RNA synthesis, perhaps by clearing ribosomes from the viral RNA, thus enabling it to serve as a template for RNA synthesis.

5

MATERIALS AND METHODS

Cells, viruses, and virus titration. Vero E6 and 293/ACE2 cells (157) were cultured and infected with CHIKV Leiden Synthetic 3 (LS3) (GenBank accession number KC149888) or enhanced green fluorescent protein (eGFP)-expressing reporter virus CHIKV LS3-GFP (GenBank accession number KC149887) as described previously (69). CHIKV LS3 is an infectious clone-derived virus with a genome sequence based on the consensus sequence of 'recent A226V strains', with growth kinetics and other properties similar to those of natural isolates (69). All experiments were performed with this virus unless indicated otherwise. CHIKV variants expressing *Renilla* luciferase either as an nsP3 fusion (ICRES1-P3Rluc) or from a duplicated subgenomic RNA (sgRNA) promoter (ICRES1-2SG-Rluc) were generated by standard cloning techniques, based on previously described constructs (117). The ICRES1 CHIKV variants were based on the sequence of natural isolate LR2006-OPY1. A replication-deficient variant (ICRES1-P3Rluc-nsP4-GAA) was created by mutating the GDD motif of nsP4 (amino acids [aa] 465 to 467) to GAA using QuikChange site-directed mutagenesis. CHIKV strain ITA07-RA1 (GenBank accession number EU244823) was isolated during the 2007 outbreak in Italy (69). Virus titers were determined by plaque assay on Vero E6 cells in six-well clusters in medium containing 1.2% Avicel RC-581 (FMC BioPolymer) as described previously (69). All work with live CHIKV was performed inside biosafety cabinets in a biosafety level 3 facility. CHIKV LR2006-OPY1-nsP4/FLAG, which was used for colocalization studies, encodes a 3× FLAG-tagged nsP4 (unpublished data). SINV-GFP was created by cloning eGFP into the previously described SINV MRE16 infectious clone (268) using standard techniques (details available upon request). CVB3-GFP (269) was a kind gift from Frank van Kuppeveld (Utrecht University, the Netherlands).

In vitro transcription and RNA transfection. *In vitro* transcription and RNA transfection were essentially performed as described previously (69). The ICRES1-P3Rluc and ICRES1-2SG-Rluc plasmids were linearized with NotI and transcribed using the mMessage mMachine SP6 kit (Ambion).

Indirect immunofluorescence microscopy. For visualization of SGs, Vero E6 cells were grown on coverslips and treated for 60 min with 0.5 mM sodium arsenite (Sigma). Disassembly of SGs was induced by treatment with 100 µg/ml of cycloheximide (CHX) for 30 min. Cells were processed for indirect immunofluorescence microscopy as described previously (69). Double-stranded RNA was detected using mouse monoclonal antibody J2 (English & Scientific Consulting; 10010500). Mouse anti-G3BP1 (BD Transduction Laboratories; 61126) or rabbit anti-G3BP1 (Aviva; ARP37713) was used to detect G3BP1. G3BP2 was detected with a rabbit antiserum (262) generously provided by Christer Larsson (Lund University, Sweden) or using a commercially available antibody (Assay Biotech; C18193-2). Other SG components were visualized using antibodies against eIF3α (Santa Cruz; sc-16377), TIA-1 (Santa Cruz; sc-1751), TIAR (Santa Cruz; sc-1749), p-eIF2α (Cell Signaling; 9721), or PABP (Santa Cruz, sc-32318).

Primary antibodies were detected with Cy3- or Alexa 488-conjugated secondary antibodies (Jackson/Life Technologies). Nuclei were stained with Hoechst 33342. The coverslips were analyzed using a Leica TCS SP5 confocal microscope and LAS AF Lite software (Leica).

To assess colocalization of G3BPs with CHIKV nsPs, Vero cells were grown on coverslips and infected with CHIKV LR2006-OPY1-nsP4/FLAG at a multiplicity of infection (MOI) of 5. At 6 h p.i. cells were fixed with 4% paraformaldehyde (PFA) in phosphate-buffered saline (PBS) and permeabilized with ice-cold methanol. The nsPs were visualized using mouse anti-FLAG, rabbit anti-o'nyong-nyong nsP1, anti-CHIKV helicase (nsP2), and anti-CHIKV nsP3 sera. Primary antibodies were detected with Alexa 488- or Alexa 568-conjugated secondary antibodies. The coverslips were analyzed using a Zeiss LSM 710 confocal microscope.

Western blot analysis. Western blot analysis was performed basically as described previously (69) using the primary antibodies listed in the previous paragraph. In addition, rabbit antisera against CHIKV nsP1 and nsP4 (raised against bacterially expressed full-length recombinant proteins), nsP2 (aa 453 to 798), and nsP3 (aa 1 to 320) were used. Rabbit antiserum against CHIKV E2 (161) was kindly provided by Gorben Pijlman (Wageningen University, the Netherlands).

Cellular fractionation experiments. The subcellular fractionation and isolation of active replication complexes from CHIKV-infected Vero E6 cells have been described elsewhere (270). Briefly, CHIKV LS3-infected cells were harvested at 6 h p.i. by trypsinization and lysed using a Dounce homogenizer. Unlysed cells, debris, and nuclei were pelleted by centrifugation at $1,000 \times g$, and the resulting postnuclear supernatant (PNS) was further fractionated in a $15,000 \times g$ pellet (P15) and supernatant (S15).

RNA interference. ON-TARGETplus SMARTpool small interfering RNAs (siRNAs) targeting G3BP1 (L-012099-00), G3BP2 (L-015329-01), the corresponding G3BP2-specific deconvoluted pool, and scrambled (non-targeting pool) control siRNAs (D-001810-10) were obtained from Dharmacon. C911 mutant siRNAs (271) and a nontargeting control siRNA were custom made by Sigma. 293/ACE2 cells were transfected with a final concentration of 50 to 100 nM siRNA using DharmaFECT1 (Dharmacon) according to the manufacturer's instructions. Cells that were transfected with two siRNA pools, targeting both G3BPs, received in total the same amount of siRNA and transfection reagent as the cells transfected with one SMARTpool. At 48 h posttransfection (p.t.), cells were infected with CHIKV or harvested to determine the silencing efficiency by Western blotting. To quantify the replication of the eGFP-expressing reporter virus, siRNA-transfected cells in 96-well clusters were infected with CHIKV LS3-GFP. Cells were fixed with 3% paraformaldehyde in PBS at 16 to 24 h p.i., depending on the MOI that was used. In parallel, the viability of siRNA-transfected cells was assessed at 48 h p.t. using the CellTiter 96 AQueous nonradioactive cell proliferation assay (Promega). Absorbance and eGFP expression were quantified using a Berthold Mithras LB 940 96-well plate reader.

Rescue experiments with an siRNA-resistant G3BP2 expression plasmid. G3BP2 expression plasmid pCMV-FLAG-G3BP2 was created by cloning the G3BP2 coding sequence obtained from MRC5 cDNA into p3xFLAG-CMV-10 (Sigma). Transcripts from the resulting construct are resistant to G3BP2 siRNAs 2 and 4, which target the 3′ untranslated region (UTR) of the natural G3BP2 mRNA. During rescue experiments the G3BP2 expression plasmid or the empty vector was cotransfected with the G3BP2 siRNAs using Lipofectamine 2000 (Life Technologies) according to the manufacturer's instructions. These cells were infected with CHIKV at 24 h p.t.

RNA isolation, gel electrophoresis, and in-gel hybridization. CHIKV RNA isolation using acid phenol, denaturing gel electrophoresis, and detection by in-gel hybridization with ^{32}P-labeled oligonucleotides specific for positive or negative-strand RNA were performed as described previously (69).

qRT-PCR. An internally controlled multiplex quantitative TaqMan real-time PCR (qRT-PCR) was used to determine the copy number of CHIKV genomic RNA (probe in nsP1-coding region) and total RNA (probe in E1-coding region). Briefly, forward (CTAGCTATAAAACTAAUAGAGCAGGAAATTG) and reverse (GACTTTTCCTGCGGCAGATGC) primers and a probe (Texas red-TCCGACATCATCCTCCTTGCTGGCG-black hole quencher 2 [BHQ2]) in the nsP1-encoding region were used in combination with a set of primers and 6-carboxyfluorescein (FAM)-labeled probe specific for the E1-coding region that has been described previously (272). Samples were analyzed using the SensiFast Probe (Bioline) or TaqMan Fast Virus 1-Step (ABI) qRT-PCR kit and a CFX384 Touch Real-Time PCR detection system (Bio-Rad) according to the manufacturers' instructions. Serial dilutions of *in vitro*-transcribed RNA were used as standards for copy number determination, and the cellular PGK1 mRNA was used as an internal control in multiplex reactions.

Luciferase assays. 293/ACE2 cells (5 × 10^3 per well) were seeded in 96-well plates and transfected with siRNAs (described above). After 48 h, the cells were infected with ICRES1-P3Rluc or ICRES1-2SG-Rluc at an MOI of 5. Alternatively, the cells were transfected with 100 ng of *in vitro*-transcribed full-length viral RNA (ICRES1-P3Rluc, ICRES1-2SG-Rluc, or ICRES1-P3Rluc-nsP4-GAA) using Lipofectamine 2000. At the desired time points, cells were lysed in passive lysis buffer (Promega) and luciferase substrate was added according to the manufacturer's instructions. Luciferase activity was measured in a GloMax 96 microplate luminometer (Promega).

Metabolic labeling and immunoprecipitation. Proteins synthesized in infected 293/ACE2 cells were labeled with [^{35}S]methionine and [^{35}S]cysteine ([^{35}S]Met/Cys) as described previously (69). Cells were lysed in Laemmli sample buffer, and antibody binding was carried out overnight at 4°C in AVIP buffer (20 mM Tris-HCl [pH 7.6], 150 mM NaCl, 1% NP-40, 0.1%

SDS, 0.5% deoxycholine) containing a final concentration of 0.5% SDS. Immune complexes were pulled down using a 1:1 mixture of protein A/G-Sepharose beads (GE Healthcare). Beads were washed three times in AVIP buffer before elution by boiling in Laemmli sample buffer for 5 min. Eluted proteins were separated in 10% polyacrylamide gels, and detection was done by autoradiography with phosphorimager screens and a Typhoon-9410 scanner (GE Healthcare).

Data analysis. Band intensities were quantified using Quantity One v4.5.1 (Bio-Rad) or ImageQuant TL software (GE Healthcare). Two or three independent experiments were quantified (one representative experiment is shown in figures). Statistical significance was calculated using a two-tailed Student t test in GraphPad Prism 5 (*, $P < 0.05$; **, $P < 0.01$; ***, $P < 0.001$).

5

RESULTS

CHIKV replication induces G3BP-containing foci that resemble SGs. A variety of viruses, including alphaviruses, induce the formation of SGs or SG-like cytoplasmic granules. To investigate whether CHIKV infection induces SGs, Vero E6 cells were infected and the localization of the SG marker G3BP2 was monitored (Fig. 1A). Arsenite, commonly used to induce SGs via oxidative stress, was employed as a positive control. In uninfected cells, G3BP2 displayed a diffuse cytoplasmic distribution, whereas in CHIKV-infected cells, G3BP2-containing foci appeared by 6 to 8 h p.i., continued to grow in size until ~10 h p.i., and remained present thereafter. Similar observations were made for G3BP1 (data not shown), and costaining for G3BP1 and G3BP2 revealed that the two proteins localize to the same puncta (Fig. 1B). These G3BP puncta did not possess the typical rounded morphology of arsenite- or heat shock-induced SGs but had a more rod-like appearance (Fig. 1A to C). Genuine SGs are dispersed upon cycloheximide (CHX) treatment, which stabilizes polysomes and prevents their disassembly, a crucial step in SG formation. As expected, arsenite-induced G3BP1 puncta readily dispersed upon CHX treatment. However, the CHIKV-induced G3BP1 puncta were not affected by CHX treatment (Fig. 1C). Identical observations were made when the granules were stained for G3BP2 (data not shown). To exclude the possibility that the induction of G3BP-containing puncta was a unique feature of the infectious clone-derived strain LS3, which is based on the consensus sequence of several CHIKV strains, we also analyzed cells infected with other strains. Natural isolate CHIKV ITA07-RA1 and CHIKV LR2006-OPY1-nsP4/FLAG, which is based on a clinical isolate from La Reunion, induced similar G3BP2-containing granules (Fig. 1D), suggesting that this is a general CHIKV property.

The composition of CHIKV-induced granules differs from that of genuine SGs. The composition of the CHIKV-induced granules was examined by immunostaining for several SG markers. In arsenite-induced SGs, G3BP1, G3BP2, TIA-1, TIAR, PABP, and eIF3 could readily be detected (Fig. 2). However, the CHIKV-induced granules were labeled only for G3BP1 and G3BP2, demonstrating that they differ not only in morphology and response to CHX treatment but also in protein composition. Some viruses, e.g., poliovirus (273), block SG formation by cleaving key SG components, like G3BP1. To assess whether the CHIKV-induced granules lack SG components due to their degradation or downregulation, the expression level of a number of SG markers in CHIKV-infected cells was determined. Western blot analysis showed that G3BP1 and G3BP2 protein levels did not change during the course of CHIKV infection (Fig. 3). Also, the expression levels of eIF3 and PABP remained unchanged during CHIKV infection. As expected, the level of eIF2α phosphorylation increased strongly in CHIKV-infected cells between 6 and 12 h p.i. (Fig. 3). The expression level of TIA-1 and TIAR proteins increased ~2-fold within 6 h p.i. (Fig. 3).

G3BPs colocalize with CHIKV nsP2 and nsP3 but not with nsP1, nsP4, or dsRNA. To investigate if the G3BP granules represent CHIKV replication complexes, we analyzed the possible colocalization of G3BP2 with CHIKV nsPs and dsRNA. Vero cells were infected with CHIKV at an MOI of 5, fixed at 6 h p.i., and immunostained for G3BP2 and CHIKV nsPs. This staining confirmed the previously reported nsP3-G3BP2 colocalization in cytoplasmatic granules (Fig. 4A). In addition, we observed nsP2-G3BP2 colocalization in similar foci. Strikingly, no colocalization of G3BP2 with nsP1 or nsP4 could be detected (Fig. 4A). Next, we analyzed the distribution of dsRNA and G3BP2 in CHIKV-infected cells (Fig. 4B). Only early in infection (4 h p.i.), when the dsRNA and G3BP2 signals were barely detectable, did there appear to be some colocalization of G3BP2 and dsRNA. At 6 h p.i. there was a very limited overlap between the dsRNA- and G3BP2-containing puncta, and at 8 h p.i. most of the dsRNA and G3BP2 signals were clearly not colocalizing (Fig. 4B). We did not observe complete

5
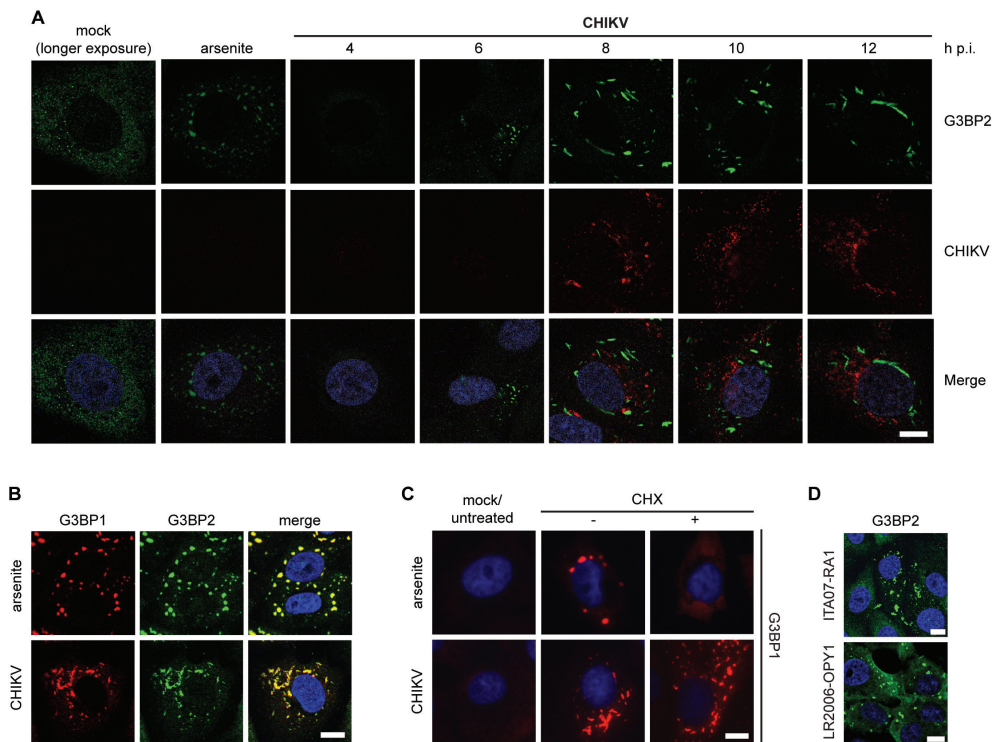
Figure 1. Induction of G3BP–containing foci by CHIKV replication. (A) Vero E6 cells were infected with CHIKV (MOI, 5), fixed at the indicated time points postinfection, and immunostained for G3BP2 and CHIKV. A longer exposure of mock-infected cells is shown to visualize diffuse G3BP2 staining. **(B)** CHIKV-induced granules (MOI, 5; 8 h p.i.) were costained for G3BP1 and G3BP2. **(C)** Vero E6 cells were infected with CHIKV (MOI, 5; analyzed at 8 h p.i.) or treated with arsenite (0.5 mM for 1 h) to induce SG formation and subsequently incubated with CHX (100 µg/ml for 30 min), followed by immunostaining for G3BP1. **(D)** G3BP2 immunostaining of Vero cells that were infected with CHIKV ITA07-RA1 or LR2006-OPY1-nsP4/FLAG (MOI, 5) and fixed at 6 h p.i. Scale bar: 10 µm.

colocalization between the nsP1 and nsP4 foci and the dsRNA puncta, which makes it impossible to unequivocally pinpoint the intracellular location of the RTC. This is likely because only a fraction of nsP1 and nsP4 is located within RTCs. Nonetheless, regardless of which of these markers most accurately identifies the CHIKV RTCs, clearly none of them colocalized with the G3BPs, suggesting that the G3BP granules did not represent the RTCs. All 4 nsPs are needed to form the RTC, but nsP2 and nsP3 also have other functions and different intracellular localizations outside the membrane-associated RTC. Thus, it is likely that the previously reported nsP3-G3BP interaction occurs with the pool of nsP3 that is not associated with the RTC.
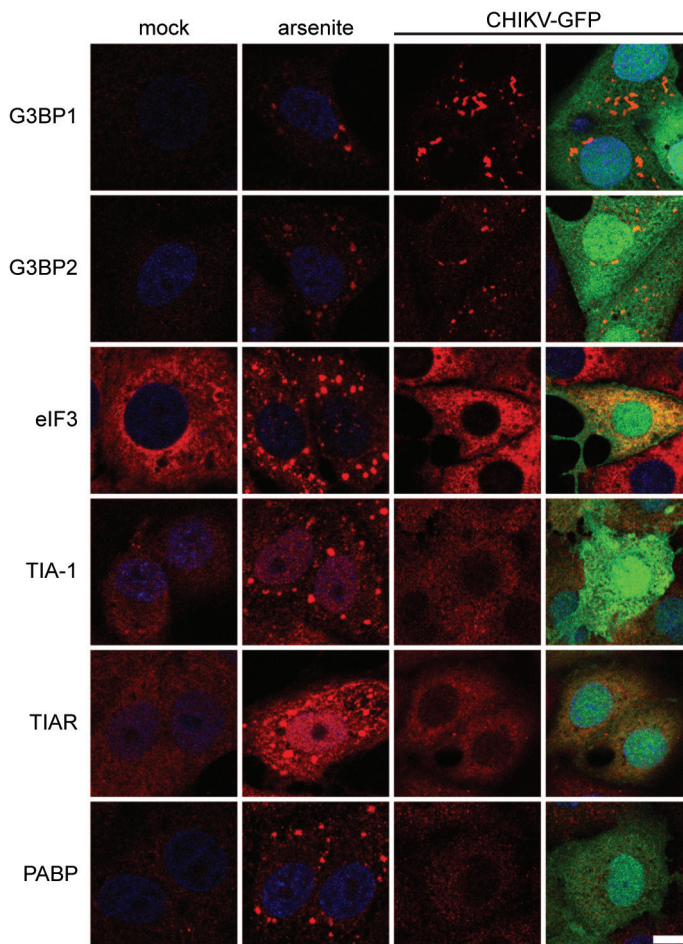
Figure 2. Composition of arsenite–induced SGs and CHIKV–induced granules. Vero E6 cells were treated with arsenite or infected with CHIKV-GFP (MOI, 5; fixed at 8 h p.i.). After fixation, the localization of the SG markers indicated to the left of each row was analyzed by immunofluorescence microscopy. The rightmost column shows the overlays of the signals of the SG marker and eGFP. Scale bar: 10 μm.

G3BPs are not associated with membrane-bound CHIKV replication complexes. To independently confirm that the G3BP granules observed in our immunofluorescence microscopy analysis were not the (membrane-associated) CHIKV RTCs, subcellular fractionation experiments were performed. CHIKV-infected cells were fractionated into a crude membrane fraction (P15) and a cytosolic fraction (S15). The P15 fraction contained 80 to 90% of the *in vitro* RNA synthesizing activity and was enriched in negative-strand RNA and nsP4, suggesting that it contained the majority of the membrane-associated RTCs (Fig. 4C). The bulk of nsP3 was found in the cytosolic S15 fraction. G3BP1 and G3BP2 were detected exclusively in the S15 fraction, suggesting that they are not associated with the RTCs. This supports the idea that the pool of nsP3 that associates with G3BPs differs from the one that is part of the RTC. The subcellular distribution of G3BPs in mock-infected cells was similar to that in CHIKV-infected cells (data not shown).

Depletion of G3BPs inhibits CHIKV replication. To further study the role of G3BP1 and G3BP2 in CHIKV replication, we assessed the effect of their knockdown on viral replication (Fig. 5). It was previously shown that G3BP expression is controlled by an apparent feedback mechanism that results in the upregulation of one G3BP when the expression of the other
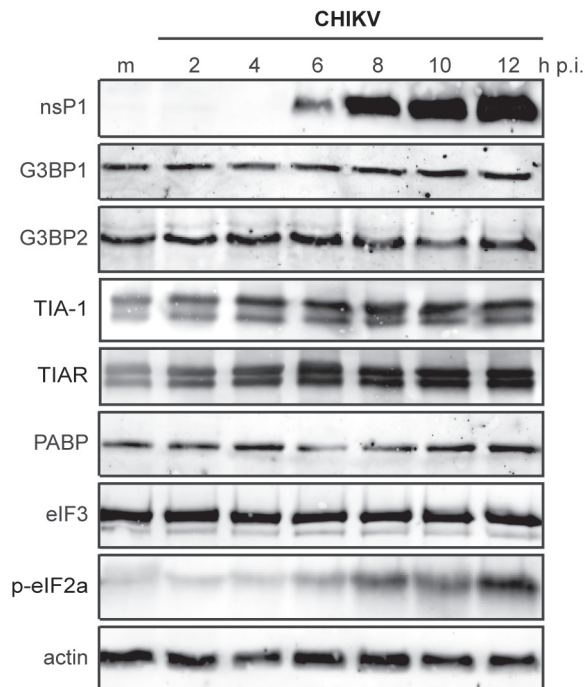

Figure 3. Levels of stress granule proteins during CHIKV infection. 293/ACE2 cells were infected with CHIKV (MOI, 5), and whole-cell lysates were prepared at the indicated time points postinfection. The expression level of the indicated proteins was determined by Western blotting. Mock-infected cells (m) were included as a negative control, and actin was used as a loading control.

is reduced (274). These observations suggest that the proteins are functionally linked, and therefore, the impact of simultaneous knockdown of G3BP1 and G3BP2 was also examined. Transfection of cells with the G3BP1-specific siRNA pool resulted in an ~90% reduction in G3BP1 expression and an ~2-fold increase in G3BP2 levels. The G3BP2 siRNA treatment achieved an ~80% reduction of G3BP2 levels, accompanied by an ~2-fold increase in G3BP1 expression (Fig. 5A). After treatment with a combination of G3BP1- plus G3BP2-targeting siRNAs, cells displayed about 40% and 30% of their original levels of expression of G3BP1
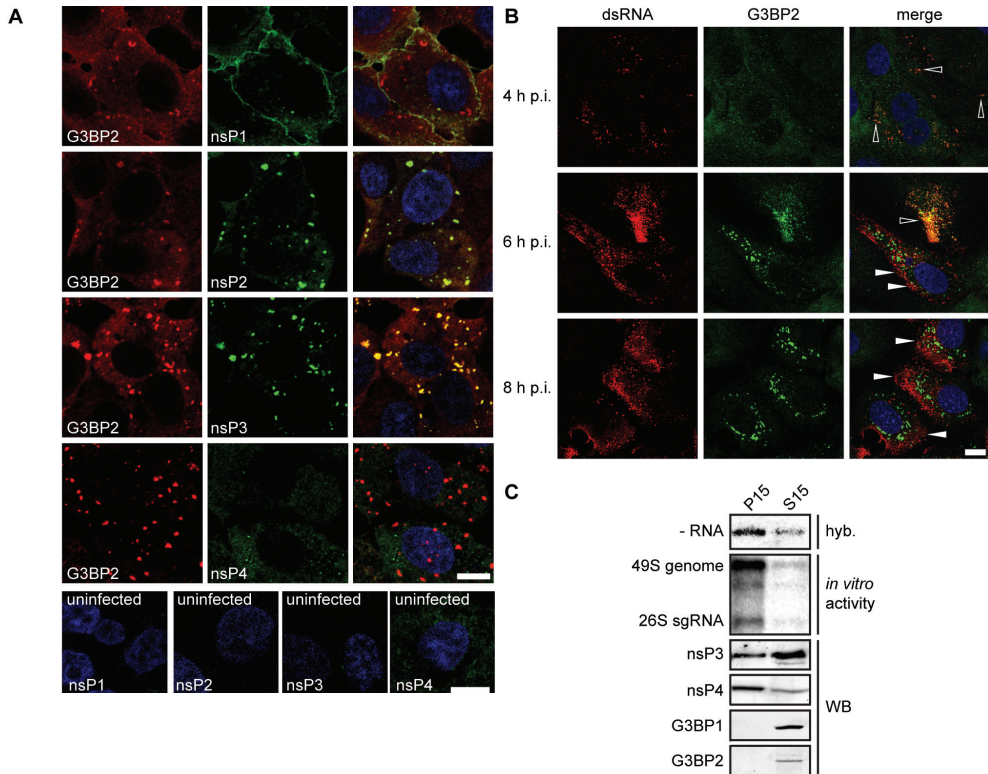
Figure 4. Localization of CHIKV nonstructural proteins, dsRNA, and G3BP. (A) Vero cells were infected with a CHIKV encoding nsP4-FLAG (LR2006-OPY1- nsP4/FLAG) at an MOI of 5, fixed at 6 h p.i., and stained for G3BP2, nsP1, nsP2, nsP3, and nsP4/FLAG. The bottom part of panel A shows the staining of uninfected cells, with the antibodies indicated in each frame. **(B)** Vero E6 cells were infected with CHIKV (MOI, 5), fixed at the indicated time points p.i., and stained for G3BP2 and dsRNA. Open arrowheads indicate colocalization of dsRNA with G3BP2, whereas closed arrowheads indicate some examples of nonoverlapping signals. Scale bar: 10 μm. **(C)** Distribution of G3BPs and CHIKV nsPs between the "heavy membrane" fraction P15 and "cytoplasmic" fraction S15. Vero E6 cells were infected with CHIKV (MOI, 5) and then harvested, lysed, and subjected to subcellular fractionation at 6 h p.i. The presence of CHIKV negative-stranded RNA was determined by hybridization with a specific probe (hyb). The RNA synthesizing activity was assessed with an *in vitro* assay in which the incorporation of [^{32}P]CTP into CHIKV RNA was determined (270). The levels of CHIKV nsP3, nsP4, G3BP1, and G3BP2 in the P15 and S15 fractions were determined by Western blotting (WB).

and G3BP2, respectively. The siRNA-transfected cells were infected with a CHIK reporter virus at MOIs of 0.05, 1, and 5, and cells were fixed at 24, 20, and 16 h p.i., respectively. The eGFP expression was quantified, and cell viability assays performed in parallel showed no negative effect of G3BP depletion (Fig. 5B). Despite efficient knockdown, G3BP1 depletion had little effect on CHIKV replication. G3BP2 depletion reduced eGFP levels in cells infected at an MOI of 0.05 by ~55%, and the combined depletion of G3BP1 and G3BP2 reduced eGFP levels even further (~80%). The effect of G3BP depletion was less pronounced in cells infected at an MOI of 1 or 5 (Fig. 5B). Because silencing of G3BP1 alone had little effect, and because the simultaneous depletion of both G3BPs exerted a stronger effect on CHIKV replication than depletion of G3BP2 alone (Fig. 5C), all subsequent knockdown experiments were done with siRNA pools that targeted G3BP1 and G3BP2 simultaneously. The combined depletion of G3BP1 and G3BP2 resulted in severely reduced negative-strand RNA levels, which were about 85 to 90% lower (6 to 8 h p.i.) than in control cells (Fig. 5D). Consequently, positive-stranded RNA levels were also affected (80 to 85% lower than in control cells). The strongly reduced genomic RNA levels in G3BP-depleted cells resulted in a reduction of nsP and E2 levels (Fig. 5E). It is noteworthy that G3BP depletion affected the accumulation of nsP3 more strongly than the other nsPs, as the amount of protein could not be quantified at 6 h p.i., and was ~80% lower at 8 h p.i. than in control cells. Viral progeny titers from G3BP-depleted cells were approximately 1 log lower at 8 h p.i. (Fig. 5F). In conclusion, G3BP2 depletion caused an ~2-h delay in the accumulation of viral RNA and proteins and the production of infectious progeny, while a less pronounced effect was observed at later time points, suggesting that the G3BPs play a role early in the CHIKV replication cycle.

The sensitivity of CHIKV replication to G3BP depletion is striking, as SINV was previously reported to replicate slightly better in G3BP-depleted cells (274). We therefore also infected G3BP-depleted cells with a SINV reporter virus (SINV-GFP) to investigate the effect of G3BP depletion. As observed for CHIKV, simultaneous depletion of the two G3BPs also inhibited SINV replication in our experimental setup (Fig. 5G). Depletion of G3BP1 alone barely affected SINV replication, whereas depletion of G3BP2 alone strongly affected SINV replication (Fig. 5G).

To ensure that the observed inhibition of CHIKV (and SINV) replication was not due to a general negative effect of G3BP2 depletion on cellular homeostasis, we infected G3BP-depleted cells with an unrelated reporter virus: the picornavirus coxsackie B3 virus (CVB3-GFP). CVB3 is not expected to be negatively affected by G3BP2 depletion, as its protease has been reported to cleave G3BP1 (275) and possibly also G3BP2. Indeed, G3BP2-depletion had no effect on GFP expression by CVB3, and depletion of G3BP1 alone or both G3BPs simultaneously even enhanced CVB3-GFP replication (Fig. 5G). This demonstrated that CVB3 replication was not negatively affected in G3BP-depleted cells, suggesting that the knockdown did not lead to serious negative effects on cellular physiology.

Another issue that needs to be addressed when using siRNAs is the possibility that the observed phenotype is due to off-target effects. Therefore, the pools of four G3BP siRNAs
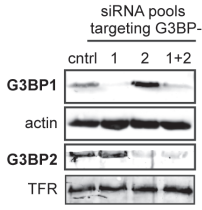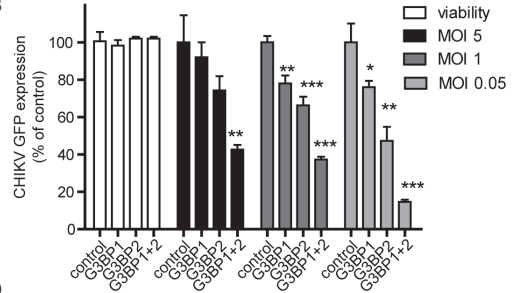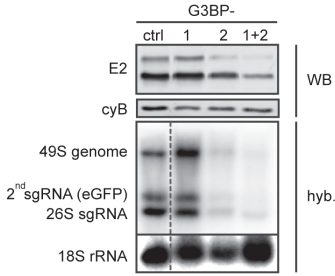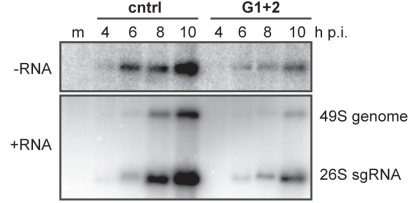
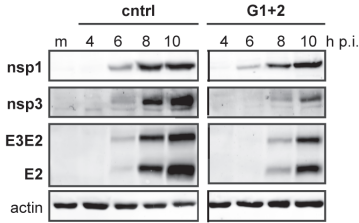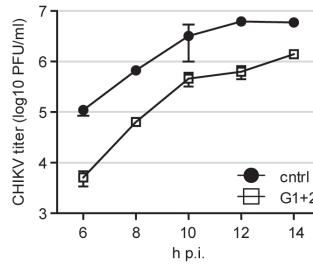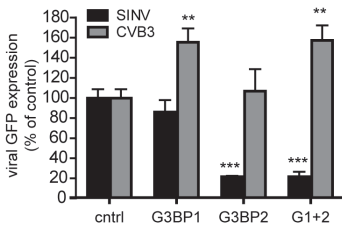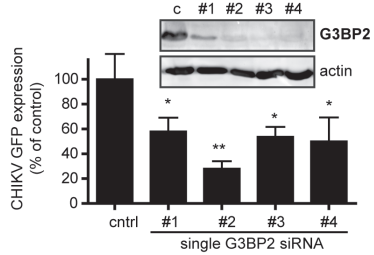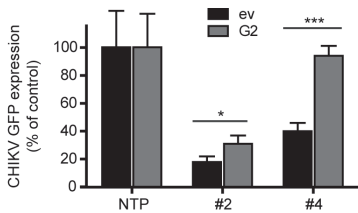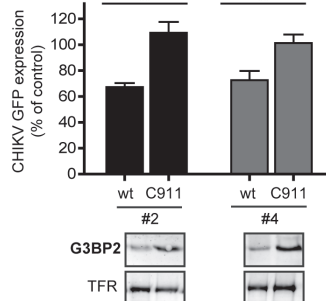**Figure 5. Effect of siRNA–mediated depletion of G3BP1 and G3BP2 on CHIKV replication. (A)** Western blot analysis of the protein levels of G3BP1 and G3BP2 in 293/ACE2 cells transfected with control siRNAs or those targeting G3BP1, G3BP2, or both. The transferrin receptor (TFR) and actin were used as loading controls. **(B)** Cell viability and CHIKV-driven eGFP expression in cells that were depleted of G3BP1 and G3BP2 and subsequently infected with reporter virus CHIKV LS3-GFP at an MOI of 5 (black bars), 1 (dark gray bars), or 0.05 (light gray bars). Cell viability was determined at 48 h p.t. (white bars), and eGFP expression was quantified at 16, 20, or 24 h p.i., depending on the MOI used. **(C)** G3BP-depleted, CHIKV-infected cells (MOI, 0.05) were analyzed for E2 expression (by Western blotting using cyclophilin B as a loading control) and positive-strand RNA levels (by in-gel hybridization [hyb]) at 24 h p.i. **(D)** In-gel hybridization analysis of CHIKV RNA levels with probes specific for negative-strand (−RNA) or positive-strand (+RNA) RNA in G3BP-depleted 293/ACE2 cells. The cells were infected with CHIKV (MOI, 5) 48 h after siRNA transfection, and total RNA was isolated at the indicated time points. cntrl, control. **(E)** Western blot analysis of CHIKV protein expression levels after G3BP depletion. 293/ACE2 cells were transfected with control or G3BP-specific siRNAs and 48 h later infected with CHIKV (MOI, 5). Cell lysates for Western blot analysis were harvested at the indicated time points and analyzed for the viral proteins indicated, using actin as a loading control. **(F)** Infectious progeny titers of CHIKV-infected cells (MOI, 5) that were transfected with control or G3BP-specific siRNAs. **(G)** G3BP-depleted 293/ACE2 cells were infected with SINV-GFP or CVB3-GFP (MOI, 1) and fixed at 16 or 10 h p.i., respectively. The level of GFP expressed by the viruses was normalized to infected cells transfected with control siRNAs. **(H)** 293/ACE2 cells were transfected with 50 nM individual siRNA duplexes (deconvoluted pool) and infected with CHIKV-GFP (MOI, 1) 2 days later, followed by quantification of GFP expression at 20 h p.i. The (remaining) level of G3BP2 expression was determined by Western blotting. **(I)** Analysis of GFP expressed by CHIKV in cells depleted for G3BP2 with siRNA 2 or 4 and cotransfected with a plasmid encoding siRNA-resistant G3BP2 (G2) or an empty vector (ev). **(J)** Cells were transfected with C911 mutant siRNAs (C911) or the corresponding G3BP2-targeting siRNAs (wt), followed 24 h later by infection with CHIKV-GFP (MOI, 1) and quantification of GFP expression at 20 h p.i. GFP levels were normalized to cells transfected with a nontargeting control siRNA (100%). G3BP2 knockdown efficiency at 24 h p.t. was determined by Western blotting.

were deconvoluted and the siRNA duplexes were tested individually. As anticipated based on the results obtained with the G3BP1 pool, none of the four single G3BP1 siRNAs had a strong effect on CHIKV replication, despite the fact that 3 out of 4 siRNAs (1 to 3) significantly reduced G3BP1 levels (data not shown). Transfection of 3 out of the 4 individual G3BP2 siRNAs (2, 3, and 4) resulted in a strong reduction in G3BP2 expression (Fig. 5H), whereas transfection of siRNA 1 was somewhat less effective in reducing G3BP2 protein levels. Single siRNA duplexes 2 to 4 reduced CHIKV replication to various extents, but all single siRNAs reduced GFP expression by ~50% or more (Fig. 5H). It should be noted that a larger effect was not expected, as depletion of G3BP2 alone with the SMARTpool resulted in a similar reduction in GFP expression (Fig. 5B and C). The correlation between the level of CHIKV replication and remaining G3BP expression indicates that the siRNA-mediated inhibition is unlikely due to off-target effects. This is further supported by the fact that expression of an siRNA-resistant form of G3BP2 restored CHIKV replication to ~30 to 90% of that in control cells (Fig. 5I). The rescue of CHIKV replication by G3BP2 overexpression was more efficient in cells in which G3BP2 was depleted with siRNA 4 than in those transfected with siRNA 2. This suggests that besides G3BP2 depletion, siRNA 2 also caused some off-target effects. To further exclude potential off-target effects, we employed C911 mutant siRNAs (271), in which the "targeting"

residues 9 to 11 are mutated. These mutant siRNAs should no longer induce knockdown of the target while still causing the same off-target effects as the corresponding targeting siRNA. We designed and tested C911 mutant siRNA corresponding to G3BP2 single siRNAs 2 and 4 (Fig. 5J). These custom-synthesized targeting siRNAs did not deplete G3BP2 protein levels to the same extent as the original (modified) Dharmacon siRNAs and only reduced CHIKV replication by ~30%. However, no reduction in CHIKV-driven eGFP expression was observed in cells transfected with the corresponding C911 mutant siRNAs, indicating that the inhibition of CHIKV replication was due to G3BP2 depletion rather than off-target effects of the siRNAs (Fig. 5J).

G3BP levels do not influence nonstructural polyprotein processing. We noticed that—especially early in infection—G3BP depletion affected the level of structural proteins (E2) more than that of nsPs (Fig. 5E). The expression of structural proteins is dependent on sgRNA synthesis, which for alphaviruses is controlled by the extent to which nsP123 is proteolytically processed (64). SFV mutants lacking the G3BP-binding domain exhibited delayed polyprotein processing, resulting in the appearance of an extra uncleaved processing intermediate (63). Therefore, we assessed CHIKV polyprotein processing in G3BP-depleted cells. Pulse-chase metabolic labeling with [^{35}S]Met/Cys, followed by immunoprecipitation of nsP3, showed no differences in the kinetics of processing of the P123 precursor when G3BP-depleted and control cells were compared (Fig. 6A). The total level of viral protein was lower in G3BP-depleted cells at this early time point, but P123 was processed at the same rate and no additional uncleaved intermediates were found, indicating that polyprotein processing was not specifically affected by the absence of G3BP.

G3BP levels do not affect CHIKV entry or RNA synthesis. We noticed that viral protein accumulation, as analyzed by Western blotting, appeared to be delayed by ~2 h in G3BP-depleted cells. Comparison of the kinetics of CHIKV RNA accumulation in control and G3BP-depleted cells by qRT-PCR revealed that RNA production was also delayed by ~2 h but occurred at the same rate, since a semilog plot of the copy number over time had the same slope as the curve obtained for control cells (Fig. 6B). These results suggested a role for G3BPs early in the CHIKV replication cycle. We therefore investigated whether G3BPs are involved in viral entry by transfecting control and G3BP-depleted cells with *in vitro*-transcribed CHIKV full-length genomic RNA, a procedure that bypasses virion attachment and entry. The transfection of control cells with CHIKV RNA led to readily detectable amounts of negative-strand RNA by 4 h p.t., after which genome and sgRNA levels increased rapidly in the next 2 h (Fig. 6C). Also in G3BP-depleted cells replication of transfected CHIKV RNA was detected, although negative-strand RNA levels were much lower than in control cells and the accumulation of positive-strand RNA was impaired (Fig. 6C). The observation that bypassing CHIKV entry still resulted in a delayed replication indicates that the G3BPs are involved in an early, but postentry, step of the CHIKV replication cycle. The effect of G3BP depletion in

these transfection experiments appeared to be smaller than that observed upon (low-MOI) infection (Fig. 5D). This may have been due to the large amount of RNA transfected into the cells, probably mimicking a very high-MOI infection, which makes the effect of G3BP depletion less pronounced (as shown in Fig. 5B) for reasons discussed below. However, we cannot formally exclude a (minor) additional role for the G3BPs during entry and/or uncoating.

G3BP depletion does not affect translation, but G3BPs appear to regulate the switch to minus-strand synthesis. Our experiments indicated that the G3BPs are likely involved in an early step of the CHIKV replication cycle. This could be either translation or early (negative-strand) RNA synthesis. Unfortunately, it is difficult to study translation and genome replication separately, as these processes are interdependent. Incoming viral genome first serves as an mRNA for nsP production and then is copied into the negative-strand template for genome replication, which produces novel positive-strand RNA that, in turn, serves as an mRNA for polyprotein production. However, infection at a very high MOI is thought to provide enough input RNA to render translation largely independent of newly synthesized
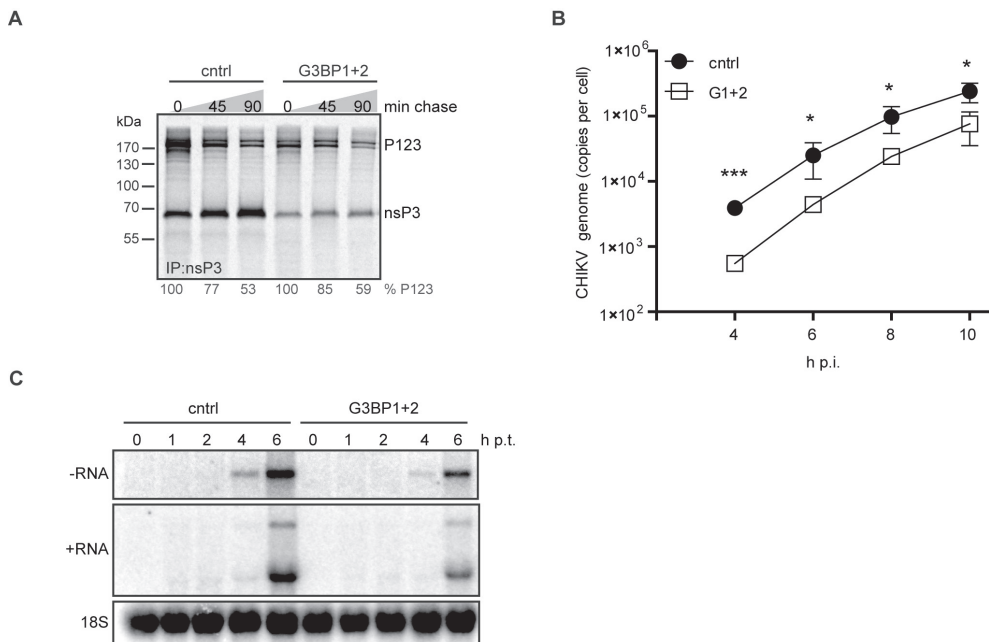
5

Figure 6. Effect of G3BP depletion on CHIKV nonstructural polyprotein processing, rate of RNA synthesis, and entry. 293/ACE2 cells were transfected with siRNAs targeting the G3BPs and 48 h later infected with CHIKV (MOI, 5) or transfected with *in vitro*-transcribed CHIKV genomic RNA. **(A)** Cells were metabolically labeled at 5 h p.i. and chased for 0, 45, or 90 min before lysis and immunoprecipitation. **(B)** Total RNA from infected cells was isolated at the indicated time points, and CHIKV genome copy numbers were determined using qRT-PCR. **(C)** G3BP-depleted cells were transfected with 1 μg of viral RNA (*in vitro* transcript) and harvested at the indicated time points. CHIKV RNA was analyzed using in-gel hybridization using probes specific for negative- or positive-strand RNA. The 18S rRNA was probed as a loading control.

RNA, enabling analysis of the translation of incoming genomes. To investigate if the incoming CHIKV genome is translated normally in G3BP-depleted cells, these cells were infected at an MOI of 50, and total cell lysates were harvested at the desired time points. Western blot analysis revealed only minor differences in nsP levels between G3BP-depleted and control cells (Fig. 7A). Only the nsP3 level was clearly lower in G3BP-depleted cells. In contrast, the accumulation of CHIKV negative-strand RNA and (consequently also) positive-strand RNA was strongly reduced in G3BP-depleted cells infected at an MOI of 50 and analyzed at 5 h p.i. (Fig. 7B), indicating that the G3BPs are involved in (early) RNA synthesis. To further examine the effect of G3BP depletion on CHIKV translation and RNA synthesis, reporter viruses were used that express *Renilla* luciferase either as part of the nonstructural polyprotein (fused to nsP3; P3Rluc) or under the control of a duplicated subgenomic promoter (2SG-Rluc). G3BP-depleted and control cells were infected with these reporter viruses (MOI, 5). Quantification of luciferase activity at 8 h p.i. showed a decrease in luciferase expressed from the duplicated subgenomic promoter in G3BP-depleted cells (Fig. 7C). This is in line with the effect of G3BP depletion on eGFP reporter gene expression (from the second sgRNA) that was observed with our reporter virus. Surprisingly, G3BP depletion resulted in an increased luciferase signal from P3Rluc virus, indicating that the translation of genomic RNA was not affected or even slightly enhanced by G3BP depletion. The increase of nsP3-Rluc signal in the luciferase assay contrasts with the apparent nsP3 decrease shown by Western blotting but can be explained by the fact that the degradation signal present in nsP3 (276) was lost in the nsP3-Rluc fusion. Alternatively, a larger amount of nsP3-Rluc could have been solubilized from G3BP-depleted cells compared to control cells, in which the protein is expected to be in G3BP-containing aggregates. Taken together, these data suggest that G3BP depletion does not directly affect translation and might even slightly stimulate nonstructural polyprotein translation.

In addition to performing infections at an MOI of 50, we have employed a replication-deficient CHIKV RNA (nsP4 GDD motif mutated to GAA), encoding luciferase fused to nsP3. G3BP-depleted or control cells were transfected with replication-deficient CHIKV nsP3-Rluc RNA, and the luciferase expression was quantified at various time points (Fig. 7D). Translation of this transfected RNA resulted in a peak of luciferase activity around 5 h p.t., followed by a decrease at later time points, likely due to degradation of the nonreplicating RNA and luciferase turnover. The luciferase signals in G3BP-depleted and control cells were very similar, indicating that G3BP depletion did not affect the translation of the CHIKV genome into nonstructural polyproteins (Fig. 7D). We performed a similar experiment with replication-competent CHIKV-nsP3-Rluc RNA, which allowed us to study translation as well as genome amplification. In control cells, an initial peak of luciferase activity was detected at 4 h posttransfection. After a small decrease in luciferase expression at 6 h p.i. (likely due to degradation of mRNA), a further increase in luciferase signal was observed, likely driven by translation of newly synthesized positive-strand RNA (Fig. 7E). Strikingly, this second increase did not occur in G3BP-depleted cells, indicating that the G3BPs play a role not in translation

but in the switch from translation of the (incoming) positive-strand RNA to negative-strand synthesis and RNA replication.
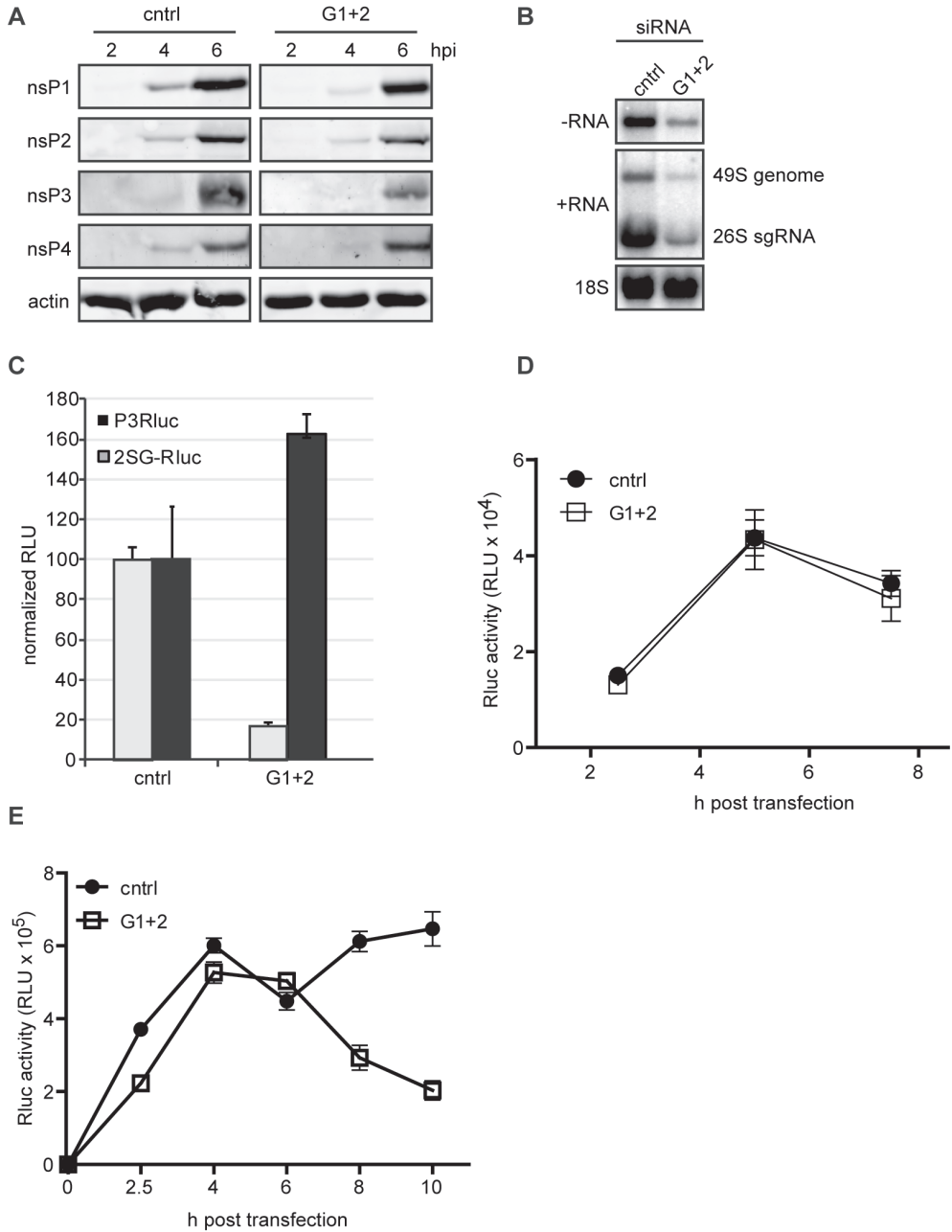
Figure 7. Effect of G3BP depletion on translation of genomic RNA and early–strand RNA synthesis.
(A) Cells transfected with control (cntrl) or G3BP1- and G3BP2-targeting (G1 + 2) siRNAs were infected with CHIKV at an MOI of 50 and harvested at the indicated time points, after which viral protein levels were analyzed by Western blotting. **(B)** siRNA-treated cells were infected with CHIKV (MOI, 50), and viral RNA was isolated at 5 h p.i. and analyzed by in-gel hybridization. The 18S rRNA was probed as a loading control. **(C)** G3BP-depleted cells were infected with reporter viruses that express *Renilla* luciferase either fused to nsP3 (P3Rluc) or from a duplicated subgenomic promoter (2SG-Rluc) at an MOI of 5. Luciferase activity was determined at 8 h p.i. and normalized to the activity in cells transfected with control siRNAs. **(D)** Replication-deficient CHIKV-P3Rluc RNA was transfected into control and G3BP-depleted cells and luciferase activity was assessed at the indicated time points. **(E)** Replication-competent CHIKV-P3Rluc RNA was transfected into control and G3BP-depleted cells, followed by measurement of luciferase activity at the indicated time points.

DISCUSSION

Many viruses manipulate the formation and dynamics of SGs, likely because their formation results in inhibition of translation. G3BP1 is an extensively studied SG marker, while the related G3BP2 remains less well characterized. These proteins, collectively referred to as G3BPs, are multifunctional RNA-binding proteins that have been implicated in the replication of several RNA viruses (273, 277-280). G3BPs have also been implicated in the alphavirus replication cycle, as they have been identified as binding partners of SINV nsP2, nsP3, and nsP4 (136-138, 266, 274) and SFV nsP3 (63, 66). Replication of a CHIKV replicon was shown to induce G3BP1-containing granules, and the expression of nsP3 alone was sufficient to sequester G3BP1 into granules (62). In addition, CHIKV-induced G3BP1-capsid protein foci have been described (281).

We found that late in infection, CHIKV induced foci that contained both G3BP1 and G3BP2 but that differed from bona fide SGs in morphology, CHX sensitivity, and composition (Fig. 1). These granules are probably similar to those observed in an earlier study using a CHIKV replicon (62). CHIKV-induced granules did not contain other SG markers, like TIA-1, TIAR, eIF3, or PABP, and the nsP3-G3BP aggregates therefore likely block the formation of genuine SGs by sequestering G3BPs. The expression level of these other SG components did not change over the course of infection, with the exception of TIA-1 and TIAR, which even slightly increased (Fig. 3). Therefore, the lack of these proteins in the CHIKV-induced granules was not due to their absence in the infected cell. SFV- and CHIKV replicon-induced G3BP-granules also lack other typical SG markers (62, 63).

SGs and G3BPs are generally thought to exert an antiviral effect on alphavirus replication. Surprisingly, we found by siRNA-mediated depletion that G3BPs were also required for efficient CHIKV replication (Fig. 5). CHIKV replication was affected most strongly when G3BP1 and G3BP2 were depleted simultaneously, which resulted in reduced viral RNA levels, diminished CHIKV protein expression, and an ~10-fold reduction in progeny titers. G3BP1 is generally considered an antiviral protein, and it was therefore surprising that depletion of G3BP1 did not stimulate CHIKV replication. However, proviral roles have also

been described for G3BPs in the replication of respiratory syncytial virus (277) and hepatitis C virus (HCV) (278). The observed inhibition of CHIKV replication in siRNA-transfected cells could be rescued by expressing siRNA-resistant G3BP2, demonstrating that it was not due to off-target effects. This was further corroborated by the use of C911 mutant siRNAs and by demonstrating that coxsackievirus replication was not affected in G3BP2-depleted cells. Our results demonstrate that simply studying the role of G3BP1 in viral replication, without taking G3BP2 into consideration, can lead to the misinterpretation or underestimation of the role of the G3BPs, as these homologous proteins can likely complement each other (in part) but also possess unique properties. This is illustrated by the fact that knockdown of G3BP1 did not affect CHIKV replication, possibly due to the concomitant increase in G3BP2 expression. Our data show that G3BP2 colocalized with CHIKV nsP2 and nsP3 in cytoplasmic granules but not with nsP1, nsP4, or dsRNA. In addition, subcellular fractionation experiments demonstrated that G3BPs were undetectable in the fraction (P15) enriched for CHIKV RTCs, suggesting that G3BPs are not associated with the active membrane-associated RTCs that can be isolated from infected cells (Fig. 4). SFV induces true SGs very early in infection, which disappear and are replaced by different nsP3-containing structures later in infection (63). For SINV, two types of nsP3-containing granules have been described: one type is likely associated with RTCs, while the other lacks dsRNA (137). Our findings suggest that most CHIKV nsP3 (and interacting G3BPs) is in the second type of granule. In contrast, G3BPs were found to be present in a fraction containing active SFV RTCs in a proteomics analysis of isolated cytopathic vacuoles (119). Which proportion of total cellular G3BPs was present in this fraction, however, was not determined. Clearly, we cannot formally exclude that trace amounts of G3BPs were present in our CHIKV RTC-containing membrane fraction. Unfortunately, technical limitations did not allow us to study the composition and *in vitro* activity of the early (negative-strand RNA-synthesizing) RTCs. Therefore, it is well possible and even likely (see below) that G3BPs play a role in negative-strand RNA synthesis. This is supported by the fact that G3BP depletion caused a delay in the replication cycle and affected an early postentry step. Translation of viral mRNA and nonstructural polyprotein processing were not impaired in G3BP-depleted cells, suggesting a role for G3BPs in early RNA synthesis. Indeed, infecting G3BP-depleted cells at a very high MOI in order to render viral mRNA translation to a certain extent independent from RNA synthesis showed that negative-strand RNA levels were severely reduced, despite the production of almost normal nsP levels (Fig. 7A and B). Therefore, G3BPs appear to be involved in the switch from translation of the incoming genome to negative-strand RNA synthesis. The G3BPs might clear the viral genome of proteins and/or translating ribosomes that would otherwise interfere with a negative-strand-synthesizing RTC moving in the opposite direction. A similar proviral role has been proposed for G3BPs during HCV replication, in which they were shown to be important during viral genome amplification but not translation (278). By analogy, impairing G3BP-induced CHIKV mRNA clearance would not affect nsP synthesis, which is in line with the observed close-to-normal nsP levels and the slightly enhanced luciferase signal of a recombinant

virus expressing an nsP3-Rluc fusion protein in G3BP-depleted cells. A less efficient switch from translation to genome amplification after G3BP depletion would explain the observed reduction of RNA levels and structural protein expression, which is dependent on sgRNA synthesis.

Our findings that G3BP depletion reduced CHIKV replication may appear to disagree with data from an earlier study on SINV (274). Cristea et al. observed enhanced SINV polyprotein expression (similar to what we found for CHIKV), but they also found similar or even slightly (though not statistically significant) increased RNA levels and virion production. It is possible that G3BP2 protein levels were not sufficiently depleted in this earlier study, as only mRNA levels were analyzed, which does not necessarily mean there was a similar reduction in G3BP protein levels. If G3BP2 protein levels were not sufficiently depleted, it would be compatible with our observation that G3BP1 depletion alone had little effect on CHIKV replication. When we analyzed SINV in G3BP2-depleted cells using our own experimental setup, we did observe reduced replication, similar to what we found for CHIKV (Fig. 5G). Of course, the differences between our data and those previously reported by Cristea et al. may also be due to differences in experimental setup or the cell lines used. We have not analyzed the effect of G3BP depletion on SINV in much detail, and it remains possible that CHIKV and SINV respond differently to G3BP depletion. Previous reports have identified at least one other RNA-binding protein that has different effects on CHIKV and SFV replication (119), so a similar difference between SINV and CHIKV would not be unimaginable.

Commonly, G3BP1 is implicated in SG formation, and therefore, its effect on viral replication has often been attributed to this function. However, both G3BPs possess multiple domains and a wide range of other functions unrelated to SG formation, which may (also) be relevant for CHIKV replication. G3BPs are part of the HCV replication complex (278), but it is unlikely that they are essential components of the CHIKV RTC, at least not in the membrane-associated complexes that produce the bulk of the genomic and sgRNA during the later stages of the replication cycle. This is in line with the recently identified interaction between CHIKV nsP3 and G3BPs (61, 62) that we have confirmed in this study (Fig. 4A). This interaction between nsP3 and G3BPs appears to occur not in RTCs (Fig. 4) but in SG-like structures that differed in composition and behavior from traditional SGs. The at-first-sight contradicting pro- and antiviral roles of G3BPs could perhaps be reconciled in a more refined model that would discriminate between early and late events in the replication cycle. Early in infection, nsP3 is present at low levels (and as part of the polyprotein), and it could then recruit G3BPs to the genomic RNA that is being translated, to mediate or support the switch from translation to the synthesis of negative-strand RNA. G3BPs might be involved in clearing ribosomes or proteins from the RNA and/or stabilize the naked viral RNA. Alternatively, G3BPs could be involved in a very early step of RTC formation, although they do not appear to be a major component of, or required for the activity of, the positive-strand RNA-synthesizing RTCs. Later in infection, when negative-strand RNA synthesis ceases, and higher levels of fully processed nsP3 are present, a cytosolic (non-RTC-associated) pool of nsP3 might sequester G3BPs

into the aggregates that prevent the formation of true SGs, which could otherwise exert an antiviral effect on the translation of viral mRNAs. This model is supported by the notions that the G3BPs seem to play a (proviral) role only early in CHIKV replication and that at this stage genuine SGs can still be formed in alphavirus-infected cells, as we and others (63) have observed. Indeed, at 4 h p.i. we observed some colocalization of dsRNA and G3BPs, while at 8 h p.i. there clearly was no colocalization of dsRNA with the nsP3- and G3BP2-containing granules.

Since G3BP1 and G3BP2 have so many (sometimes poorly understood) functions (reviewed in reference (282)), they might be involved in more steps of the CHIKV replication cycle, besides their proposed role in the translation-replication switch. For example, the G3BPs could be involved in stabilizing viral RNAs via their RNA-binding properties or even in NF-κB signaling or ubiquitin-mediated degradation, in which they have also been implicated (265, 283). NF-κB phosphorylation and protein levels were suggested by Zhang et al. to be affected by G3BP depletion (284), but we could not detect any changes in NF-κB protein levels or intracellular localization (data not shown). Another intriguing observation was that nsP3 levels appeared to be more strongly affected by G3BP depletion than the other nonstructural proteins, suggesting a role for G3BPs in stabilizing nsP3. Future work should assess the additional roles that the G3BPs might play during CHIKV replication.

ACKNOWLEDGEMENTS

6.

Inhibition of Dengue and Chikungunya Virus Infections by RIG–I–Mediated Type I Interferon–Independent Stimulation of the Innate Antiviral Response
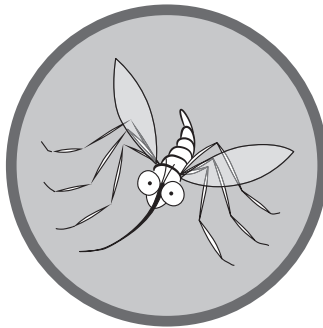
David Olagnier[1*], Florine E.M. Scholte[2*], Cindy Chiang[1], Irina C. Albulescu[2], Carmen Nichols[1], Zhong He[1], Rongtuan Lin[3], Eric J. Snijder[2], Martijn J. van Hemert[2#], John Hiscott[1#]

[1]Vaccine & Gene Therapy Institute of Florida, Port St. Lucie, Florida, USA. [2]Molecular Virology Laboratory, Department of Medical Microbiology, Leiden University Medical Center, Leiden, The Netherlands. Lady Davis Institute, Jewish General Hospital–McGill University, Montreal, Canada.
*,# These authors contributed equally to this work.

ABSTRACT

RIG-I is a cytosolic sensor critically involved in the activation of the innate immune response to RNA virus infection. In the present study, we evaluated the inhibitory effect of a RIG-I agonist on the replication of two emerging arthropod-borne viral pathogens, dengue virus (DENV) and chikungunya virus (CHIKV), for which no therapeutic options currently exist. We demonstrate that when a low, noncytotoxic dose of an optimized 5′triphosphorylated RNA (5′pppRNA) molecule was administered, RIG-I stimulation generated a robust antiviral response against these two viruses. Strikingly, 5′pppRNA treatment before or after challenge with DENV or CHIKV provided protection against infection. In primary human monocytes and monocyte-derived dendritic cells, the RIG-I agonist blocked both primary infection and antibody-dependent enhancement of DENV infection. The protective response against DENV and CHIKV induced by 5′pppRNA was dependent on an intact RIG-I/MAVS/TBK1/IRF3 axis and was largely independent of the type I IFN response. Altogether, this *in vitro* analysis of the antiviral efficacy of 5′pppRNA highlights the therapeutic potential of RIG-I agonists against emerging viruses such as DENV and CHIKV.

IMPORTANCE

DENV and CHIKV are two reemerging mosquito-borne viruses for which no therapeutic options currently exist. Both viruses overlap geographically in tropical regions of the world, produce similar fever-like symptoms, and are difficult to diagnose. This study investigated the inhibitory effect of a RIG-I agonist on the replication of these two viruses. RIG-I stimulation using 5′pppRNA before or after DENV or CHIKV infection generated a protective antiviral response against both pathogens in immune and nonimmune cells; interestingly, the protective response against the viruses was largely independent of the classical type I interferon response. The antiviral efficacy of 5′pppRNA highlights the therapeutic potential of RIG-I agonists against emerging viruses such as DENV and CHIKV.

INTRODUCTION

During infection, nucleic acids synthesized by viral replicases are the main pathogen-associated molecular patterns (PAMPs) recognized by the innate immune system (285). Sensing of PAMPs results in the control of the first waves of viral infection through the production of antiviral effector molecules and contributes to the mobilization of the adaptive arm of the immune response (286-288). Double-stranded RNA (dsRNA), generated during the replicative cycle of many viruses, is sensed by receptors such as Toll-like receptor 3 (TLR3) and different members of the RIG-I-like receptor (RLR) family, including RIG-I (retinoic acid-inducible gene I), MDA5 (melanoma differentiation factor 5), and LGP-2 (laboratory of genetics and physiology-2). RIG-I and MDA5 consist of two N-terminal caspase activation and recruitment domains (CARD), a DExD/H-box RNA helicase-sensing domain, and a C-terminal regulatory domain (RD). LGP-2 contains the RNA helicase-sensing domain and the RD but lacks the CARD (288-292).

Viral RNA extracted from infected cells has been shown to potently activate RIG-I (293, 294). Chemically or enzymatically synthesized dsRNA molecules bearing an exposed 5′-triphosphate end (5′ppp) were first identified as RIG-I inducers (295, 296), with the presence of the 5′ppp moiety being essential for RIG-I activation. Further characterization of a potent RIG-I ligand demonstrated that the presence of a blunt base pairing at the 5′ end, as well as a minimum length of 20 nucleotides, were essential for optimal RIG-I recognition of the molecule (295, 296). While short dsRNAs bearing a 5′ppp end are preferentially recognized by RIG-I, long dsRNA lacking the triphosphate moiety, such as poly(I:C), are recognized by TLR3 and MDA5 (297). More recently, a SELEX technology identified RNA aptamers that specifically target the RIG-I protein. The selected aptamers contained poly(U) motifs that were crucial for RIG-I activation of the immune response but, unexpectedly, activated RIG-I in a 5′-triphosphate-independent manner (298).

Binding of 5′ppp dsRNA to RIG-I leads to a conformational alteration, resulting in dissociation of the CARD from the helicase domain and exposure of the CARD (299, 300). This conformational change results in the generation of an active state characterized by ATP hydrolysis and ATP-driven translocation of RNA along the RIG-I molecule (299-302). RIG-I first forms a small binding unit upon recognition of the 5′ppp dsRNA, which occurs independently of ATP binding (303). In a second step, RIG-I oligomerizes on the 5′ppp dsRNA in an ATP hydrolysis-dependent manner, and the length of dsRNA dictates the strength of the type I interferon (IFN) response (303). Activated RIG-I is then able to interact with its mitochondrial adaptor MAVS via a CARD-CARD interaction. MAVS triggers the activation of IRF3, IRF7, and NF-κB through the IKK-related kinases TBK1 and IKKε, leading to the induction of type I IFN (IFN-β and IFN-α), proinflammatory cytokines, and selected antiviral genes, such as IFN-stimulated gene 15 (ISG15), ISG54, and ISG56 (304). Expansion of the antiviral response is then driven by the binding of type I IFN on its receptor, which activates the induction of hundreds of ISGs through the JAK-STAT pathway (287, 288, 305-308).

6

Given the importance of the innate immune response for host survival, TLR and RLR agonists have been the subject of intense study. Treatment with agonists of TLRs 2, 3, 4, 5, 7, and 9 inhibited hepatitis B virus as well as herpes simplex virus-2 replication in a type I IFN-dependent manner (309-311). Furthermore, pretreatment of cells with poly(I:C) also inhibited the replication of hepatitis C virus (HCV), human immunodeficiency virus (HIV), influenza virus, respiratory syncytial virus (RSV), DENV, and CHIKV (312-318). More recently, an RNA-based agonist of RIG-I was shown to block the replication of multiple viruses, including influenza virus, HIV, HCV, vesicular stomatitis virus (VSV), and vaccinia virus *in vitro*, as well as influenza virus *in vivo* (319). This broad-spectrum antiviral activity was in part attributed to the potent and specific stimulation of antiviral and inflammatory genes through IRF3/7, STAT1, and NF-κB transcription factors (319).

DENV and CHIKV are arthropod-borne viruses belonging to the *Flavivirus* and *Alphavirus* genera, respectively. Illness caused by CHIKV is usually diagnosed based on febrile symptoms and arthralgia and is often confused with dengue fever, given the similarities in clinical signs. CHIKV causes a severe arthralgia that may persist for many months but is not associated with the hemorrhagic fever that develops in a small proportion of severe dengue cases. Most DENV infections are asymptomatic or cause a self-limiting dengue fever, while a small proportion of infections leads to severe and potentially lethal manifestations, such as dengue hemorrhagic fever (DHF) and dengue shock syndrome (DSS), which are associated with antibody-dependent enhanced infections (320-322). Dengue fever, with millions of cases reported each year (320, 321), is already a leading infectious disease in tropical areas, while chikungunya fever is a lesser-known disease also affecting the same subtropical regions of the world. After a 50-year period of relative quiescence (76), CHIKV has reemerged with millions of estimated cases since 2005 (323, 324). The dramatic geographic expansion and increased incidence of DENV infections, as well as the emergence of CHIKV strains with an increased epidemic potential, highlight the increased burden of both viruses in tropical regions. The current lack of vaccines and effective antivirals stresses the importance of investigating new strategies to combat these serious human pathogens. Ideally, such strategies should target both viruses, as they cause similar symptoms, have an overlapping geographic distribution, and occur in regions in which the capacity to perform (differential) diagnosis is often limited. The present study describes the protective innate immune response against DENV and CHIKV infection triggered by a well-characterized 5′ triphosphorylated RIG-I agonist. The current study demonstrates that treatment with 5′pppRNA triggers a protective antiviral response sufficient to prevent DENV and CHIKV infection in both immune and nonimmune cells. The protective antiviral response was largely independent of the IFN-α/β receptor (IFNAR)/STAT1 axis but dependent on an intact RIG-I/MAVS/TBK1/IRF3 axis.

MATERIALS AND METHODS

***In vitro* synthesis of 5'pppRNA.** The sequence of 5'pppRNA was derived from the 5' and 3' untranslated regions (UTR) of the VSV genome as previously described (299). *In vitro*-transcribed RNA was prepared as previously described (319). Briefly, RNA was prepared using the Ambion MEGAscript T7 kit according to the manufacturer's guidelines (Invitrogen, NY, USA). 5'pppRNA was purified using the Qiagen miRNA minikit (Qiagen, Valencia, CA). An RNA with the same sequence but lacking the 5'ppp moiety was purchased from IDT (Integrated DNA Technologies Inc., IA, USA). This RNA generated results identical to those obtained with 5'pppRNA that was dephosphorylated enzymatically with calf intestinal alkaline phosphatase (Invitrogen, NY, USA).

Cell culture and transfections. A549 cells were grown in F12K medium (ATCC, Manassas, VA) supplemented with 10% fetal bovine serum (FBS) and antibiotics. C6/36 insect cells were cultured in Dulbecco's modified Eagle medium (DMEM) supplemented with 10% FBS and antibiotics. Lipofectamine RNAiMax (Invitrogen, NY, USA) was used for transfections of 5'pppRNA in A549 cells according to the manufacturer's instructions. For short interfering RNA (siRNA) knockdown, A549 cells were transfected with 50 nM (30 pmol) human RIG-I (sc-6180), IFN-α/βR α chain (sc-35637) and β chain (sc-40091), STING (sc-92042), TLR3 (sc-36685), MDA5 (sc-61010), MAVS (sc-75755), interleukin-28R (IL-28R; sc-62497), IL-10Rβ (sc-75331), STAT1 p844/91 (sc-44123), IRF1 (sc-35706), IRF3 (sc-35710), IRF7 (sc-38011), and control siRNA (sc-37007) (Santa Cruz Biotechnology, Dallas, T) using Lipofectamine RNAiMax according to the manufacturer's guidelines.

MRC-5 cells (ATCC CCL-171) were grown in Earle's minimum essential medium (EMEM) supplemented with 10% FBS, 2 mM L-glutamine, 1% nonessential amino acids (PAA), and antibiotics. For siRNA-mediated knockdown of gene expression, MRC-5 cells were transfected with 16.7 nM (10 pmol) siRNA using Dharmafect1 (Dharmacon) according to the manufacturer's guidelines.

Mouse embryonic fibroblast cells (MEFs) were grown in DMEM with 10% FBS and antibiotics.

Primary cell isolation. Human peripheral blood mononuclear cells (PBMC) were isolated from the blood of healthy volunteers in a study approved by the institutional review board and by the VGTI-FL Institutional Biosafety Committee (2011-6-JH1). Written informed consent, approved by the VGTI-FL Inc. ethics review board (FWA number 161), was provided and signed by study participants. Research conformed to ethical guidelines established by the ethics committee of the OHSU VGTI and Martin Health System. Briefly, PBMC were isolated from freshly collected blood using Ficoll-Paque plus medium (GE Healthcare Bio, Uppsala, Sweden) per the manufacturer's instructions. Monocytes were then isolated using the negative selection human monocyte enrichment kit (Stem Cell, Vancouver, Canada) per the kit's instructions and used for further experiments. To obtain monocyte-derived dendritic cells (MDDC), monocytes were allowed to adhere to 100-mm dishes for 1 h in serum-free

6

RPMI at 37°C. After adherence, remaining platelets and nonadherent cells were removed by two washes with serum-free RPMI. The cells were differentiated into MDDC by culturing for 7 days in MDDC differentiation medium (Miltenyi Biotec, Auburn, GA). Medium was replenished after 3 days of differentiation.

Virus production, quantification, and infection. Confluent monolayers of C6/36 insect cells were infected with DENV serotype 2 strain New Guinea C (DENV NGC) at a multiplicity of infection (MOI) of 0.5. Virus was allowed to adsorb for 1 h at 28°C in a minimal volume of serum-free DMEM. After adsorption, the monolayer was washed once with serum-free medium and covered with DMEM containing 2% FBS. After 7 days of infection, medium was harvested, cleared by centrifugation (500 × g, 5 min), and concentrated down by centrifugation (2,000 × g, 8 min) through a 15-ml Millipore Amicon centrifugal filter unit (Millipore, Billerica, MA). The virus was concentrated by ultracentrifugation on a sucrose density gradient (20% sucrose cushion) using a Sorvall WX 100 ultracentrifuge (ThermoScientific, Rockford, IL) for 2 h at 134,000 × g and 10°C with the brake turned off. Concentrated virus was then washed to remove sucrose using a 15-ml Amicon tube. After 2 washes, the virus was resuspended in DMEM plus 0.1% bovine serum albumin (BSA) and stored at −80°C. Titers of DENV stocks were determined by fluorescence-activated cell sorting (FACS), infecting Vero cells with 10-fold serial dilutions of the stock, and then immunofluorescence staining of intracellular DENV E protein at 24 h post infection (p.i.). Titers were expressed as IU/ml. DENV titers in cell culture supernatants from 5'ppp-treated and control cells were determined by plaque assay on confluent Vero cells. Cells in 6-well clusters were incubated with 10-fold serial dilutions of the sample in a total volume of 500 μl of DMEM without serum. After 1 h of infection, the inoculum was removed and cells were overlaid with 3 ml of 2% agarose in complete DMEM. The cells were fixed and stained, and plaques were counted 5 days post infection.

In infection experiments, A549 cells, monocytes, or MDDC were infected in a small volume of medium without FBS for 1 h at 37°C and then incubated with complete medium for 24 to 72 h prior to analysis. All procedures with live DENV were performed in a biosafety level 2+ facility at the Vaccine and Gene Therapy Institute, Florida.

CHIKV strain LS3 and enhanced green fluorescent protein (EGFP)-expressing reporter virus CHIKV LS3-GFP have been described (69). Virus production, titration, and infection were performed essentially as described previously (69). Working stocks of CHIKV were routinely produced in Vero E6 cells at 37°C, and infections were performed in EMEM with 25 mM HEPES (Lonza) supplemented with 2% fetal calf serum (FCS), L-glutamine, and antibiotics. After 1 h, the inoculum was replaced with fresh culture medium. All procedures with live CHIKV were performed in a biosafety level 3 facility at the Leiden University Medical Center.

Flow cytometry analysis. The percentage of cells infected with DENV was determined by standard intracellular staining (ICS) with a mouse IgG2a monoclonal antibody (MAb) specific for DENV-E protein (clone 4G2), followed by staining with a secondary anti-mouse antibody

coupled to phycoerythrin (PE) (BioLegend, San Diego, CA). Cells were analyzed on an LSRII flow cytometer (Becton, Dickinson, New Jersey, USA). Calculations as well as population analyses were done using FACS Diva software.

Cell viability analysis. Cell surface expression of phosphatidylserine was measured using an allophycocyanin (APC)-conjugated annexin V antibody, as recommended by the manufacturer (BioLegend, San Diego, CA). Briefly, specific annexin V binding was achieved by incubating A549 cells in annexin V binding buffer (Becton, Dickinson, NJ, USA) containing a saturating concentration of APC-annexin V antibody and 7-amino-actinomycin D (7-AAD) (Becton, Dickinson, New Jersey, USA) for 15 min in the dark. APC-annexin V and 7-AAD binding to the cells was analyzed by flow cytometry, as described previously, using an LSRII flow cytometer and FACS Diva software. Alternatively, the viability of siRNA- or 5′pppRNA-transfected cells was assessed using the CellTiter 96 aqueous nonradioactive cell proliferation assay (Promega). Absorbance was measured using a Berthold Mithras LB 940 96-well plate reader.

Protein extraction and immunoblot analysis. DENV-infected cells were washed twice in ice-cold phosphate-buffered saline (PBS) and lysed in radioimmunoprecipitation assay (RIPA) buffer (50 mM Tris-HCl, pH 8, 1% sodium deoxycholate, 1% NP-40, 5 mM EDTA, 150 mM NaCl, 0.1% sodium dodecyl sulfate), and the insoluble fraction was removed by centrifugation at $17,000 \times g$ for 15 min (4°C). Protein concentration was determined using the Pierce bicinchoninic (BCA) protein assay kit (Thermo Scientific, Rockford, IL). Protein extracts were resolved by SDS-PAGE on 4 to 20% acrylamide Mini-Protean TGX precast gels (Bio-Rad, Hercules, CA) in a 1× Tris-glycine-SDS buffer (Bio-Rad, Hercules, CA). Proteins were electrophoretically transferred to an Immobilon-P^{SQ}polyvinylidene difluoride (PVDF) membrane (Millipore, Billerica, MA) for 1 h at 100 V in a buffer containing 30 mM Tris, 200 mM glycine, and 20% methanol. Membranes were blocked for 1 h at room temperature in Odyssey blocking buffer (Odyssey, USA) and then probed with the following primary antibodies: anti-IRF1 (Santa Cruz Biotechnology, Dallas, TX), anti-pIRF3 at Ser 396 (EMD Millipore, MA, USA), anti-IRF3 (IBL, Japan), anti-IRF7 (Cell Signaling, MA, USA), anti-RIG-I (EMD Millipore, MA, USA), anti-IFIT1 (Thermo Fisher Scientific, Rockford, IL, USA), anti-ISG15 (Cell Signaling Technology, Danvers, MA), anti-pSTAT1 at Tyr701 (Cell Signaling, MA, USA), anti-STAT1 (Cell Signaling, MA, USA), anti-STING (Novus Biologicals, Littleton, CO), anti-DENV (Santa Cruz Biotechnology, USA), and anti-β-actin (Odyssey, USA). Antibody signals were detected by immunofluorescence using the IRDye 800CW and IRDye 680RD secondary antibodies (Odyssey, USA) and the LiCor imager (Odyssey, USA). Protein expression levels were determined and normalized to β-actin using ImageJ software (National Institutes of Health, Bethesda, MD).
CHIKV-infected cells were lysed and proteins were analyzed by Western blotting as described previously (69). CHIKV proteins were detected with rabbit antisera against nsP1 (a generous

gift of Andres Merits, University of Tartu, Estonia) and E2 (161). Mouse monoclonal antibodies against β-actin (Sigma), the transferrin receptor (Zymed), cyclophilin A (Abcam), and cyclophilin B (Abcam) were used for detection of loading controls. Biotin-conjugated swine α-rabbit (Dako), goat α-mouse (Dako), and Cy3-conjugated mouse α-biotin (Jackson) were used for fluorescent detection of the primary antibodies with a Typhoon-9410 scanner (GE Healthcare).

RT-qPCR. Total RNA was isolated from cells using an RNeasy kit (Qiagen, Valencia, CA) per the manufacturer's instructions. RNA was reverse transcribed using the SuperScript VILO cDNA synthesis kit according to the manufacturer's instructions (Invitrogen, Carlsbad, CA). PCR primers were designed using Roche's Universal Probe Library Assay Design Center (Roche). Quantitative reverse transcription-PCR (RT-qPCR) was performed on a LightCycler 480 system using LightCycler 480 probes master (Roche, Penzberg, Germany). All data are presented as a relative quantification with efficiency correction based on the relative expression of target gene versus glyceraldehyde-3-phosphate dehydrogenase (GAPDH) as the invariant control. The N-fold differential mRNA expression of genes in samples was expressed as $2^{\Delta\Delta CT}$. Primers used in this study were the following: DENV2 (probe 5) forward, 5′-ATCCTCCTATGGTACGCACAAA-3′; reverse, 5′-CTCCAGTATTATTGAAGCTGCTATCC-3′; GAPDH (probe 60) forward, 5′-AGCCACATCGCTCAGACAC-3′; reverse, 5′-GCCCAATACGACCAAATCC-3′; IFNA2 (probe 49) forward, 5′-AATGGCCTTGACCTTTGCTT-3′; reverse, 5′-CACAGAGCAGCTTGACTTGC-3′; IFNAR1 (probe 65) forward, 5′-ATTTACACCATTTCGCAAAGC-3′; reverse, 5′-CACTATTGCCTTATCTTCAGCTTCTA-3′; IFNAR2 (probe 87) forward, 5′-TAGCCTCCCCAAAGTCTTGA-3′; reverse, 5′-AAATGACCTCCACCATATCCA-3′; IFNB1 (probe 20) forward, 5′-CTTTGCTATTTTCAGACAAGATTCA-3′; reverse, 5′-GCCAGGAGGTTCTCAACAAT-3′; ILA (probe 66) forward, 5′-TGACGCCCTCAATCAAAGTA-3′; reverse, 5′-TGACTTATAAGCACCCATGTCAA-3′; IL-6 (probe 7) forward, 5′-CAGGAGCCCAGCTATGAACT-3′; reverse, 5′-GAAGGCAGCAGGCAACAC-3′; IL28RA (probe 12) forward, 5′-CCCCCACTGGATCTGAAGTA-3′; reverse, 5′-GAGTGACTGGAAATAGGGTCTTG-3′; IL-29 (probe 75) forward, 5′-CCTGAGGCTTCTCCAGGTG-3′; reverse, 5′-CCAGGACCTTCAGCGTCA-3′; TNFA (probe 79) forward, 5′-GACAAGCCTGTAGCCCATGT-3′; reverse, 5′-TCTCAGCTCCACGCCATT-3′.

RNA isolation, denaturing agarose electrophoresis, and in-gel hybridization. CHIKV RNA isolation and analysis were performed essentially as described previously (69). Briefly, total RNA was isolated by lysis in 20 mM Tris-HCl (pH 7.4), 100 mM LiCl, 2 mM EDTA, 5 mM dithiothreitol (DTT), 5% (wt/vol) lithium dodecyl sulfate, and 100 µg/ml proteinase K. After acid phenol (Ambion) extraction, RNA was precipitated with isopropanol, washed with 75% ethanol, and dissolved in 1 mM sodium citrate (pH 6.4). RNA samples were separated in 1.5% denaturing formaldehyde-agarose gels using the morpholinepropanesulfonic acid (MOPS) buffer system. RNA molecules were detected by direct hybridization of the dried gel with ^{32}P-labeled oligonucleotides. CHIKV genomic and subgenomic RNAs (sgRNAs) were visualized with

probe CHIKV-hyb4 (5′-TGTGGGTTCGGAGAATCGTGGAAGAGTT-3′), and negative-stranded RNA was detected with probe CHIKV-hyb2 (5′-AACCCATCATGGATCCTGTGTACGTGGA-3′). Probes (10 pmol) were labeled with 10 μCi [γ-^{32}P]ATP (PerkinElmer). Prehybridization (1 h) and hybridization (overnight) were done at 55°C in 5× SSPE (0.9 M NaCl, 50 mM NaH$_2$PO$_4$, 5 mM EDTA, pH 7.4), 5× Denhardt's solution, 0.05% SDS, and 0.1 mg/ml homomix I. Storage Phosphor screens were exposed to hybridized gels and scanned with a Typhoon-9410 scanner (GE Healthcare), and data were quantified with Quantity One v4.5.1 (Bio-Rad).

Statistical analysis. Values were expressed as the means ± standard errors of the means (SEM), and statistical analysis was performed with Microsoft Excel using an unpaired, two-tailed Student's t test to determine significance. Differences were considered significant at $P < 0.05$.

6

RESULTS

5′pppRNA inhibits DENV infection. To determine the capacity of the 5′pppRNA RIG-I agonist to induce a protective antiviral response to DENV infection, A549 cells were challenged with DENV at different multiplicities of infection (MOI); infection and replication were monitored by flow cytometry, RT-qPCR, plaque assay, and immunoblotting (Fig. 1A to F). DENV established infection in A549 cells which was completely abrogated in cells pretreated with 1 ng/ml of 5′pppRNA (Fig. 1A). A similar antiviral effect was observed at higher concentrations of 5′pppRNA (10 ng/ml). Importantly, the antiviral effect was strictly dependent on the 5′ppp moiety, as transfection of cells with the identical RNA sequence lacking the 5′ppp did not prevent DENV infection (Fig. 1B). Pretreatment of cells with 5′pppRNA also led to an 8.5-fold decrease in DENV RNA synthesis (Fig. 1C). Release of infectious DENV was completely suppressed by 5′pppRNA treatment (4.3×10^6 PFU/ml in untreated cells versus undetectable in 5′pppRNA-treated cells) (Fig. 1D), leading to a complete inhibition of DENV E protein expression (Fig. 1D, lane 3). To compare the effect of 5′pppRNA to that of the dsRNA ligand poly(I:C), A549 cells were pretreated with 5′pppRNA or poly(I:C) (0.1 to 1 ng/ml) and subsequently challenged with DENV (Fig. 1E). Treatment with 1 ng/ml of 5′pppRNA almost completely suppressed DENV infection, whereas at the same concentration, only a 1.8-fold decrease of the number of DENV-infected cells was observed upon poly(I:C) treatment (Fig. 1E). Cytosolic delivery of dsRNA by transfection was required in A549 cells, as demonstrated by the absence of a protective antiviral effect in cells in medium to which 5 μg/ml of 5′pppRNA or poly(I:C) had just been added (Fig. 1E). To determine whether pretreatment with 5′pppRNA maintained a protective effect, A549 cells were transfected with 5′pppRNA prior to DENV challenge and the virus was allowed to replicate up to 72 h p.i. (Fig. 1F). The combination treatment completely inhibited DENV infection at all time points for up to 72 h p.i. (Fig. 1F). The viability of uninfected cells and cells protected from infection by 5′pppRNA was indistinguishable (Fig. 1G). Altogether, these results demonstrate the antiviral potential of 5′pppRNA against DENV infection in nonimmune cells.

To assess the potential of 5′pppRNA as a post-infection treatment, A549 cells were first infected with DENV, subsequently treated with the RIG-I agonist at 4 h and 8 h after infection, and analyzed 48 h later to detect DENV infection. Interestingly, infection was almost completely inhibited even when cells were treated at 8 h p.i., as shown by the 12.4-fold reduction of the number of DENV-infected cells (Fig. 2A). This suggests that as DENV replicates over time, 5′pppRNA prevents further spread of the virus by protecting uninfected cells and clearing virus from infected cells. The observed effects of 5′pppRNA on DENV infection were confirmed by RT-qPCR, yielding a 3.6-fold (+4 h) and 10.8-fold (+8 h) decrease in DENV viral RNA levels at 48 h p.i. (Fig. 2B). Cell viability was not significantly affected by a 24-h 5′pppRNA treatment, and an ~20% decrease in viability was observed at 48 h p.i. in cells protected from infection by 5′pppRNA (Fig. 2C and D).

To investigate the antiviral response triggered by 5′pppRNA, various signaling parameters were monitored by immunoblotting and RT-qPCR in cells treated with increasing doses of

5′pppRNA in the presence or absence of DENV infection (Fig. 2E and F). Interferon signaling was detected by immunoblotting in 5′pppRNA-treated cells, both in the presence or absence of DENV, as demonstrated by increased STAT1 Tyr701 phosphorylation and ISG expression of STAT1, RIG-I, and IFIT1 (Fig. 2E, lanes 2 to 8). Although DENV can evade the host innate response (325-327), we did not observe a significant inhibition of IFN signaling based on the expression of antiviral markers STAT1, RIG-I, and IFIT1 in infected or uninfected cells (Fig. 2E, lanes 2 to 8). 5′pppRNA treatment elicited a strong antiviral response in uninfected and DENV-infected A549 cells (Fig. 2E), and delivery of 5′pppRNA at 4 h p.i. potently stimulated type I IFN and inflammatory responses via the upregulation of genes, such as those of IFN-α, IFN-β, IL-6, and IL-1α (Fig. 2F).

5′pppRNA-restricted DENV infection requires an intact RIG-I pathway. Introduction of RIG-I siRNA (10 and 30 pmol) into A549 cells severely reduced RIG-I as well as IFIT1 induction in response to 5′pppRNA treatment (Fig. 3A, lanes 5 to 8). Induction of the type I and type III IFNs, as well as the inflammatory response, were all dependent on intact RIG-I signaling, since the mRNA levels of IFN-β, IFN-α, IL-29, and tumor necrosis factor alpha (TNF-α) were drastically decreased in the absence of a functional RIG-I sensor (Fig. 3B). To explore the respective involvement of RIG-I, TLR3, and MDA5 in the 5′pppRNA-mediated anti-DENV effect, the expression of these immune sensors was knocked down in A549 cells by siRNA (Fig. 3C). While impairing RIG-I expression completely suppressed the 5′pppRNA-mediated antiviral effect, this was not the case upon knockdown of TLR3/MDA5 (Fig. 3C). The efficacy of poly(I:C) in preventing DENV infection was reduced to a larger extent in the absence of TLR3/MDA5 than in the absence of RIG-I, suggesting a predominant role for TLR3/MDA5 in mediating poly(I:C) antiviral effect in A549 cells (Fig. 3C). To demonstrate that the antiviral activity of 5′pppRNA against DENV relies on a functional RIG-I axis, the expression of RIG-I, STING, MAVS, and TBK1 was depleted in A549 cells using specific siRNAs. In addition, suitable knockout MEFs were used (Fig. 3D to F). Following 5′pppRNA treatment, DENV viral replication was assessed by flow cytometry. Whereas ~35% of A549 cells were infected with DENV in the untreated population, the absence of RIG-I led to an ~1.5-fold increase in the number of infected cells (Fig. 3D). Transient knockdown of RIG-I resulted in the abrogation of the protective response induced by 5′pppRNA in control cells (Fig. 3D), whereas the absence of STING did not affect DENV infection and did not significantly reduce the 5′pppRNA-induced antiviral response (Fig. 3D). Similar results were observed with A549 cells depleted for the mitochondrial adaptor MAVS; depletion of MAVS strongly reduced the 5′pppRNA-mediated protective antiviral response (Fig. 3E). Finally, TBK1-deficient MEFs were more susceptible to DENV infection than wild-type MEFs and were not responsive to the 5′pppRNA treatment, as demonstrated by the high level of DENV infection (Fig. 3F). In conclusion, 5′pppRNA treatment efficiently generates a RIG-I/MAVS/TBK1-dependent antiviral response that limits DENV infection *in vitro*.
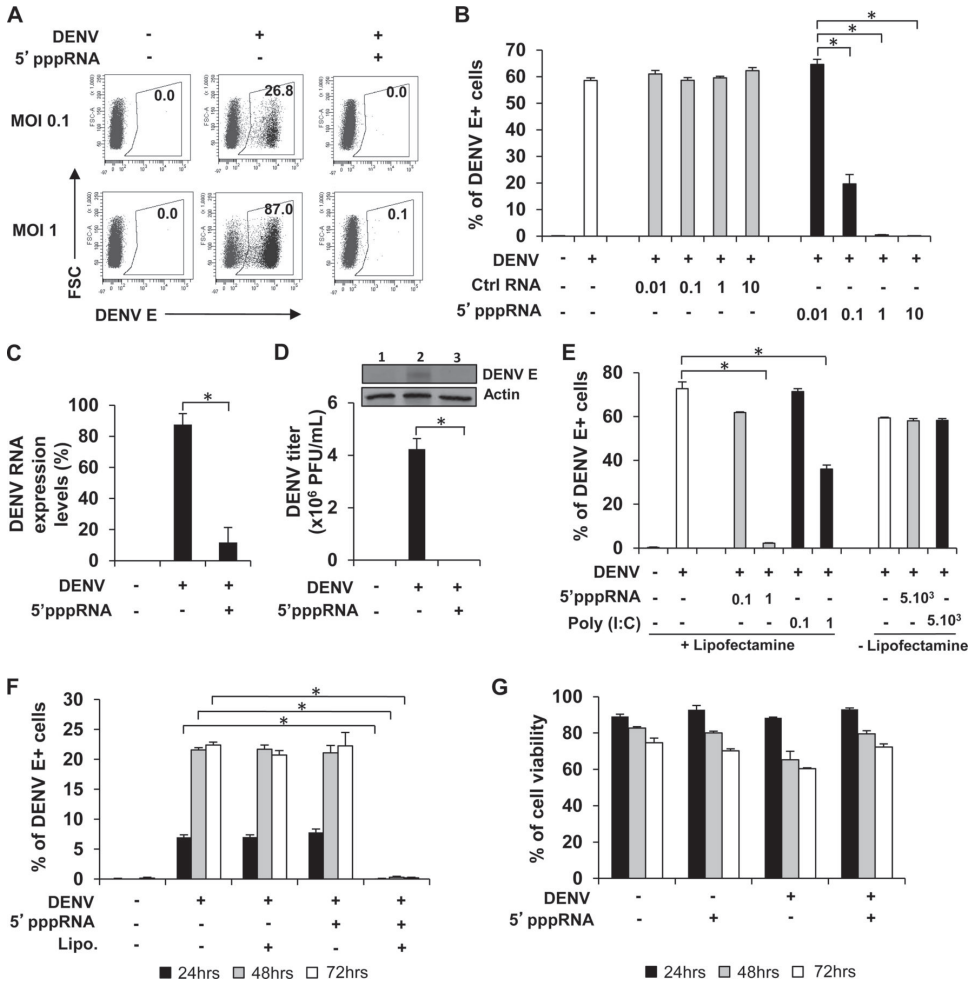
Figure 1. Pretreatment with 5'pppRNA inhibits DENV replication *in vitro*. (A and **B)** A549 cells were pretreated with various concentrations of 5'pppRNA (0.01 to 10 ng/ml) or control (Ctrl) RNA lacking the 5'ppp at the same concentrations for 24 h prior to DENV challenge. The percentage of DENV-infected cells was determined by intracellular staining (ICS) of DENV E protein expression using flow cytometry. Data are from two independent experiments performed in triplicate and represent the means ± SEM. *, $P <$ 0.05. FSC, forward scatter. (C and D) A549 cells were pretreated with 5'pppRNA (1 ng/ml) for 24 h prior to DENV challenge (MOI, 0.1). DENV RNA level **(C)**, viral titers **(D)**, and DENV E protein expression level **(D)** were determined by RT-qPCR, plaque assay, and Western blotting, respectively. Error bars represent SEM from three independent samples. *, $P < 0.05$. One representative DENV E protein Western blot out of three independent triplicates is shown. **(E)** A549 cells were transfected using Lipofectamine (Lipo.) RNAiMax with increasing concentrations of 5'pppRNA and poly(I:C) (0.1 to 1 ng/ml) or treated with the same dsRNA sequences (5,000 ng/ml) in the absence of transfection reagent. Cells were then challenged with DENV (MOI, 1), and the percentage of infected cells was determined by FACS 24 h after infection. Data are the means ± SEM from two independent experiments performed in triplicate. *, $P < 0.05$. **(F and G)** The percentage of A549 DENV-infected cells and cell viability were assessed by flow cytometry and determined at 24 h (black bars), 48 h (gray bars), and 72 h (white bars) after DENV challenge (MOI, 0.01). Cells were pretreated with 5'pppRNA (1 ng/ml) for 24 h before DENV challenge. Data are the means ± SEM from a representative experiment performed in triplicate. *, $P < 0.05$.

5′pppRNA generates an IRF3-dependent and IFNAR/STAT1-independent antiviral protective effect. To determine whether the potent RIG-I activation could compensate for the type I and type III IFN response, expression of the type I IFN receptor (IFN-α/βR) as well as the type III IFN receptor (IL-28R plus IL-10Rβ) was knocked down using siRNA in A549 cells (Fig. 4A to C). Expression of both type I and III IFN receptor was efficiently reduced, as shown by the downregulation of IFNAR1 (IFN-α/βR α chain), IFNAR2 (IFN-α/βR β chain), and IL-28R mRNA expression levels (Fig. 4A). Furthermore, knockdown of type I IFN signaling was highly efficient, as demonstrated by the reduction of IFIT1 and RIG-I induction following IFN-α2b stimulation (6.2-fold reduction of IFIT1 versus control siRNA [siCTRL]; Fig. 4B, lane 3 versus lane 6). Knocking down the type III IFN receptor did not interfere with the ability of 5′pppRNA and IFN-α2b to induce IFIT1 and RIG-I expression Fig. 4B, lanes 2 and 3 versus lanes 8 and 9). Interestingly, induction of IFIT1 but not RIG-I was only partially reduced following 5′pppRNA treatment in the absence of type I IFN receptor (1.6-fold reduction of IFIT1 versus siCTRL; Fig. 4B, lane 2 versus lane 5), suggesting that certain ISGs were upregulated by 5′pppRNA in an IFN-independent manner. Knocking down expression of both type I and type III IFN receptors did not limit IFIT1 induction by 5′pppRNA, as the increase of IFIT1 was only reduced 1.9 times compared to the siRNA control (Fig. 4B). This type I and III IFN-independent activation of the innate system was sufficient to suppress DENV infection in A549 cells stimulated with a higher (10 ng/ml) but not a low dose (0.1 to 1 ng/ml) of 5′pppRNA (Fig. 4C). To further confirm that type I IFN signaling was not necessarily required to mediate an immune response to 5′pppRNA, STAT1 was depleted in A549 cells using siRNA (Fig. 4D, lanes 5 to 8). The increased expression of IFIT1 following 5′pppRNA treatment was not impacted by the absence of the STAT1 transcription factor (Fig. 4D, lanes 2 to 4 versus lanes 6 to 8). The STAT1-independent induction of the antiviral response was sufficient to block DENV infection in A549 cells stimulated with a high 5′pppRNA concentration (Fig. 4E). Finally, to determine which IRF transcription factor downstream of RIG-I was involved in the antiviral protective effect, IRF1, IRF3, and IRF7 expression was knocked down using siRNA (Fig. 4F). Depletion of these different transcription factors was highly efficient, as shown in Fig. 4F. Only IRF3 knockdown resulted in inhibition of the protective antiviral response generated by 5′pppRNA treatment. Indeed, the absence of either IRF1 or IRF7 did not impair 5′pppRNA-mediated antiviral protection (Fig. 4G). Altogether, these data demonstrate that the 5′pppRNA-mediated anti-DENV effect *in vitro* is largely independent of the type I or type III IFN responses but requires the activation of a functional RIG-I/IRF3 axis to mediate its protective effect.
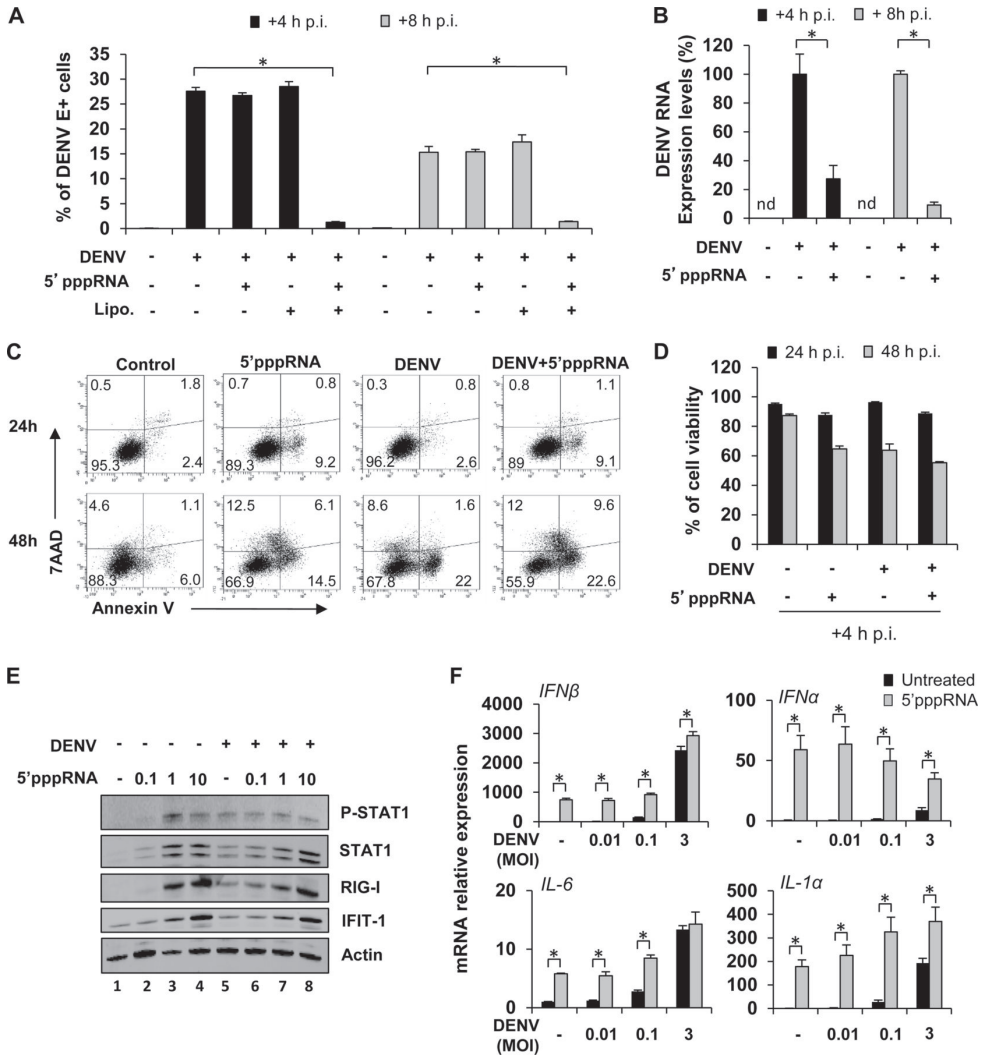
6

Figure 2. Post–infection treatment with 5′pppRNA inhibits *de novo* DENV infection. (A) A549 cells were treated with 5′pppRNA (1 ng/ml) 4 h (black bars) or 8 h (gray bars) following DENV challenge (MOI, 0.01). The percentage of DENV-infected cells was determined by intracellular staining (ICS) of DENV E protein expression using flow cytometry at 48 h after infection. Data represent the means ± SEM from a representative experiment performed in triplicate. *, $P < 0.05$. **(B)** DENV RNA levels were determined by RT-qPCR (48 h after infection) on A549 cells treated with 5′pppRNA (1 ng/ml) 4 h (black bars) and 8 h (gray bars) after infection. *, $P < 0.05$. **(C and D)** Cell viability of A549 cells was measured by flow cytometry 24 h (black bars) and 48 h (gray bars) after infection. Cells were treated with 5′pppRNA 4 h after DENV infection. Data are the means ± SEM from a representative experiment performed in triplicate. **(E)** A549 cells were challenged with DENV (MOI, 0.1) for 4 h and transfected with 5′pppRNA (0.1 to 10 ng/ml) and incubated for an additional 20 h. Whole-cell extracts (WCEs) were prepared and subjected to immunoblot analysis 24 h post-infection. Data are from one representative experiment. **(F)** A549 cells were infected with DENV at different MOI and were transfected with 5′pppRNA (1 ng/ml) 4 h after infection. The expression level of genes was determined by RT-qPCR 24 h after DENV challenge. Data are the means ± SEM from a representative experiment performed in triplicate. *, $P < 0.05$.
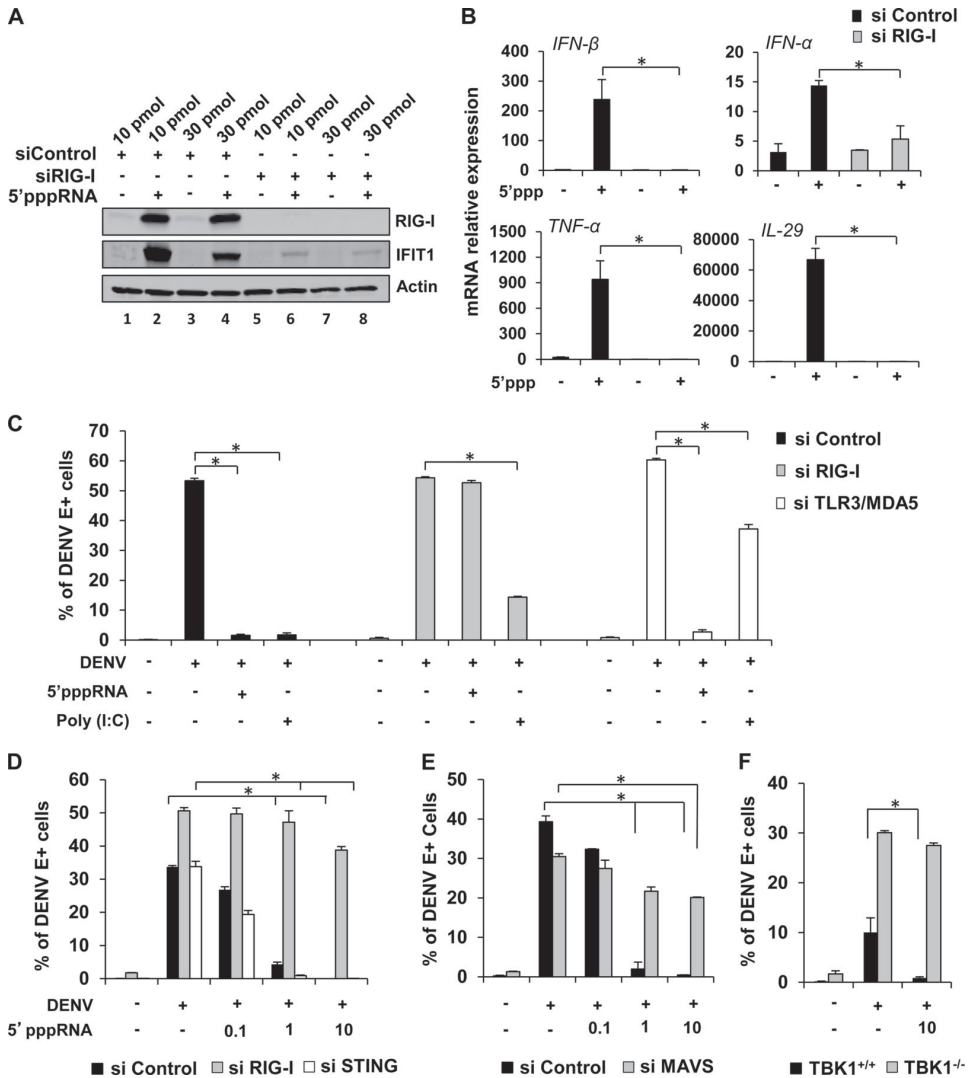
Figure 3. 5'pppRNA inhibits DENV infection *in vitro* in a RIG–I/MAVS/TBK1–dependent manner. (A) A549 cells were transfected with control or RIG-I siRNA (10 or 30 pmol), and 48 h later they were treated with 5'pppRNA (10 ng/ml) for 24 h. Expression of IFIT1, RIG-I, and β-actin was evaluated by Western blotting. RIG-I knockdown and impairment of the 5'ppp-induced immune response is representative of at least 3 independent experiments. (B) A549 cells were transfected with control siRNA or RIG-I siRNA (30 pmol), and 48 h later they were treated with 5'pppRNA (10 ng/ml) for 24 h. mRNA expression level of IFN-β, IFN-α, TNF-α, and IL-29 was evaluated by RT-qPCR. Data are from a representative experiment performed in triplicate and show the means ± SEM. *, $P < 0.05$. (C) A549 cells were transfected with control (black bars), RIG-I (gray bars), or a combination of TLR3/MDA5 (white bars) siRNA (30 pmol each), and 48 h later they were treated with 5'pppRNA (10 ng/ml) or poly(I:C) (1 ng/ml). Cells were then infected with DENV (MOI, 0.5), and at 24 h p.i. the percentage of infected cells was assessed by intracellular staining of DENV E protein using flow cytometry. Data are from a representative experiment performed in triplicate and show the means ± SEM. *, $P < 0.05$. (D and E) A549 cells were treated with 5'pppRNA (0.1 to 10 ng/ml) for 24 h 2 days after transfection with 30 pmol of control (black bars), RIG-I (gray bars), or STING

(white bars) siRNA **(D)** or with 30 pmol of control (black bars) or MAVS (gray bars) siRNA **(E)**. Cells were then challenged with DENV (MOI, 0.1) for 24 h. The percentage of DENV-infected cells was determined by intracellular staining of DENV E protein and flow cytometry 24 h after infection. Data are the means ± SEM from a representative experiment performed in triplicate. *, $P < 0.05$. (F) TBK1$^{+/+}$ (black bars) and TBK1$^{-/-}$ (gray bars) MEF cells were treated with 10 ng/ml of 5'pppRNA 24 h before DENV challenge at an MOI of 5. The percentage of DENV-infected cells was evaluated by flow cytometry. Data are the means ± SEM of a representative experiment performed in triplicate. *, $P < 0.05$.

Figure 4. 5'pppRNA–induced antiviral effect is IRF3 dependent but IFNAR and STAT1 independent.
(A) A549 cells were transfected with control, IFN-α/βR α chain (IFNAR1), IFN-α/βR β chain (IFNAR2), or IL-28R siRNA, and 48 h later mRNA levels of IFNAR1, IFNAR2, and IL-28R were evaluated by RT-qPCR. Data are from a representative experiment performed in triplicate. *, $P < 0.05$ **(B)** A549 cells were transfected with the control siRNA, IFN-α/βR or IL-28R siRNA, or a combination of both. After 48 h, cells were treated with 5'pppRNA (10 ng/ml) or IFN-α2b (100 UI/ml) for 24 h. Expression of IFIT1, RIG-I, and β-actin was evaluated by Western blotting. The evaluation of 5'ppp-induced immune response by Western blotting

in the absence of type I IFN receptor, representative of three independent experiments, and in the absence of type III IFN receptor, representative of one experiment. **(C)** After siRNA knockdown of IFN-α/βR as described for panel B, cells were treated with increasing concentrations of 5′pppRNA (0.1 to 10 ng/ml) and then infected with DENV (MOI, 0.1). The percentage of DENV-infected cells was evaluated by flow cytometry. Data are the means ± SEM of a repre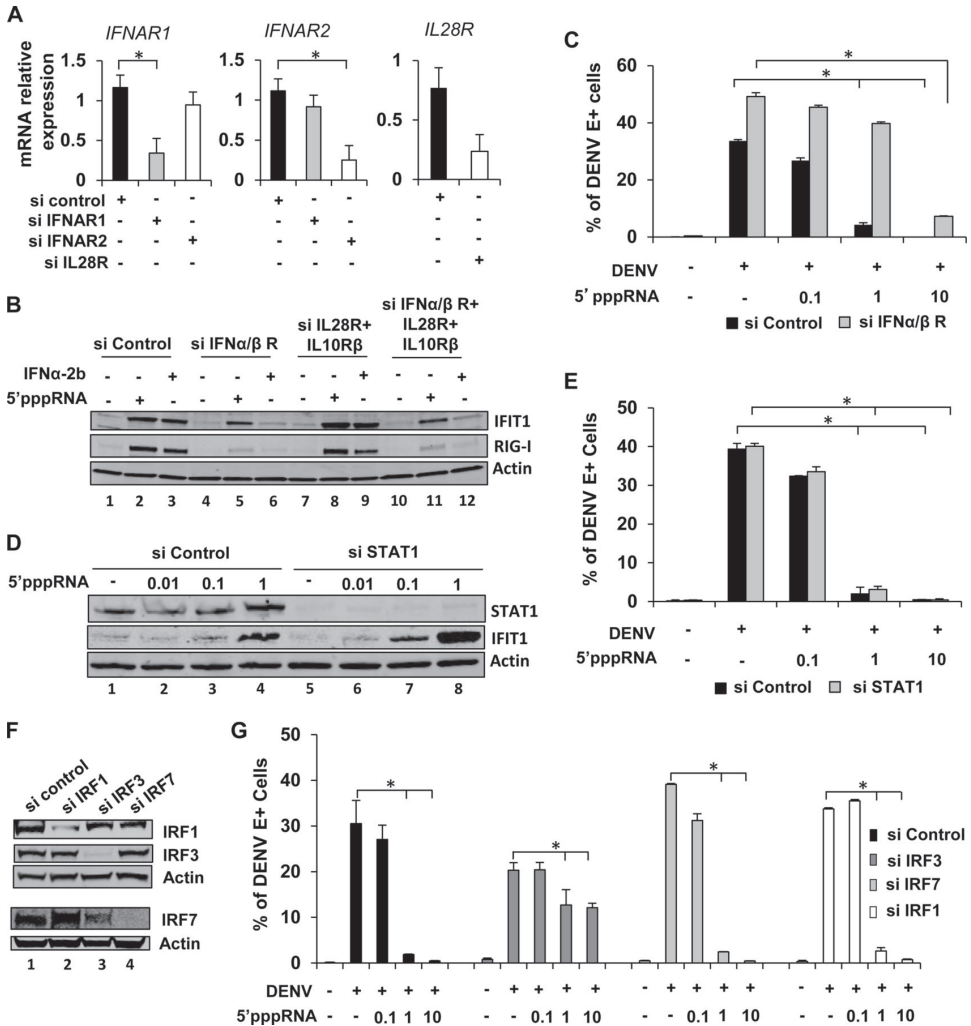sentative experiment performed in triplicate. *, $P < 0.05$. **(D)** A549 cells were transfected with control and STAT1 siRNA, and 48 h later they were treated with 5′pppRNA (0.01 to 1 ng/ml) for 24 h. Expression of STAT1, IFIT1, and β-actin was evaluated by Western blotting. The induction of 5′ppp-induced immune response in the absence of STAT is representative of two independent experiments. **(E)** A549 cells were transfected with control or STAT1 siRNA and incubated for 48 h. Cells were treated with increasing concentrations of 5′pppRNA (0.1 to 10 ng/ml) and then infected with DENV (MOI, 0.1). The percentage of DENV-infected cells was evaluated by flow cytometry. Data are the means ± SEM from a representative experiment performed in triplicate. *, $P < 0.05$. **(F)** A549 cells were transfected with control, IRF1, IRF3, or IRF7 siRNA for 48 h, and the protein expression level of these transcription factors was evaluated by Western blotting. This panel is representative of one experiment. **(G)** A549 cells were transfected with control IRF1, IRF3, or IRF7 and then treated as described for panel E. The percentage of DENV-infected cells was evaluated by flow cytometry. Data are the means ± SEM from a representative experiment performed in triplicate. *, $P < 0.05$.

6

A protective antiviral response against DENV in primary human myeloid cells. Cells of the myeloid lineage, including monocyte/macrophages and dendritic cells, are the primary target cells for DENV infection among human peripheral blood mononuclear immune cells (328, 329). Severe and potentially lethal manifestations associated with secondary DENV infection are often related to antibody-dependent enhancement (ADE) of infection (320-322). To address the impact of 5′pppRNA on ADE-mediated DENV infection, we demonstrated, using isolated human monocytes, that anti-DENV E 4G2 antibody increased DENV infectivity from 16.4% to 24.4% (Fig. 5A), whereas a control isotype IgG2a antibody did not significantly increase viral infectivity (Fig. 5A). Both primary and ADE DENV infections were completely suppressed by 5′pppRNA treatment (16.4% and 24.4% in untreated cells versus 0.1% and 0.3% in 5′pppRNA-treated cells, respectively). Similarly, in primary human MDDC, which are highly permissive to DENV, infection decreased 8.4-fold in the presence of 5′pppRNA in combination with Lyovec (Fig. 5B), and cell viability was not affected by increasing concentrations of 5′pppRNA (Fig. 5C). MDDC treated with 5′pppRNA at 4 h p.i. were assessed for markers of activation of the innate immune response (Fig. 5D). Increased levels of phosphorylated IRF3 and STAT1 were observed, and a 2- to 10-fold increase in the expression of ISGs RIG-I and IFIT1 following 5′pppRNA treatment were observed (Fig. 5D, lane 2). A similar response was observed with DENV infection alone (Fig. 5D, lane 3). The innate DNA sensor STING was previously shown to be cleaved and inactivated by DENV NS2/3 protease (325); in the current experiments, STING expression was not modulated by 5′pppRNA or DENV infection alone (Fig. 5D, lane 2 and 3). Also, post-infection treatment with 5′pppRNA moderately increased the levels of the following markers of the innate immune response compared to virus alone: phospho-STAT1 (3-fold increase), STAT1 (1.4-fold increase), IFIT1 (1.3-fold increase), and RIG-I (1.3-fold increase) (Fig. 5D, lanes 3 and 4). Surprisingly, 5′pppRNA did not further increase the level of phospho-IRF3 compared to DENV infection alone (Fig. 5D, lane 3 and 4), an observation
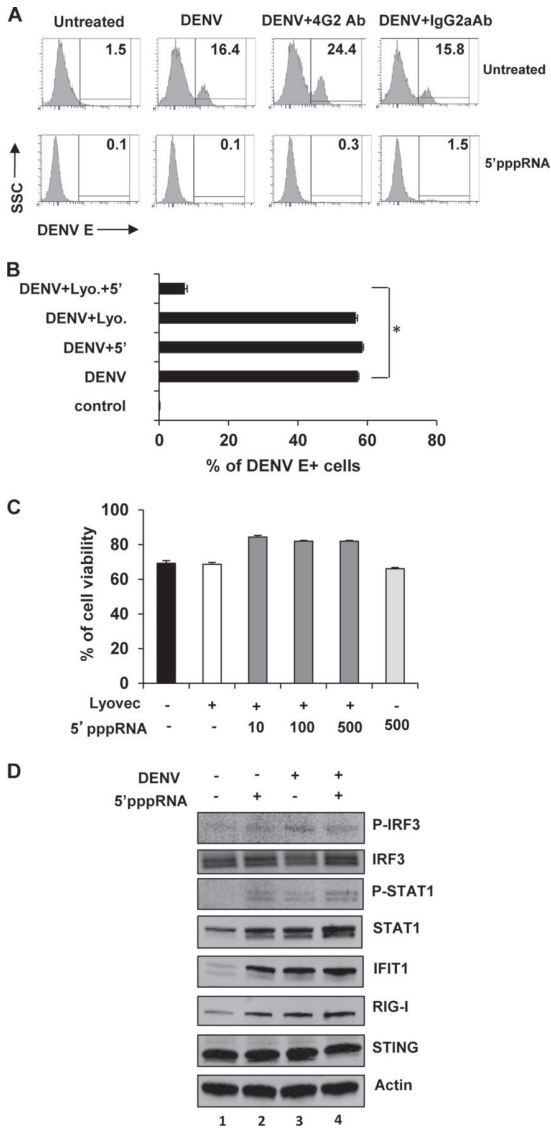
Figure 5. 5′pppRNA treatment protects human myeloid cells from primary and ADE DENV infection.
(A) Negatively selected monocytes were challenged with DENV (MOI, 20) in the presence or absence of the enhancing antibody 4G2 (0.5 µg/ml) for 4 h. They were subsequently transfected with 5′pppRNA (100 ng/ml) using Lyovec and incubated for 20 h. An IgG2a antibody (0.5 µg/ml) served as a negative control. The percentage of DENV-infected cells was determined by flow cytometry 24 h after infection. **(B)** CD14⁻ MDDCs were challenged with DENV (MOI, 10) for 4 h, followed by transfection with 5′pppRNA (100 ng/ml) and incubation for an additional 20 h. Data represent the means ± SEM of an experiment performed in triplicate. *, $P < 0.05$. **(C)** Cell viability was assessed by flow cytometry on CD14⁻ MDDC and determined 24 h after 5′pppRNA treatment (10 to 500 ng/ml) in the presence of Lyovec. Data are the means ± SEM of a representative experiment performed in triplicate. **(D)** CD14⁻ MDDCs were challenged with DENV (MOI, 10) for 4 h and then were treated with 5′pppRNA (100 ng/ml) for an additional 20 h. WCEs were resolved by SDS-PAGE and analyzed by immunoblotting for phospo-IRF3, IRF3, phospho-STAT1, STAT1, IFIT1, RIG-I, STING, and β-actin. Results are from one representative experiment that was repeated once.

that is in part attributable to the early and transient kinetics of IRF3 phosphorylation. These data demonstrate that RIG-I activation by 5′pppRNA triggers an immune response capable of inhibiting DENV in both primary and ADE models of infection.

5′pppRNA treatment inhibits CHIKV replication in a RIG-I-dependent manner. To explore the potential of the 5′pppRNA agonist to prevent CHIKV infection, human fibroblast MRC-5 cells were pretreated with increasing concentrations of 5′pppRNA prior to challenge with a CHIKV LS3-GFP reporter virus (Fig. 6A). CHIKV replication was strongly inhibited in a dose-dependent manner in cells treated with 5′pppRNA 1 h prior to infection (Fig. 6A); as little as 1 ng/ml completely blocked CHIKV EGFP reporter gene expression, and the 5′pppRNA concentration required to completely block CHIKV replication in MRC-5 cells was 10-fold lower than that required to inhibit DENV in A549 cells. It is currently unclear whether this is due to virus-specific immune evasion or cell type-specific differences, as CHIKV does not replicate in A549 cells. Also, introduction of control RNA lacking the 5′ triphosphate moiety only led to a minor reduction of GFP reporter gene expression in CHIKV LS3-GFP-infected cells (Fig. 6A). Cell viability, monitored in parallel, was not significantly affected by transfection of either 5′pppRNA or control RNA lacking the 5′ triphosphate (Fig. 6B). Analysis of intracellular RNA of CHIKV-infected cells pretreated with 5′pppRNA or control RNA showed that treatment with 0.1 ng/ml 5′pppRNA reduced CHIKV positive- and negative-strand RNA accumulation to minimally detectable levels (Fig. 6C), and at higher doses of 5′pppRNA viral RNA was undetectable. Transfection of cells with control RNA prior to infection had no significant effect on the accumulation of CHIKV RNA (Fig. 6C). To determine the effect of RIG-I agonist treatment on the expression of CHIKV nonstructural proteins (translated from genomic RNA) and structural proteins (translated from the sgRNA), cells were pretreated with 5′pppRNA or control RNA and infected with CHIKV, and nsP1 and E2 expression was analyzed by Western blotting (Fig. 6D). Transfection of 0.1 ng/ml 5′pppRNA led to a 4-fold reduction in nsP1 expression and an 8-fold reduction in E2 expression. Higher doses of 5′pppRNA reduced nsP1 and E2 expression over 30-fold (Fig. 6D). Transfection of control RNA lacking the 5′ triphosphate had no noticeable effect on CHIKV protein expression (Fig. 6D). Finally, the effect of 5′pppRNA treatment on the production of infectious progeny was determined. Compared to untreated cells, transfection of MRC-5 cells with 0.1 ng/ml of 5′pppRNA 1 h prior to CHIKV infection led to an ~1 log reduction in virus titer, while transfection with 1 ng/ml and 10 ng/ml 5′pppRNA reduced viral progeny titers by ~2 and ~3 logs, respectively (Fig. 6E). Transfection of control RNA lacking the 5′ triphosphate did not significantly affect CHIKV progeny titers (Fig. 6E).
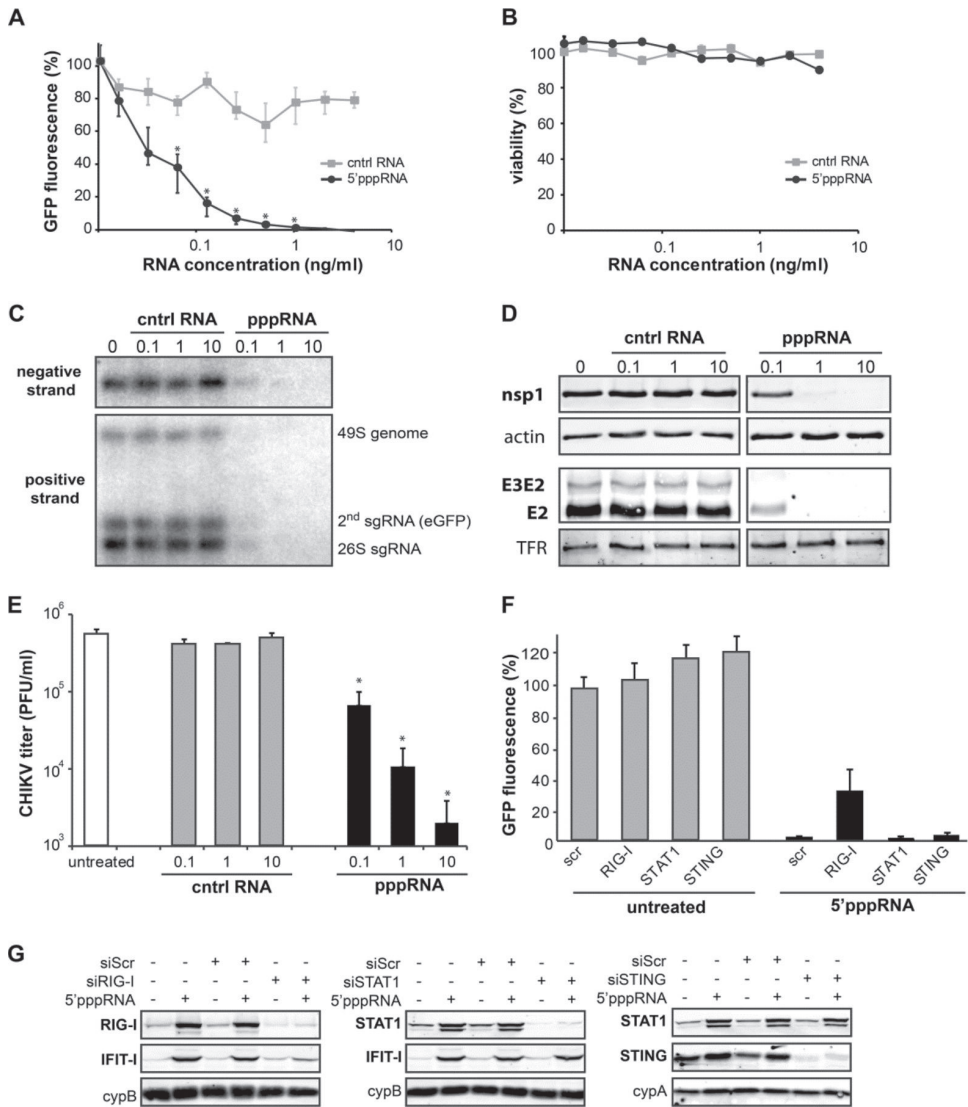
Figure 6. Treatment with 5′pppRNA inhibits CHIKV replication in a RIG–I–dependent manner. (A) MRC-5 cells were treated with 0.015 to 4 ng/ml of control RNA or 5′pppRNA from 1 h prior to infection to 24 h post-infection with CHIKV LS3-GFP (MOI, 0.1). At 24 h p.i., cells were fixed and EGFP reporter gene expression was quantified. *, $P < 0.05$. cntrl, control. **(B)** To assess potential cytotoxicity, MRC-5 cell viability was measured 24 h posttransfection of 5′pppRNA or control RNA lacking the 5′ triphosphate. Data are represented as the means ± SEM from a representative experiment performed in quadruplicate. **(C)** The intracellular accumulation of CHIKV positive- and negative-strand RNA was determined by in-gel hybridization of RNA isolated from MRC-5 cells that were treated with 5′pppRNA (0.1 to 10 ng/ml) 1 h prior to infection (MOI, 0.1). **(D)** CHIKV E2, E3E2, and nsP1 protein expression was assessed by Western blotting of lysates of MRC-5 cells that were treated with various concentrations of control RNA or 5′pppRNA 1 h prior to infection with CHIKV. Data are representative of at least two independent experiments. **(E)** The effect of 5′pppRNA and control RNA treatment on CHIKV progeny titers as assessed by plaque assay. **(F)** siRNA-transfected MRC-5 cells were either left untreated or were transfected with 5′pppRNA, after which they

were infected with CHIKV LS3-GFP (MOI, 0.1). CHIKV-driven EGFP reporter gene expression was measured at 24 h p.i. and was normalized to the expression level in CHIKV-infected cells that had been transfected with a nontargeting scrambled siRNA (scr). *, $P < 0.05$. **(G)** MRC-5 cells were transfected with 10 pmol of scrambled siRNA (siScr) or siRNA targeting RIG-I, STAT1, or STING 48 h prior to treatment with 1 ng/ml of 5′pppRNA. Expression levels of RIG-I, STAT1, STING, and IFIT1 were monitored by Western blotting. Cyclophilin A or B was used as a loading control. Data are representative of at least two independent experiments.

To determine which innate immune pathways are involved in the 5′pppRNA-mediated inhibition of CHIKV replication, several key proteins of the IFN signaling pathway (RIG-I, STAT1, and STING) were depleted in MRC-5 cells using siRNAs. Knockdown levels were assessed by Western blotting (Fig. 6G). Subsequently, cells depleted for RIG-I, STAT1, or STING were treated with 5′pppRNA and infected 1 h later with CHIKV LS3-GFP (Fig. 6F). CHIKV-driven GFP reporter gene activity was reduced to almost background levels in 5′pppRNA-treated cells that were depleted for STAT1 and STING, suggesting these proteins are not involved in the 5′pppRNA-mediated antiviral response to CHIKV. In contrast, CHIKV replication was observed in cells depleted of RIG-I and treated with 5′pppRNA, although EGFP reporter gene expression was ~30% of that in untreated cells transfected with scrambled (or RIG-I-targeting) siRNAs (Fig. 6F). This partial recovery of replication might be due to incomplete knockdown of RIG-I in a fraction of the cells and/or paracrine IFN signaling of those cells, which could affect CHIKV replication of RIG-I-depleted cells. CHIKV replication in cells depleted for RIG-I, STAT1, or STING, but not treated with 5′pppRNA, was similar or slightly increased compared to that of cells transfected with a scrambled control siRNA. In parallel, the siRNA-treated cells were transfected with 1 ng/ml 5′pppRNA, and 24 h later the IFN signaling response was analyzed by monitoring the upregulation of IFITI or STAT1 (Fig. 6G). Knockdown of RIG-I expression resulted in a strong reduction of 5′pppRNA-induced IFITI upregulation, whereas the 5′pppRNA-induced upregulation of IFITI was not affected by STAT1 depletion. siRNA-mediated knockdown of STING also did not block the 5′pppRNA-induced upregulation of STAT1, indicating that STAT1 and STING are dispensable for the response to 5′pppRNA, whereas RIG-I is required.

Post-infection treatment with 5′pppRNA inhibits CHIKV replication and stimulates the RIG-I pathway in both uninfected and CHIKV-infected cells. To explore the antiviral potential of 5′pppRNA against CHIKV, MRC-5 cells were first infected with CHIKV LS3-GFP at an MOI of 0.1, followed by transfection with 5′pppRNA (1 ng/ml) or control RNA at several time points post-infection. Measurement of EGFP expression by the reporter virus in infected MRC-5 cells that were fixed at 24 h p.i. indicated that treatment with 5′pppRNA at 1 or 3 h p.i. reduced reporter gene expression to less than 20% of that in untreated infected control cells (Fig. 7A). Even when treatment was initiated as late as 5 h p.i., a more than 50% reduction in EGFP expression was observed (Fig. 7A). Transfection of control RNA merely led to a ~20% reduction in EGFP reporter gene expression, largely independent of the time of addition.
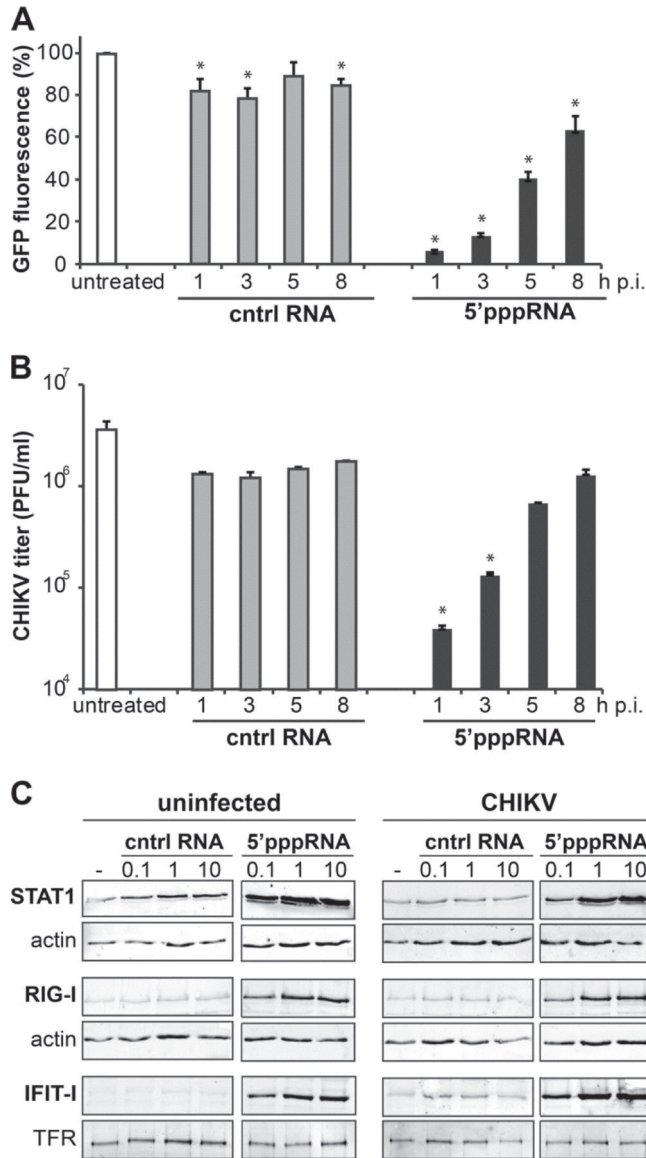
Figure 7. Post–infection treatment with 5'pppRNA inhibits CHIKV replication in an addition–dependent manner. MRC-5 cells were infected with CHIKV LS3-GFP at an MOI of 0.1, and at the indicated time points post-infection they were transfected with 1 ng/ml 5'pppRNA or control RNA. **(A)** Cells were fixed at 24 h p.i., and EGFP reporter gene expression was quantified and normalized to that in untreated cells. *, $P < 0.05$. **(B)** CHIKV progeny titers 24 h p.i. and after 5'pppRNA or control RNA treatment were determined by plaque assay. **(C)** MRC-5 cells were transfected with 0.1, 1, or 10 ng/ml 5'pppRNA or control RNA 1 h prior to infection with CHIKV LS3-GFP (MOI, 0.1). At 24 h p.i., cell lysates were prepared and STAT1, RIG-I, and IFIT-I protein levels were determined by Western blotting. Actin or the transferrin receptor were used as loading controls. Data are representative of at least two independent experiments.

Post-infection treatment of CHIKV-infected cells with 5′pppRNA also reduced viral progeny titers at 24 h p.i., depending on the time of addition (Fig. 7B). CHIKV titers in the medium of untreated infected cells were 6×10^6 PFU/ml at 24 h p.i., while treatment from 1 h p.i. onward led to a more than 2-log reduction in infectious progeny, i.e., 5×10^4 PFU/ml. When treatment was initiated at 3, 5, or 8 h p.i., CHIKV titers of 2×10^5, 7×10^5, and 1×10^6, respectively, were measured at 24 h p.i. Transfection of CHIKV-infected cells with control RNA resulted in a less than 1-log reduction in infectious progeny titer (Fig. 7B).

To assess the activation of the RIG-I signaling pathway in MRC-5 cells after 5′pppRNA treatment in the presence or absence of CHIKV infection, the expression levels of STAT1, RIG-I, and IFIT1 were analyzed by immunoblotting (Fig. 7C). Both in mock-infected and CHIKV-infected cells, transfection of 0.1 ng/ml 5′pppRNA induced a strong upregulation of STAT1, RIG-I, and IFITI (Fig. 7C), an effect that was more pronounced with treatment of 1 or 10 ng/ml of 5′pppRNA. In contrast, introduction of control RNA had no effect on expression of these proteins. CHIKV infection alone did not lead to increased STAT1, RIG-I, and IFIT1 expression, and CHIKV infection did not inhibit the 5′pppRNA-induced upregulation of RIG-I or downstream IFN signaling (Fig. 7C).

6

DISCUSSION

The absence of directly acting antivirals and registered vaccines for the treatment of important human pathogens, such as DENV and CHIKV, has emphasized the need for the development of therapeutic strategies. Initiated within minutes of virus binding to target cells, the innate immune response is the first natural barrier against viral infection. The innate response triggers an array of protective processes, resulting in the production of antiviral effectors and the induction of adaptive immune responses (285-288). Mimicking the early steps of the host antiviral response through stimulation of innate recognition receptors represents a novel therapeutic strategy for the treatment of emerging diseases, such as those caused by DENV and CHIKV.

We previously demonstrated that a 5′pppRNA derived from the 5′ and 3′ UTRs of VSV blocked the replication of multiple viruses both *in vitro* and *in vivo* (319). In the present study, we further characterized the antiviral potential of 5′pppRNA and demonstrated that 5′pppRNA treatment restricted DENV and CHIKV infection in human myeloid, epithelial, and fibroblastic cells. The antiviral effect was observed when 5′pppRNA was administered both pre- and post-infection, with demonstrated inhibition of DENV and CHIKV protein expression, RNA levels, and production of infectious progeny. The *in vitro* protective antiviral effect was dependent on an intact RIG-I/MAVS/TBK1/IRF3 axis but largely independent of IFNAR and STAT1. The protective effect was sustained over time, as cells remained free from infection even 72 h after infection, and 5′pppRNA also blocked antibody-dependent enhancement of DENV infectivity, a phenomenon that is associated with complications and disease severity in dengue patients. The present data on the 5′pppRNA immune-stimulating effect on human cells, combined with previous observations demonstrating that 5′pppRNA triggered a full range of antiviral and inflammatory responses in serum, lungs, and spleens of treated mice (319), highlights the importance of evaluating the efficacy of RIG-I agonists as a potential immune stimulator in humans.

The type I IFN system represents an important innate antiviral response to DENV and CHIKV. Indeed, type I IFN has been shown to restrict the propagation of DENV and CHIKV in both *in vitro* and *in vivo* models. Treatment with either IFN-α or IFN-β suppressed the replication of both DENV (330) and CHIKV (77) in cell culture. Moreover, infection of mice lacking IFNAR led to a significantly higher lethality after DENV (331) or CHIKV infection (81, 332). Among the viral RNA sensors, RIG-I, MDA5, and TLR3 are activated upon DENV infection and are essential for host defense against the virus (333). RIG-I appears to play a major role in the response to CHIKV infection, as CHIKV-induced IFN-β expression was more strongly reduced in RIG-I-deficient MEFs than in those lacking MDA5 (194). The antiviral activity of 5′pppRNA observed in previous studies has been attributed to the potent activation of inflammatory and antiviral programs driven by transcription factors such as IRF3, IRF7, STAT1, and NF-κB (319). In this study, the antiviral protective response was dependent on a functional RIG-I pathway but was largely independent of STAT signaling. We also demonstrated that 5′pppRNA treatment triggered a robust host antiviral response associated with the expression of several IFN-

stimulated genes (ISGs), including RSAD2 (Viperin), IFIT, and IFITM proteins MX1 and OAS. Although hundreds of ISGs have been identified, only a few of them have been fully characterized with respect to their inhibitory function. Recently, Schoggins et al. identified a panel of broadly active antiviral molecules that facilitate inhibition of viral infection (308), with IFITM proteins and Viperin characterized as important ISGs required for inhibition of CHIKV (120, 334, 335). Although most of these essential antiviral genes were upregulated following RIG-I stimulation (319), an in-depth analysis is now required to identify which IRF3-driven ISGs mediate the 5′pppRNA antiviral effect observed against DENV and CHIKV infection *in vitro*.

Poly(I:C), another dsRNA innate immune stimulator, has been extensively studied *in vitro* and *in vivo* and has demonstrated a broad range of efficacy against many viral infections, including those by DENV and CHIKV (314, 315, 336-339). *In vitro* studies have shown that the poly(I:C)-mediated DENV antiviral response was dependent primarily on IFN-β induction and was reversed by IKK inhibitors (315). Poly(I:C), in combination with TLR7/8 agonists, not only prevented DENV infection *in vitro* but also decreased DENV viremia *in vivo* through increased inflammatory and humoral responses (315, 338). The immune response generated by poly(I:C) was previously evaluated in a phase 1 clinical trial with healthy volunteers, and whole-genome transcriptional analysis of peripheral blood mononuclear cells demonstrated upregulation of genes involved in multiple innate pathways, including antiviral and inflammasome signaling (340). This observation underscores the fact that synthetic dsRNA remains an attractive innate immune stimulator in humans.

Vaccination is the primary approach to prevent viral infection. Increasing the immunogenicity of vaccines with molecular immune modulators that elicit immune responses is crucial to enhance vaccine efficacy. Poly(I:C) and, more recently, 5′pppRNA have been used as adjuvants and were shown in combination with influenza vaccine to improve protection in mice (310, 341-343). Interestingly, we observed that RIG-I activation using 5′pppRNA not only induced antiviral effectors but also mobilized cytokines and chemokines involved in trafficking processes of immune cells, including CXCL10, CCL5, and CCL3. The proinflammatory cytokine IL-6, which was potentiated by the 5′pppRNA treatment, also is crucial to maintain and potentiate CD8^{+} T cell survival and killing *in vivo* (344). A significant type III IFN response was observed in cells challenged with 5′pppRNA. Recent studies have shown that type I and III IFNs activate similar components of the JAK-STAT pathways, although type III IFNs induced a delayed and stronger induction of ISGs than type I IFNs (345). We did not find a significant antiviral role for type III IFN in DENV-infected A549 cells, although the induction of type III IFN may have biological relevance *in vivo* by bridging the innate and adaptive immune responses. Indeed, IL-28A stimulation presented antiviral immunostimulatory effects by increasing the total number of lymphocytes and CD4^{+} T cells in lung lymphocyte preparations of vaccinia virus-infected mice (346). The present study demonstrates the antiviral effect of 5′pppRNA but also suggests new perspectives on the use of RIG-I agonists as vaccine adjuvants in the context of DENV and CHIKV infection.

Taken together, our study provides compelling evidence that stimulation of the natural host defense with 5'pppRNA represents a valuable alternative strategy to conventional antiviral drugs directed against specific viral targets. RIG-I activation mimics and stimulates evolutionarily conserved immune responses to infection and induces multiple antiviral factors that block viral infection at different steps, reducing the possible development of antiviral resistance. These novel approaches to boost host antiviral innate and inflammatory immune responses are broad spectrum in nature rather than virus specific. Such a broadly acting antiviral molecule may be desirable in tropical areas where the population is exposed to multiple pathogens, e.g., where both DENV and CHIKV are endemic and cause co-infections and where the facilities for (differential) diagnosis are limited.
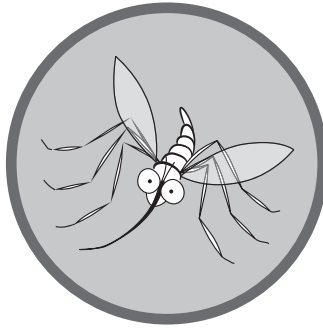
ACKNOWLEDGEMENTS

7.

General Discussion

Identifying and understanding host factors involved in CHIKV replication

Over the past decade, the status of CHIKV has shifted from relatively uncommon and poorly documented to being a wide-spread emerging virus. At present, it is even considered a global public health concern with the potential of high morbidity and a large social impact. CHIKV transmission has been reported in all inhabited continents (both Americas, Europe, Africa, Asia, and Oceania), illustrating the rapid globalization of the virus. Especially Latin America may be facing large epidemics in the near future. Many infected travelers return to non-endemic areas, providing the opportunity for local transmission and new outbreaks. Despite this rapid spread and the increasing social and economic burden that CHIKV poses, no registered vaccines or effective antiviral drugs are available. A thorough understanding of the viral replicative cycle will provide a better basis for the development of antiviral strategies. CHIKV is expected to rely heavily on cellular factors for its replication, but only a handful of host factors involved in CHIKV replication have been identified thus far. Research tools can aid in identifying these host factors and thus increase our understanding of this pathogen. This thesis describes the development and characterization of a novel infectious cDNA clone (**chapter 2**), and its application in a kinome-directed siRNA screen aimed at identifying host factors involved in CHIKV replication (**chapter 3**). A selection of these and other identified host factors were described in more detail in this thesis. The involvement of MAPK signaling during CHIKV replication was studied in **chapter 4**, and the role of stress granule components G3BP1 and -2 in **chapter 5**. **Chapter 6** describes that both CHIKV and DENV replication can be inhibited using a RIG-I agonist (5'pppRNA), which may represent a suitable starting point for antiviral treatment in a clinical setting.

Construction and characterization of a synthetic CHIKV cDNA clone

An infectious cDNA clone is a plasmid that contains a full-length DNA copy of the viral genomic sequence. Infectious RNA is generated by *in vitro* transcription and can subsequently be transfected into cells to launch and recover the (mutant) virus, although in recent years also DNA-launched systems have been developed. Full-length cDNA clones are valuable research tools that enable reverse genetics and can be tailored to specific requirements. They enable the insertion of reporter genes and mutational analyses, for example to assess the function of a specific residue or viral protein, or examine mutations related to drug resistance. When we set out to create the synthetic infectious cDNA clone CHIKV LS3 (Leiden synthetic 3), already several other infectious CHIKV clones existed (e.g. (62, 69, 114-117)). However, some of these clones were based on older and/or different genotypes than the genotype that caused the major outbreak in 2005. We decided not to use a single isolate and a single sequence thereof as a basis for our infectious cDNA clone, but to base it on the consensus sequence of all deposited CHIKV genomes that contained the A226V mutation present in GenBank at the moment of design. The designed sequence was created by gene synthesis and the resulting cDNA clone was termed LS3. There is the risk that a virus based on such a consensus sequence of several variants is hampered in its replication if certain sequence combinations

are incompatible with each other. If this would have been the case, LS3 could have easily been converted to the sequence of a natural isolate by introducing only a few mutations. The synthetic virus and its derived GFP-reporter virus were extensively characterized in cell culture, and they behaved very similar to natural isolate, ITA07-RA1. Also in a mouse model it caused a lethal infection comparable to that caused by a natural isolate (chapter 2) (69).

The majority of previously developed CHIKV infectious clones are transcribed into genomic RNA using an upstream SP6 promoter. This is a strong promoter that yields high amounts of RNA *in vitro*. However, it also generates capped CHIKV RNA with a non-native 5' terminus, as it will contain m7Gppp**G** (instead of m7Gppp**A**) at the 5'end (Figure 1). This additional 5'-terminal G residue will eventually be removed during subsequent passages and the virus will return to its native sequence, as was shown for Rubella virus (347), but it may take several replication cycles to achieve this. It is unclear what the exact implications of the additional 5'-terminal G are for viral replication. We therefore placed our molecular clone under control of a phi2.5 promoter, which generates a genuine 5' terminus. A disadvantage of using this promoter is that it is less efficient and yields lower amounts of RNA. A full-length CHIKV clone under control of the routinely used SP6 promoter (named CHIKV LS2) was also generated, and it would be interesting to compare virus derived from both constructs side-by-side to determine the effect of the extra 5'-terminal G on CHIKV replication. DNA-launched CHIKV infectious clones have been constructed that use a CMV early promoter to drive production of viral RNAs in the nucleus of infected cells, which results in native 5' termini (e.g (348)).

As CHIKV spreads globally and infections are becoming increasingly common, the number of CHIKV-related studies is growing fast. Unfortunately, this results in a growing diversity of CHIKV strains being studied, ranging from the 'old' African S27 and Ross isolates to a myriad of (often ill-defined) clinical isolates. These different CHIKV variants may have different characteristics, potentially leading to contradictory reports. Therefore it would be advisable to confirm key findings with at least one other CHIKV isolate. We preferred to work with our consensus-based virus instead of a clone based on a single genome derived from a quasispecies population. The bulk of the experiments described in this thesis were performed with CHIKV LS3(-GFP), but frequently one or more other CHIKV strains were used to confirm results. In general these different CHIKV variants behaved the same, although e.g. NL10/152 showed a delayed onset of CPE compared to other strains. This suggests that the synthetic virus is a good representative of the currently circulating CHIKV Indian/Indian Ocean strains and constitutes an appropriate tool to study various aspects of the viral replication cycle, including the role of host factors.

RNAi screening to identify host factors involved in CHIKV replication

Despite the enormous surge in CHIKV-related research efforts and publications since its re-emergence in 2005, its replicative cycle is still not completely elucidated. Especially our comprehension of the involvement of cellular components remains incomplete. The identification of host factors is the first step towards testing their importance for viral

replication. A number of host factors involved in CHIKV replication have been described (e.g. (118-122)), but till date large-scale RNAi approaches have not been published for CHIKV. Functional genomics represent an unbiased approach to identify host factors involved in viral replication, including siRNA (short interfering RNA) and shRNA (short hairpin RNA) screening, which are based on RNA interference (RNAi). RNAi is a highly conserved cellular process characterized by sequence-specific transcript cleavage and degradation. The silencing process is controlled by the RNA-induced silencing complex (RISC) and is initiated by short (~21-nt) dsRNA molecules, which can be introduced endogenously or exogenously. One strand of the dsRNA/siRNA molecule is loaded into RISC (the antisense or guide strand) and functions as a template for the sequence-dependent mRNA cleavage. Full sequence complementarity triggers enzymatic cleavage opposite of position 10 of the siRNA, and cleaved RNAs are degraded rapidly (349) Selective depletion of cellular mRNAs results in knockdown of the encoded protein.

Like every screening approach, also siRNA-mediated knock-down of expression has its drawbacks. A major concern are the potential "off-target" effects of the siRNAs (imperfect gene targeting), which can result in false positive hits (Figure 2). Off-target effects are caused by the fact that siRNAs with an imperfect sequence similarity can still bind to mRNAs they are not intended to target (350). Imperfect sequence similarity will not lead to RISC-induced cleavage of the mRNA bound by the siRNA, but it will result in translational repression by ribosome interference (351). The risk of finding false positive hits due to off-target binding increases when a high concentration of siRNA is used. The likelihood of false positives due to off-target binding can be reduced by (a) using lower amounts of siRNA, (b) using pooled siRNA that target different parts of the mRNA (and thus also lower concentrations of each individual siRNA), or (c) separately testing several individual siRNAs that target the same gene. Strikingly, the reduction in off-target effect that is observed when pooled siRNA are used is
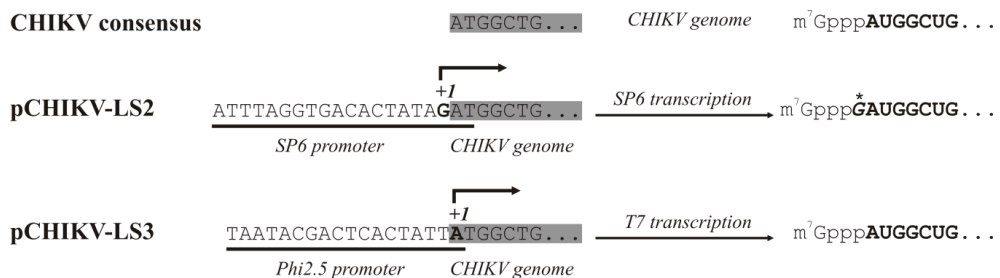
Figure 1. Comparison of the 5' termini of *in vitro* transcribed RNA produced with SP6 and phi2.5 promoters. The top line shows the 5'-end of the consensus genome sequence, based on the selected CHIKV strains described in the text. Minimal promoter sequences are underlined. The +1 nucleotide (transcription start) is indicated in bold. The CHIKV genome is shaded in grey. The products resulting from SP6 transcription (using a m7GpppG cap analog) and T7 transcription (using a m7GpppA cap analog) are shown. The extra G at the 5'-end of the genome resulting from SP6 polymerase transcription on LS2 constructs is indicated with a *.

not only due to lower amounts of the individual siRNAs. The effect could not be reproduced to the same extent by using low concentrations of a single siRNA, thus indicating that it is rather the competition between the different siRNAs than the concentration (352). Off-target binding can further be reduced by chemical modifications of the siRNA, for example by 2'-O-methylation of the guide (antisense) strand (353). The passenger (sense) strand can be modified to prevent interaction with RISC, and thus favor guide strand uptake (and reduce passenger strand-induced off-target effects). In addition, the seed region of the guide strand is often modified to destabilize off-target binding, hence increasing target specificity (353).

Some siRNA can cause off-target effects by behaving as microRNA (miRNA). The latter are encoded by mammalian cells and resemble siRNAs in the sense that they are also short RNA sequences that can affect mRNA levels, using the same cellular machinery. They are involved in many cellular processes, but mostly play a regulatory role, as they can induce only modest
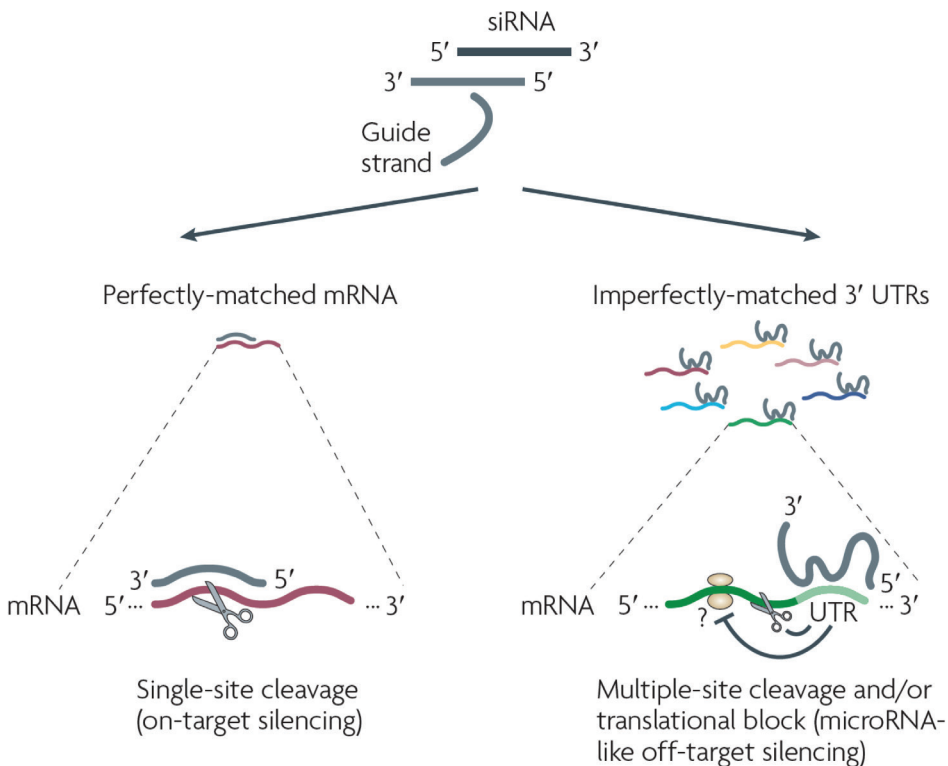
Figure 2. Schematic overview of sequence–specific transcript depletion by RNAi. One strand of the siRNA duplex (guide strand) is loaded into the RISC and functions as a template for sequence-dependent transcript cleavage. A siRNA with perfect sequence similarity ideally targets only one transcript, and siRNA/RISC binding results in mRNA cleavage and degradation (left). Off-target effects are caused by siRNA that bind with imperfect sequence similarity, often to the 3' UTR of mRNAs. As only limited sequence similarity is needed, many different transcripts can be targeted by a single siRNA. Reproduced (and adapted) with permission from (350).

(~2-fold) changes in mRNA levels (354). It is striking that a single miRNA can regulate dozens of transcripts, thus having a widespread effect on cellular processes. siRNA can behave as miRNA by sequence-specific imperfect pairing with motifs that are located mostly in the 3'UTR of an mRNA. As only short regions of sequence complementarity are required, many different transcripts can be affected, thus resulting in sequence-dependent miRNA-like off-target effects (Figure 2). As with genuine miRNA binding, this interaction results in modest (less than 2-fold) changes of transcript levels (355).

Another concern when utilizing siRNAs is the possible activation of the cellular innate immune response, which can be stimulated by either the oligonucleotides or the delivery method. Activation can occur through Toll-like receptors or cytoplasmic RNA sensors, such as RIG-I (reviewed in (356)). The degree of innate immune activation depends on the siRNA structure, sequence, delivery method, and cell type. It can result in the production of high levels of inflammatory cytokines and interferons, especially in animal models and primary human blood cells (357-359). Presently, siRNAs are often modified by introducing chemically modified nucleotides in order to avoid recognition by Toll-like receptors and other nucleic acid sensors (360, 361).

Taken together, off-target binding and activation of the innate immune response can result in false-positive hits in siRNA screens. RNAi screening can also yield the opposite: false-negative results. False negatives may occur when the degree of target gene knockdown is insufficient. This can be due to suboptimal siRNA sequences, or when the mRNA half-life is very short or the protein turn-over time very long. Optimization for these factors (assay timing) is often not possible in a large(r)-scale screen, as the optimal time frame to achieve depletion for the majority of the targets needs to be taken into consideration. Biological redundancy is another potential source of false-negative results. Parallel pathways or homologous genes with (partially) overlapping functions may mask the effect of target depletion. In addition, false negatives can occur when the targeted gene is not expressed in the cell type/line chosen for the experiments. The number of expressed genes in a given cell type can vary greatly, between ~500 genes in ovary tissue to over 6,000 in B lymphoblasts (362). The CHIKV siRNA screen described in chapter 3 was performed using MRC5 cells, which are lung fibroblasts. Assuming these cells express the same number of genes as adult lung tissue (362), about ~3,000 genes are expressed, approximately ~15% of all genes in the human genome. This suggests there is some potential for false-negative results in our screen.

Proper controls and quality control can reduce false discoveries, but can never completely prevent them. Therefore, it is crucial to confirm the hits (potential host factors) identified in a screen to exclude false discoveries.

Whole-genome RNAi screens are feasible nowadays, but are expensive and need special robotic equipment. In addition, they yield enormous amounts of data, which often requires collaborating with data analysis experts. Many groups choose to screen a subset of the genome, for example the druggable genome (subset of the ~30.000 genes in the human genome that encode proteins able to bind drug-like molecules), or the kinome. Chapter 3

describes a siRNA library screen targeting the human kinome for its potential involvement in CHIKV replication. Obviously, the choice to use a siRNA library targeting the human kinome is associated with its own merits and potential problems. The kinome is more often selected to identify host factors involved in viral replication (190, 191, 363, 364), because kinases play key roles in many, if not all, cellular processes and are therefore undoubtedly also involved in viral replication. However, the fact that kinases perform key functions in many cellular pathways also presents a problem. Depletion of a key protein may disturb a range of downstream signaling pathways. Therefore it can be troublesome to determine which downstream effect was responsible for the abrogation of viral replication.

In recent years, quite a number of siRNA screens have been performed that aimed at identifying viral co-factors. However, when comparing independent RNAi screens done using the same virus, there is often only very limited overlap between identified targets. For example, between the hits of four genome-wide siRNA screens aiming to identify host factors in influenza A virus replication, only ~6.7% overlap was found when comparing the screens pairwise (193, 194, 365-367). However, there was a larger overlap when comparing the screens at the level of enriched categories, rather than individual genes. The same observation was also made for CHIKV proteomic screens (142). It is therefore speculated that the limited overlap is mostly due to false-negative hits, rather than false-positives (i.e. each screen identified a (different) fraction of truly involved proteins) (368). This is further supported by the observation that hits from different screens are highly connected in interaction networks (e.g. protein-protein interactions), at a significantly higher frequency than they would be by chance. This observation underscores the notion that RNAi screening is a powerful tool to identify host factors involved in viral replication, but that it is by no means perfect, and often provides only a partial answer. Confirmed hits do provide valuable starting points for further, in-depth studies.

To summarize, RNAi is a powerful forward genetics tool to dissect CHIKV-host interactions, but needs to be used with caution. It is a relatively young technique that can be employed for unprecedented large-scale loss-of function studies, but also contains various potential drawbacks, including aspecificity of siRNA targeting, variability and incomplete knockdown, and a restriction to use cell lines that can be efficiently transfected and are subsequently still permissive to viral infection. The above-mentioned potential drawbacks of RNAi may paint a dark picture of the benefits of using RNAi screening; however, it is a tremendously versatile tool, if used with caution. RNAi enables loss-of-function studies at a scale and with an ease that cannot be achieved using mouse embryonic fibroblasts (MEFs) or other loss-of-function techniques. In addition, it allows the identification of host proteins that are either directly or indirectly involved in CHIKV replication, in contrast to other techniques used to identify host factors (Y2H, pull-down experiments, etc.). RNAi screening has the potential to provide valuable information about genes and especially pathways involved in viral replication and can provide many starting points for further characterization of the involvement of those genes.

7

MAPK signaling during CHIKV replication

Chapter 4 describes the role of MAPK signaling during CHIKV replication. MAPK signaling pathways mediate key responses when triggered by a range of stimuli, including viral infection. MAPK signaling can roughly be divided into three major pathways: Ras-Raf-MEK-ERK, p38 MAPK and SAPK/JNK signaling (reviewed in (208)). SAPK/JNK and p38 MAPK are induced by various stresses, whereas the Ras-Raf-MEK-ERK signaling cascade regulates growth factor responsive targets and is thus linked with cell proliferation and differentiation. Disturbances in Ras-Raf-MEK-ERK signaling are associated with cancer, as an increased signaling activity is often found in tumors (369, 370). Ras and Raf are both oncogenes, and are thought to transform cells by prolonging the activated state of MAPKK and downstream components. Overexpression of constitutively active MAPKK promotes cell transformation (371). ERK1 and ERK2 are the central effectors of the Ras-Raf-MEK-ERK pathway. They are related protein-serine/threonine kinases whose cascade regulates a wide range of processes related to survival (cell adhesion, migration, metabolism, differentiation, cell cycle progression, and transcription) (210). ERK can inhibit Raf by phosphorylation, thus creating a negative feedback loop (Figure 3). Beside the negative feedback loop, several phosphatases are involved in the inactivation of ERK. These include MKP3 (also known as DUSP6), MKP4 (DUSP9), and PAC1 (DUSP2) (210, 372). Raf and MEK have narrow substrate specificities, but ERK can catalyze the phosphorylation of hundreds of nuclear and cytoplasmic substrates, including regulatory molecules and transcription factors. Several viruses have been described to induce the Ras-Raf-MEK-ERK pathway (213, 221, 232-238, 243, 244) and many of them benefit from an activated Ras-Raf-MEK-ERK axis, through a mechanism that is not yet fully understood. Little is known about the activation of the Ras-Raf-MEK-ERK pathway by alphaviruses, with the exception of VEEV, which activates MEK/ERK signaling, and depends on this activation (239). Chapter 4 shows that CHIKV does not activate MEK/ERK signaling, and is not affected by its pharmacological modulation. Also inhibition of the upstream kinase b-Raf did not affect CHIKV replication. This was rather surprising, as many other +RNA viruses, including the distantly related VEEV, depend on an activated MEK/ERK signaling pathway (233, 238, 239, 243, 244). It is hypothesized that a (virally) activated MEK/ERK pathway eventually results in a downregulation of the innate immune (IFN) response, which obviously is beneficial for the invading virus (247, 248). Another potential proviral aspect of activated Ras-Raf-MEK-ERK signaling is its positive effect on cellular transcription and translation, which may also extend to viral transcription and translation. ERK can positively regulate transcription, either directly or indirectly by phosphorylation of ribosomal protein S6 kinases, mitogen- and stress-activated protein kinases and ternary complex factors (reviewed in (210)).

Clearly, further experiments are needed to elucidate the exact involvement of MAPK signaling in CHIKV replication, and how MEK/ERK activation can be beneficial for the replication of some viruses (e.g. VEEV, CVB3, Influenza A and Junin) (233, 238, 239, 243, 244). It would be interesting to examine the apparent differences between CHIKV and VEEV, two viruses from the same genus, and elucidate the underlying molecular mechanisms.
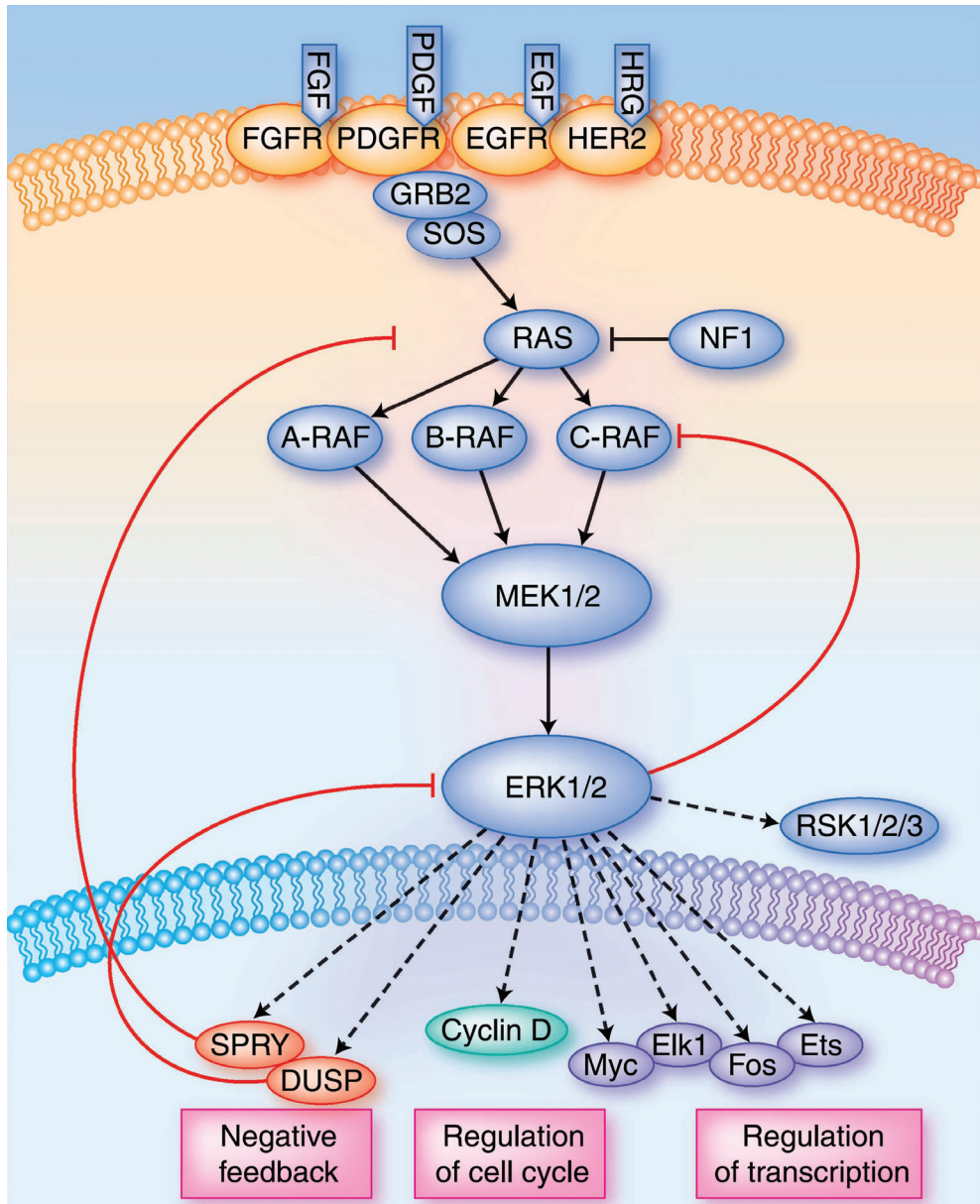
Figure 3. Ras–Raf–MEK–ERK signaling. The Ras-Raf-MEK-ERK signaling cascade is activated when growth-stimulating ligands bind to the receptor tyrosine kinases, eventually resulting in phosphorylation and activation of the downstream components. The Ras-Raf-MEK-ERK cascade contains a negative feedback loop, the level of ERK activity regulates SPRY and DUSP family proteins, which in turn negatively regulate Ras or ERK. ERK can also phosphorylate the upstream Rafs, thus inducing an inhibitory feedback loop. Reproduced from (373).

Finally, CHIKV-induced activation of p38 MAPK occurs only very late in infection, and therefore this response is most likely associated with the onset of apoptosis, rather than a specific antiviral response. Nevertheless, it would be interesting to further pursue the mechanisms behind this activation of the p38 MAPK cascade.

Stress granules and CHIKV replication – an unexpected proviral role for G3BPs

The G3BPs (G3BP1 and G3BP2) are a good example of the aforementioned risk of overlooking host factors during RNAi screens due to redundancy in protein function or pathways. Chapter 4 describes that depletion of a single G3BP did not have a major effect on CHIKV replication, while the simultaneous depletion of both G3BPs strongly affected CHIKV replication. The G3BPs are multi-functional, multi-domain proteins that share a conserved acidic domain, a Nuclear Transport Factor 2-like domain, an arginine/glycine-rich box, and an RNA recognition motif (282, 374). The latter two elements are associated with RNA binding. G3BP was originally identified as a binding partner of the Ras-GTPase-activating protein, but that property was later disputed (44, 45). G3BP1 has two SH3 domain-binding motifs, whereas G3BP2 possesses - depending on the splice variant - 5 or 6 of such motifs. The G3BP1 and G3BP2 proteins share several domains and may thus be (partly) functionally redundant, as is illustrated by our observation that simultaneous depletion exerts a stronger effect on CHIKV replication. G3BP1 and G3BP2 are encoded by genes located on different chromosomes (5 and 4) and, despite their similarities, are thought to have different functions despite their many shared characteristics. Indeed, G3BP1 is a negative regulator of wnt/β-catenin signaling (375) whereas G3BP2 is a positive regulator (376).

The G3BPs have been studied most extensively in relation to their role in stress granule formation. Stress granules (SGs) are formed in response to cellular stress and result in translational inhibition (253, 377). The G3BPs have been previously implicated in the replication of alphaviruses, including CHIKV. For example, nsP3 of SINV, SFV, and CHIKV was shown to bind to G3BP (62, 63, 138, 274). Generally, this nsP3-G3BP interaction is thought to partially block the cellular antiviral response, as nsP3 prevents the formation of genuine stress granules by sequestering G3BP, thus preventing translational inhibition. Translational inhibition can be considered both an antiviral response by the cell to limit the production of viral proteins and thus viral replication, as well as a proviral manipulation of the host cell machinery by the virus, to reduce competition of host transcripts with viral mRNAs. CHIKV structural proteins are still produced when host translation is blocked, possibly due to a translational enhancer sequence in the subgenomic mRNA, similar to those described for other alphaviruses (68). The data presented in chapter 4 does not dispute the antiviral role described for G3BPs during alphavirus replication, but demonstrates that the G3BPs have an additional, proviral role early in CHIKV infection. G3BP depletion did not affect entry, translation or polyprotein processing, but seriously affected +RNA accumulation. Infections performed with a replication-deficient virus indicated that the G3BPs were likely needed for the switch from protein synthesis to genome amplification. During CHIKV replication the viral

genome is used as a template by both the viral polymerase and cellular ribosomes. However, they operate in opposite directions, thus requiring some form of regulation. Chapter 4 proposes a role for G3BPs in clearing ribosomes and/or other proteins from the template during the switch to genome amplification (Figure 4). In recent years our understanding of the complexity of SGs has grown significantly, and they are more and more seen as complex signaling hubs instead of the static RNA-protein aggregates they were once thought to be. Diverse signaling molecules, including scaffolding proteins, are recruited to stress granules (378-381). The recruitment of scaffolding proteins (e.g. RACK1, TRAF2) inhibits the signaling pathways they are involved in. For example, RACK1 is an adaptor molecule that integrates input from several signaling pathways and plays a key role in cellular processes including cell proliferation, transcription and protein synthesis (382). Its recruitment to SGs inhibits stress-activated p38/JNK signaling, which would otherwise trigger apoptosis (383). Alternatively, recruitment of specific proteins can also induce downstream signaling. For example, there is a clear link between SG formation and the activation of the innate immune response. RIG-I and PKR were found to be sequestered to SG structures, and this RIG-I sequestering is needed for IFN-stimulated gene (ISG) activation (378). G3BP1 directly interacts with inactive PKR and recruits it to SGs, resulting in phosphorylation of eIF2α which leads to translational inhibition (379). These examples illustrate the central role SG formation plays during many cellular processes, including antiviral responses. Blocking stress granule assembly, for example during viral infection, can affect these signaling cascades.

As mentioned earlier, also functions (thus far) not linked to stress granule formation and regulation are attributed to G3BPs. For example, G3BP2 was described to bind the N-terminal domain of IκBα, thus enforcing cytoplasmic anchoring of IκBα/NF-κB complexes (265). Nuclear translocation of NF-κB results in the induction of numerous genes involved in immune and inflammatory responses (384, 385). Therefore, depletion of G3BP2 may enhance the antiviral response to CHIKV infection, although we could not observe changes in NF-κB protein expression or cellular localization. Furthermore, G3BP2 modulates the activity of GSK3β (376), which in turn modulates pro-inflammatory gene expression, and inhibition of GSK-3β reduced VEEV replication (386). It is therefore possible that GSK-3β activity is also needed for CHIKV replication, which is disturbed upon G3BP knockdown. Another aspect of G3BPs and their function is related to its methylation. The C-terminus of G3BP contains prominent target motifs for protein arginine methyl transferases (PRMTs). Methylation can affect protein-protein interaction, but also RNA binding activity and intracellular localization of the targeted protein (387). The exact role and function of G3BP methylation is not completely understood yet. Clearly, we have only just begun to unravel the complexity of functions associated with SGs in general, and G3BPs in particular. Future experiments should assess the exact function of the G3BPs and its associated signaling profile during CHIKV infection.

Innate immune stimulation inhibits CHIKV and DENV replication

Both CHIKV and DENV are important human pathogens for which no therapeutic options are available. In contrast to CHIKV, DENV is associated with hemorrhagic symptoms and mortality. Both viruses have overlapping geographic distributions and initially present with similar symptoms. This makes it challenging to distinguish the viruses clinically, especially considering the fact that both viruses are mostly endemic in areas where diagnostic capacity is limited. An antiviral therapy that would target both viruses would be ideal.

Infection with either virus elicits a strong, protective innate immune response and treatment with IFN-α or IFN-β reduces the replication of these viruses in cell culture (77, 330). Unfortunately, treating patients with IFN is only effective when started early in disease. However, harnessing the host's own IFN response might be an interesting alternative strategy to IFN therapy to treat infections with DENV, CHIKV and other viruses. Chapter 6 describes the effect of the exogenous stimulation of the innate immune response on DENV and CHIKV infection. A small 5' triphosphorylated RNA molecule (5'pppRNA) was used as a RIG-I agonist, which induced an antiviral state that blocked both DENV and CHIKV replication in cell culture (Figure 5). The innate immune response triggered by the RIG-I agonist was characterized by increased levels of RIG-I, IFIT-1, STAT1 and phospho-STAT1, resulting in increased levels of IFN-α, IFN-β, IL-6, and IL-1α. This activation is dependent on intact RIGI-MAVS-TBK1 signaling, but largely independent of the IFN receptor and STAT1. Treatment with 5'pppRNA was still protective in cell culture when started after infection, and the activated IFN response could prevent viral spread to neighboring cells and tissues. In addition, the protective effect induced by the 5'pppRNA is long-lasting, as cells were still protected from DENV infection 72 h post treatment (*in vitro*) (192). The protective effect of 5'pppRNA treatment is at least partially IFN independent, as 5'pppRNA was still able to induce an innate immune response in cell culture when the IFN receptor (IFNAR) was depleted using siRNA (192). In addition, IFNAR knockout mice could still be protected against a lethal influenza challenge by treating them with
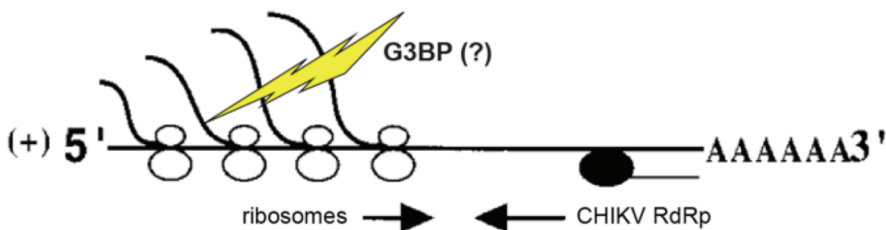
Figure 4. Model depicting the proposed proviral function of G3BP during CHIKV replication. Genomic CHIKV RNA is initially translated by ribosomes into non-structural proteins, which assemble into a replication complex that synthesizes a complementary negative strand CHIKV RNA. However, ribosomes and the replication complex use the same genomic RNA as a template, which could lead to collisions as they move in opposite directions (towards each other), stressing the importance of regulation. The G3BPs may be involved in regulation the switch from translation to negative strand synthesis, possibly by clearing ribosomes and other proteins from the genomic RNA from. Adapted from (388).

5'pppRNA (319). This latter experiment illustrates that the RIG-I agonist is not only suitable for *in vitro* experiments (as described in chapter 6), but also has potential for clinical application. In recent years *in vivo* transfection reagents have been developed that enable delivery of nucleic acids in various animal models. Indeed, as mentioned above, also the 5'pppRNA could be effectively delivered to mice using intravenous administration, protecting them from a lethal influenza virus challenge (319). Prolonged 5'pppRNA administration further reduced viral replication, thus indicating that therapeutic use is a realistic scenario for patients already infected when seeking medical attention. The application of innate immune stimulation is assumed to have a broad-spectrum antiviral effect rather than providing protection against a specific virus, and may therefore have broad therapeutic potential in the clinic. The RIG-I agonist induces a general immune response that includes multiple antiviral effectors that block viral replication at different steps, therefore raising the barrier for development of resistant virus mutants. RIG-I agonists are attractive potential therapeutic agents, as they mimic the earliest step of virus recognition by the immune system and triggers its subsequent response. A previous study showed that 5'pppRNA stimulation could induce a complete IFN response, inducing 97% of the genes activated after IFNα-2b treatment (319). Obviously, the patient should be closely monitored, to control the strength of the IFN response and reduce potential side effects.

Although not the main focus of this thesis, the innate immune response to viral infection is currently considered an important focus area by the scientific society. It is one of the first hurdles the invading virus needs to pass, and is triggered within minutes of viral attachment and entry. Furthermore, the activation of the innate immune system is essential for subsequent adaptive immune activation. It is therefore not surprising that many viruses have developed strategies to disable or evade the innate immune response, and CHIKV is not an exception. Still, our understanding of exactly how viruses achieve such a feat is incomplete. Gaining more insight into these immuno-modulatory mechanisms may provide us with tools to combat viral infections, as well as potential treatment options for other (uncontrolled) infections in the human body, e.g. autoimmune diseases. In conclusion, CHIKV (and DENV) induces a strong, protective IFN response, apparently via the RIGI-MAVS-TBK1-IRF3 cascade and downstream ISGs, including viperin (81, 88, 120). Although in recent years some light was shed on innate immune activation and evasion by CHIKV, more in-depth analyses are still needed to completely elucidate the mechanisms by which CHIKV induces and manipulates the innate immune response.

Concluding remarks

CHIKV is serious human pathogen that has exhibited a dramatic spread over the globe in the past decade, resulting in severe human suffering and economic damage. The fact that no registered vaccine or antiviral drugs are available is very troublesome, considering the high numbers of new infections yearly. However, several promising vaccine candidates are currently tested in clinical trials, and will hopefully be available to the public soon. Antiviral

leads against CHIKV are followed with fervor and will hopefully soon result in the design of intervention strategies. A more complete knowledge of all cellular components involved in the CHIKV replication cycle is critical for our understanding of this important human pathogen, and indispensable to understand the long-term sequelae often observed. In recent years the amount of scientific interest in CHIKV has seen a sharp increase, and our knowledge about this fascinating pathogen is expanding equally fast. Unfortunately, there are still many unknowns, and future work should assess the exact requirements for CHIKV replication, and solve the puzzle of how to prevent and treat CHIKV-induced arthritis.
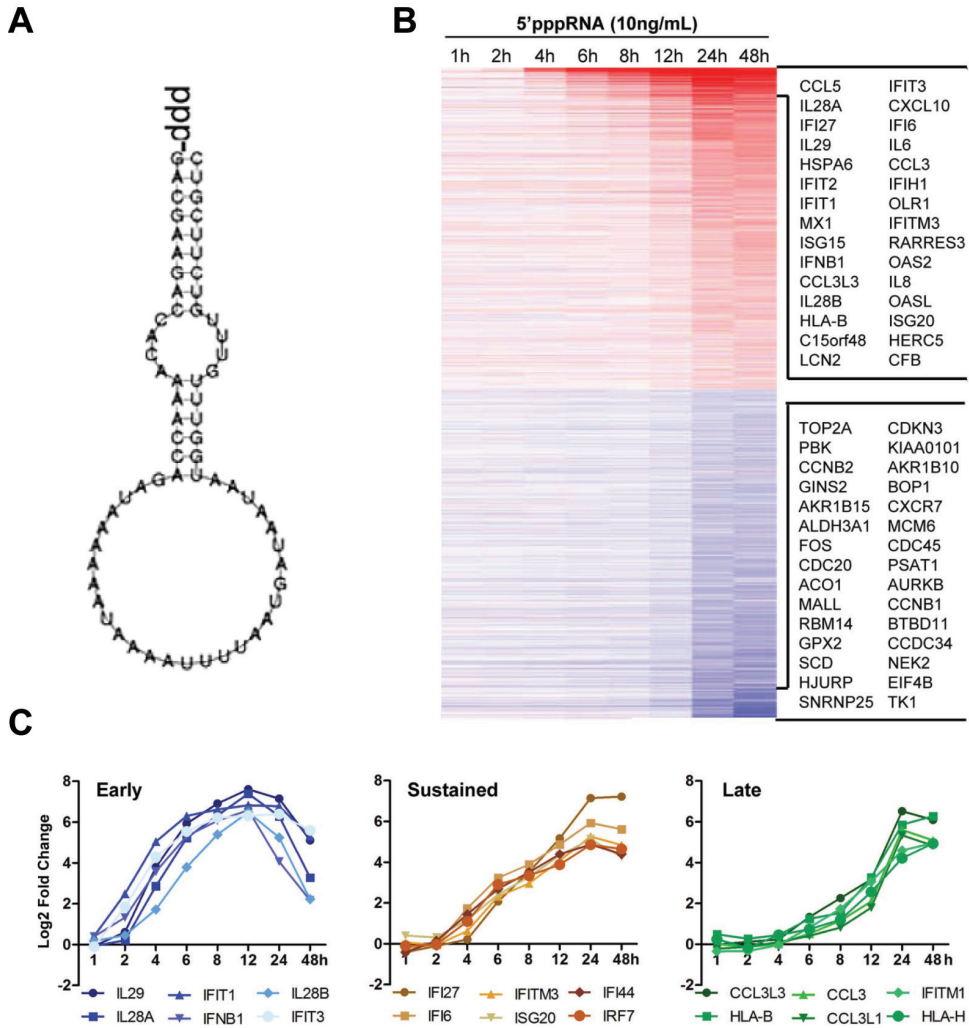
Figure 5. Induction of the innate immune response by the RIG–I agonist 5'pppRNA. (A) Schematic overview of the panhandle structure formed by the 5' and 3' UTRs of the VSV genome that forms the 5'pppRNA. **(B)** Heatmap of genes affected by 5'pppRNA treatment, sorted by fold-change (red: upregulated, blue: downregulated). **(C)** Genes among the top 30 upregulated genes could be divided based on different expression patterns: early, sustained or late. Adapted from (319).

REFERENCES

1. **Burt FJ, Rolph MS, Rulli NE, Mahalingam S, Heise MT.** 2012. Chikungunya: a re-emerging virus. Lancet **379:**662-671.
2. **Taubitz W, Cramer JP, Kapaun A, Pfeffer M, Drosten C, Dobler G, Burchard GD, Loscher T.** 2007. Chikungunya fever in travelers: clinical presentation and course. Clin Infect Dis **45:**e1-4.
3. **Rajapakse S, Rodrigo C, Rajapakse A.** 2010. Atypical manifestations of chikungunya infection. Trans R Soc Trop Med Hyg **104:**89-96.
4. **Touret Y, Randrianaivo H, Michault A, Schuffenecker I, Kauffmann E, Lenglet Y, Barau G, Fourmaintraux A.** 2006. [Early maternal-fetal transmission of the Chikungunya virus]. Presse Med **35:**1656-1658.
5. **Gérardin P, Barau G, Michault A, Bintner M, Randrianaivo H, Choker G, Lenglet Y, Touret Y, Bouveret A, Grivard P, Roux KL, Blanc S, Schuffenecker I, Couderc T, Arenzana-Seisdedos F, Lecuit M, Robillard P-Y.** 2008. Multidisciplinary Prospective Study of Mother-to-Child Chikungunya Virus Infections on the Island of La Réunion. PLoS Med **5:**e60.
6. **Ross RW.** 1956. The Newala epidemic. III. The virus: isolation, pathogenic properties and relationship to the epidemic. J Hyg (Lond) **54:**177-191.
7. **Powers AM, Brault AC, Tesh RB, Weaver SC.** 2000. Re-emergence of Chikungunya and O'nyong-nyong viruses: evidence for distinct geographical lineages and distant evolutionary relationships. J Gen Virol **81:**471-479.
8. **Weaver SC.** 2014. Arrival of chikungunya virus in the new world: prospects for spread and impact on public health. PLoS Negl Trop Dis **8:**e2921.
9. **Chretien JP, Anyamba A, Bedno SA, Breiman RF, Sang R, Sergon K, Powers AM, Onyango CO, Small J, Tucker CJ, Linthicum KJ.** 2007. Drought-associated chikungunya emergence along coastal East Africa. Am J Trop Med Hyg **76:**405-407.
10. **Schuffenecker I, Iteman I, Michault A, Murri S, Frangeul L, Vaney MC, Lavenir R, Pardigon N, Reynes JM, Pettinelli F, Biscornet L, Diancourt L, Michel S, Duquerroy S, Guigon G, Frenkiel MP, Brehin AC, Cubito N, Despres P, Kunst F, Rey FA, Zeller H, Brisse S.** 2006. Genome microevolution of chikungunya viruses causing the Indian Ocean outbreak. PLoS Med **3:**e263.
11. **Gerardin P, Guernier V, Perrau J, Fianu A, Le Roux K, Grivard P, Michault A, de Lamballerie X, Flahault A, Favier F.** 2008. Estimating Chikungunya prevalence in La Reunion Island outbreak by serosurveys: Two methods for two critical times of the epidemic. BMC Infectious Diseases **8:**99.
12. http://www.cdc.gov/chikungunya/geo/united-states.html**.** 13 april 2015. *on* Centers for Disease Control and Prevention. http://www.cdc.gov/chikungunya/geo/united-states.html. Accessed
13. **PAHO.** Number of reported cases of chikungunya fever in the Americas. http://www.paho.org/hq/index.php?option=com_topics&view=readall&cid=5927&Itemid=40931&lang=en. http://www.paho.org/hq/index.php?option=com_topics&view=readall&cid=5927&Itemid=40931&lang=en. Accessed
14. **Fischer M, Staples JE.** 2014. Notes from the field: chikungunya virus spreads in the Americas - Caribbean and South America, 2013-2014. MMWR Morb Mortal Wkly Rep **63:**500-501.
15. **Gibney KB, Fischer M, Prince HE, Kramer LD, St George K, Kosoy OL, Laven JJ, Staples JE.** 2011. Chikungunya fever in the United States: a fifteen year review of cases. Clin Infect Dis **52:**e121-126.
16. **Simon F, Parola P, Grandadam M, Fourcade S, Oliver M, Brouqui P, Hance P, Kraemer P, Ali Mohamed A, de Lamballerie X, Charrel R, Tolou H.** 2007. Chikungunya infection: an emerging rheumatism among travelers returned from Indian Ocean islands. Report of 47 cases. Medicine (Baltimore) **86:**123-137.

17. **Oliver M, Grandadam M, Marimoutou C, Rogier C, Botelho-Nevers E, Tolou H, Moalic J-L, Kraemer P, Morillon M, Morand J-J, Jeandel P, Parola P, Simon F.** 2009. Persisting Mixed Cryoglobulinemia in Chikungunya Infection. PLoS Negl Trop Dis **3:**e374.

18. **Powers AM, Brault AC, Shirako Y, Strauss EG, Kang W, Strauss JH, Weaver SC.** 2001. Evolutionary relationships and systematics of the alphaviruses. J Virol **75:**10118-10131.

19. **RIVM.** http://wwwrivmnl/dsresource?type=pdf&disposition=inline&objectid=rivmp:268473&versionid=&subobjectname= **Chikungunya surveillance overview Dutch Caribbean islands, 1 October 2013 – 22th December 2014 (week 52)**.

20. **Reusken CBEM, Bakker J, Reimerink JHJ, Zelena H, Koopmans MGP.** 2013. Underdiagnosis of Chikungunya Virus Infections in Symptomatic Dutch Travelers Returning From the Indian Ocean Area. Journal of Travel Medicine **20:**44-46.

21. **Angelini P, Macini P, Finarelli AC, Pol C, Venturelli C, Bellini R, Dottori M.** 2008. Chikungunya epidemic outbreak in Emilia-Romagna (Italy) during summer 2007. Parassitologia **50:**97-98.

22. **Rezza G, Nicoletti L, Angelini R, Romi R, Finarelli AC, Panning M, Cordioli P, Fortuna C, Boros S, Magurano F, Silvi G, Angelini P, Dottori M, Ciufolini MG, Majori GC, Cassone A.** 2007. Infection with chikungunya virus in Italy: an outbreak in a temperate region. Lancet **370:**1840-1846.

23. **Bonilauri P, Bellini R, Calzolari M, Angelini R, Venturi L, Fallacara F, Cordioli P, Angelini P, Venturelli C, Merialdi G, Dottori M.** 2008. Chikungunya Virus in Aedes albopictus, Italy. Emerging Infectious Diseases **14:**852-854.

24. **Grandadam M, Caro V, Plumet S, Thiberge JM, Souares Y, Failloux AB, Tolou HJ, Budelot M, Cosserat D, Leparc-Goffart I, Despres P.** 2011. Chikungunya virus, southeastern France. Emerg Infect Dis **17:**910-913.

25. **Gould EA, Gallian P, De Lamballerie X, Charrel RN.** 2010. First cases of autochthonous dengue fever and chikungunya fever in France: from bad dream to reality! Clin Microbiol Infect **16:**1702-1704.

26. **France WuCi.** WHO update Chikungunya in France. http://www.who.int/csr/don/23-october-2014-chikungunya/en/. Accessed

27. **Delisle E RC, Broche B, Leparc-Goffart I, L'Ambert G, Cochet A, Prat C, Foulongne V, Ferré JB, Catelinois O, Flusin O, Tchernonog E, Moussion IE, Wiegandt A, Septfons A, Mendy A, Moyano MB, Laporte L, Maurel J, Jourdain F, Reynes J, Paty MC, Golliot F. .** 2015. Chikungunya outbreak in Montpellier, France, September to October 2014. http://www.eurosurveillance.org/ViewArticle.aspx?ArticleId=21108. Accessed

28. **McCarthy M.** 2014. First case of locally acquired chikungunya is reported in US. BMJ **349:**g4706.

29. **MMWR.** 2010. Locally acquired Dengue--Key West, Florida, 2009-2010. MMWR Morb Mortal Wkly Rep **59:**577-581.

30. **Santhosh SR, Dash PK, Parida MM, Khan M, Tiwari M, Lakshmana Rao PV.** 2008. Comparative full genome analysis revealed E1: A226V shift in 2007 Indian Chikungunya virus isolates. Virus Res **135:**36-41.

31. **Parola P, de Lamballerie X, Jourdan J, Rovery C, Vaillant V, Minodier P, Brouqui P, Flahault A, Raoult D, Charrel RN.** 2006. Novel chikungunya virus variant in travelers returning from Indian Ocean islands. Emerg Infect Dis **12:**1493-1499.

32. **Suhrbier A, Jaffar-Bandjee MC, Gasque P.** 2012. Arthritogenic alphaviruses--an overview. Nat Rev Rheumatol **8:**420-429.

33. **Steele KE, Twenhafel NA.** 2010. REVIEW PAPER: pathology of animal models of alphavirus encephalitis. Vet Pathol **47:**790-805.

34. http://www.cdc.gov/chikungunya/geo/index.html**.** 2015. Geographic distribution of chikungunya virus. http://www.cdc.gov/chikungunya/geo/index.html. Accessed 11 may 2015.

35. **Turell MJ, Beaman JR, Tammariello RF.** 1992. Susceptibility of Selected Strains of Aedes aegypti and Aedes albopictus (Diptera: Culicidae) to Chikungunya Virus, vol 29.

36. **Mangiafico JA.** 1971. Chikungunya virus infection and transmission in five species of mosquito. Am J Trop Med Hyg **20:**642-645.

37. **Tsetsarkin KA, Vanlandingham DL, McGee CE, Higgs S.** 2007. A single mutation in chikungunya virus affects vector specificity and epidemic potential. PLoS Pathogens **3:**e201.

38. **Dubrulle M, Mousson L, Moutailler S, Vazeille M, Failloux AB.** 2009. Chikungunya virus and Aedes mosquitoes: saliva is infectious as soon as two days after oral infection. PLoS One **4:**e5895.

39. **Hapuarachchi HC, Bandara KB, Sumanadasa SD, Hapugoda MD, Lai YL, Lee KS, Tan LK, Lin RT, Ng LF, Bucht G, Abeyewickreme W, Ng LC.** 2010. Re-emergence of Chikungunya virus in South-east Asia: virological evidence from Sri Lanka and Singapore. Journal of General Virology **91:**1067-1076.

40. **de Lamballerie X, Leroy E, Charrel RN, Ttsetsarkin K, Higgs S, Gould EA.** 2008. Chikungunya virus adapts to tiger mosquito via evolutionary convergence: a sign of things to come? Virology Journal **5:**33.

41. **Sam IC, Chan YF, Chan SY, Loong SK, Chin HK, Hooi PS, Ganeswrie R, Abubakar S.** 2009. Chikungunya virus of Asian and Central/East African genotypes in Malaysia. J Clin Virol **46:**180-183.

42. **Kumar NP, Joseph R, Kamaraj T, Jambulingam P.** 2008. A226V mutation in virus during the 2007 chikungunya outbreak in Kerala, India. Journal of General Virology **89:**1945-1948.

43. **Lambrechts L, Scott TW, Gubler DJ.** 2010. Consequences of the Expanding Global Distribution of <italic>Aedes albopictus</italic> for Dengue Virus Transmission. PLoS Negl Trop Dis **4:**e646.

44. **Strauss JH, Strauss EG.** 1994. The alphaviruses: gene expression, replication, and evolution. Microbiol Rev **58:**491-562.

45. **Kuhn RJ.** 2007. Fields virology: Togaviridae: The Viruses and Their Replication, 5th ed. ed, vol 5th ed. Lippincott Williams & Wilkins.

46. **Wang KS, Kuhn RJ, Strauss EG, Ou S, Strauss JH.** 1992. High-affinity laminin receptor is a receptor for Sindbis virus in mammalian cells. J Virol **66:**4992-5001.

47. **Klimstra WB, Ryman KD, Johnston RE.** 1998. Adaptation of Sindbis virus to BHK cells selects for use of heparan sulfate as an attachment receptor. J Virol **72:**7357-7366.

48. **Kielian M, Chanel-Vos C, Liao M.** 2010. Alphavirus Entry and Membrane Fusion. Viruses **2:**796-825.

49. **Martín CS-S, Liu CY, Kielian M.** 2009. Dealing with low pH: entry and exit of alphaviruses and flaviviruses. Trends in Microbiology **17:**514-521.

50. **Gomatos PJ, Kaariainen L, Keranen S, Ranki M, Sawicki DL.** 1980. Semliki Forest virus replication complex capable of synthesizing 42S and 26S nascent RNA chains. J Gen Virol **49:**61-69.

51. **Kujala P, Ikaheimonen A, Ehsani N, Vihinen H, Auvinen P, Kaariainen L.** 2001. Biogenesis of the Semliki Forest virus RNA replication complex. J Virol **75:**3873-3884.

52. **Spuul P, Balistreri G, Kaariainen L, Ahola T.** 2010. Phosphatidylinositol 3-kinase-, actin-, and microtubule-dependent transport of Semliki Forest Virus replication complexes from the plasma membrane to modified lysosomes. J Virol **84:**7543-7557.

53. **Strauss EG, Levinson R, Rice CM, Dalrymple J, Strauss JH.** 1988. Nonstructural proteins nsP3 and nsP4 of Ross River and O'Nyong-nyong viruses: sequence and comparison with those of other alphaviruses. Virology **164:**265-274.

54. **Firth AE, Wills NM, Gesteland RF, Atkins JF.** 2011. Stimulation of stop codon readthrough: frequent presence of an extended 3' RNA structural element. Nucleic Acids Res **39:**6679-6691.

55. **Ahola T, Kaariainen L.** 1995. Reaction in alphavirus mRNA capping: formation of a covalent complex of nonstructural protein nsP1 with 7-methyl-GMP. Proc Natl Acad Sci U S A **92:**507-511.

56. **Ahola T, Lampio A, Auvinen P, Kaariainen L.** 1999. Semliki Forest virus mRNA capping enzyme requires association with anionic membrane phospholipids for activity. EMBO J **18:**3164-3172.

57. **Metz SW, Pijlman GP.** 2011. Arbovirus vaccines; opportunities for the baculovirus-insect cell expression system. Journal of Invertebrate Pathology **107, Supplement:**S16-S30.

58. **Gorchakov R, Frolova E, Frolov I.** 2005. Inhibition of Transcription and Translation in Sindbis Virus-Infected Cells. Journal of Virology **79:**9397-9409.

59. **Malet H, Coutard B, Jamal S, Dutartre H, Papageorgiou N, Neuvonen M, Ahola T, Forrester N, Gould EA, Lafitte D, Ferron F, Lescar J, Gorbalenya AE, de Lamballerie X, Canard B.** 2009. The crystal structures of Chikungunya and Venezuelan equine encephalitis virus nsP3 macro domains define a conserved adenosine binding pocket. J Virol **83:**6534-6545.

60. **Shin G, Yost SA, Miller MT, Elrod EJ, Grakoui A, Marcotrigiano J.** 2012. Structural and functional insights into alphavirus polyprotein processing and pathogenesis. Proc Natl Acad Sci U S A **109:**16534-16539.

61. **Panas MD, Ahola T, McInerney GM.** 2014. The C-terminal repeat domains of nsP3 from the Old World alphaviruses bind directly to G3BP. J Virol doi:10.1128/JVI.00439-14.

62. **Fros JJ, Domeradzka NE, Baggen J, Geertsema C, Flipse J, Vlak JM, Pijlman GP.** 2012. Chikungunya virus nsP3 blocks stress granule assembly by recruitment of G3BP into cytoplasmic foci. J Virol **86:**10873-10879.

63. **Panas MD, Varjak M, Lulla A, Eng KE, Merits A, Karlsson Hedestam GB, McInerney GM.** 2012. Sequestration of G3BP coupled with efficient translation inhibits stress granules in Semliki Forest virus infection. Mol Biol Cell **23:**4701-4712.

64. **Shirako Y, Strauss JH.** 1994. Regulation of Sindbis virus RNA replication: uncleaved P123 and nsP4 function in minus-strand RNA synthesis, whereas cleaved products from P123 are required for efficient plus-strand RNA synthesis. J Virol **68:**1874-1885.

65. **Levis R, Schlesinger S, Huang HV.** 1990. Promoter for Sindbis virus RNA-dependent subgenomic RNA transcription. Journal of Virology **64:**1726-1733.

66. **McInerney GM, Kedersha NL, Kaufman RJ, Anderson P, Liljestrom P.** 2005. Importance of eIF2alpha phosphorylation and stress granule assembly in alphavirus translation regulation. Mol Biol Cell **16:**3753-3763.

67. **Frolov I, Schlesinger S.** 1996. Translation of Sindbis virus mRNA: analysis of sequences downstream of the initiating AUG codon that enhance translation. J Virol **70:**1182-1190.

68. **Sjoberg EM, Suomalainen M, Garoff H.** 1994. A significantly improved Semliki Forest virus expression system based on translation enhancer segments from the viral capsid gene. Biotechnology (N Y) **12:**1127-1131.

69. **Scholte FE, Tas A, Martina BE, Cordioli P, Narayanan K, Makino S, Snijder EJ, van Hemert MJ.** 2013. Characterization of synthetic Chikungunya viruses based on the consensus sequence of recent E1-226V isolates. PLoS One **8:**e71047.

70. **Perera R, Owen KE, Tellinghuisen TL, Gorbalenya AE, Kuhn RJ.** 2001. Alphavirus nucleocapsid protein contains a putative coiled coil alpha-helix important for core assembly. J Virol **75:**1-10.

71. **Ekström M, Liljeström P, Garoff H.** 1994. Membrane protein lateral interactions control Semliki Forest virus budding. The EMBO Journal **13:**1058-1064.

72. **Fuller SD.** The T=4 envelope of sindbis virus is organized by interactions with a complementary T=3 capsid. Cell **48:**923-934.

73. **Simizu B, Yamamoto K, Hashimoto K, Ogata T.** 1984. Structural proteins of Chikungunya virus. Journal of Virology **51:**254-258.

74. **Uchime O, Fields W, Kielian M.** 2013. The role of E3 in pH protection during alphavirus assembly and exit. J Virol **87:**10255-10262.

75. **Lobigs M, Zhao HX, Garoff H.** 1990. Function of Semliki Forest virus E3 peptide in virus assembly: replacement of E3 with an artificial signal peptide abolishes spike heterodimerization and surface expression of E1. J Virol **64:**4346-4355.

76. **Schwartz O, Albert ML.** 2010. Biology and pathogenesis of chikungunya virus. Nat Rev Microbiol **8:**491-500.

77. **Sourisseau M, Schilte C, Casartelli N, Trouillet C, Guivel-Benhassine F, Rudnicka D, Sol-Foulon N, Le Roux K, Prevost MC, Fsihi H, Frenkiel MP, Blanchet F, Afonso PV, Ceccaldi**

PE, Ozden S, Gessain A, Schuffenecker I, Verhasselt B, Zamborlini A, Saib A, Rey FA, Arenzana-Seisdedos F, Despres P, Michault A, Albert ML, Schwartz O.** 2007. Characterization of reemerging chikungunya virus. PLoS Pathog **3:**e89.

78. **Robin S, Ramful D, Zettor J, Benhamou L, Jaffar-Bandjee MC, Riviere JP, Marichy J, Ezzedine K, Alessandri JL.** 2010. Severe bullous skin lesions associated with Chikungunya virus infection in small infants. Eur J Pediatr **169:**67-72.

79. **Couderc T, Chrétien F, Schilte C, Disson O, Brigitte M, Guivel-Benhassine F, Touret Y, Barau G, Cayet N, Schuffenecker I, Desprès P, Arenzana-Seisdedos F, Michault A, Albert ML, Lecuit M.** 2008. A Mouse Model for Chikungunya: Young Age and Inefficient Type-I Interferon Signaling Are Risk Factors for Severe Disease. PLoS Pathog **4:**e29.

80. **Ozden S, Huerre M, Riviere J-P, Coffey LL, Afonso PV, Mouly V, de Monredon J, Roger J-C, El Amrani M, Yvin J-L, Jaffar M-C, Frenkiel M-P, Sourisseau M, Schwartz O, Butler-Browne G, Desprès P, Gessain A, Ceccaldi P-E.** 2007. Human Muscle Satellite Cells as Targets of Chikungunya Virus Infection. PLoS ONE **2:**e527.

81. **Schilte C, Couderc T, Chretien F, Sourisseau M, Gangneux N, Guivel-Benhassine F, Kraxner A, Tschopp J, Higgs S, Michault A, Arenzana-Seisdedos F, Colonna M, Peduto L, Schwartz O, Lecuit M, Albert ML.** 2010. Type I IFN controls chikungunya virus via its action on nonhematopoietic cells. J Exp Med **207:**429-442.

82. **Couderc T, Khandoudi N, Grandadam M, Visse C, Gangneux N, Bagot S, Prost JF, Lecuit M.** 2009. Prophylaxis and therapy for Chikungunya virus infection. J Infect Dis **200:**516-523.

83. **Gardner J, Anraku I, Le TT, Larcher T, Major L, Roques P, Schroder WA, Higgs S, Suhrbier A.** 2010. Chikungunya virus arthritis in adult wild-type mice. J Virol **84:**8021-8032.

84. **Hawman DW, Stoermer KA, Montgomery SA, Pal P, Oko L, Diamond MS, Morrison TE.** 2013. Chronic joint disease caused by persistent Chikungunya virus infection is controlled by the adaptive immune response. J Virol **87:**13878-13888.

85. **Ng LF, Chow A, Sun YJ, Kwek DJ, Lim PL, Dimatatac F, Ng LC, Ooi EE, Choo KH, Her Z, Kourilsky P, Leo YS.** 2009. IL-1beta, IL-6, and RANTES as biomarkers of Chikungunya severity. PLoS One **4:**e4261.

86. **Chow A, Her Z, Ong EK, Chen JM, Dimatatac F, Kwek DJ, Barkham T, Yang H, Renia L, Leo YS, Ng LF.** 2011. Persistent arthralgia induced by Chikungunya virus infection is associated with interleukin-6 and granulocyte macrophage colony-stimulating factor. J Infect Dis **203:**149-157.

87. **Fros JJ, van der Maten E, Vlak JM, Pijlman GP.** 2013. The C-terminal domain of chikungunya virus nsP2 independently governs viral RNA replication, cytopathicity, and inhibition of interferon signaling. J Virol **87:**10394-10400.

88. **White LK, Sali T, Alvarado D, Gatti E, Pierre P, Streblow D, Defilippis VR.** 2011. Chikungunya virus induces IPS-1-dependent innate immune activation and protein kinase R-independent translational shutoff. J Virol **85:**606-620.

89. **Garmashova N, Gorchakov R, Volkova E, Paessler S, Frolova E, Frolov I.** 2007. The Old World and New World alphaviruses use different virus-specific proteins for induction of transcriptional shutoff. J Virol **81:**2472-2484.

90. **Fros JJ, Liu WJ, Prow NA, Geertsema C, Ligtenberg M, Vanlandingham DL, Schnettler E, Vlak JM, Suhrbier A, Khromykh AA, Pijlman GP.** 2010. Chikungunya virus nonstructural protein 2 inhibits type I/II interferon-stimulated JAK-STAT signaling. J Virol **84:**10877-10887.

91. **Hoarau JJ, Jaffar Bandjee MC, Krejbich Trotot P, Das T, Li-Pat-Yuen G, Dassa B, Denizot M, Guichard E, Ribera A, Henni T, Tallet F, Moiton MP, Gauzere BA, Bruniquet S, Jaffar Bandjee Z, Morbidelli P, Martigny G, Jolivet M, Gay F, Grandadam M, Tolou H, Vieillard V, Debre P, Autran B, Gasque P.** 2010. Persistent chronic inflammation and infection by Chikungunya arthritogenic alphavirus in spite of a robust host immune response. J Immunol **184:**5914-5927.

92. **Wauquier N, Becquart P, Nkoghe D, Padilla C, Ndjoyi-Mbiguino A, Leroy EM.** 2011. The acute phase of Chikungunya virus infection in humans is associated with strong innate immunity and T CD8 cell activation. J Infect Dis **204:**115-123.

93. **Teo TH, Lum FM, Claser C, Lulla V, Lulla A, Merits A, Renia L, Ng LF.** 2013. A pathogenic role for CD4+ T cells during Chikungunya virus infection in mice. J Immunol **190:**259-269.

94. **Borgherini G, Poubeau P, Staikowsky F, Lory M, Le Moullec N, Becquart JP, Wengling C, Michault A, Paganin F.** 2007. Outbreak of chikungunya on Reunion Island: early clinical and laboratory features in 157 adult patients. Clin Infect Dis **44:**1401-1407.

95. **Kamphuis E, Junt T, Waibler Z, Forster R, Kalinke U.** 2006. Type I interferons directly regulate lymphocyte recirculation and cause transient blood lymphopenia. Blood **108:**3253-3261.

96. **Brighton SW, Prozesky OW, de la Harpe AL.** 1983. Chikungunya virus infection. A retrospective study of 107 cases. S Afr Med J **63:**313-315.

97. **Borgherini G, Poubeau P, Jossaume A, Gouix A, Cotte L, Michault A, Arvin-Berod C, Paganin F.** 2008. Persistent arthralgia associated with chikungunya virus: a study of 88 adult patients on reunion island. Clin Infect Dis **47:**469-475.

98. **Staikowsky F, Le Roux K, Schuffenecker I, Laurent P, Grivard P, Develay A, Michault A.** 2008. Retrospective survey of Chikungunya disease in Reunion Island hospital staff. Epidemiol Infect **136:**196-206.

99. **Schilte C, Staikowsky F, Couderc T, Madec Y, Carpentier F, Kassab S, Albert ML, Lecuit M, Michault A.** 2013. Chikungunya virus-associated long-term arthralgia: a 36-month prospective longitudinal study. PLoS Negl Trop Dis **7:**e2137.

100. **Chen W, Foo S-S, Sims NA, Herrero LJ, Walsh NC, Mahalingam S.** 2015. Arthritogenic alphaviruses: new insights into arthritis and bone pathology. Trends in Microbiology **23:**35-43.

101. **Miner JJ, Aw-Yeang HX, Fox JM, Taffner S, Malkova ON, Oh ST, Kim AH, Diamond MS, Lenschow DJ, Yokoyama WM.** 2015. Chikungunya viral arthritis in the United States: A mimic of seronegative rheumatoid arthritis. Arthritis Rheumatol doi:10.1002/art.39027.

102. **Manimunda SP, Vijayachari P, Uppoor R, Sugunan AP, Singh SS, Rai SK, Sudeep AB, Muruganandam N, Chaitanya IK, Guruprasad DR.** 2010. Clinical progression of chikungunya fever during acute and chronic arthritic stages and the changes in joint morphology as revealed by imaging. Trans R Soc Trop Med Hyg **104:**392-399.

103. **Bouquillard E, Combe B.** 2009. A report of 21 cases of rheumatoid arthritis following Chikungunya fever. A mean follow-up of two years. Joint Bone Spine **76:**654-657.

104. **Dupuis-Maguiraga L, Noret M, Brun S, Le Grand R, Gras G, Roques P.** 2012. Chikungunya Disease: Infection-Associated Markers from the Acute to the Chronic Phase of Arbovirus-Induced Arthralgia. PLoS Neglected Tropical Diseases **6:**e1446.

105. **Suhrbier A, Mahalingam S.** 2009. The immunobiology of viral arthritides. Pharmacol Ther **124:**301-308.

106. **Labadie K, Larcher T, Joubert C, Mannioui A, Delache B, Brochard P, Guigand L, Dubreil L, Lebon P, Verrier B, de Lamballerie X, Suhrbier A, Cherel Y, Le Grand R, Roques P.** 2010. Chikungunya disease in nonhuman primates involves long-term viral persistence in macrophages. The Journal of Clinical Investigation **120:**894-906.

107. **Morrison TE, Oko L, Montgomery SA, Whitmore AC, Lotstein AR, Gunn BM, Elmore SA, Heise MT.** 2011. A Mouse Model of Chikungunya Virus–Induced Musculoskeletal Inflammatory Disease: Evidence of Arthritis, Tenosynovitis, Myositis, and Persistence. The American Journal of Pathology **178:**32-40.

108. **Carey DE.** 1971. Chikungunya and dengue: a case of mistaken identity? J Hist Med Allied Sci **26:**243-262.

109. **Caron M, Paupy C, Grard G, Becquart P, Mombo I, Nso BB, Kassa Kassa F, Nkoghe D, Leroy EM.** 2012. Recent introduction and rapid dissemination of Chikungunya virus and Dengue virus serotype 2 associated with human and mosquito coinfections in Gabon, central Africa. Clin Infect Dis **55:**e45-53.

110. **Chahar HS, Bharaj P, Dar L, Guleria R, Kabra SK, Broor S.** 2009. Co-infections with Chikungunya Virus and Dengue Virus in Delhi, India. Emerging Infectious Diseases **15:**1077-1080.
111. **Leroy EM, Nkoghe D, Ollomo B, Nze-Nkogue C, Becquart P, Grard G, Pourrut X, Charrel R, Moureau G, Ndjoyi-Mbiguino A, De-Lamballerie X.** 2009. Concurrent chikungunya and dengue virus infections during simultaneous outbreaks, Gabon, 2007. Emerg Infect Dis **15:**591-593.
112. **Omarjee R, Prat C, Flusin O, Boucau S, Tenebray B, Merle O, Huc-Anais P, Cassadou S, Leparc-Goffart I.** 2014. Importance of case definition to monitor ongoing outbreak of chikungunya virus on a background of actively circulating dengue virus, St Martin, December 2013 to January 2014. Euro Surveill **19**.
113. **Laoprasopwattana K, Kaewjungwad L, Jarumanokul R, Geater A.** 2012. Differential Diagnosis of Chikungunya, Dengue Viral Infection and Other Acute Febrile Illnesses in Children. The Pediatric Infectious Disease Journal **31:**459-463.
114. **Tsetsarkin K, Higgs S, McGee CE, De Lamballerie X, Charrel RN, Vanlandingham DL.** 2006. Infectious clones of Chikungunya virus (La Reunion isolate) for vector competence studies. Vector Borne Zoonotic Dis **6:**325-337.
115. **Vanlandingham DL, Tsetsarkin K, Hong C, Klingler K, McElroy KL, Lehane MJ, Higgs S.** 2005. Development and characterization of a double subgenomic chikungunya virus infectious clone to express heterologous genes in Aedes aegypti mosquitoes. Insect Biochem Mol Biol **35:**1162-1170.
116. **Kummerer BM, Grywna K, Glasker S, Wieseler J, Drosten C.** 2012. Construction of an infectious Chikungunya virus cDNA clone and stable insertion of mCherry reporter genes at two different sites. Journal of General Virology **93:**1991-1995.
117. **Pohjala L, Utt A, Varjak M, Lulla A, Merits A, Ahola T, Tammela P.** 2011. Inhibitors of alphavirus entry and replication identified with a stable Chikungunya replicon cell line and virus-based assays. PLoS ONE **6:**e28923.
118. **Scholte FE, Tas A, Albulescu IC, Zusinaite E, Merits A, Snijder EJ, van Hemert MJ.** 2015. Stress Granule Components G3BP1 and G3BP2 Play a Proviral Role Early in Chikungunya Virus Replication. J Virol **89:**4457-4469.
119. **Varjak M, Saul S, Arike L, Lulla A, Peil L, Merits A.** 2013. Magnetic fractionation and proteomic dissection of cellular organelles occupied by the late replication complexes of Semliki Forest virus. J Virol **87:**10295-10312.
120. **Teng TS, Foo SS, Simamarta D, Lum FM, Teo TH, Lulla A, Yeo NK, Koh EG, Chow A, Leo YS, Merits A, Chin KC, Ng LF.** 2012. Viperin restricts chikungunya virus replication and pathology. J Clin Invest **122:**4447-4460.
121. **Treffers EE, Tas A, Scholte FE, Van MN, Heemskerk MT, de Ru AH, Snijder EJ, van Hemert MJ, van Veelen PA.** 2015. Temporal SILAC-based quantitative proteomics identifies host factors involved in chikungunya virus replication. Proteomics doi:10.1002/pmic.201400581.
122. **Bourai M, Lucas-Hourani M, Gad HH, Drosten C, Jacob Y, Tafforeau L, Cassonnet P, Jones LM, Judith D, Couderc T, Lecuit M, Andre P, Kummerer BM, Lotteau V, Despres P, Tangy F, Vidalain PO.** 2012. Mapping of Chikungunya virus interactions with host proteins identified nsP2 as a highly connected viral component. J Virol **86:**3121-3134.
123. **Fire A, Xu S, Montgomery MK, Kostas SA, Driver SE, Mello CC.** 1998. Potent and specific genetic interference by double-stranded RNA in Caenorhabditis elegans. Nature **391:**806-811.
124. **Tai AW, Benita Y, Peng LF, Kim SS, Sakamoto N, Xavier RJ, Chung RT.** 2009. A functional genomic screen identifies cellular cofactors of hepatitis C virus replication. Cell Host Microbe **5:**298-307.
125. **Randall G, Panis M, Cooper JD, Tellinghuisen TL, Sukhodolets KE, Pfeffer S, Landthaler M, Landgraf P, Kan S, Lindenbach BD, Chien M, Weir DB, Russo JJ, Ju J, Brownstein MJ, Sheridan R, Sander C, Zavolan M, Tuschl T, Rice CM.** 2007. Cellular cofactors affecting hepatitis C virus infection and replication. Proc Natl Acad Sci U S A **104:**12884-12889.

126. **Li Q, Brass AL, Ng A, Hu Z, Xavier RJ, Liang TJ, Elledge SJ.** 2009. A genome-wide genetic screen for host factors required for hepatitis C virus propagation. Proc Natl Acad Sci U S A **106:**16410-16415.

127. **Ng TI, Mo H, Pilot-Matias T, He Y, Koev G, Krishnan P, Mondal R, Pithawalla R, He W, Dekhtyar T, Packer J, Schurdak M, Molla A.** 2007. Identification of host genes involved in hepatitis C virus replication by small interfering RNA technology. Hepatology **45:**1413-1421.

128. **Krishnan MN, Ng A, Sukumaran B, Gilfoy FD, Uchil PD, Sultana H, Brass AL, Adametz R, Tsui M, Qian F, Montgomery RR, Lev S, Mason PW, Koski RA, Elledge SJ, Xavier RJ, Agaisse H, Fikrig E.** 2008. RNA interference screen for human genes associated with West Nile virus infection. Nature **455:**242-245.

129. **Le Sommer C, Barrows NJ, Bradrick SS, Pearson JL, Garcia-Blanco MA.** 2012. G protein-coupled receptor kinase 2 promotes flaviviridae entry and replication. PLoS Negl Trop Dis **6:**e1820.

130. **Sessions OM, Barrows NJ, Souza-Neto JA, Robinson TJ, Hershey CL, Rodgers MA, Ramirez JL, Dimopoulos G, Yang PL, Pearson JL, Garcia-Blanco MA.** 2009. Discovery of insect and human dengue virus host factors. Nature **458:**1047-1050.

131. **Kwon YJ, Heo J, Wong HE, Cruz DJ, Velumani S, da Silva CT, Mosimann AL, Duarte Dos Santos CN, Freitas-Junior LH, Fink K.** 2014. Kinome siRNA screen identifies novel cell-type specific dengue host target genes. Antiviral Res **110C:**20-30.

132. **Panda D, Rose PP, Hanna SL, Gold B, Hopkins KC, Lyde RB, Marks MS, Cherry S.** 2013. Genome-wide RNAi screen identifies SEC61A and VCP as conserved regulators of Sindbis virus entry. Cell Rep **5:**1737-1748.

133. **Ooi YS, Stiles KM, Liu CY, Taylor GM, Kielian M.** 2013. Genome-wide RNAi screen identifies novel host proteins required for alphavirus entry. PLoS Pathog **9:**e1003835.

134. **Varble A, Benitez AA, Schmid S, Sachs D, Shim JV, Rodriguez-Barrueco R, Panis M, Crumiller M, Silva JM, Sachidanandam R, tenOever BR.** 2013. An in vivo RNAi screening approach to identify host determinants of virus replication. Cell Host Microbe **14:**346-356.

135. **Balistreri G, Horvath P, Schweingruber C, Zünd D, McInerney G, Merits A, Mühlemann O, Azzalin C, Helenius A.** 2014. The Host Nonsense-Mediated mRNA Decay Pathway Restricts Mammalian RNA Virus Replication. Cell Host & Microbe **16:**403-411.

136. **Atasheva S, Gorchakov R, English R, Frolov I, Frolova E.** 2007. Development of Sindbis viruses encoding nsP2/GFP chimeric proteins and their application for studying nsP2 functioning. J Virol **81:**5046-5057.

137. **Gorchakov R, Garmashova N, Frolova E, Frolov I.** 2008. Different types of nsP3-containing protein complexes in Sindbis virus-infected cells. J Virol **82:**10088-10101.

138. **Cristea IM, Carroll JW, Rout MP, Rice CM, Chait BT, MacDonald MR.** 2006. Tracking and elucidating alphavirus-host protein interactions. J Biol Chem **281:**30269-30278.

139. **Thio CL, Yusof R, Abdul-Rahman PS, Karsani SA.** 2013. Differential proteome analysis of chikungunya virus infection on host cells. PLoS One **8:**e61444.

140. **Dhanwani R, Khan M, Alam SI, Rao PV, Parida M.** 2011. Differential proteome analysis of Chikungunya virus-infected new-born mice tissues reveal implication of stress, inflammatory and apoptotic pathways in disease pathogenesis. Proteomics **11:**1936-1951.

141. **Dhanwani R, Khan M, Lomash V, Rao PV, Ly H, Parida M.** 2014. Characterization of chikungunya virus induced host response in a mouse model of viral myositis. PLoS One **9:**e92813.

142. **Abraham R, Mudaliar P, Jaleel A, Srikanth J, Sreekumar E.** 2015. High throughput proteomic analysis and a comparative review identify the nuclear chaperone, Nucleophosmin among the common set of proteins modulated in Chikungunya virus infection. J Proteomics **120:**126-141.

143. **Issac TH, Tan EL, Chu JJ.** 2014. Proteomic profiling of chikungunya virus-infected human muscle cells: reveal the role of cytoskeleton network in CHIKV replication. J Proteomics **108:**445-464.

144. **Fraisier C, Koraka P, Belghazi M, Bakli M, Granjeaud S, Pophillat M, Lim SM, Osterhaus A, Martina B, Camoin L, Almeras L.** 2014. Kinetic Analysis of Mouse Brain Proteome Alterations Following Chikungunya Virus Infection before and after Appearance of Clinical Symptoms. PLoS ONE **9:**e91397.

145. **Smith DR.** 2015. Global protein profiling studies of chikungunya virus infection identify different proteins but common biological processes. Rev Med Virol **25:**3-18.

146. **Burnham AJ, Gong L, Hardy RW.** 2007. Heterogeneous nuclear ribonuclear protein K interacts with Sindbis virus nonstructural proteins and viral subgenomic mRNA. Virology **367:**212-221.

147. **Frank C, Schoneberg I, Stark K.** 2011. Trends in imported chikungunya virus infections in Germany, 2006-2009. Vector Borne Zoonotic Dis **11:**631-636.

148. **Lemant J, Boisson V, Winer A, Thibault L, Andre H, Tixier F, Lemercier M, Antok E, Cresta MP, Grivard P, Besnard M, Rollot O, Favier F, Huerre M, Campinos JL, Michault A.** 2008. Serious acute chikungunya virus infection requiring intensive care during the Reunion Island outbreak in 2005-2006. Crit Care Med **36:**2536-2541.

149. **Robin S, Ramful D, Le Seach F, Jaffar-Bandjee MC, Rigou G, Alessandri JL.** 2008. Neurologic manifestations of pediatric chikungunya infection. J Child Neurol **23:**1028-1035.

150. **Volk SM, Chen R, Tsetsarkin KA, Adams AP, Garcia TI, Sall AA, Nasar F, Schuh AJ, Holmes EC, Higgs S, Maharaj PD, Brault AC, Weaver SC.** 2010. Genome-scale phylogenetic analyses of chikungunya virus reveal independent emergences of recent epidemics and various evolutionary rates. Journal of Virology **84:**6497-6504.

151. **Tsetsarkin KA, Chen R, Leal G, Forrester N, Higgs S, Huang J, Weaver SC.** 2011. Chikungunya virus emergence is constrained in Asia by lineage-specific adaptive landscapes. Proceedings of the National Academy of Sciences of the United States of America **108:**7872-7877.

152. **Tsetsarkin KA, McGee CE, Volk SM, Vanlandingham DL, Weaver SC, Higgs S.** 2009. Epistatic roles of E2 glycoprotein mutations in adaption of chikungunya virus to Aedes albopictus and Ae. aegypti mosquitoes. PLoS One **4:**e6835.

153. **Gorchakov R, Wang E, Leal G, Forrester NL, Plante K, Rossi SL, Partidos CD, Adams AP, Seymour RL, Weger J, Borland EM, Sherman MB, Powers AM, Osorio JE, Weaver SC.** 2012. Attenuation of Chikungunya virus vaccine strain 181/clone 25 is determined by two amino acid substitutions in the E2 envelope glycoprotein. Journal of Virology **86:**6084-6096.

154. **Tsetsarkin KA, Weaver SC.** 2011. Sequential adaptive mutations enhance efficient vector switching by Chikungunya virus and its epidemic emergence. PLoS Pathog **7:**e1002412.

155. **Liu WJ, Rourke MF, Holmes EC, Aaskov JG.** 2011. Persistence of multiple genetic lineages within intrahost populations of Ross River virus. Journal of Virology **85:**5674-5678.

156. **Igarashi A.** 1978. Isolation of a Singh's Aedes albopictus cell clone sensitive to Dengue and Chikungunya viruses. J Gen Virol **40:**531-544.

157. **Kamitani W, Narayanan K, Huang C, Lokugamage K, Ikegami T, Ito N, Kubo H, Makino S.** 2006. Severe acute respiratory syndrome coronavirus nsp1 protein suppresses host gene expression by promoting host mRNA degradation. Proc Natl Acad Sci U S A **103:**12885-12890.

158. **Coleman TM, Wang G, Huang F.** 2004. Superior 5' homogeneity of RNA from ATP-initiated transcription under the T7 phi 2.5 promoter. Nucleic Acids Research **32:**e14.

159. **van Marle G, Luytjes W, van der Most RG, van der Straaten T, Spaan WJ.** 1995. Regulation of coronavirus mRNA transcription. J Virol **69:**7851-7856.

160. **de Vries AA, Chirnside ED, Bredenbeek PJ, Gravestein LA, Horzinek MC, Spaan WJ.** 1990. All subgenomic mRNAs of equine arteritis virus contain a common leader sequence. Nucleic Acids Research **18:**3241-3247.

161. **Metz SW, Geertsema C, Martina BE, Andrade P, Heldens JG, van Oers MM, Goldbach RW, Vlak JM, Pijlman GP.** 2011. Functional processing and secretion of Chikungunya virus E1 and E2 glycoproteins in insect cells. Virol J **8:**353.

162. **Lelli D, Moreno A, Lavazza A, Sozzi E, Luppi A, Canelli E, Tamba M, Capucci L, Cordioli P.** Chikungunya: Monoclonal Antibodies Production and Their Empoyment in Serological Diagnosis, abstr. 18.162, p. *In* (ed),

163. **Werneke SW, Schilte C, Rohatgi A, Monte KJ, Michault A, Arenzana-Seisdedos F, Vanlandingham DL, Higgs S, Fontanet A, Albert ML, Lenschow DJ.** 2011. ISG15 is critical in the control of Chikungunya virus infection independent of UbE1L mediated conjugation. PLoS Pathog **7:**e1002322.

164. **Katoh K, Misawa K, Kuma K, Miyata T.** 2002. MAFFT: a novel method for rapid multiple sequence alignment based on fast Fourier transform. Nucleic Acids Research **30:**3059-3066.

165. **de Wilde AH, Zevenhoven-Dobbe JC, van der Meer Y, Thiel V, Narayanan K, Makino S, Snijder EJ, van Hemert MJ.** 2011. Cyclosporin A inhibits the replication of diverse coronaviruses. Journal of General Virology **92:**2542-2548.

166. **de Wilde AH, Wannee KF, Scholte FE, Goeman JJ, Ten Dijke P, Snijder EJ, Kikkert M, van Hemert MJ.** 2015. A kinome-wide siRNA screen identifies proviral and antiviral host factors in SARS-coronavirus replication, including PKR and early secretory pathway proteins. J Virol doi:10.1128/JVI.01029-15.

167. **Warrier R, Linger BR, Golden BL, Kuhn RJ.** 2008. Role of sindbis virus capsid protein region II in nucleocapsid core assembly and encapsidation of genomic RNA. J Virol **82:**4461-4470.

168. **Degroot RJ, Rumenapf T, Kuhn RJ, Strauss EG, Strauss JH.** 1991. Sindbis Virus-Rna Polymerase Is Degraded by the N-End Rule Pathway. Proceedings of the National Academy of Sciences of the United States of America **88:**8967-8971.

169. **Weber F, Wagner V, Rasmussen SB, Hartmann R, Paludan SR.** 2006. Double-stranded RNA is produced by positive-strand RNA viruses and DNA viruses but not in detectable amounts by negative-strand RNA viruses. J Virol **80:**5059-5064.

170. **Ziegler SA, Lu L, da Rosa AP, Xiao SY, Tesh RB.** 2008. An animal model for studying the pathogenesis of chikungunya virus infection. Am J Trop Med Hyg **79:**133-139.

171. **Hong Z, Cameron CE.** 2002. Pleiotropic mechanisms of ribavirin antiviral activities. Prog Drug Res **59:**41-69.

172. **Moreno H, Gallego I, Sevilla N, de la Torre JC, Domingo E, Martin V.** 2011. Ribavirin can be mutagenic for arenaviruses. J Virol **85:**7246-7255.

173. **McCammon JR, Riesser VW.** 1979. Effects of ribavirin on BHK-21 cells acutely or persistently infected with mumps virus. Antimicrob Agents Chemother **15:**356-360.

174. **McTighe SP, Vaidyanathan R.** 2012. Vector competence of Aedes albopictus from Virginia and Georgia for chikungunya virus isolated in the Comoros Islands, 2005. Vector Borne and Zoonotic Diseases **12:**867-871.

175. **Ruiz-Moreno D, Vargas IS, Olson KE, Harrington LC.** 2012. Modeling dynamic introduction of Chikungunya virus in the United States. PLoS Neglected Tropical Diseases **6:**e1918.

176. **Coffey LL, Vignuzzi M.** 2011. Host alternation of chikungunya virus increases fitness while restricting population diversity and adaptability to novel selective pressures. Journal of Virology **85:**1025-1035.

177. **Weaver SC, Brault AC, Kang W, Holland JJ.** 1999. Genetic and fitness changes accompanying adaptation of an arbovirus to vertebrate and invertebrate cells. J Virol **73:**4316-4326.

178. **De Lamballerie X, Boisson V, Reynier JC, Enault S, Charrel RN, Flahault A, Roques P, Le Grand R.** 2008. On chikungunya acute infection and chloroquine treatment. Vector Borne and Zoonotic Diseases **8:**837-839.

179. **Delogu I, de Lamballerie X.** 2011. Chikungunya disease and chloroquine treatment. Journal of Medical Virology **83:**1058-1059.

180. **Khan M, Santhosh SR, Tiwari M, Lakshmana Rao PV, Parida M.** 2010. Assessment of in vitro prophylactic and therapeutic efficacy of chloroquine against Chikungunya virus in vero cells. Journal of Medical Virology **82:**817-824.

181. **Briolant S, Garin D, Scaramozzino N, Jouan A, Crance JM.** 2004. In vitro inhibition of Chikungunya and Semliki Forest viruses replication by antiviral compounds: synergistic effect of interferon-alpha and ribavirin combination. Antiviral Res **61:**111-117.

182. **Khan M, Dhanwani R, Patro IK, Rao PV, Parida MM.** 2011. Cellular IMPDH enzyme activity is a potential target for the inhibition of Chikungunya virus replication and virus induced apoptosis in cultured mammalian cells. Antiviral Res **89:**1-8.

183. **Shah NR, Sunderland A, Grdzelishvili VZ.** 2010. Cell type mediated resistance of vesicular stomatitis virus and Sendai virus to ribavirin. PLoS One **5:**e11265.

184. **Baugh J, Gallay P.** 2012. Cyclophilin involvement in the replication of hepatitis C virus and other viruses. Biological Chemistry **393:**579-587.

185. **De Clercq E.** 1998. Carbocyclic adenosine analogues as S-adenosylhomocysteine hydrolase inhibitors and antiviral agents: recent advances. Nucleosides and Nucleotides **17:**625-634.

186. **Sourisseau M, Schilte C, Casartelli N, Trouillet C, Guivel-Benhassine F, Rudnicka D, Sol-Foulon N, Le Roux K, Prevost MC, Fsihi H, Frenkiel MP, Blanchet F, Afonso PV, Ceccaldi PE, Ozden S, Gessain A, Schuffenecker I, Verhasselt B, Zamborlini A, Saib A, Rey FA, Arenzana-Seisdedos F, Despres P, Michault A, Albert ML, Schwartz O.** 2007. Characterization of reemerging chikungunya virus. PLoS Pathogens **3:**e89.

187. **Frolova EI, Fayzulin RZ, Cook SH, Griffin DE, Rice CM, Frolov I.** 2002. Roles of Nonstructural Protein nsP2 and Alpha/Beta Interferons in Determining the Outcome of Sindbis Virus Infection. Journal of Virology **76:**11254-11264.

188. **Paingankar MS, Arankalle VA.** 2014. Identification of chikungunya virus interacting proteins in mammalian cells. J Biosci **39:**389-399.

189. **Fongsaran C, Jirakanwisal K, Kuadkitkan A, Wikan N, Wintachai P, Thepparit C, Ubol S, Phaonakrop N, Roytrakul S, Smith DR.** 2014. Involvement of ATP synthase beta subunit in chikungunya virus entry into insect cells. Arch Virol **159:**3353-3364.

190. **Atkins C, Evans CW, Nordin B, Patricelli MP, Reynolds R, Wennerberg K, Noah JW.** 2014. Global Human-Kinase Screening Identifies Therapeutic Host Targets against Influenza. J Biomol Screen **19:**936-946.

191. **Reiss S, Rebhan I, Backes P, Romero-Brey I, Erfle H, Matula P, Kaderali L, Poenisch M, Blankenburg H, Hiet M-S, Longerich T, Diehl S, Ramirez F, Balla T, Rohr K, Kaul A, Bühler S, Pepperkok R, Lengauer T, Albrecht M, Eils R, Schirmacher P, Lohmann V, Bartenschlager R.** 2011. Recruitment and Activation of a Lipid Kinase by Hepatitis C Virus NS5A Is Essential for Integrity of the Membranous Replication Compartment. Cell Host & Microbe **9:**32-45.

192. **Olagnier D, Scholte FE, Chiang C, Albulescu IC, Nichols C, He Z, Lin R, Snijder EJ, van Hemert MJ, Hiscott J.** 2014. Inhibition of dengue and chikungunya virus infections by RIG-I-mediated type I interferon-independent stimulation of the innate antiviral response. J Virol **88:**4180-4194.

193. **Konig R, Stertz S, Zhou Y, Inoue A, Hoffmann HH, Bhattacharyya S, Alamares JG, Tscherne DM, Ortigoza MB, Liang Y, Gao Q, Andrews SE, Bandyopadhyay S, De Jesus P, Tu BP, Pache L, Shih C, Orth A, Bonamy G, Miraglia L, Ideker T, Garcia-Sastre A, Young JAT, Palese P, Shaw ML, Chanda SK.** 2010. Human host factors required for influenza virus replication. Nature **463:**813-817.

194. **Brass AL, Huang IC, Benita Y, John SP, Krishnan MN, Feeley EM, Ryan BJ, Weyer JL, van der Weyden L, Fikrig E, Adams DJ, Xavier RJ, Farzan M, Elledge SJ.** 2009. The IFITM Proteins Mediate Cellular Resistance to Influenza A H1N1 Virus, West Nile Virus, and Dengue Virus. Cell **139:**1243-1254.

195. **Borawski J, Troke P, Puyang X, Gibaja V, Zhao S, Mickanin C, Leighton-Davies J, Wilson CJ, Myer V, Cornellataracido I, Baryza J, Tallarico J, Joberty G, Bantscheff M, Schirle M, Bouwmeester T, Mathy JE, Lin K, Compton T, Labow M, Wiedmann B, Gaither LA.** 2009. Class III phosphatidylinositol 4-kinase alpha and beta are novel host factor regulators of hepatitis C virus replication. J Virol **83:**10058-10074.

196. **Panda D, Das A, Dinh PX, Subramaniam S, Nayak D, Barrows NJ, Pearson JL, Thompson J, Kelly DL, Ladunga I, Pattnaik AK.** 2011. RNAi screening reveals requirement for host cell secretory pathway in infection by diverse families of negative-strand RNA viruses. Proc Natl Acad Sci U S A **108:**19036-19041.

197. **Maynell LA, Kirkegaard K, Klymkowsky MW.** 1992. Inhibition of poliovirus RNA synthesis by brefeldin A. J Virol **66:**1985-1994.

198. **Cherry S, Kunte A, Wang H, Coyne C, Rawson RB, Perrimon N.** 2006. COPI activity coupled with fatty acid biosynthesis is required for viral replication. PLoS Pathog **2:**e102.

199. **Liu X, Erikson RL.** 2003. Polo-like kinase (Plk)1 depletion induces apoptosis in cancer cells. Proceedings of the National Academy of Sciences of the United States of America **100:**5789-5794.

200. **Hartsink-Segers SA, Exalto C, Allen M, Williamson D, Clifford SC, Horstmann M, Caron HN, Pieters R, Den Boer ML.** 2013. Inhibiting Polo-like kinase 1 causes growth reduction and apoptosis in pediatric acute lymphoblastic leukemia cells. Haematologica **98:**1539-1546.

201. **Yoshimura A, Naka T, Kubo M.** 2007. SOCS proteins, cytokine signalling and immune regulation. Nat Rev Immunol **7:**454-465.

202. **Shao R-X, Zhang L, Hong Z, Goto K, Cheng D, Chen W-C, Jilg N, Kumthip K, Fusco DN, Peng LF, Chung RT.** 2013. SOCS1 abrogates IFN's antiviral effect on hepatitis C virus replication. Antiviral Research **97:**101-107.

203. **Sun K, Salmon S, Yajjala VK, Bauer C, Metzger DW.** 2014. Expression of Suppressor of Cytokine Signaling 1 (SOCS1) Impairs Viral Clearance and Exacerbates Lung Injury during Influenza Infection. PLoS Pathog **10:**e1004560.

204. **Kaluza G, Scholtissek C, Rott R.** 1972. Inhibition of the multiplication of enveloped RNA-viruses by glucosamine and 2-deoxy-D-glucose. J Gen Virol **14:**251-259.

205. **Kilbourne ED.** 1959. Inhibition of influenza virus multiplication with a glucose antimetabolite (2-deoxy-D-glucose). Nature **183:**271-272.

206. **Kaluza G, Schmidt MFG, Scholtissek C.** 1973. Effect of 2-deoxy-d-glucose on the multiplication of semliki forest virus and the reversal of the block by mannose. Virology **54:**179-189.

207. **Noch E, Khalili K.** 2012. Oncogenic viruses and tumor glucose metabolism: like kids in a candy store. Mol Cancer Ther **11:**14-23.

208. **Cargnello M, Roux PP.** 2011. Activation and function of the MAPKs and their substrates, the MAPK-activated protein kinases. Microbiol Mol Biol Rev **75:**50-83.

209. **Dong C, Davis RJ, Flavell RA.** 2002. MAP kinases in the immune response. Annu Rev Immunol **20:**55-72.

210. **Roskoski R, Jr.** 2012. ERK1/2 MAP kinases: structure, function, and regulation. Pharmacol Res **66:**105-143.

211. **Clifton AD, Young PR, Cohen P.** 1996. A comparison of the substrate specificity of MAPKAP kinase-2 and MAPKAP kinase-3 and their activation by cytokines and cellular stress. FEBS Letters **392:**209-214.

212. **Gaestel M.** 2006. MAPKAP kinases - MKs - two's company, three's a crowd. Nat Rev Mol Cell Biol **7:**120-130.

213. **Liao Y, Wang X, Huang M, Tam JP, Liu DX.** 2011. Regulation of the p38 mitogen-activated protein kinase and dual-specificity phosphatase 1 feedback loop modulates the induction of interleukin 6 and 8 in cells infected with coronavirus infectious bronchitis virus. Virology **420:**106-116.

214. **Geiss GK, Salvatore M, Tumpey TM, Carter VS, Wang X, Basler CF, Taubenberger JK, Bumgarner RE, Palese P, Katze MG, Garcia-Sastre A.** 2002. Cellular transcriptional profiling in influenza A virus-infected lung epithelial cells: the role of the nonstructural NS1 protein in the evasion of the host innate defense and its potential contribution to pandemic influenza. Proc Natl Acad Sci U S A **99:**10736-10741.

215. **Tachado SD, Zhang J, Zhu J, Patel N, Koziel H.** 2005. HIV impairs TNF-alpha release in response to Toll-like receptor 4 stimulation in human macrophages in vitro. Am J Respir Cell Mol Biol **33:**610-621.

216. **Caunt CJ, Keyse SM.** 2013. Dual-specificity MAP kinase phosphatases (MKPs): shaping the outcome of MAP kinase signalling. FEBS J **280:**489-504.

217. **Su WC, Chen YC, Tseng CH, Hsu PW, Tung KF, Jeng KS, Lai MM.** 2013. Pooled RNAi screen identifies ubiquitin ligase Itch as crucial for influenza A virus release from the endosome during virus entry. Proc Natl Acad Sci U S A **110:**17516-17521.

218. **Shapira SD, Gat-Viks I, Shum BO, Dricot A, de Grace MM, Wu L, Gupta PB, Hao T, Silver SJ, Root DE, Hill DE, Regev A, Hacohen N.** 2009. A physical and regulatory map of host-influenza interactions reveals pathways in H1N1 infection. Cell **139:**1255-1267.

219. **Tran AT, Rahim MN, Ranadheera C, Kroeker A, Cortens JP, Opanubi KJ, Wilkins JA, Coombs KM.** 2013. Knockdown of specific host factors protects against influenza virus-induced cell death. Cell Death Dis **4:**e769.

220. **Ngo HT, Pham LV, Kim JW, Lim YS, Hwang SB.** 2013. Modulation of mitogen-activated protein kinase-activated protein kinase 3 by hepatitis C virus core protein. J Virol **87:**5718-5731.

221. **Luig C, Kother K, Dudek SE, Gaestel M, Hiscott J, Wixler V, Ludwig S.** 2010. MAP kinase-activated protein kinases 2 and 3 are required for influenza A virus propagation and act via inhibition of PKR. Faseb j **24:**4068-4077.

222. **Naz F, Anjum F, Islam A, Ahmad F, Hassan MI.** 2013. Microtubule affinity-regulating kinase 4: structure, function, and regulation. Cell Biochem Biophys **67:**485-499.

223. **Schmitt-Ulms G, Matenia D, Drewes G, Mandelkow EM.** 2009. Interactions of MAP/microtubule affinity regulating kinases with the adaptor complex AP-2 of clathrin-coated vesicles. Cell Motil Cytoskeleton **66:**661-672.

224. **Bernard E, Solignat M, Gay B, Chazal N, Higgs S, Devaux C, Briant L.** 2010. Endocytosis of chikungunya virus into mammalian cells: role of clathrin and early endosomal compartments. PLoS One **5:**e11479.

225. **Parks WC, Wilson CL, Lopez-Boado YS.** 2004. Matrix metalloproteinases as modulators of inflammation and innate immunity. Nat Rev Immunol **4:**617-629.

226. **Migliaccio E, Giorgio M, Mele S, Pelicci G, Reboldi P, Pandolfi PP, Lanfrancone L, Pelicci PG.** 1999. The p66shc adaptor protein controls oxidative stress response and life span in mammals. Nature **402:**309-313.

227. **Zona L, Lupberger J, Sidahmed-Adrar N, Thumann C, Harris Helen J, Barnes A, Florentin J, Tawar Rajiv G, Xiao F, Turek M, Durand Sarah C, Duong François HT, Heim Markus H, Cosset F-L, Hirsch I, Samuel D, Brino L, Zeisel Mirjam B, Le Naour F, McKeating Jane A, Baumert Thomas F.** 2013. HRas Signal Transduction Promotes Hepatitis C Virus Cell Entry by Triggering Assembly of the Host Tetraspanin Receptor Complex. Cell Host & Microbe **13:**302-313.

228. **Camps M, Nichols A, Arkinstall S.** 2000. Dual specificity phosphatases: a gene family for control of MAP kinase function. FASEB J **14:**6-16.

229. **James SJ, Jiao H, Teh HY, Takahashi H, Png CW, Phoon MC, Suzuki Y, Sawasaki T, Xiao H, Chow VT, Yamamoto N, Reynolds JM, Flavell RA, Dong C, Zhang Y.** 2015. MAPK Phosphatase 5 Expression Induced by Influenza and Other RNA Virus Infection Negatively Regulates IRF3 Activation and Type I Interferon Response. Cell Rep doi:10.1016/j.celrep.2015.02.030.

230. **Hammer M, Mages J, Dietrich H, Servatius A, Howells N, Cato AC, Lang R.** 2006. Dual specificity phosphatase 1 (DUSP1) regulates a subset of LPS-induced genes and protects mice from lethal endotoxin shock. J Exp Med **203:**15-20.

231. **Jeffrey KL, Camps M, Rommel C, Mackay CR.** 2007. Targeting dual-specificity phosphatases: manipulating MAP kinase signalling and immune responses. Nat Rev Drug Discov **6:**391-403.

232. **Ludwig S, Ehrhardt C, Neumeier ER, Kracht M, Rapp UR, Pleschka S.** 2001. Influenza virus-induced AP-1-dependent gene expression requires activation of the JNK signaling pathway. J Biol Chem **276:**10990-10998.

233. **Pleschka S, Wolff T, Ehrhardt C, Hobom G, Planz O, Rapp UR, Ludwig S.** 2001. Influenza virus propagation is impaired by inhibition of the Raf/MEK/ERK signalling cascade. Nat Cell Biol **3:**301-305.

234. **Kujime K, Hashimoto S, Gon Y, Shimizu K, Horie T.** 2000. p38 mitogen-activated protein kinase and c-jun-NH2-terminal kinase regulate RANTES production by influenza virus-infected human bronchial epithelial cells. J Immunol **164:**3222-3228.

235. **Lee DC, Cheung CY, Law AH, Mok CK, Peiris M, Lau AS.** 2005. p38 mitogen-activated protein kinase-dependent hyperinduction of tumor necrosis factor alpha expression in response to avian influenza virus H5N1. J Virol **79:**10147-10154.

236. **Hayashi J, Aoki H, Kajino K, Moriyama M, Arakawa Y, Hino O.** 2000. Hepatitis C virus core protein activates the MAPK/ERK cascade synergistically with tumor promoter TPA, but not with epidermal growth factor or transforming growth factor alpha. Hepatology **32:**958-961.

237. **Huber M, Watson KA, Selinka HC, Carthy CM, Klingel K, McManus BM, Kandolf R.** 1999. Cleavage of RasGAP and phosphorylation of mitogen-activated protein kinase in the course of coxsackievirus B3 replication. J Virol **73:**3587-3594.

238. **Luo H, Yanagawa B, Zhang J, Luo Z, Zhang M, Esfandiarei M, Carthy C, Wilson JE, Yang D, McManus BM.** 2002. Coxsackievirus B3 replication is reduced by inhibition of the extracellular signal-regulated kinase (ERK) signaling pathway. J Virol **76:**3365-3373.

239. **Voss K, Amaya M, Mueller C, Roberts B, Kehn-Hall K, Bailey C, Petricoin E, 3rd, Narayanan A.** 2014. Inhibition of host extracellular signal-regulated kinase (ERK) activation decreases new world alphavirus multiplication in infected cells. Virology **468-470:**490-503.

240. **Favata MF, Horiuchi KY, Manos EJ, Daulerio AJ, Stradley DA, Feeser WS, Van Dyk DE, Pitts WJ, Earl RA, Hobbs F, Copeland RA, Magolda RL, Scherle PA, Trzaskos JM.** 1998. Identification of a novel inhibitor of mitogen-activated protein kinase kinase. J Biol Chem **273:**18623-18632.

241. **Raines MA, Kolesnick RN, Golde DW.** 1993. Sphingomyelinase and ceramide activate mitogen-activated protein kinase in myeloid HL-60 cells. J Biol Chem **268:**14572-14575.

242. **Kayali AG, Austin DA, Webster NJ.** 2000. Stimulation of MAPK cascades by insulin and osmotic shock: lack of an involvement of p38 mitogen-activated protein kinase in glucose transport in 3T3-L1 adipocytes. Diabetes **49:**1783-1793.

243. **Wong J, Zhang J, Si X, Gao G, Luo H.** 2007. Inhibition of the extracellular signal-regulated kinase signaling pathway is correlated with proteasome inhibitor suppression of coxsackievirus replication. Biochem Biophys Res Commun **358:**903-907.

244. **Rodriguez ME, Brunetti JE, Wachsman MB, Scolaro LA, Castilla V.** 2014. Raf/MEK/ERK pathway activation is required for Junin virus replication. J Gen Virol **95:**799-805.

245. **Uddin S, Majchrzak B, Woodson J, Arunkumar P, Alsayed Y, Pine R, Young PR, Fish EN, Platanias LC.** 1999. Activation of the p38 mitogen-activated protein kinase by type I interferons. J Biol Chem **274:**30127-30131.

246. **Arora T, Floyd-Smith G, Espy MJ, Jelinek DF.** 1999. Dissociation between IFN-alpha-induced anti-viral and growth signaling pathways. J Immunol **162:**3289-3297.

247. **Battcock SM, Collier TW, Zu D, Hirasawa K.** 2006. Negative regulation of the alpha interferon-induced antiviral response by the Ras/Raf/MEK pathway. J Virol **80:**4422-4430.

248. **Noser JA, Mael AA, Sakuma R, Ohmine S, Marcato P, Lee PW, Ikeda Y.** 2007. The RAS/Raf1/MEK/ERK signaling pathway facilitates VSV-mediated oncolysis: implication for the defective interferon response in cancer cells. Mol Ther **15:**1531-1536.

249. **Frolov I.** 2004. Persistent infection and suppression of host response by alphaviruses. Arch Virol Suppl**:**139-147.

250. **Nikonov A, Molder T, Sikut R, Kiiver K, Mannik A, Toots U, Lulla A, Lulla V, Utt A, Merits A, Ustav M.** 2013. RIG-I and MDA-5 detection of viral RNA-dependent RNA polymerase activity restricts positive-strand RNA virus replication. PLoS Pathog **9:**e1003610.

251. **White JP, Lloyd RE.** 2012. Regulation of stress granules in virus systems. Trends Microbiol **20:**175-183.

252. **Tsai W-C, Lloyd RE.** 2014. Cytoplasmic RNA Granules and Viral Infection. Annual Review of Virology **1:**147-170.

253. **Kedersha N, Anderson P.** 2002. Stress granules: sites of mRNA triage that regulate mRNA stability and translatability. Biochem Soc Trans **30:**963-969.

254. **Kimball SR, Horetsky RL, Ron D, Jefferson LS, Harding HP.** 2003. Mammalian stress granules represent sites of accumulation of stalled translation initiation complexes. Am J Physiol Cell Physiol **284:**C273-284.

255. **Tourriere H, Chebli K, Zekri L, Courselaud B, Blanchard JM, Bertrand E, Tazi J.** 2003. The RasGAP-associated endoribonuclease G3BP assembles stress granules. J Cell Biol **160:**823-831.

256. **Kedersha NL, Gupta M, Li W, Miller I, Anderson P.** 1999. RNA-binding proteins TIA-1 and TIAR link the phosphorylation of eIF-2 alpha to the assembly of mammalian stress granules. J Cell Biol **147:**1431-1442.

257. **Williams BR.** 2001. Signal integration via PKR. Sci STKE **2001:**re2.

258. **Harding HP, Novoa I, Zhang Y, Zeng H, Wek R, Schapira M, Ron D.** 2000. Regulated translation initiation controls stress-induced gene expression in mammalian cells. Mol Cell **6:**1099-1108.

259. **Kimball SR.** 2001. Regulation of translation initiation by amino acids in eukaryotic cells. Prog Mol Subcell Biol **26:**155-184.

260. **Han AP, Yu C, Lu L, Fujiwara Y, Browne C, Chin G, Fleming M, Leboulch P, Orkin SH, Chen JJ.** 2001. Heme-regulated eIF2alpha kinase (HRI) is required for translational regulation and survival of erythroid precursors in iron deficiency. EMBO J **20:**6909-6918.

261. **Gilks N, Kedersha N, Ayodele M, Shen L, Stoecklin G, Dember LM, Anderson P.** 2004. Stress granule assembly is mediated by prion-like aggregation of TIA-1. Mol Biol Cell **15:**5383-5398.

262. **Kobayashi T, Winslow S, Sunesson L, Hellman U, Larsson C.** 2012. PKCalpha binds G3BP2 and regulates stress granule formation following cellular stress. PLoS One **7:**e35820.

263. **Matsuki H, Takahashi M, Higuchi M, Makokha GN, Oie M, Fujii M.** 2013. Both G3BP1 and G3BP2 contribute to stress granule formation. Genes Cells **18:**135-146.

264. **Tourriere H, Gallouzi IE, Chebli K, Capony JP, Mouaikel J, van der Geer P, Tazi J.** 2001. RasGAP-associated endoribonuclease G3Bp: selective RNA degradation and phosphorylation-dependent localization. Mol Cell Biol **21:**7747-7760.

265. **Prigent M, Barlat I, Langen H, Dargemont C.** 2000. IkappaBalpha and IkappaBalpha /NF-kappa B complexes are retained in the cytoplasm through interaction with a novel partner, RasGAP SH3-binding protein 2. J Biol Chem **275:**36441-36449.

266. **Frolova E, Gorchakov R, Garmashova N, Atasheva S, Vergara LA, Frolov I.** 2006. Formation of nsP3-specific protein complexes during Sindbis virus replication. J Virol **80:**4122-4134.

267. **Foy NJ, Akhrymuk M, Akhrymuk I, Atasheva S, Bopda-Waffo A, Frolov I, Frolova EI.** 2013. Hypervariable domains of nsP3 proteins of New World and Old World alphaviruses mediate formation of distinct, virus-specific protein complexes. J Virol **87:**1997-2010.

268. **Myles KM, Pierro DJ, Olson KE.** 2003. Deletions in the putative cell receptor-binding domain of Sindbis virus strain MRE16 E2 glycoprotein reduce midgut infectivity in Aedes aegypti. J Virol **77:**8872-8881.

269. **Lanke KH, van der Schaar HM, Belov GA, Feng Q, Duijsings D, Jackson CL, Ehrenfeld E, van Kuppeveld FJ.** 2009. GBF1, a guanine nucleotide exchange factor for Arf, is crucial for coxsackievirus B3 RNA replication. J Virol **83:**11940-11949.

270. **Albulescu IC, Tas A, Scholte FE, Snijder EJ, van Hemert MJ.** 2014. An in vitro assay to study chikungunya virus RNA synthesis and the mode of action of inhibitors. J Gen Virol doi:10.1099/vir.0.069690-0.

271. **Buehler E, Chen Y-C, Martin S.** 2012. C911: A Bench-Level Control for Sequence Specific siRNA Off-Target Effects. PLoS ONE **7:**e51942.

272. **Pastorino B, Bessaud M, Grandadam M, Murri S, Tolou HJ, Peyrefitte CN.** 2005. Development of a TaqMan RT-PCR assay without RNA extraction step for the detection and quantification of African Chikungunya viruses. J Virol Methods **124:**65-71.

273. **White JP, Cardenas AM, Marissen WE, Lloyd RE.** 2007. Inhibition of cytoplasmic mRNA stress granule formation by a viral proteinase. Cell Host & Microbe **2:**295-305.

274. **Cristea IM, Rozjabek H, Molloy KR, Karki S, White LL, Rice CM, Rout MP, Chait BT, MacDonald MR.** 2010. Host Factors Associated with the Sindbis Virus RNA-Dependent RNA Polymerase: Role for G3BP1 and G3BP2 in Virus Replication. Journal of Virology **84:**6720-6732.

275. **Fung G, Ng CS, Zhang J, Shi J, Wong J, Piesik P, Han L, Chu F, Jagdeo J, Jan E, Fujita T, Luo H.** 2013. Production of a Dominant-Negative Fragment Due to G3BP1 Cleavage Contributes to the Disruption of Mitochondria-Associated Protective Stress Granules during CVB3 Infection. PLoS ONE **8:**e79546.

276. **Varjak M, Žusinaite E, Merits A.** 2010. Novel Functions of the Alphavirus Nonstructural Protein nsP3 C-Terminal Region. J Virol **84:**2352-2364.

277. **Lindquist ME, Lifland AW, Utley TJ, Santangelo PJ, Crowe JE.** 2010. Respiratory Syncytial Virus Induces Host RNA Stress Granules To Facilitate Viral Replication. Journal of Virology **84:**12274-12284.

278. **Yi ZG, Pan TT, Wu XF, Song WH, Wang SS, Xu Y, Rice CM, MacDonald MR, Yuan ZH.** 2011. Hepatitis C Virus Co-Opts Ras-GTPase-Activating Protein-Binding Protein 1 for Its Genome Replication. Journal of Virology **85:**6996-7004.

279. **Ward AM, Bidet K, Ang YL, Ler SG, Hogue K, Blackstock W, Gunaratne J, Garcia-Blanco MA.** 2011. Quantitative mass spectrometry of DENV-2 RNA-interacting proteins reveals that the DEAD-box RNA helicase DDX6 binds the DB1 and DB2 3 ' UTR structures. Rna Biology **8:**1173-1186.

280. **Matthews JD, Frey TK.** 2012. Analysis of subcellular G3BP redistribution during rubella virus infection. Journal of General Virology **93:**267-274.

281. **Zheng Y, Kielian M.** 2013. Imaging of the alphavirus capsid protein during virus replication. J Virol **87:**9579-9589.

282. **Irvine K, Stirling R, Hume D, Kennedy D.** 2004. Rasputin, more promiscuous than ever: a review of G3BP. International Journal of Developmental Biology **48:**1065-1077.

283. **Soncini C, Berdo I, Draetta G.** 2001. Ras-GAP SH3 domain binding protein (G3BP) is a modulator of USP10, a novel human ubiquitin specific protease. Oncogene **20:**3869-3879.

284. **Zhang H, Zhang S, He H, Zhao W, Chen J, Shao RG.** 2012. GAP161 targets and downregulates G3BP to suppress cell growth and potentiate cisplaitin-mediated cytotoxicity to colon carcinoma HCT116 cells. Cancer Sci **103:**1848-1856.

285. **Goubau D, Deddouche S, Reis ESC.** 2013. Cytosolic sensing of viruses. Immunity **38:**855-869.

286. **Akira S, Uematsu S, Takeuchi O.** 2006. Pathogen recognition and innate immunity. Cell **124:**783-801.

287. **Liu SY, Sanchez DJ, Cheng G.** 2011. New developments in the induction and antiviral effectors of type I interferon. Curr Opin Immunol **23:**57-64.

288. **Takeuchi O, Akira S.** 2010. Pattern recognition receptors and inflammation. Cell **140:**805-820.

289. **Belgnaoui SM, Paz S, Hiscott J.** 2011. Orchestrating the interferon antiviral response through the mitochondrial antiviral signaling (MAVS) adapter. Curr Opin Immunol **23:**564-572.

290. **Kumar H, Kawai T, Akira S.** 2011. Pathogen recognition by the innate immune system. Int Rev Immunol **30:**16-34.

291. **Loo YM, Gale M, Jr.** 2011. Immune signaling by RIG-I-like receptors. Immunity **34:**680-692.

292. **Wilkins C, Gale M, Jr.** 2010. Recognition of viruses by cytoplasmic sensors. Curr Opin Immunol **22:**41-47.

293. **Rehwinkel J, Reis e Sousa C.** 2010. RIGorous detection: exposing virus through RNA sensing. Science **327:**284-286.

294. **Rehwinkel J, Tan CP, Goubau D, Schulz O, Pichlmair A, Bier K, Robb N, Vreede F, Barclay W, Fodor E, Reis e Sousa C.** 2010. RIG-I detects viral genomic RNA during negative-strand RNA virus infection. Cell **140:**397-408.

295. **Hornung V, Ellegast J, Kim S, Brzozka K, Jung A, Kato H, Poeck H, Akira S, Conzelmann KK, Schlee M, Endres S, Hartmann G.** 2006. 5'-Triphosphate RNA is the ligand for RIG-I. Science **314:**994-997.

296. **Pichlmair A, Schulz O, Tan CP, Naslund TI, Liljestrom P, Weber F, Reis e Sousa C.** 2006. RIG-I-mediated antiviral responses to single-stranded RNA bearing 5'-phosphates. Science **314:**997-1001.

297. **Kato H, Takeuchi O, Mikamo-Satoh E, Hirai R, Kawai T, Matsushita K, Hiiragi A, Dermody TS, Fujita T, Akira S.** 2008. Length-dependent recognition of double-stranded ribonucleic acids by retinoic acid-inducible gene-I and melanoma differentiation-associated gene 5. J Exp Med **205:**1601-1610.

298. **Hwang SY, Sun HY, Lee KH, Oh BH, Cha YJ, Kim BH, Yoo JY.** 2012. 5'-Triphosphate-RNA-independent activation of RIG-I via RNA aptamer with enhanced antiviral activity. Nucleic Acids Res **40:**2724-2733.

299. **Schlee M, Roth A, Hornung V, Hagmann CA, Wimmenauer V, Barchet W, Coch C, Janke M, Mihailovic A, Wardle G, Juranek S, Kato H, Kawai T, Poeck H, Fitzgerald KA, Takeuchi O, Akira S, Tuschl T, Latz E, Ludwig J, Hartmann G.** 2009. Recognition of 5' triphosphate by RIG-I helicase requires short blunt double-stranded RNA as contained in panhandle of negative-strand virus. Immunity **31:**25-34.

300. **Yoneyama M, Kikuchi M, Natsukawa T, Shinobu N, Imaizumi T, Miyagishi M, Taira K, Akira S, Fujita T.** 2004. The RNA helicase RIG-I has an essential function in double-stranded RNA-induced innate antiviral responses. Nat Immunol **5:**730-737.

301. **Kowalinski E, Lunardi T, McCarthy AA, Louber J, Brunel J, Grigorov B, Gerlier D, Cusack S.** 2011. Structural basis for the activation of innate immune pattern-recognition receptor RIG-I by viral RNA. Cell **147:**423-435.

302. **Myong S, Cui S, Cornish PV, Kirchhofer A, Gack MU, Jung JU, Hopfner KP, Ha T.** 2009. Cytosolic viral sensor RIG-I is a 5'-triphosphate-dependent translocase on double-stranded RNA. Science **323:**1070-1074.

303. **Patel JR, Jain A, Chou YY, Baum A, Ha T, Garcia-Sastre A.** 2013. ATPase-driven oligomerization of RIG-I on RNA allows optimal activation of type-I interferon. EMBO Rep doi:10.1038/embor.2013.102.

304. **Grandvaux N, Servant MJ, tenOever B, Sen GC, Balachandran S, Barber GN, Lin R, Hiscott J.** 2002. Transcriptional profiling of interferon regulatory factor 3 target genes: direct involvement in the regulation of interferon-stimulated genes. J Virol **76:**5532-5539.

305. **Kawai T, Akira S.** 2007. SnapShot: Pattern-recognition receptors. Cell **129:**1024.

306. **Kawai T, Akira S.** 2011. Toll-like receptors and their crosstalk with other innate receptors in infection and immunity. Immunity **34:**637-650.

307. **Sadler AJ, Williams BR.** 2008. Interferon-inducible antiviral effectors. Nat Rev Immunol **8:**559-568.

308. **Schoggins JW, Wilson SJ, Panis M, Murphy MY, Jones CT, Bieniasz P, Rice CM.** 2011. A diverse range of gene products are effectors of the type I interferon antiviral response. Nature **472:**481-485.

309. **Wu J, Lu M, Meng Z, Trippler M, Broering R, Szczeponek A, Krux F, Dittmer U, Roggendorf M, Gerken G, Schlaak JF.** 2007. Toll-like receptor-mediated control of HBV replication by nonparenchymal liver cells in mice. Hepatology **46:**1769-1778.

310. **Isogawa M, Robek MD, Furuichi Y, Chisari FV.** 2005. Toll-like receptor signaling inhibits hepatitis B virus replication in vivo. J Virol **79:**7269-7272.

311. **Svensson A, Bellner L, Magnusson M, Eriksson K.** 2007. Role of IFN-alpha/beta signaling in the prevention of genital herpes virus type 2 infection. J Reprod Immunol **74:**114-123.

312. **Boukhvalova MS, Sotomayor TB, Point RC, Pletneva LM, Prince GA, Blanco JC.** 2010. Activation of interferon response through toll-like receptor 3 impacts viral pathogenesis and pulmonary toll-like receptor expression during respiratory syncytial virus and influenza infections in the cotton rat Sigmodon hispidus model. J Interferon Cytokine Res **30:**229-242.

313. **Lau YF, Tang LH, Ooi EE, Subbarao K.** 2010. Activation of the innate immune system provides broad-spectrum protection against influenza A viruses with pandemic potential in mice. Virology **406:**80-87.

314. **Li YG, Siripanyaphinyo U, Tumkosit U, Noranate N, A AN, Pan Y, Kameoka M, Kurosu T, Ikuta K, Takeda N, Anantapreecha S.** 2012. Poly (I:C), an agonist of toll-like receptor-3, inhibits replication of the Chikungunya virus in BEAS-2B cells. Virol J **9:**114.

315. **Liang Z, Wu S, Li Y, He L, Wu M, Jiang L, Feng L, Zhang P, Huang X.** 2011. Activation of Toll-like receptor 3 impairs the dengue virus serotype 2 replication through induction of IFN-beta in cultured hepatoma cells. PLoS One **6:**e23346.

316. **Trapp S, Derby NR, Singer R, Shaw A, Williams VG, Turville SG, Bess JW, Jr., Lifson JD, Robbiani M.** 2009. Double-stranded RNA analog poly(I:C) inhibits human immunodeficiency virus amplification in dendritic cells via type I interferon-mediated activation of APOBEC3G. J Virol **83:**884-895.

317. **Wang N, Liang Y, Devaraj S, Wang J, Lemon SM, Li K.** 2009. Toll-like receptor 3 mediates establishment of an antiviral state against hepatitis C virus in hepatoma cells. J Virol **83:**9824-9834.

318. **Zhou Y, Wang X, Liu M, Hu Q, Song L, Ye L, Zhou D, Ho W.** 2010. A critical function of toll-like receptor-3 in the induction of anti-human immunodeficiency virus activities in macrophages. Immunology **131:**40-49.

319. **Goulet ML, Olagnier D, Xu Z, Paz S, Belgnaoui SM, Lafferty EI, Janelle V, Arguello M, Paquet M, Ghneim K, Richards S, Smith A, Wilkinson P, Cameron M, Kalinke U, Qureshi S, Lamarre A, Haddad EK, Sekaly RP, Peri S, Balachandran S, Lin R, Hiscott J.** 2013. Systems analysis of a RIG-I agonist inducing broad spectrum inhibition of virus infectivity. PLoS Pathog **9:**e1003298.

320. **Halstead SB.** 2007. Dengue. Lancet **370:**1644-1652.

321. **Halstead SB, Suaya JA, Shepard DS.** 2007. The burden of dengue infection. Lancet **369:**1410-1411.

322. **Rothman AL.** 2011. Immunity to dengue virus: a tale of original antigenic sin and tropical cytokine storms. Nat Rev Immunol **11:**532-543.

323. **Her Z, Kam YW, Lin RT, Ng LF.** 2009. Chikungunya: a bending reality. Microbes Infect **11:**1165-1176.

324. **Powers AM, Logue CH.** 2007. Changing patterns of chikungunya virus: re-emergence of a zoonotic arbovirus. J Gen Virol **88:**2363-2377.

325. **Aguirre S, Maestre AM, Pagni S, Patel JR, Savage T, Gutman D, Maringer K, Bernal-Rubio D, Shabman RS, Simon V, Rodriguez-Madoz JR, Mulder LC, Barber GN, Fernandez-Sesma A.** 2012. DENV inhibits type I IFN production in infected cells by cleaving human STING. PLoS Pathog **8:**e1002934.

326. **Morrison J, Aguirre S, Fernandez-Sesma A.** 2012. Innate immunity evasion by Dengue virus. Viruses **4:**397-413.

327. **Rodriguez-Madoz JR, Belicha-Villanueva A, Bernal-Rubio D, Ashour J, Ayllon J, Fernandez-Sesma A.** 2010. Inhibition of the type I interferon response in human dendritic cells by dengue virus infection requires a catalytically active NS2B3 complex. J Virol **84:**9760-9774.

328. **Blackley S, Kou Z, Chen H, Quinn M, Rose RC, Schlesinger JJ, Coppage M, Jin X.** 2007. Primary human splenic macrophages, but not T or B cells, are the principal target cells for dengue virus infection in vitro. J Virol **81:**13325-13334.

329. **Kou Z, Quinn M, Chen H, Rodrigo WW, Rose RC, Schlesinger JJ, Jin X.** 2008. Monocytes, but not T or B cells, are the principal target cells for dengue virus (DV) infection among human peripheral blood mononuclear cells. J Med Virol **80:**134-146.

330. **Diamond MS, Edgil D, Roberts TG, Lu B, Harris E.** 2000. Infection of human cells by dengue virus is modulated by different cell types and viral strains. J Virol **74:**7814-7823.

331. **Johnson AJ, Roehrig JT.** 1999. New mouse model for dengue virus vaccine testing. J Virol **73:**783-786.

332. **Couderc T, Chretien F, Schilte C, Disson O, Brigitte M, Guivel-Benhassine F, Touret Y, Barau G, Cayet N, Schuffenecker I, Despres P, Arenzana-Seisdedos F, Michault A, Albert ML, Lecuit M.** 2008. A mouse model for Chikungunya: young age and inefficient type-I interferon signaling are risk factors for severe disease. PLoS Pathog **4:**e29.

333. **Nasirudeen AM, Wong HH, Thien P, Xu S, Lam KP, Liu DX.** 2011. RIG-I, MDA5 and TLR3 synergistically play an important role in restriction of dengue virus infection. PLoS Negl Trop Dis **5:**e926.

334. **Brass AL, Huang IC, Benita Y, John SP, Krishnan MN, Feeley EM, Ryan BJ, Weyer JL, van der Weyden L, Fikrig E, Adams DJ, Xavier RJ, Farzan M, Elledge SJ.** 2009. The IFITM proteins mediate cellular resistance to influenza A H1N1 virus, West Nile virus, and dengue virus. Cell **139:**1243-1254.

335. **Helbig KJ, Carr JM, Calvert JK, Wati S, Clarke JN, Eyre NS, Narayana SK, Fiches GN, McCartney EM, Beard MR.** 2013. Viperin is induced following dengue virus type-2 (DENV-2) infection and has anti-viral actions requiring the C-terminal end of viperin. PLoS Negl Trop Dis **7:**e2178.

336. **Gaajetaan GR, Geelen TH, Grauls GE, Bruggeman CA, Stassen FR.** 2012. CpG and poly(I:C) stimulation of dendritic cells and fibroblasts limits herpes simplex virus type 1 infection in an IFNbeta-dependent and -independent way. Antiviral Res **93:**39-47.

337. **Mazaleuskaya L, Veltrop R, Ikpeze N, Martin-Garcia J, Navas-Martin S.** 2012. Protective role of Toll-like Receptor 3-induced type I interferon in murine coronavirus infection of macrophages. Viruses **4:**901-923.

338. **Sariol CA, Martinez MI, Rivera F, Rodriguez IV, Pantoja P, Abel K, Arana T, Giavedoni L, Hodara V, White LJ, Anglero YI, Montaner LJ, Kraiselburd EN.** 2011. Decreased dengue replication and an increased anti-viral humoral response with the use of combined Toll-like receptor 3 and 7/8 agonists in macaques. PLoS One **6:**e19323.

339. **Zhao J, Wohlford-Lenane C, Zhao J, Fleming E, Lane TE, McCray PB, Jr., Perlman S.** 2012. Intranasal treatment with poly(I*C) protects aged mice from lethal respiratory virus infections. J Virol **86:**11416-11424.

340. **Caskey M, Lefebvre F, Filali-Mouhim A, Cameron MJ, Goulet JP, Haddad EK, Breton G, Trumpfheller C, Pollak S, Shimeliovich I, Duque-Alarcon A, Pan L, Nelkenbaum A, Salazar AM, Schlesinger SJ, Steinman RM, Sekaly RP.** 2011. Synthetic double-stranded RNA induces innate immune responses similar to a live viral vaccine in humans. J Exp Med **208:**2357-2366.

341. **Ichinohe T, Kawaguchi A, Tamura S, Takahashi H, Sawa H, Ninomiya A, Imai M, Itamura S, Odagiri T, Tashiro M, Chiba J, Sata T, Kurata T, Hasegawa H.** 2007. Intranasal immunization with H5N1 vaccine plus Poly I:Poly C12U, a Toll-like receptor agonist, protects mice against homologous and heterologous virus challenge. Microbes Infect **9:**1333-1340.

342. **Ichinohe T, Watanabe I, Ito S, Fujii H, Moriyama M, Tamura S, Takahashi H, Sawa H, Chiba J, Kurata T, Sata T, Hasegawa H.** 2005. Synthetic double-stranded RNA poly(I:C) combined with mucosal vaccine protects against influenza virus infection. J Virol **79:**2910-2919.

343. **Martinez-Gil L, Goff PH, Hai R, Garcia-Sastre A, Shaw ML, Palese P.** 2013. A Sendai virus-derived RNA agonist of RIG-I as a virus vaccine adjuvant. J Virol **87:**1290-1300.

344. **Dejean AS, Beisner DR, Ch'en IL, Kerdiles YM, Babour A, Arden KC, Castrillon DH, DePinho RA, Hedrick SM.** 2009. Transcription factor Foxo3 controls the magnitude of T cell immune responses by modulating the function of dendritic cells. Nat Immunol **10:**504-513.

345. **Maher SG, Sheikh F, Scarzello AJ, Romero-Weaver AL, Baker DP, Donnelly RP, Gamero AM.** 2008. IFNalpha and IFNlambda differ in their antiproliferative effects and duration of JAK/STAT signaling activity. Cancer Biol Ther **7:**1109-1115.

346. **Bartlett NW, Buttigieg K, Kotenko SV, Smith GL.** 2005. Murine interferon lambdas (type III interferons) exhibit potent antiviral activity in vivo in a poxvirus infection model. J Gen Virol **86:**1589-1596.

347. **Pugachev KV, Abernathy ES, Frey TK.** 1997. Improvement of the specific infectivity of the rubella virus (RUB) infectious clone: determinants of cytopathogenicity induced by RUB map to the nonstructural proteins. J Virol **71:**562-568.

348. **Delogu I, Pastorino B, Baronti C, Nougairede A, Bonnet E, de Lamballerie X.** 2011. In vitro antiviral activity of arbidol against Chikungunya virus and characteristics of a selected resistant mutant. Antiviral Res **90:**99-107.

349. **Elbashir SM, Lendeckel W, Tuschl T.** 2001. RNA interference is mediated by 21- and 22-nucleotide RNAs. Genes Dev **15:**188-200.

350. **Jackson AL, Linsley PS.** 2010. Recognizing and avoiding siRNA off-target effects for target identification and therapeutic application. Nat Rev Drug Discov **9:**57-67.

351. **Good L.** 2003. Translation repression by antisense sequences. Cell Mol Life Sci **60:**854-861.

352. **Kittler R, Surendranath V, Heninger AK, Slabicki M, Theis M, Putz G, Franke K, Caldarelli A, Grabner H, Kozak K, Wagner J, Rees E, Korn B, Frenzel C, Sachse C, Sonnichsen B, Guo J, Schelter J, Burchard J, Linsley PS, Jackson AL, Habermann B, Buchholz F.** 2007. Genome-wide resources of endoribonuclease-prepared short interfering RNAs for specific loss-of-function studies. Nat Methods **4:**337-344.

353. **Jackson AL, Burchard J, Leake D, Reynolds A, Schelter J, Guo J, Johnson JM, Lim L, Karpilow J, Nichols K, Marshall W, Khvorova A, Linsley PS.** 2006. Position-specific chemical modification of siRNAs reduces "off-target" transcript silencing. Rna **12:**1197-1205.

354. **Ha M, Kim VN.** 2014. Regulation of microRNA biogenesis. Nat Rev Mol Cell Biol **15:**509-524.

355. **Jackson AL, Burchard J, Schelter J, Chau BN, Cleary M, Lim L, Linsley PS.** 2006. Widespread siRNA "off-target" transcript silencing mediated by seed region sequence complementarity. Rna **12:**1179-1187.

356. **Robbins M, Judge A, MacLachlan I.** 2009. siRNA and innate immunity. Oligonucleotides **19:**89-102.

357. **Judge AD, Sood V, Shaw JR, Fang D, McClintock K, MacLachlan I.** 2005. Sequence-dependent stimulation of the mammalian innate immune response by synthetic siRNA. Nat Biotech **23:**457-462.

358. **Hornung V, Guenthner-Biller M, Bourquin C, Ablasser A, Schlee M, Uematsu S, Noronha A, Manoharan M, Akira S, de Fougerolles A, Endres S, Hartmann G.** 2005. Sequence-specific potent induction of IFN-alpha by short interfering RNA in plasmacytoid dendritic cells through TLR7. Nat Med **11:**263-270.

359. **Sioud M.** 2005. Induction of inflammatory cytokines and interferon responses by double-stranded and single-stranded siRNAs is sequence-dependent and requires endosomal localization. J Mol Biol **348:**1079-1090.

360. **Sioud M.** 2006. Single-stranded small interfering RNA are more immunostimulatory than their double-stranded counterparts: A central role for 2'-hydroxyl uridines in immune responses. European Journal of Immunology **36:**1222-1230.

361. **Sioud M, Furset G, Cekaite L.** 2007. Suppression of immunostimulatory siRNA-driven innate immune activation by 2'-modified RNAs. Biochemical and Biophysical Research Communications **361:**122-126.

362. **Lopes TJ, Schaefer M, Shoemaker J, Matsuoka Y, Fontaine JF, Neumann G, Andrade-Navarro MA, Kawaoka Y, Kitano H.** 2011. Tissue-specific subnetworks and characteristics of publicly available human protein interaction databases. Bioinformatics **27:**2414-2421.

363. **Nousiainen L, Sillanpaa M, Jiang M, Thompson J, Taipale J, Julkunen I.** 2013. Human kinome analysis reveals novel kinases contributing to virus infection and retinoic-acid inducible gene I-induced type I and type III IFN gene expression. Innate Immun **19:**516-530.

364. **Kwon Y-J, Heo J, Wong HEE, Cruz DJM, Velumani S, da Silva CT, Mosimann ALP, Duarte dos Santos CN, Freitas-Junior LH, Fink K.** 2014. Kinome siRNA screen identifies novel cell-type specific dengue host target genes. Antiviral Research **110:**20-30.

365. **Chou YC, Lai MM, Wu YC, Hsu NC, Jeng KS, Su WC.** 2015. Variations in genome-wide RNAi screens: lessons from influenza research. J Clin Bioinforma **5:**2.

366. **Karlas A, Machuy N, Shin Y, Pleissner KP, Artarini A, Heuer D, Becker D, Khalil H, Ogilvie LA, Hess S, Maurer AP, Muller E, Wolff T, Rudel T, Meyer TF.** 2010. Genome-wide RNAi screen identifies human host factors crucial for influenza virus replication. Nature **463:**818-822.

367. **Hao L, Sakurai A, Watanabe T, Sorensen E, Nidom CA, Newton MA, Ahlquist P, Kawaoka Y.** 2008. Drosophila RNAi screen identifies host genes important for influenza virus replication. Nature **454:**890-893.

368. **Hao L, He Q, Wang Z, Craven M, Newton MA, Ahlquist P.** 2013. Limited Agreement of Independent RNAi Screens for Virus-Required Host Genes Owes More to False-Negative than False-Positive Factors. PLoS Comput Biol **9:**e1003235.

369. **McCubrey JA, Steelman LS, Chappell WH, Abrams SL, Wong EWT, Chang F, Lehmann B, Terrian DM, Milella M, Tafuri A, Stivala F, Libra M, Basecke J, Evangelisti C, Martelli AM, Franklin RA.** 2007. Roles of the Raf/MEK/ERK pathway in cell growth, malignant transformation and drug resistance. Biochimica et Biophysica Acta (BBA) - Molecular Cell Research **1773:**1263-1284.

370. **Roberts PJ, Der CJ.** 2007. Targeting the Raf-MEK-ERK mitogen-activated protein kinase cascade for the treatment of cancer. Oncogene **26:**3291-3310.

371. **Mansour SJ, Matten WT, Hermann AS, Candia JM, Rong S, Fukasawa K, Vande Woude GF, Ahn NG.** 1994. Transformation of mammalian cells by constitutively active MAP kinase kinase. Science **265:**966-970.

372. **Zhang Z, Kobayashi S, Borczuk AC, Leidner RS, Laframboise T, Levine AD, Halmos B.** 2010. Dual specificity phosphatase 6 (DUSP6) is an ETS-regulated negative feedback mediator of oncogenic ERK signaling in lung cancer cells. Carcinogenesis **31:**577-586.

373. **Pratilas CA, Solit DB.** 2010. Targeting the mitogen-activated protein kinase pathway: physiological feedback and drug response. Clin Cancer Res **16:**3329-3334.

374. **Kennedy D, French J, Guitard E, Ru KL, Tocque B, Mattick J.** 2002. Characterization of G3BPs: Tissue specific expression, chromosomal localisation and rasGAP(120) binding studies. Journal of Cellular Biochemistry **84:**173-187.

375. **Bikkavilli RK, Malbon CC.** 2011. Arginine methylation of G3BP1 in response to Wnt3a regulates beta-catenin mRNA. J Cell Sci **124:**2310-2320.

376. **Bikkavilli RK, Malbon CC.** 2012. Wnt3a-stimulated LRP6 phosphorylation is dependent upon arginine methylation of G3BP2. J Cell Sci **125:**2446-2456.

377. **Kedersha N, Anderson P.** 2007. Mammalian stress granules and processing bodies. Methods Enzymol **431:**61-81.

378. **Onomoto K, Jogi M, Yoo J-S, Narita R, Morimoto S, Takemura A, Sambhara S, Kawaguchi A, Osari S, Nagata K, Matsumiya T, Namiki H, Yoneyama M, Fujita T.** 2012. Critical Role of an Antiviral Stress Granule Containing RIG-I and PKR in Viral Detection and Innate Immunity. PLoS ONE **7:**e43031.

379. **Reineke LC, Kedersha N, Langereis MA, van Kuppeveld FJ, Lloyd RE.** 2015. Stress granules regulate double-stranded RNA-dependent protein kinase activation through a complex containing G3BP1 and Caprin1. MBio **6:**e02486.

380. **Reineke LC, Lloyd RE.** 2015. The stress granule protein G3BP1 recruits protein kinase R to promote multiple innate immune antiviral responses. J Virol **89:**2575-2589.

381. **Kedersha N, Ivanov P, Anderson P.** 2013. Stress granules and cell signaling: more than just a passing phase? Trends Biochem Sci **38:**494-506.

382. **Adams DR, Ron D, Kiely PA.** 2011. RACK1, A multifaceted scaffolding protein: Structure and function. Cell Commun Signal **9:**22.

383. **Arimoto K, Fukuda H, Imajoh-Ohmi S, Saito H, Takekawa M.** 2008. Formation of stress granules inhibits apoptosis by suppressing stress-responsive MAPK pathways. Nat Cell Biol **10:**1324-1332.

384. **Baldwin AS, Jr.** 1996. The NF-kappa B and I kappa B proteins: new discoveries and insights. Annu Rev Immunol **14:**649-683.

385. **May MJ, Ghosh S.** 1998. Signal transduction through NF-kappa B. Immunol Today **19:**80-88.

386. **Kehn-Hall K, Narayanan A, Lundberg L, Sampey G, Pinkham C, Guendel I, Van Duyne R, Senina S, Schultz KL, Stavale E, Aman MJ, Bailey C, Kashanchi F.** 2012. Modulation of GSK-3beta activity in Venezuelan equine encephalitis virus infection. PLoS One **7:**e34761.

387. **Aletta JM, Hu JC.** 2008. Protein arginine methylation in health and disease. Biotechnol Annu Rev **14:**203-224.

388. **Barton DJ, Morasco BJ, Flanegan JB.** 1999. Translating ribosomes inhibit poliovirus negative-strand RNA synthesis. J Virol **73:**10104-10112.

ABBREVIATIONS

-RNA	negative-stranded RNA
+RNA	positive-stranded RNA
aa	amino acid
ACE2	angiotensin-converting enzyme 2
ActD	actinomycin D
Ae.	Aedes
Arbo	arthropod borne
BHK	baby hamster kidney
BSL3	biosafety level 3
CDK	cyclin-dependent protein kinase
CHIKV	chikungunya virus
CHIKF	chikungunya fever
COP	coatomer protein complex
CPE	cytopathic effect
CPV	cytopathic vacuoles
Cy3	indocarbocyanine 3
DENV	dengue virus
DMEM	Dulbecco's Modified Eagle Medium
DMSO	dimethyl sulfoxide
DNA	deoxyribonucleic acid
ds	double-stranded
DTT	dithiothreitol
eIF	eukaryotic translation initiation factor
ECSA	East-Central-South African
EMEM	Eagle's Minimal Essential Medium
ER	endoplasmic reticulum
FA	formaldehyde
FACS	fluorescence-activated cell sorting
FCS	fetal calve serum
FDA	Food and Drug Administration
g	genomic
GAPDH	glyceraldehyde 3-phosphate dehydrogenase
GFP	green fluorescent protein
HCV	hepatitis C virus
HEPES	4-(2-hydroxyethyl)-1-piperazineethanesulfonic acid
hnRNP	heterogeneous nuclear ribonucleoprotein
hpi	hours post infection
hpt	hours post transfection
IC50	half maximal inhibitory concentration

IFA	immunofluorescence assay
IFN	interferon
IgG	immunoglobulin G
IgM	immunoglobulin M
IL	interleukin
IRF	IFN-regulatory factor
ISG	interferon-stimulated gene
IVRA	in vitro RNA synthesis assay
kb	kilobase
kDa	kilo Dalton
Mabs	monoclonal antibodies
MCP-1	monocyte chemoattractant protein 1
MOI	multiplicity of infection
MRC5	Medical Research Council-5
mRNA	messenger RNA
nsP	non-structural protein
ORF	open reading frame
PABP	poly(A)-binding protein
PAGE	polyacrylamide gel electrophoresis
PBS	phosphate-buffered saline
PBST	phosphate buffered saline with 0.05% Tween
PCBP	poly(C)-binding protein
PERK	PKR-like endoplasmic reticulum kinase
PFA	paraformaldehyde
p.i.	post infection
PKR	double-stranded RNA-activated protein kinase
PNS	post-nuclear supernatant
p.t.	post transfection
RC	replication complex
RdRp	RNA-dependent RNA polymerase
RIG-I	retinoic acid-inducible gene 1
RISC	RNA-induced silencing complex
RNA	ribonucleic acid
RNAi	RNA interference
RNase	ribonuclease
RRV	Ross River virus
rt	room temperature
RTC	replication and transcription complex
RT-PCR	reverse transcriptase- polymerase chain reaction
SD	standard deviation

SDS	sodium dodecyl sulphate
SDS-PAGE	sodium-dodecyl sulfate polyacrylamide gel electrophoresis
SINV	Sindbis virus
SFV	Semliki Forest virus
sg	subgenomic
shRNA	short-hairpin RNA
siRNA	small interfering RNA
ss	single-stranded
TBS(T)	tris-buffered saline (with 0.05% Tween-20)
TfR	transferrin receptor
UPR	unfolded protein response
USAMRIID	U.S. Army Institute of Infectious Diseases
UTR	untranslated region
VEEV	Venezuelan equine encephalitis virus
VLP	virus-like particle
WB	Western Blot
WNV	West Nile virus
wt	wild-type
Y2H	yeast two-hybrid

NEDERLANDSE SAMENVATTING

Infectieziekten veroorzaken jaarlijks wereldwijd aanzienlijke morbiditeit en mortaliteit. Ze kunnen worden veroorzaakt door bacteriën, schimmels, parasieten, prionen en virussen. Een belangrijk deel van deze infectieziekten wordt veroorzaakt door virussen, bijvoorbeeld griep en verkoudheid, maar ook AIDS en ebola. Virussen bevolken onze planeet vermoedelijk al miljarden jaren, en kunnen praktisch elke levensvorm infecteren, van bacteriën en planten tot vissen en mensen. Deze kleine, maar flexibele micro-organismen blinken uit op het gebied van adaptatie. Met slechts een klein wapenarsenaal (de kleine genomen van RNA virussen, bijvoorbeeld, coderen meestal voor slechts een handjevol eiwitten), zijn virussen toch in staat om een gastheercel compleet over te nemen. Ook het tegenovergestelde is mogelijk: een virus kan erin slagen om onopgemerkt te blijven in een gastheer, ondanks de aanwezigheid van een functioneel immuunsysteem.

Om zich te kunnen vermenigvuldigen moeten virussen hun erfelijk materiaal (RNA of DNA) kopiëren. Veel RNA virussen bezitten geen mechanisme om fouten te corrigeren, waardoor er mutaties ontstaan in het virale genoom. In het algemeen levert elke replicatieronde unieke veranderingen per virusgenoom op. 'Een virus' bestaat dus eigenlijk uit een hele zwerm van varianten. Meestal hebben mutaties geen effect, soms zijn ze nadelig voor het virus, bijvoorbeeld als het daardoor minder efficiënt repliceert, maar mutaties kunnen er ook toe leiden dat virussen nieuwe eigenschappen ontwikkelen. Door deze genomische plasticiteit kan een virus zich snel aanpassen aan een veranderende omgeving.

Grote virusuitbraken leiden met enige regelmaat tot aanzienlijke maatschappelijke onrust en economische schade, zoals bijvoorbeeld is gebleken bij de jongste uitbraak van het Ebolavirus (2013-heden (2015)), maar ook van MERS-CoV (2012-heden), en SARS-CoV (2002-2004). Ook het chikungunya virus (CHIKV) is een voorbeeld van een virus dat de afgelopen 10 jaar een behoorlijke impact heeft gehad op het leven van miljoenen mensen in tientallen landen. CHIKV wordt door muggen overgedragen en veroorzaakt koorts, huiduitslag en ernstige spier- en gewrichtspijn. De spier- en gewrichtsklachten kunnen weken tot maanden aanhouden. CHIKV werd voor het eerst geïsoleerd en beschreven in 1952 tijdens een uitbraak in het huidige Tanzania. Tussen 1952 en 2005 werden er af en toe uitbraken van relatief beperkte omvang gerapporteerd in Afrika en Azië. In 2005 startte echter een uitbraak van ongekende omvang. Deze begon relatief ongemerkt in Afrika, maar kwam wereldwijd in het nieuws nadat 30-50% van de bevolking van het Franse La Réunion en omliggende eilanden in de Indische oceaan geïnfecteerd raakte binnen een periode van slechts enkele maanden. De uitbraak verspreidde zich vervolgens snel naar het Indische subcontinent en andere delen van Azië waarbij miljoenen mensen geïnfecteerd raakten. Eind 2013 werden de eerste CHIKV infecties gerapporteerd in het Caribbisch gebied, alwaar het zich ook snel over omliggende (ei)landen verspreidde. In een tijdspanne van een jaar werden bijna 1 miljoen infecties gemeld in het Caribbisch gebied en omliggende landen. Recentelijk is ook in Noord- en Zuid-Amerika lokale overdracht van het virus gemeld, en met name in Zuid-Amerika is de kans op aanzienlijke uitbraken groot, onder andere doordat Zuid-Amerikaanse landen

over minder diagnostische capaciteit beschikken, waardoor een beginnende uitbraak langer onopgemerkt kan blijven. Ondanks uitgebreide onderzoeksinspanningen in de afgelopen jaren is men er tot op heden niet in geslaagd om een commercieel verkrijgbaar vaccin of antiviraal middel te ontwikkelen. Het feit dat CHIKV onverminderd nieuwe infecties blijft veroorzaken en de langdurig aanhoudende gewrichtsklachten waar veel patiënten mee kampen, onderstrepen het belang van de ontwikkeling van effectieve antivirale strategieën tegen dit belangrijke humane pathogeen.

Het werk beschreven in dit proefschrift verschaft meer inzicht in de replicatiecyclus van CHIKV. Het virus is (net als andere RNA virussen) vanwege zijn kleine genoom sterk afhankelijk van gastheer factoren voor zijn replicatie. Daarom is in dit proefschrift met name aandacht besteed aan het identificeren van deze cellulaire eiwitten, en wat hun rol is. Hiervoor dienden er eerst diverse reagentia te worden ontwikkeld, waaronder een infectieuze cDNA kloon. Een cDNA kloon is een waardevol hulpmiddel omdat het (onder andere) de gerichte genetische modificatie van CHIKV mogelijk maakt, bijvoorbeeld het aanbrengen van puntmutaties of de introductie van zogenaamde reporter genen in het virale genoom, waarmee de replicatie eenvoudig kan worden gemeten. Dit soort reporter virussen zijn erg handig bij het uitvoeren van grootschalige screens naar bijvoorbeeld antivirale middelen of gastheerfactoren betrokken bij de virusreplicatie. **Hoofdstuk 2** beschrijft het ontwerp, de constructie en de karakterisatie van een nieuwe CHIKV cDNA kloon (LS3). De LS3 cDNA kloon is gebaseerd op de consensus-sequentie van alle destijds bekende CHIKV genomen (met de de E1-A2226V mutatie) die in de periode 2006-2008 geïsoleerd zijn. Diverse aspecten van de replicatiecyclus van dit virus werden bestudeerd en vergeleken met die van een natuurlijk isolaat uit Italië (CHIKV ITA07). Hieruit bleek dat CHIKV LS3 zich net zo gedraagt als het natuurlijke isolaat en dus een geschikt modelvirus is voor verder onderzoek aan CHIKV.

Tijdens een virusinfectie gaan virale eiwitten de interactie aan met cellulaire componenten, zowel om de virusreplicatie mogelijk te maken, als om het immuunsysteem van de gastheer te manipuleren. Het bestuderen van deze virus-gastheer interacties kan interessante fundamentele inzichten verschaffen, maar dit soort gastheerfactoren kunnen ook geschikte aangrijpingspunten vormen voor nieuwe antivirale therapieën. Helaas is voor CHIKV nog weinig bekend over welke specifieke cellulaire componenten betrokken zijn bij replicatie, en wat hun rol precies is. **Hoofdstuk 3** beschrijft een zogenaamde siRNA screen die uitgevoerd is om gastheereiwitten te identificeren die (direct of indirect) een effect hebben op de replicatie van CHIKV. De primaire screen leverde een lijst met potentiële anti- of provirale eiwitten op waarvan er een aantal bevestigd zijn in een onafhankelijke secundaire analyse. Zo kon worden vastgesteld dat de cellulaire eiwitten COPB2, DUSP1, SHC1 en MARK4 een proviraal effect hebben, dus nodig zijn voor efficiënte replicatie. Het onderzoek beschreven in hoofdstuk 3 heeft waardevolle inzichten verschaft in cellulaire eiwitten en signaaltransductieroutes die betrokken zijn bij CHIKV replicatie, en biedt vele interessante aanknopingspunten voor vervolgstudies.

Hoofdstuk 4 beschrijft onderzoek naar de rol van MAPK (mitogen-activated protein kinase) signaaltransductie in CHIKV geïnfecteerde cellen. MAPK-signaaltransductie is betrokken bij vele processen waaronder de afweerrespons, celdeling en homeostase. Voorgaande studies hebben aangetoond dat verscheidene virussen MAPK-signaaltransductie manipuleren, en met name de MEK/ERK-cascade. Remming van de MEK/ERK-cascade had een nadelig effect op de replicatie van deze virussen, terwijl activatie van deze signaaltransductieroute juist een positief effect had op virusreplicatie. In tegenstelling tot wat is gevonden voor andere virussen, leek stimulatie of remming van de MEK/ERK signaaltransductie geen meetbaar effect te hebben op CHIKV replicatie. Hetzelfde geldt voor manipulatie van p38 MAPK-signaaltransductie, die wel wordt geactiveerd in CHIKV-geïnfecteerde cellen, maar tamelijk laat tijdens de infectie, waardoor het aannemelijk is dat dit een algemene apoptotische respons is, en niet zozeer een specifieke reactie op het virus.

Hoofdstuk 5 beschrijft de interactie tussen CHIKV en stress granule componenten, met name G3BP1 en G3BP2. Stress granules zijn aggregaten van eiwitten en RNA die gevormd worden in de cel als reactie op diverse vormen van stress, zoals hitte, oxidatieve stress of infectie. Ze bevatten onder andere vastgelopen (pre-initiatie) translatiecomplexen, met daarin mRNA en RNA-bindende eiwitten. Verscheidene virussen hebben manieren ontwikkeld om de vorming van deze stress granules te voorkomen, of reeds gevormde stress granules uiteen te laten vallen. De voornaamste reden hiervoor is waarschijnlijk dat de vorming van stress granules leidt tot verminderde translatie, wat ongunstig kan zijn voor de productie van virale eiwitten. De vorming van stress granules wordt over het algemeen als een antivirale reactie gezien. Daarom was het verassend dat G3BP1 en G3BP2, belangrijke stress granule componenten, nodig bleken te zijn voor efficiënte replicatie van CHIKV.

Tenslotte beschrijft **hoofdstuk 6** het antivirale effect van een speciaal RNA molecuul (5'pppRNA) tegen CHIKV en dengue virus (DENV) infectie. 5'pppRNA is een zogenaamde RIG-I agonist en kan de aangeboren immuunrespons stimuleren. Zowel CHIKV als DENV worden door muggen overgedragen en de initiële symptomen kunnen erg op elkaar lijken. Aangezien de twee virussen circuleren in dezelfde gebieden, waar de mogelijkheden voor (differentiaal) diagnostiek meestal beperkt zijn, zou een breedwerkend antiviraal middel dat beide virussen remt ideaal zijn. Hoofdstuk 6 laat zien dat behandeling met 5'pppRNA de gastheercel in een antivirale staat brengt en CHIKV en DENV infectie effectief remt. Deze respons berust op de activatie van de RIG-I/MAVS signaaltransductieroute, maar is grotendeels onafhankelijk van de interferon response. Verder onderzoek naar potentiële bijwerkingen zal nodig zijn voordat 5'pppRNA getest kan worden in klinische studies om te bepalen of het ook werkelijk therapeutisch ingezet kan worden.

Samenvattend, biedt dit proefschrift meer inzicht in de replicatie cyclus van CHIKV en de gastheer factoren die hierbij betrokken zijn. Naast het vergroten van onze algemene kennis omtrent CHIKV en CHIKV-gastheer interacties, biedt dit proefschrift tevens waardevolle aanknopingspunten voor vervolgonderzoek dat mogelijk kan leiden tot de ontwikkeling van antivirale middelen.

CURRICULUM VITAE / ABOUT THE AUTHOR

Florine Elisabeth Maria Scholte was born on December 17th 1985 in Hoogeveen, the Netherlands. She completed her pre-university secondary education (VWO) at the 'Menso Alting College' in 2004, and moved to Utrecht to continue her scientific education. She enrolled in the Bachelor Biomedical Sciences at the University of Utrecht, and it was during the Bachelor virology course, enthusiastically coordinated by dr. Raoul de Groot and prof. dr. Peter Rottier, that her interest in viruses was first sparked. After obtaining her Bachelor's degree in 2008, she continued her training with the research Master 'Biology of Disease' at the same university. As part of her Master's education, she performed two laboratory rotations with research teams studying virus-host interactions, which further intensified her interest in viruses and their interactions with the host cell. She completed her first research internship at the University of Utrecht, Veterinary Medicine, at the Department of Infectious Diseases and Immunology/Virology, in the laboratory of prof. dr. Peter Rottier (under supervision of dr. Erik de Vries). Subsequently, she was provided the opportunity to spend 8 months in the lab of prof. dr. Grant McFadden at the University of Florida, Gainesville, at the department of Molecular Genetics & Microbiology, for her second master research project. She obtained her Master's degree in 2010, and aimed to continue studying viruses as a PhD student. In October 2010 she started her PhD training at the Leiden University Medical Center, under supervision of dr. Martijn J. van Hemert and prof. dr. Eric J. Snijder. This research project was aimed at identifying host factors involved in chikungunya virus replication, and elucidating their function during viral replication. Near the end of her PhD project, Florine had the opportunity to participate in the response to the massive Ebola outbreak in 2014/15, and spent several weeks performing diagnostic tests in Sinje, Liberia. In August 2015 Florine started working as a postdoctoral researcher at the Centers for Disease Control and Prevention, division of High-Consequence Pathogens and Pathology, Viral Special Pathogens branch, in Atlanta, USA. Under supervision of dr. Eric Bergeron she is studying the role of the ovarian tumor domain of Crimean-Congo Haemorrhagic Fever virus during its replication.

LIST OF PUBLICATIONS

1. **Scholte FEM**, **Tas A**, **Albulescu IC**, **Žusinaite E**, **Merits A**, **Snijder EJ**, **van Hemert MJ**. 2015. Stress granule components G3BP1 and G3BP2 play a proviral role early in Chikungunya virus replication. Journal of Virology **89**:4457–4469.

2. **de Wilde AH**, **Wannee KF**, **Scholte FEM**, **Goeman JJ**, **Dijke Ten P**, **Snijder EJ**, **Kikkert M**, **van Hemert MJ**. 2015. A Kinome-Wide Small Interfering RNA Screen Identifies Proviral and Antiviral Host Factors in Severe Acute Respiratory Syndrome Coronavirus Replication, Including Double-Stranded RNA-Activated Protein Kinase and Early Secretory Pathway Proteins. Journal of Virology **89**:8318–8333.

3. **Treffers EE**, **Tas A**, **Scholte FEM**, **Van MN**, **Heemskerk MT**, **de Ru AH**, **Snijder EJ**, **van Hemert MJ**, **van Veelen PA**. 2015. Temporal SILAC-based quantitative proteomics identifies host factors involved in chikungunya virus replication. Proteomics **15**:2267–2280.

4. **Fros JJ**, **Major LD**, **Scholte FEM**, **Gardner J**, **van Hemert MJ**, **Suhrbier A**, **Pijlman GP**. 2015. Chikungunya virus non-structural protein 2-mediated host shut-off disables the unfolded protein response. J Gen Virol **96**:580–589.

5. **Albulescu IC**, **Tas A**, **Scholte FEM**, **Snijder EJ**, **van Hemert MJ**. 2014. An in vitro assay to study chikungunya virus RNA synthesis and the mode of action of inhibitors. J Gen Virol **95**:2683–2692.

6. **Scholte FEM**[*], **Olagnier D***, **Chiang C**, **Albulescu IC**, **Nichols C**, **He Z**, **Lin R**, **Snijder EJ**, **van Hemert MJ**, **Hiscott J**. 2014. Inhibition of dengue and chikungunya virus infections by RIG-I-mediated type I interferon-independent stimulation of the innate antiviral response. Journal of Virology **88**:4180–4194.

7. **Scholte FEM**, **Tas A**, **Martina BEE**, **Cordioli P**, **Narayanan K**, **Makino S**, **Snijder EJ**, **van Hemert MJ**. 2013. Characterization of synthetic Chikungunya viruses based on the consensus sequence of recent E1-226V isolates. PLoS ONE **8**:e71047.

8. **de Vries E**, **Tscherne DM**, **Wienholts MJ**, **Cobos-Jiménez V**, **Scholte F**, **García-Sastre A**, **Rottier PJM**, **de Haan CAM**. 2011. Dissection of the influenza A virus endocytic routes reveals macropinocytosis as an alternative entry pathway. PLoS Pathog **7**:e1001329.

Scholte FEM, Tas A, Snijder EJ, van Hemert MJ. MEK/ERK and p38 MAPK signalling is not induced by nor affecting CHIKV replication. *Submitted*

Scholte FEM, Tas A, de Wilde AH, Wannee KF, Goeman J, ten Dijke P, Snijder EJ, van Hemert, MJ. Identification of host factors involved in chikungunya virus replication by RNAi screening of the human kinome. *Manuscript in preparation*.